Università degli Studi di Ferrara

DOTTORATO DI RICERCA IN
FARMACOLOGIA E ONCOLOGIA MOLECOLARE

CICLO XXII

COORDINATORE Prof. Pier Andrea Borea

Nociceptin/orphanin FQ and motor activity: behavioural, biochemical and electrophysiological studies in models of Parkinson's disease

Settore Scientifico Disciplinare BIO/14

Dottorando
Dott. Riccardo Viaro

Tutore
Prof. Michele Morari

Anni 2007/2009

Doctoral dissertation

Nociceptin/orphanin FQ and motor activity: behavioural, biochemical and electrophysiological studies in models of Parkinson's disease

by

Riccardo Viaro

Al sole, naturalmente.

Abstract

Nociceptin/orphanin FQ (N/OFQ) is an opioid-like neuropeptide which activates the NOP receptor. N/OFQ exerts an inhibitory control on locomotion through inhibition of dopamine (DA) neurons located in the substantia nigra (SN), which degenerate in Parkinson's disease (PD). In the present study, we demonstrated that NOP receptor antagonists facilitated and inhibited motor behavior in 1-methyl-4-phenyl-1,2,5,6-tetrahydropyridine (MPTP)-treated mice and nonhuman primates depending on dose. In naïve mice, we found that dual response to NOP receptor antagonists was DA-dependent and mediated by D_2 postsynaptic (facilitation) and D_2 presynaptic receptors (inhibition). Consistently, inhibition induced by high doses of NOP receptor antagonists in MPTP-treated mice was reversed by D_2 receptor blockade, leading to a widening of their therapeutic window. Evidence that endogenous N/OFQ not only sustains symptoms but also contributes to neurodegeneration in PD was also provided. In fact, NOP receptor knockout mice were found to be partially resistant against MPTP-induced loss of nigral DA cells. In order to understand the mechanisms underlying motor effects of endogenous N/OFQ, we investigated the role of nigral NOP receptors in the control of motor cortex (M1) output. Motor inhibition induced by exogenous N/OFQ was associated with reduction in M1 excitability while the opposite was true for motor facilitation induced by NOP receptor antagonists. Finally, we investigated M1 reorganization in parkinsonian conditions and found that M1 excitability was decreased after 6-OHDA lesioning in rats. We concluded that endogenous N/OFQ controls motor activity via NOP receptors located in SN and through modulation of DA transmission, leading to changes in activity of the basal ganglia-thalamo-cortical pathway and M1 output. Moreover, we provide evidence that NOP receptor antagonists may represent a novel approach for symptomatic and neuroprotective therapy of PD.

Table of content

Introduction

Parkinson's disease

Classified as the second most common neurodegenerative disorder, Parkinson's disease (PD) is a disabling motor disease that affects approximately 0.1% of the world population and 1% of the population over 60 years of age. Clinical symptoms of PD are related to impairment of motor function such as akinesia (absence of movement or temporary paralysis), bradykinesia (abnormal slowness of movement execution), resting tremor, rigidity an abnormalities in gait and posture. Many parkinsonian patients also display non motor symptoms such as sleep disturbance, depression, anxiety, cognitive impairment and autonomic dysfunctions.

Neuropathology

Postmortem analysis of brains from PD patients demonstrated that the key pathological characteristics are loss of melanin-pigmented cells in the substantia nigra pars compacta (SNc) and presence of insoluble proteinaceous cytoplasmic inclusions termed Lewy bodies in the remaining cells (Irizarry et al., 1998). SNc, a nucleus located in the ventral mesencephalon, contains DA-producing neurons that project to the striatum, where they form synaptic connections with the GABAergic medium spiny neurons. Nevertheless, motor symptoms appear only when the level of degeneration exceeds the critical threshold of ~70% of nerve terminals and ~50% of midbrain DA neurons. However, neurodegeneration in PD extends beyond DA neurons; it is also detected in noradrenergic locus coeruleus, serotonergic raphe nuclei, cholinergic nucleus basalis of Meynert, cerebral cortex, olfactory bulb and autonomic nervous system. In recent times, a new concept has emerged in the understanding of PD pathology (Braak et al., 2003) proposing that PD neurodegeneration progresses from lower brainstem nuclei to cerebral cortical areas. The first appearance of disease-related symptoms correlates with functional deficits in the lower brainstem and olfactory bulb, then dysfunction impacts the brainstem to produce classical PD motor symptoms (Braak et al., 2003). Changes in other nuclei are observed and are thought to be secondary to the primary disease (Henderson et al., 2005). The disease progresses until cortical and cognitive changes develop.

Etiology

The cause of PD is poorly understood. Epidemiological studies have shown that while sporadic PD usually occurs at an average of 60 years of age, familial onset tends to develop at a younger age (<50 years) and occurs in approximately 1% of all PD cases (Polymeropoulos et al., 1996). Pathogenic mutations in specific genes (PARK loci) were observed in familial PD giving emphasis to the genetics of parkinsonism. Mutations in the alpha-synuclein (α-syn), Parkin, PTEN-Induced putative Kinase 1 (PINK1), DJ-1, Leucine-rich repeat kinase 2 (LRRK2), UCH-L1 and ATP13A2 genes have all been shown to be associated with familial PD (George et al., 2009). Although mutations in LRRK2 have also been detected in sporadic PD, genetic mutations alone cannot explain the majority of disease cases. The discovery of 1-methyl-4-phenyl—1,2,3,6-tetrahydropyridine (MPTP; Langston, 1983) which causes DA neuron degeneration and parkinsonism in humans, suggested that environmental factors may play a pivotal role, most likely through toxicity pathways involving oxidative stress, mitochondrial dysfunction and inflammation (Przedborski et al., 2000). Various environmental toxins such as drugs of abuse (amphetamine, ecstasy, cocaine), agricultural chemicals (paraquat, rotenone), transition metals (iron, copper, manganese, aluminium) are known to cause the disease (George et al., 2009). In addition, proteasome dysfunction has been observed in DA neurons in PD patients, suggesting that the failure to clear damaged and cytotoxic protein aggregates contributes to neurodegeneration (Olanow and McNaught, 2006).

Motor circuitry

Motor information is generated in the cerebral cortex, processed in the basal ganglia and transmitted back to the motor cortex via the thalamic relay. This forms a functional loop which regulates movement initiation and execution (i.e. the so-called “cortico-basal ganglia-thalamo-cortical” loop; Albin et al, 1989; Alexander and Crutcher, 1990). The disruption of coherent information flow, (mediated by different neurotransmitters), between these structures results in disturbed motor activity. Primary neurotransmitters in the CNS are γ-amino butyric acid (GABA), glutamate (GLU) and dopamine (DA). GABA is the main inhibitory amino acid neurotransmitter, GLU is the main excitatory

one and DA, depending on the receptor subtype activated, causes inhibitory (D_2-like) or excitatory (D_1-like) responses.

The basal ganglia

The basal ganglia are a subcortical interconnected group of nuclei, comprised of the striatum, the globus pallidus (GP), the subthalamic nucleus (STN) and the substantia nigra (SN). Basal ganglia are involved in motor, cognitive and limbic functions (Alexander et al., 1986; Albin et al., 1989; DeLong, 1990; Obeso et al., 2000). In primates, the striatum is further divided into the caudate and the putamen, while in rodents these two structures are not separated from each other. In primates, also the GP is divided an external (GPe) and an internal (GPi) portion, which are referred to as the GP and the entopeduncolar nucleus, respectively, in rodents. At last, SN is separated in the SNc and the SNr. The striatum is the major input nucleus and receives excitatory (glutamatergic) afferents mainly from the cerebral cortex and the thalamus. The striatum also receives a dopaminergic input from the SNc. DA exerts a modulatory effect on GABAergic striatal medium spiny neurons which, in turn, regulate the BG output structures (GPi and SNr) via two distinct neuronal pathway: the so-called direct and indirect pathways. The neuronal populations originating the two pathways can be identified based on distinctive patterns of DA receptor subtypes and opioid co-transmitters. Neurons of the direct pathway predominantly express excitatory D_1 receptors and prodynorphin mRNA, while neurons of the indirect pathway mainly express inhibitory D_2 receptors and preproenkephalins mRNA (Gerfen et al., 1990). The direct pathway makes monosynaptic contacts with GPi/SNr neurons, whereas the indirect pathway connects to the GPi/SNr via GPe and STN. Both GPi and SNr send inhibitory projections to the thalamus which, in turn, sends excitatory projections back to the cortex. Activation of the direct pathway inhibits GPi/SNr neurons, leading to disinhibition of thalamo-cortical glutamatergic projections and facilitation of movement initiation and execution. Conversely, activation of the indirect pathway, causes GPe inhibition and STN disinhibition. This will excite GPi/SNr neurons leading to thalamic inhibition and movement suppression, In PD, the lack of DA leads to an imbalance between the two pathways (Wichmann and DeLong, 1996). The lack of D_1 receptor stimulation leads to hypoactivation of the direct pathway while the lack of D_2 receptor stimulation leads to hyperactivation of the indirect pathway. This imbalance eventually

causes hyperactivation of the inhibitory GPi/SNr neurons, which leads to thalamic inhibition and motor impairment (Obeso et al., 2000).

Motor cortex

In mammals, the hierarchical organization among the cortical motor areas is under investiagtion. The primary motor cortex (M1) was identified based on its agranular cytoarchitectonic (Brecht et al., 2004). The division between M1 and premotor cortex is notoriously fuzzy: it may be more of a gradient than a border (Graziano et al., 2002). Premotor cortex projects to and controls M1, which in turn projects to and controls the spinal cord. Damage to M1 does not cause a general loss of the ability to move; instead, it results in a specific deficit in fine manual coordination. Many new motor areas have been described, including the supplementary motor area, the cingulated motor areas and many subdivisions of the premotor cortex. However, M1 is the most important region for movement control. It contains a somatotopic representation of the major subdivisions of the body musculature and predominantly controls the limb muscles on the contralateral side of the body albeit only at the level of head, limbs and trunk. Within representations of body parts, M1 map appears to be organized in mostly distributed and overlapping patches (Schieber, 2001). The cortical map of movements is thought to be an emergent property of distributed, horizontal, modifiable network within the cortex (Donoghue, 1995). In recent years, evidence has been provided that PD is a complex network disorder in which abnormal activity of BG neurons strongly affects the excitability, oscillatory activity, synchrony responses of those areas of the cerebral cortex involved in planning and execution of movement (Galvan and Wichmann, 2008). However, the nature and the time at which these abnormalities appear are unknown. Previous studies indicate that M1 activity is reduced (Buhmann et al. 2003; Escola et al. 2002, 2003; Parr-Brownlie and Hyland, 2005; Lefaucheur, 2005; Brown et al., 2009), increased (Sabatini et al., 2000; Pelled et al., 2002; Seiss and Praamstra, 2004, Lefaucheur, 2005) or normal (Dick et al., 1984; Metz et al., 2004) under parkinsonian conditions in animals and humans. This variability could be attributed to precise experimental factors (i.e. methods, time and region of interest) since more recent studies performed in PD patients (Thickbroom et al., 2006; Huang et al., 2007) indicate a biphasic reorganization into M1 (i.e. increase and decrease of excitability). Indeed, these findings indicate that there is a dynamic reorganisation of the corticomotor representation even at a relatively early stage of the disease and suggest a dynamic

process of M1 reorganisation with progressive increases and decreases in regional metabolism at key nodes of the motor and cognitive networks.

Treatment options for PD

PD is presently incurable. Alleviation of parkinsonian symptoms to improve the quality of life for patients is the principal goal of PD management in clinical practice. Most patients in early stages of PD will improve in response to medications that are directed at correcting DA biochemical deficit and enhancing DA transmission with the DA precursor L-3,4-dihydroxyphenylalanine (L-dopa) or with DA receptor agonists.

L-dopa

Administration of the immediate DA precursor, L-dopa, is the gold standard of PD therapy (Carlsson, 2002). L-dopa is a small neutral molecule (3,4-dihydroxyphenylalanine) that crosses the blood brain barrier using the large aminoacid transporter and can be converted to DA in (spared) DA (and also serotonergic) neurons. Indeed, these neurons contain the enzyme that convert L-dopa to DA, the L-aromatic aminoacid decarboxylase (AADC). In order to avoid peripheral decarboxylation of L-dopa, the drug is combined with a decarboxylase inhibitor that does not significantly cross the blood brain barrier, such as carbidopa or benserazide (Hornykiewicz, 2002). L-dopa effectively alleviates PD symptoms in the early stages of disease. The current "storage hypothesis" holds that at this stage of PD the available DA neurons and pre-synaptic DA terminals maintain the capacity to process exogenous L-dopa and carry out physiological handling of synthesized DA (Obeso et al., 2004). It has been suggested that the benefits of L-dopa wear off with disease progression and ongoing death of DA neurons (Lee et al., 2008) This view may be misleading due to the inability to discriminate between treatment effects and natural progression of the disease. According to the "storage hypothesis", in the absence of DA neurons, L-dopa is metabolized to DA by neural cells that lack "dopaminergic machinery" (George et al., 2009). As a result, DA release becomes pulsatile rather than continuous, and eventually leads to changes in post-synaptic receptor signalling and development of motor complications (Agid et al., 1985). Therefore, as the disease progresses, leading to fewer and fewer functional DA terminals in the striatum that can convert the L-dopa to DA

and store it, higher and more frequent doses are required to obtain the same efficacy as in the early phases of the disease. Inevitably, the long-term use of high doses and the increased frequency of administration, leads, in the majority of the PD patients, to the development of debilitating motor effects such as motor fluctuations and abnormal involuntary movements (dyskinesias) and non motor effects such as hallucinations and psychosis (due to overdosing of "normosensitive" DA receptors).

DA receptors agonists

The rationale for using direct DA receptor agonists was the delivery of continuous stimulation of DA receptors, thought to be necessary to prevent development of motor fluctuations in long-term (Radad et al., 2005). This approach was put forward as an alternative to L-dopa treatment, based on the hypothesis that L-dopa treatment set pulsatile stimulation of postsynaptic DA receptors, promoting the development of motor fluctuations (Obeso et al., 2000). DA agonists such as pramipexole (PPX), ropinirole and rotigotine bypass the degenerating neurons and directly stimulate the intact, although denervated, postsynaptic receptors in the striatum (Factor et al., 2008). These agonists are not as effective as L-dopa in relieving PD motor symptoms, however, their addition to L-dopa therapy can significantly reduce dyskinesias (Calne, 1993). Numerous in vitro and in vivo pre-clinical studies have established the neuroprotective potential of DA agonists, that can be mediated via several mechanisms including free radical scavenging and anti-oxidative properties (George et al., 2009). However, data from human trials are still not conclusive in this respect.

Other therapeutic options

Alternative treatments have been used with varying degrees of success such as GLU antagonists (Kornhuber et al., 1991), monoamine oxidase inhibitors (Birkmayer et al., 1975), catechol-O-methytransferase inhibitors (Ruottinen and Rinne, 1998), A_{2A} receptor antagonists (Jenner et al., 2009) and cholinergic antagonists (Duvoisin, 1967). Beside pharmacological treatment, some surgical procedures have been performed on PD patients, among which ablative surgery (i.e. pallidotomy or thalamotomy) or deep brain stimulation (DBS) of the thalamus, GPi or STN. The aim of pallidotomy and DBS is to reduce the excessive inhibitory output from GPi and SNr (Ashkan et al., 2004). Taken together, it is clear that the currently available treatments for PD are lacking in some key areas such as therapeutic longevity and side effect profiles. For these reasons,

investigators continue to search for alternative therapies with an emphasis on neuroprotective agents to slow or halt the progression of the disease. However, the majority of PD patients will gradually deteriorate. It is thought that an ongoing apoptotic death of DA neurons in SN underpins this relentless natural history of PD. Novel restorative therapies for PD under investigation are transplantation of fetal DA neurons or stem cells, and gene therapy based on viral-mediated delivery of enzymes critical for DA metabolism or neurotrophic factors.

Animal models of Parkinson's disease

Until now, very little is known about why and how the PD neurodegenerative process begins and progresses. Consequently, investigators still rely heavily on animal models to obtain greater insights into PD pathogenesis, and, in particular, to predict the clinical efficacy of new treatments. Whereas recent genetic discoveries have led to a number of genetic models of PD, none of these shows the typical degeneration of DA neurons. Therefore, neurotoxins such as 6-OHDA and MPTP still remain the most popular tools to produce selective neuronal death both in in vitro and in vivo systems.

MPTP

The protoxin MPTP, which is structurally similar to a number of commonly used herbicides and pesticides, can induce specific loss of substantia nigra neurons in many vertebrate species, from human to mouse. After systemic administration, MPTP rapidly enters the brain where it is processed into glial cells. MPTP first is metabolized by the enzyme MAO-B to 1-methyl-4-phenyl-2, 3-dihydropyridium ($MPDP^+$) that then deprotonates to generate the corresponding pyridium species (MPP^+). MPP^+ enters in DA cells and accumulates in the mitochondria, where it inhibits cellular respiration through the blockade of the electron transport enzyme NADH:ubiquinone oxidoreductase (complex I). Blockade of this complex inhibits ATP production and stimulates superoxide radical formation (Przedborski et al., 2000). The produced superoxide radicals react with nitric oxide (NO) to produce peroxynitrite, a highly reactive tissue-damaging species that damages proteins by oxidation and nitration. Among these proteins is found tyrosine hydroxylase (TH), the rate limiting enzyme in DA synthesis. The process of nitration inactivates TH and, consequently DA

production. Peroxynitrite also nicks DNA, which, in turn, activates poly(ADP-ribose) polymerase (PARP). PARP activation consumes ATP, and thus acutely depletes cell energy stores. This latter event aggravates the preexisting energy failure due to MPP^+-induced mitochondrial respiration blockade and precipitates cell death (Smeyne and Jackson-Lewis, 2005). Studies using MPTP have led to the development of useful animal models of PD. MPTP-treated mouse is commonly used to investigate the neurotoxicity pathways underlying PD and test the neuroprotective potential of antiparkinsonian drugs. Nonetheless, this model has failed to reproduce the motor impairment seen in PD patients or consistently replicate the phenotype observed in other parkinsonism models. Indeed, mice treated with MPTP can display no change in motor behavior (Miller et al., 1991; Itzhak et al., 1999), transient (Nishi et al., 1991; Sedelis et al., 2000) or sustained (Fredriksson et al., 1994; Haobam et al., 2005) motor impairment, and even hyperlocomotion (Colotla et al., 1990; Chia et al., 1996). Though this variability could be attributed to precise experimental factors (Sedelis et al., 2001; Jackson-Lewis and Przedborski, 2007), it has prevented the MPTP mouse model from being used to screen for symptomatic antiparkinsonian drugs, essentially limiting its applications to neurotoxicity studies. Nonhuman primate models of Parkinson's disease are a key tool to unravel PD pathophysiology and evaluate therapeutic strategies for the disease. The motor and cognitive skills of nonhuman primates as well as their neuroanatomical complexity closely resemble those of humans and thus can provide insight on issues that have clinical impact (Emborg, 2007). MPTP-treated monkeys develop a parkinsonian motor syndrome that replicates key PD features such as rigidity, bradykinesia and postural instability and that is responsive to conventional DA replacement treatments (Stephenson et al., 2005). Similar to PD patients, MPTP-treated monkeys may also present nonmotor signs, including frontostriatal cognitive deficits (Taylor et al. 1999) and changes in sleep pattern (Barcia et al., 2003). Researchers have also documented temporary autonomic disturbances affecting noradrenergic cardiac innervation (Goldstein et al. 2003). Biochemical analysis of striatal DA in PD monkeys reveals differences depending on the method of administration and, to a lesser degree, the individual (Emborg, 2007). Intramuscular, subcutaneous or intravenous injections are appropriate methods of systemic administration in monkeys. Intraperitoneal injections are not advisable as they increase the risk of infection or gastrointestinal complications. Intracarotid administration of MPTP is an appealing model because it decreases the risks to animals and investigators as well as the variability associated with

the systemic model. Administration of the neurotoxin continues as needed to develop the desired level of disability, for this reason, it is important to evaluate animals after each dosing for PD signs and general effects of MPTP intoxication in order to stop administration if necessary.

6-OHDA

The most extensively used animal model of PD is the 6-OHDA rat (Ungerstedt, 1968). 6-OHDA is a toxin that enters DA neurons through the high affinity DA transporter (DAT) and accumulates in the cytosol. It then inhibits the mitochondrial complexes I and IV (Glinka and Youdim, 1995; Glinka et al., 1996) and simultaneously forms free radicals causing oxidative stress (Olanow, 1993), which synergistically leads to degeneration of DA neurons (Glinka et al., 1997). The toxin does not cross the blood barrier brain and, therefore, has to be injected directly into the brain, in an area containing DA fibers. Following 6-OHDA-induced DA degeneration, the rat exhibits many of the disease-related symptoms observed in PD, including motor deficits and development of L-dopa-induced dyskinesias. In order to obtain an almost complete destruction of the nigrostriatal DA pathway, 6-OHDA is injected into the medial forebrain bundle (MFB), in close vicinity to the SNc DA cell bodies (Ungerstedt, 1968). Following the injection, a rapid loss of DA neurons occurs within the first days, leading to a severe depletion (>97%) of striatal DA content and loss of SNc DA neurons (Ungerstedt, 1968; Kirik et al., 1998). The MFB lesion also depletes the VTA by up to 80% (Kirik et al., 1998). This lesion is most commonly performed unilaterally. Indeed, animals receiving bilateral injections develop aphagia and adipsia, requiring extensive monitoring and care to be kept alive (Ungerstedt, 1971; Zigmod and Stricker, 1972). In addition, the unilateral model has the advantage that behavioural deficit affects muscles at the body side contralateral to the lesion. The intact side can therefore be used as an internal control.

The nociceptin/orphanin FQ neuropeptide

The identification of nociceptin/orphanin FQ (N/OFQ; Meunier et al., 1995; Reinscheid et al., 1995) represented the first successful use of reverse pharmacology, and led to deorphanization of a particular G-protein coupled receptor, namely opioid receptor like

1 (ORL-1; Mollereau et al., 1994) or, more recently, N/OFQ peptide receptor (NOP; Cox et al., 2000).

The N/OFQ-NOP receptor system

NOP receptor activation inhibits the formation of cyclic AMP, closes voltage-gated Ca^{2+} channels and opens inwardly rectifying K^{+} channels. The net effect at cellular level is the reduction of neuronal excitability and neurotransmitter release (Mogil and Pasternak, 2001). Although the N/OFQ-NOP receptor system shares considerable structural and localization features with the classical opioid system, N/OFQ does not bind classical opioid receptors, and NOP receptor activity is insensitive to the opioid antagonist naloxone, an important property used (especially when selective antagonists were not available) to discriminate N/OFQ actions with those of classical opioids . For these reasons, the N/OFQ-NOP receptor system is considered as "a nonopioid branch of the opioid family" (Cox et al., 2000). The N/OFQ-NOP receptor system is widely expressed in cortical and subcortical areas (Darland et al, 1998; Neal et al, 1999) and is involved in a wide range of physiological responses, with effects noted in the nervous system (central and peripheral), the cardiovascular system, the airways, the gastrointestinal tract, the urogenital tract and the immune system (Lambert, 2008). A wide range of neurotransmitter systems, including glutamate, catecholamines and tachykinins, are modulated by N/OFQ (Lambert, 2008). Understanding of the complex biological roles played by endogenous N/OFQ was dependent upon the generation of useful research tools, particularly transgenic animals and selective ligands, especially antagonists. Knockout mice for the N/OFQ precursor ($ppN/OFQ^{-/-}$; Köster et al., 1999) or the NOP receptor ($NOP^{-/-}$; Nishi et al., 1997) gene are available. Recently, $NOP^{-/-}$ rats were also generated (Homberg et al., 2009). From an experimental point of view, basic pharmacological properties of selective NOP receptor ligands have been characterized. From a clinical perspective, NOP receptor agonists can be developed as an innovative drug class for the treatment of pain, water-retaining disease, anxiety, urinary incontinence, drug addiction and cough while NOP receptor antagonist may represent a novel approach for memory loss, depression, movement disorders and sepsis (Calo' et al., 2010). For all this reason, the NOP receptor is an emerging target with broad therapeutic potential.

N/OFQ and motor activity

Endogenous N/OFQ exerts a physiologically inhibitory control over motor function (Marti et al., 2004a; 2008). Indeed, NOP receptor selective antagonists such as the peptide [Nphe^{1},Arg^{14},Lys^{15}]N/OFQ-NH_2 (UFP-101; Calo' et al., 2002) and nonpeptide 1-[(3R,4R)-1-cyclooctylmethyl-3-hydroxymethyl-4-piperidyl]-3-ethyl-1,3-dihydro-2H benzimidazol-2-one (J-113397 or Compound B; Kawamoto et al., 1999) and its achiral analogue 1-[1-(cyclooctylmethyl)-1,2,3,6-tetrahydro-5-(hydroxymethyl)-4-pyridinyl]-3-ethyl-1,3-dihydro-2H-benzimidazol-2-one (Trap-101; Trapella et al., 2006) increased stepping activity, run speed and rotarod performance in naïve rats (Marti et al., 2004a; 2008, 2009). J-113397 and Trap-101 also elevated motor performance in naïve mice (Viaro et al., 2008; Marti et al., 2008), while J-113397 increased arm movement speed in nonhuman primates (Viaro et al., 2008). The view of N/OFQ as a physiological constraint over motor activity was also corroborated by the finding that $NOP^{-/-}$ mice had greater stepping activity and rotarod performance than wild-type mice (Marti et al., 2004a, 2005; Viaro et al., 2008). Recent data, however, suggested that endogenous N/OFQ may play a more complex role in motor control. Indeed, J-113397 and Trap-101 facilitated motor activity at low doses and impaired it at higher ones through NOP receptor blockade in naïve rodents (Viaro et al., 2008; Marti et al., 2008). A similar dual response was also reported after i.c.v. administration of N/OFQ, low doses facilitating (Florin et al., 1996; Jenck et al., 1997; Higgins et al., 2001; Kuzmin et al., 2004, Marti et al., 2009) and higher ones inhibiting (Reinscheid et al., 1995; Devine et al., 1996; Rizzi et al., 2001; Higgins et al., 2001; Kuzmin et al., 2004; Marti et al., 2009) spontaneous locomotion. Importantly, we found that N/OFQ-induced motor facilitation was a true motor response (Marti et al., 2009) and not a result of an anxiolytic effect of N/OFQ as previously thought (Florin et al., 1996; Jenck et al., 1997). In fact, motor improvement induced by low N/OFQ doses given i.c.v. or injected into SNr was associated with enhanced motor cortex excitability and motor output, while motor impairment induced by higher N/OFQ doses was accompanied by opposite electrophysiological changes (Marti et al., 2009). Interestingly, NOP receptor antagonists replicated the electrophysiological and behavioral changes induced by low N/OFQ doses, overall suggesting that dual motor responses to NOP receptor ligands are mediated by NOP receptors in SNr and NOP receptor antagonists and N/OFQ (at low doses) activate common pathways. Evidence that mesencephalic DA neurons transduce motor actions of NOP receptor ligands has been presented. Indeed, N/OFQ and NOP

receptor antagonists, given systemically or into SNr, inhibited and facilitated DA release in dorsal striatum, respectively (Marti et al., 2004a). Moreover, N/OFQ inhibited DA release in limbic striatum (Murphy et al., 1999; Narayanan et al., 2004) while J-113397 elevated it, although via NOP-unrelated mechanisms (Koizumi et al., 2004). Finally, even the hyperlocomotive response to N/OFQ was reported to be DA-dependent (Florin et al., 1996; Kuzmin et al., 2004).

NOP receptor antagonists and PD

Endogenous N/OFQ also seems to play an important inhibitory role on motor behaviour in pathological conditions. Indeed, we collected evidence that N/OFQ sustains symptoms and neurodegeneration associated with PD (Marti et al., 2005). Thus, NOP receptor antagonists attenuated motor impairment in rats made hypokinetic with haloperidol (Marti et al., 2004b) or 6-OHDA lesioning (Marti et al., 2005, 2007, 2008) as well as in mice and nonhuman primates treated with MPTP (Viaro et al., 2008; Visanji et al., 2008). NOP receptor antagonists act via blockade of NOP receptors in SNr causing reduction of glutamate and increase of GABA release in SNr and, consequently, overinhibition of the nigro-thalamic pathway. To support pharmacological studies, genetic deletion of the NOP receptor ($NOP^{-/-}$ mice) conferred partial protection from haloperidol-induced akinesia (Marti et al., 2005), a phenomenon linked to the reduced ability of haloperidol to elevate nigral GLU release in $NOP^{-/-}$ mice (Mabrouk et al., 2010). Interestingly, DA depletion causes up-regulation of N/OFQ synthesis (Marti et al., 2005; Brown et al., 2006; Di Benedetto et al., 2009) and release (Marti et al., 2005) in SNr, thereby exacerbating negative influence of N/OFQ on DA cells and motor output. The role of N/OFQ in parkinsonism, however, may go beyond phenotype modulation. Indeed, mice with deletion of the N/OFQ precursor (ppN/OFQ) were found to be partially resistant to MPTP toxicity as shown by the reduced loss of nigral DA cells and striatal DA terminals observed following MPTP treatment in comparison with wild-type controls (Marti et al.,. 2005; Brown et al., 2006). However, different peptides (i.e. N/OFQ, N/OFQ II and nocistatin) are generated by cleavage of the ppN/OFQ precursor (Okuda-Ashitaka and Ito, 2000), questioning the view that endogenous N/OFQ modulates MPTP-induced neurotoxicity.

Purpose

The overall goal of this interdisciplinary study was to investigate the involvement of N/OFQergic transmission in motor activity under physiological and pathological conditions, in particularly PD. Specific aims of the study were as follows:

1) In order to dissect out the role of endogenous DA and the contribution of specific DA receptor subtypes to motor responses to NOP receptor antagonists, subtype-selective DA receptor antagonists were challenged against motor facilitating and inhibitory doses of N/OFQ and NOP receptor antagonists. This behavioural and neurochemical study was performed in naïve mice.

2) In order to prove the concept that blockade of nociceptinergic transmission is a new approach for symptomatic therapy of PD, we tested the effectiveness of NOP receptor antagonists in mice intoxicated with MPTP. This behavioural study was performed by testing NOP receptor antagonists alone or in combination with classical antiparkinsonian compounds.

3) In order to confirmed the efficacy of NOP receptor antagonists also in animals models that showed symptoms that closely resemble those observed in parkinsonian patients, we tested drugs in nonhuman primates. This behavioural study was performed in naïve and then in MPTP-treated macaques.

4) In order to demonstrate that endogenous N/OFQ sustains not only symptoms but also neurodegeneration associated with PD, we tested the impact of MPTP in $NOP^{-/-}$ mice by using behavioural tests and stereological counting.

5) In order to investigate whether N/OFQ controls motor behaviour through NOP receptors located in SNr and modulation of motor cortex output, we used behavioral testing and intracortical microstimulation technique. NOP receptor ligands were locally injected in SNr (and M1, for a comparison) of naïve rats.

6) In order to study the progressive reorganization of motor cortex under parkinsonian conditions, the intracortical microstimulation technique was used in rats made hemiparkinsonians with 6-OHDA at different time points after lesion.

Materials and methods

Animals

All animals used in the study were housed with free access to food and water and kept under environmentally controlled conditions (12-h light/dark cycle with light on between 07:00 and 19:00). The experimental protocols were approved by the Italian Ministry of Health (licenses n. 94/2007B and 194/2008B) and Ethical Committee of the University of Ferrara. Adequate measures were taken to minimize animal pain and discomfort. After surgery, the skin was closed using surgical sutures and the wound was cleansed with an antibiotic solution (Rifamicina SV, Lepetit, Milano).

Mice

Young adult male (20-25 g; 10-12 weeks old) Swiss, C57BL/6J, $NOP^{+/+}$ and $NOP^{-/-}$ mice were used in this study. Swiss and C57BL/6J mice were purchased from Harlan Italy (S. Pietro al Natisone, Italy), while $NOP^{-/-}$ and $NOP^{+/+}$ mice (Nishi et al., 1997) were raised at the vivarium of the Section of Pharmacology of the University of Ferrara. $NOP^{-/-}$ mice were grown on a C57BL/6J background.

Rats

Young adult male (150-300 g; 12-16 weeks old) Sprague-Dawley and Wistar rats were used in this study. Sprague-Dawley rats were purchased from Harlan Italy (S. Pietro al Natisone, Italy), while Wistar rats were generated at the vivarium of the Section of Human Physiology of the University of Ferrara.

Nonhuman primates

Young adult male macaques (Macaca fascicularis) were included in the study. Animals were housed individually at the New England Primate Research Center. All the studies were done following NIH guidelines and were approved by the IACUC at Harvard Medical Area and the New England Regional Primate Research Center.

Lesion of the DA system

In order to obtain a destruction of the DAergic system, different protocols were used, depending on the type of lesion to obtain (partial or total, unilateral or bilateral) and the species of animal to be treated.

6-OHDA lesion in rats

Unilateral lesion of DA neurons was induced in isoflurane-anaesthetised rats (Marti et al., 2005). Eight micrograms of 6-OHDA (in 4 µl of saline containing 0.02% ascorbic acid) were stereotaxically injected in the right MFB according to the following coordinates from bregma: AP= -4.4 mm, ML= -1.2 mm, VD= -7.8 mm below dura (Paxinos and Watson, 1982).

MPTP lesion in mice

Bilateral lesion of DA neurons was induced in C57BL/6J mice using an acute protocol for MPTP administration (4 x 20 mg/Kg, 90 min apart; Marti et al., 2005; Viaro et al., 2008, 2010).

MPTP lesion in nonhuman primates

Bilateral lesion of DA neurons was induced in nonhuman primates by subcrhonic administration of MPTP (0.3 mg/kg/week, i.v. for 7.5 ± 2.5 weeks) as described by Jenkins et al. (2004) and Sanchez-Pernaute et al. (2007).

Pharmacological treatments

For systemic administration (i.p.), the volume injected was 10 µl/g body weight. For local (central) administration, different methods are used in according to stereotaxic coordinates of rat brain (Paxinos and Watson, 1982) and mouse brain (Paxinos and Franklin, 2003).

Microinjection technique in mice

The injections in the lateral cerebral ventricle (LCV) of mice were given according to the procedure described by Laursen and Belknap (1986). Briefly, the syringe was held

at an approximate 45° angle to the skull. Bregma was found by lightly rubbing the point of the needle over the skull until the suture was felt. Once found, care was taken to maintain the approximate 45° angle and the needle was inserted about 2 mm lateral to the midline. The skull is relatively thin at this point, so only mild pressure was required to insert and remove the needle. Drugs were slowly injected (0.5 µl in about 5 sec) and to prevent the substance from refluxing, the needle was withdrawn from the skull 5 sec later.

Microinjection technique in awake rats

A guide cannula (outer diameter 0.55 mm, inner diameter 0.35 mm) was stereotaxically implanted under isoflurane anesthesia (1.4 % in air delivered at 1.2 ml/min) 1 mm above the right or left LCV, M1 or SNr, according to the following coordinates from bregma: LCV, AP -0.9, ML ±1.4, VD -2; M1, AP +2, ML ±2, VD -0.5; SNr, AP -5.5, ML ±2.2, VD -7.3. The cannula was secured to the skull by acrylic dental cement and metallic screws. A stainless steel obturator (outer diameter 0.30 mm) was left in place inside the guide. After a 7 day recovery period, each rat was opportunely handled and trained before behavioral tests. The day of the experiment, the obturator was removed and drugs were injected (volume 0.5 µl) through a stainless-steel injector (outer diameter 0.30 mm; inner diameter 0.15 mm) protruding 1 mm from the cannula tip.

Microinjection technique in anaesthetized rats

The animal was anaesthetized (ketamine hydrochloride, 50 mg/kg, i.p.) and placed in a Kopf stereotaxic apparatus and a large craniotomy was performed over the frontal cortex. The dura remained intact, and was kept moist with a 0.9 % saline solution. Drug injections were performed using a Hamilton syringe connected to the injection cannula with polyethylene tubing, in the left or right LCV (AP= -0.8 mm; ML= ±1.5 mm; VD= -3.5 mm below the pial surface), layer V of central M1 (AP= 2-3 mm and ML= 2.5-3 mm; VD= -1.5 mm) and SNr (AP= -5.5 mm; ML= ±2.2 mm; VD= -7.6 mm). Drugs were slowly injected and, to prevent the substance from refluxing, the needle was withdrawn from the cortex 120 sec later.

Lidocaine injection

For performed the lidocaine injection in M1, a total of 12 µl of 3% lidocaine injected at three sites within the forelimb motor cortex (Maggiolini et al., 2008), according to the

following coordinates from bregma (AP= 1 ML= 3; AP= 2 ML= 3; AP= 3 ML= 3). The cannula was lowered into the selected site 1 mm below the pial surface and the lidocaine was slowly injected (4 µl/min) and, to prevent the substance from refluxing, the needle was withdrawn from the cortex 120 sec later. For the duration of the experiment, cortical inactivation was maintained by supplementary injections of lidocaine (1-2 times for each animal) at the same sites when the forelimb movement at these sites was ICMS-evoked at the highest current used under the present experimental condition (60µA). The injected sites were remapped every 30 minutes to confirm that sites were inactivated.

Cortical bicuculline application

Under surgical stereomicroscopy, the dura on the M1 was removed and a 30 µl solution of 50 µM bicuculline was applied to the cortical surface (Stojic et al., 2008), by using a Gilson micropipette. The temperature of the solution was 35-37°C and the volume was maintained by supplementary application (1-2 times for each animal).

Behavioural studies in rodents

Motor activity in rodents was evaluated by means of different behavioural tests specific for different motor abilities, as previously described (Marti et al., 2004a, 2004b, 2005, 2007, 2008, 2009; Viaro et al., 2008, 2010). The different tests are useful to evaluate motor functions under static conditions or dynamic conditions, as an integration of coordination, gait, balance, muscle tone and motivation to run, and wre performed in a fixed sequence In the case of evaluation of pharmacological treatment, tests were performed 10 min before drug injection (control session) and 10 and 60 min after drug injection. With this protocol, both facilitatory/inhibitory and short/long term effects can be detected (Marti et al., 2004a).

Drug-induced rotation

The rotational model (Ungerstedt and Arbuthnott, 1970) was used to select the rats which had been successfully lesioned with 6-OHDA. Two weeks after lesion, rats were injected with amphetamine (5 mg/Kg i.p., dissolved in saline) and only those rats

performing >7 ipsilateral turns/min were enrolled in the study. This behaviour has been associated with >95% loss of striatal extracellular DA levels (Marti et al., 2002).

Bar test

This test, also known as the catalepsy test (Sandberg et al., 1988), measures the ability of the animal to respond to an externally imposed static posture. Each rodent was placed gently on a table and the right and left forepaws were placed alternatively on blocks of increasing heights (1.5, 3 and 6 cm for mice and 3, 6 and 9 cm for rats). The immobility time (in sec) of each forepaw on the block was recorded (cut-off time 20 sec per step, 60 sec maximum). Akinesia was calculated as total time spent on the blocks (mean between the two forepaws).

Reaction time test

This test measures motor reactivity of the animal in a open field. Mice were allowed to habituate to the center of a square arena (150x150 cm) for 5 min, then elevated 3 cm above the surface (lifting from the tail), and finally left to fall. When the animal touched the floor, the latency time for the first forelimb movement was recorded.

Drag test

This test (modification of the ”whelbarrow” test; Schallert et al., 1979), measures the ability of the animal to balance its body posture using forelimbs in response to an externally imposed dynamic stimulus (backward dragging; Marti et al., 2005). Each rodent was gently lifted from the tail (allowing the forepaws on the table) and dragged backwards at a constant speed (about 20 cm/sec) for a fixed distance (100 cm). The number of touches made by each forepaw was counted by two separate observers (mean between the two forepaws).

Elevated body swing test

The test was conducted in a dark plastic box (40×40×50 cm). Initially, each rat was allowed to habituate in the box for 5 min then it was elevated 3 cm above the ground by holding its tail. When the animal turned with its body (i.e. head and trunk) more than 30° to either side of the vertical axis a swing was counted. The direction and the number of swings carried out in 60 sec were recorded.

Speed test

This tests essentially measure animal speed in an open field. The rodent was allowed to habituate in a square arena (150x150 cm) for 5 min then elevated 3 cm about the ground (by holding its tail) and finally positioned in the centre of the arena. When the animal touched the floor it started running. Behavior was scored online using the "correct walking" criteria (see Bouwman et al, 2005). Data acquisition was stopped when the rat changed its acceleration, velocity or direction. Run speed was calculated as distance traveled (cm/sec).

Stair climbing test

This test (modification of the SCA test; Kumar and Sehgal, 2007) analyzed the motivation and the motor skill during a climb-walk. Each mouse was positioned on the first step (2 cm height, 2 cm long, 5 cm wide) of a 45°-sloping staircase. At the top of the staircase a food pellet was lodged in a small dark goal box. The speed needed for climbing 20 consecutive steps (50 cm) was recorded. Steps made at the beginning and the end of the climb were excluded because of velocity changes or obvious acceleration/deceleration.

Grip test

This test was used to evaluate the skeletal muscular strength in mice (Meyer et al., 1979). The grip-strength apparatus (ZP-50N, IMADA, Japan) is comprised of a wire grid (5 × 5 cm) connected to an isometric force transducer (dynamometer). In the grip-strength test mice were held by their tails and allowed to grasp the grid with their forepaws. The mice were then gently pulled backward by the tail until the grid was released. The maximal and the average force exerted by the mouse before losing grip was recorded. The mean of 10 measurements for each animal was calculated and the maximal and mean force was determined. The skeletal muscular strength in mice was expressed in grams force (gf) and was recorded and processed by IMADA ZP-Recorder software.

Rotarod test

This test analyzes the ability of the rodents to run on a rotating cylinder (diameter 8 cm) and provides information on different motor parameters such as coordination, gait, balance, muscle tone and motivation to run (Rozas et al., 1997). The fixed-speed rotarod

test was employed according to a previously described protocol (Marti et al., 2004a; Viaro et al., 2008, 2010). Briefly, animals were tested at stepwise increasing speeds (180 sec each) and time spent on the rod calculated (in sec). Drug effect was calculated by monitoring motor activity within a limited speed range (four speed) causing a progressive decrement of performance to ~40% of the maximal response.

Footprinting test

This test provides information on gait patterns (Klapdor et al., 1997). Mice paws were marked with ink and gait patterns (stride length and width, foot angle, overlap, speed) analyzed after walking over a sheet of paper (Fig. 2F). The apparatus was composed of a white runway (5 cm wide, 70 cm long, with borders of 10 cm height) arranged to lead out into a dark goal box (20 x 20 x 30 cm). The parameters were measured by wetting forepaws and hindpaws with commercially available pencil nontoxic ink (the paws were painted with different colored inks) and allowing the mice to trot on a strip of paper (5 cm wide, 70 cm long) onto the runway. Pawprints made at the beginning and the end of the run were excluded because of velocity changes or obvious acceleration/deceleration. Stride length is the average distance (in mm) of forward movement between each forepaw and hindpaw footprint. Stride width is the average lateral distance (in mm) between opposite left and right forepaw and opposite left and right hindpaw. It has been calculated by measuring the perpendicular distance of a given step to a line connecting its opposite preceding and succeeding steps. Foot angle is the angle of hindpaw (in degree) with respect to main direction. It has been calculated by measuring the amplitude of angle between the direction of run and each direction of the hindpaw (line starting at center of paw to the third finger). Placement of paws is the footprint overlap (in mm) and is calculated by measuring the distance between the center of the forepaw footprint and the ipsilateral hindpaw footprint, taken from successive steps. Speed of run (in cm/sec), was calculated by the ratio between the length of runway and time spent along the runway. After the run, animals were placed in a cage filled with 0.5 cm warm water for 1 min in order to wash off the dye.

Spontaneous activity

Spontaneous motor activity and step parameters were detected in a freely-moving mouse by videotape recording (Canon Camcorder HG21) and off-line analysis. The animal was placed in a square box (50 x 50 cm) and the recorded video was then

analysed by two separate observers. Global, horizontal and fine movements were quantified together with immobility (i.e. freezing) time. Step parameters such as time for movement preparation and initiation, step speed and length were also evaluated. Activity measurements were conducted between 11:00 and 15:00 during the light phase.

Behavioural studies in nonhuman primates

In order to monitor parkinsonian phenotype and the effectiveness of drug treatments, motor activity in nonhuman primates were analysed by the movement analysis panel (MAP) test and neurologist evaluation.

Movement analysis panel (MAP)

Animals were trained to perform a computerized timed reaching task that measures the speed of arm movements (Jenkins et al., 2004). Training was carried out for an average of 6 days for the platform task and 8-12 days for the straight rod task, until the performance (time to retrieve the treats) was stable. For pharmacological evaluation, animals were tested 30 min after the administration of vehicle (saline) for two days and then with either saline or the active drugs. In addition, global motor activity data was obtained using activity monitors (Actiwatch) for a week at the naïve and parkinsonian stages (Table 1). These tests provide objective measures of bradykinesia and hypokinesia, respectively.

Parkinsonian rate scale (PRS)

For motor evaluation, animals were transferred to a Plexiglas observation cage where they were videotaped. Motor behavior was rated according to a scale based on the motor subscale of the UPDRS (Unified Parkinson Disease Rating Scale), as described (Jenkins et al., 2004; Sanchez-Pernaute et al., 2007). The following signs were scored from 0 to 3: bradykinesia in the left and right arms (L/R), tremor L/R, rigidity L/R, hypokinesia, posture/balance (for a total score from 0 to 24). Scores were obtained at 30-45 min after each drug or vehicle administration.

Intracortical microstimulation in rats

The intracortical microstimulation (ICMS) technique is commonly used to quantitatively evaluate plastic changes in the motor cortex following motor output disconnection because it is useful in evaluating the strength of functional connection between the motor cortex and the target motoneuron pool (Sanes et al., 1990). It presumes that after motor output disconnection/manipulation, the motor cortical changes in the types of evoked movements and in the minimal level of current necessary to evoke movements, reflect the adapting changes of cortical circuits. If so, the difference changes in cortical evoked movements and in their current threshold over time could reveal different underlying mechanisms in adaptive remodeling of disconnected/manipulated cortical circuits. In each animal, the movements evoked by ICMS in the frontal agranular cortex were mapped.

Surgical procedure

The anaesthetized animal was placed in a Kopf stereotaxic apparatus and a large craniotomy was performed over the frontal cortex of both hemispheres. The dura remained intact and was kept moist with an 0.9% saline solution. The electrode penetrations were regularly spaced out over a 500μm grid. Alteration in the coordinate grid, up to 50μm, was sometimes necessary to prevent the electrode from penetrating the surface blood vessels. These adjustments in the coordinate grid were not reported in the reconstructing maps. When the adjustment was over 50μm, the penetration at this site was not performed. Glass insulated tungsten electrodes (0.6-1MΩ impedance at 1kHz) were used for stimulation. The electrode was lowered perpendicularly into the cortex to a depth of 1.5 mm below the cortical surface and adjusted ±200 μm so as to evoke movement at the lowest threshold. In preliminary experiments this depth was found to correspond to layer V of the frontal agranular cortex (Franchi, 2000).

Mapping procedure

The mapping procedure was similar to the one described by Donoghue and Wise(1982) and Sanes et al. (1990), and detailed elsewhere (Franchi, 2000). Briefly, monophasic cathodal pulses (30ms train duration at 300Hz, 200μs pulse duration) of a maximum of 60 μA were passed through the electrode with a minimum interval of 2.5 s. Two observers were required to detect movement and determine threshold. One observed the

movement without knowledge of the actual current intensity and was unaware of which group the particular rat belonged to. The other observer changed the level of current. Starting with a 60μA current, intensity was decreased in 5μA steps until the movement was no longer evoked; then the intensity was increased to a level at which approximately 50% of the stimulations elicited movement. This level defined the current threshold. If no movements or twitches were evoked with 60μA, the site was recorded as negative (ineffective site). Mapping was initiated at a high current because the initial polysynaptic recruitment of remote neurons optimizes the detection of movements in this 500μm step grid mapping. Body parts activated by ICMS were identified by visual inspection and/or muscle palpation. When eye movement was observed, the current threshold was determined under optical microscope. A normal component of the output organization of rat M1 is the presence of some sites along the border region between two movement representations from which movement of both body parts can be evoked simultaneously. At such sites, both movements were recorded for that position regardless of the individual thresholds (which were determined separately for each). Hereafter such movements are identified as 'threshold-movement' and 'over-threshold movement', respectively, according to value of the individual threshold. In some sites along the border region between two movement representations, both movements can be evoked simultaneously at the current threshold level (dual movement site). Forelimb movements evoked by threshold current typically consisted of brief twitches of the elbow or shoulder (proximal limb movement), wrist and digit (distal limb movement), or simultaneous twitches of both muscles groups. Forelimbs and hindlimbs were approximately half-way between flexion and extension and were alternately flexed and extended, particularly at the representational borders.

Neurotransmitter release

The pharmacological profiles of presynaptic DA receptors modulating monoamine release from mice striatal synaptosomes were studied and compared using different dopaminergic ligand.

Synaptosome preparation

To minimize pain and discomfort, mice were decapitated under light ether anesthesia and the striatum was quickly excised to prepare synaptosomes, as previously described (Morari et al., 1998). Briefly, striata were homogenized in ice-cold 0.32 M sucrose buffer at pH 7.4 then centrifuged for 10 min at 2,500 g_{max} (4°C). The supernatant was then centrifuged for 20 min at 9,500 g_{max} (4°C) with the synaptosomal pellet being resuspended in oxygenated (95% O_2, 5% CO_2) Krebs solution (mM: NaCl 118.5, KCl 4.7, $CaCl_2$ 1.2, $MgSO_4$ 1.2, KH_2PO_4 1.2, $NaHCO_3$ 25, glucose 10) containing ascorbic acid (0.05 mM) and disodium EDTA (0.03 mM). Synaptosomes were pre-loaded with [^{3}H]-DA by incubation in medium containing 50 nM [^{3}H]-DA (specific activity 27.8 Ci/mmol, NEN DuPont, Boston, MA, USA.) for 25 min. One milliliter aliquots of the suspension (~0.35 mg protein) were slowly injected into nylon syringe filters (outer diameter 13 mm, 0.45 μM pore size, internal volume of about 100 μl; MSI, Westporo, MA, USA) which were then connected to a peristaltic pump. Filters were maintained at 36.5 °C in a thermostatic bath and superfused at a flow rate of 0.4 ml/min with a pre-oxygenated Krebs solution. Under these experimental conditions, spontaneous [^{3}H]-DA efflux was essentially unaffected by reuptake. Sample collection (every 3 min) was initiated after a 20 min period of filter washout. The effect of drugs was evaluated on both spontaneous and K^+-stimulated neurotransmitter outflow. In this case, drugs were added to the perfusion medium 6 (agonist) or 9 (antagonist) min before a 10 mM KCl pulse (120 sec) and maintained until the end of the experiment.

[^{3}H]-DA analysis

[^{3}H]-DA levels in the samples were measured by liquid scintillation spectrophotometry. Sample superfusate (1.2 ml/sample) and filter retained (dissolved with 1 ml of 1 M NaOH followed by 1 M HCl) were opportunely mixed with Ultima Gold XR scintillation fluid (Packard Instruments B.V., Groningen, The Netherlands) and radioactivity was determined by a Beckman LS 1800 β-spectrophotometer.

Histological analysis

After in vivo experiments, the animals were sacrificed for the histological evaluations. All neurons contain Nissl substance, which is primarily composed of granular

endoplasmic reticulum and ribosomes, and occurring in nerve cells body and dendrites. Because of the RNA content, Nissl substance is very basophilic and will be very sharply stained with cresyl violet acetate. This aspecific staining was used for check the placement of the probes or electrode. The tracks was verified by microscopic examination and the animals in which the tracks were not correctly positioned were discarded from the study. On contrary, tyrosine hydroxylase (TH; tyrosine 3-monooxygenase) is a selective marker, because this enzyme is content only in the cytoplasme of dopaminergic cells. TH is responsible for catalyzing the conversion of the amino acid L-tyrosine to dihydroxyphenylalanine (dopa). Dopa is a precursor for dopamine which in turn is a precursor for norepinephrine (noradrenaline) and epinephrine (adrenaline).

Tissue processing

Mice were deeply anesthetized with ketamine and xylazine (85+15 mg/Kg; i.p.) and rats were deeply anaesthetised with Zoletil 100® (10 mg/Kg, i.m.; Virbac Laboratories, Carros, France), transcardially perfused at room temperature with phosphate-buffered saline (PBS; 20 mM, pH 7.4) and fixed with cold 4% paraformaldheyde in PBS. Brains were removed, post-fixed overnight, transferred to 20% sucrose solution in PBS for cryoprotection (until they sunk) and stored at -80°C. We used a cryostat at −18°C to cut 40 µm coronal sections, which were collected free floating (in PBS) for all analysis.

Nissl staining

Sections at levels of cortex and SNc were mounted on gelatine-coated slides, stained with cresyl violet, dried in escalating alcohol concentration (50-70-90-95-100%), cleared in xylene and coverslipped with mounting medium.

TH immunohistochemistry

Sections at levels of striatum and SNc, were rinsed 3 times in PBS and incubated for 15 min in 3% H_2O_2 and 10% methanol in PBS to block the endogenous peroxidase activity. After washing in PBS, the sections were preincubated in blocking serum (5% normal horse serum and 0.3% Triton x100 in PBS) for 60 min, followed by incubation in anti-TH mouse monoclonal antibody solution (1:2000, Chemicon, Temcula, CA) for 16 hr at room temperature. The sections were then rinsed in PBS and incubated for 1 hr in biotinylated horse anti-mouse IgG secondary antibody (1:200; Vector Laboratories,

Burlingame, CA). After rinsing, sections were incubated with avidin-biotin-peroxidase complex (Vector Laboratories) for 30 min at room temperature. After rinsing with PBS, immunoreactivity was visualized by incubating the sections in a solution containing 0.05% 3,3-diaminobenzidine (DAB) in 0.013% H_2O_2 in PBS for about 1 min. The sections were rinsed in PBS, mounted on chrome-alum-coated slides, eventually counterstained with cresyl violet, dried with escalating alcohol concentration, cleared in xylene and coverslipped with mounting medium.

Optical density evaluation

The sections were viewed with a Zeiss Axioskop (Carl Zeiss, Germany). Sections were acquired (AxioCam ICc3, Carl Zeiss, Germany) and TH-immunoreactive fiber density analyzed using ImageJ software (Wayne Rasband; NIH, USA). For each animal, optical density was calculated as the mean of the 5 striatal levels and corrected for non-specific background, measured in the corpus callosum.

Stereological cell counting

For counting of TH-immunoreactive neurons (phenotypic marker) and cresyl violet stained cells (structural marker) in SNc, an unbiased stereological sampling method was used (West and Gundersen, 1990), based on optical dissector stereological probe (Bezard et al., 2003; Gross et al., 2003). Stereological analysis was performed using an Leica DMRE microscope with a motorized Z and X-Y stage encoders linked to a computer-assisted stereological system (Mercator Digital Imaging System, Explora Nova, La Rochelle, France). For each animal, SNc boundaries were delimited at low magnification (2.5×) by examining the size and shape of the different groups of TH-immunoreactive neurons and their axonal projections, as well as nearby fibre bundles according to the mouse brain atlas. SNc boundaries were drawn on every fourth section and the first was randomly chosen. SNc volume was calculated using the formula $V_{(SNc)} = \sum S\ td$; where $\sum S$ is the sum of surface areas (μm^2), t the average section thickness and d the distance between the sections (Theoret et al., 1999). The average section thickness (t) was estimated to 12 µm after immunohistochemistry processing and guard zones of 2 µm were used to ensure that top and bottom of sections are never included in the analysis. Eight sections were used for each animal. From a random start position, a computer-generated sampling grid placed the counting frames. The counting frame size was 50 µm length and 50 µm width. We left a distance of 100 µm (x) and 100 µm (y)

between each counting frame. Within each frame, all cell nuclei which came into focus (40× immersion oil objective; Gundersen et al., 1988) were counted. A neuron was counted if more than half the cell body was inside the two consecutive boundaries taken into account. To estimate the number of TH-immunoreactive neurons we used: $N= V_{(SNc)} (\sum Q^{-}/\sum V_{(dis)})$; where N is the estimation of the number of TH-immunoreactive neurons, V the volume of SNc, $\sum Q^{-}$ the number of cells counted in the frames and $\sum V_{(dis)}$ is the total volume of frames (Theoret et al., 1999).

Data presentation and statistical analysis

Data are expressed as means ± SEM of n determinations per group. Different statistical analysis was performed, as appropriate: Student's t-test, χ^2 test presented in a two-way contingency table, one-way ANOVA followed by the Newman-Keuls or PLSD test, and two-way repeated measure (RM) ANOVA followed by contrast analysis and the sequentially rejective Bonferroni test. P values <0.05 were considered to be statistically significant. In order to facilitate the readership, we reported the results of statistics performed on data in a separate section (appendix I).

Materials

6-OHDA bromide, amphetamine methylester, benserazide hydrochloride, bicuculline methochloride, L-dopa methyl ester and MPTP hydrochloride were purchased from Sigma (St. Louis, MO, USA). Amisulpride, domperidone, GBR12783, raclopride and SCH23390 were purchased from Tocris (Bristol, UK). PPX was purchased from McTony Bio&Chem (Vancouver, Canada). S33084 was provided by Institut de Recherches Servier (Croissy-sur-Seine, France). Lidocaine hydrochloride was purchased from S.Anna Hospital (Ferrara, Italy). N/OFQ, J-113397, Trap-101 and UFP-101 were synthesized in the laboratories of the Department of Pharmaceutical Chemistry at the University of Ferrara. All drugs were freshly dissolved in the vehicle just prior to use.

Results

Part I Different subpopulations of D_2 receptors mediate dual motor responses of NOP receptor antagonists in mice

Dose-response curves of NOP receptor antagonists

The motor profiles of three NOP receptor antagonists were investigated in C57BL/6J mice by using static and dynamic tests providing complementary information on motor parameters: the bar, drag and rotarod tests. The non peptide antagonist J-113397 and its achiral analogue Trap-101 were administered systemically while the peptide antagonist UFP-101 was given i.c.v. Basal activity in absolute values was 0.8 ± 0.1 sec (immobility time in the bar test), 16.5 ± 0.9 steps (drag test) and 937.9 ± 62.1 sec (time on rod). Motor activity was not different at the right and left paw so data were pooled together.

J-113397

J-113397 caused long lasting inhibition of the immobility time in the bar test at 10 mg/Kg, lower doses being ineffective (Fig. 1A). J-113397 caused a dual regulation of stepping activity in the drag test (Fig. 1B) and rotarod performance (Fig. 1C). In both tests, facilitation was observed at 0.3 and 1 mg/Kg and reduction at 10 mg/Kg.

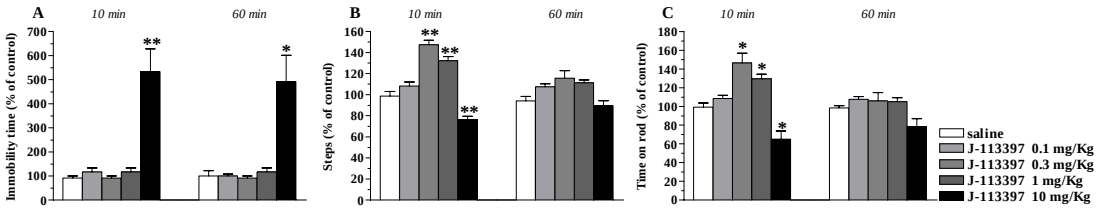

Figure 1. J-113397 dually modulated motor activity in C57BL/6J mice. Systemic administration of J-113397 (0.1-10 mg/Kg, i.p.) affected motor performance in the bar (**A**), drag (**B**) and rotarod (**C**) test. All tests were performed before (control session) and after (10 and 60 min) drug injection. Data are means ± SEM of 6 determinations per group and were expressed as percentage of the control session. *p<0.05, **p<0.01 different from saline (RM ANOVA followed by contrast analysis and the sequentially rejective Bonferrroni's test).

Trap-101

Trap-101 did not affect the immobility time at any of the doses tested (Fig. 2A). However, Trap-101 dually modulated motor activity in the drag and rotarod test, increasing the number of steps (Fig. 2B) and time on rod (Fig. 2C) at 10 mg/Kg and reducing them at 30 mg/Kg. administration. These effects were observed only at 10 min after drug administration.

UFP-101

UFP-101 increased the immobility time at 30 nmol (Fig. 2D) and caused dual responses in the drag (Fig. 2E) and rotarod test (Fig. 2F), namely facilitation at 1 and 3 nmol and marked inhibition at 30 nmol. Differently from non peptide antagonists, the effects of UFP-101 were detected also at 60 min after injection.

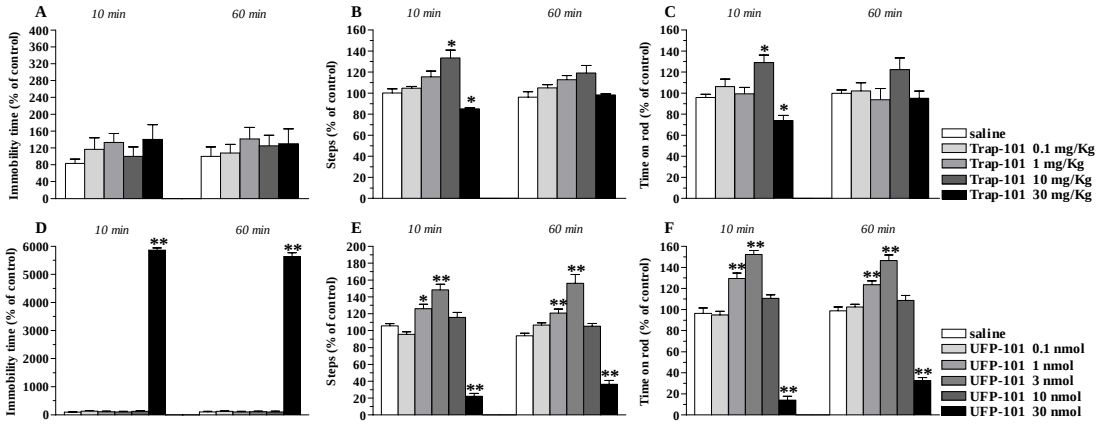

Figure 2. Trap-101 and UFP-101 dually modulated motor activity in C57BL/6J mice. Systemic administration of Trap-101 (0.1-30 mg/Kg, i.p.), or i.c.v. injection of UFP-101 (0.1-30 nmol) affected motor performance in the bar (**A, D**), drag (**B, E**) and rotarod (**C, F**) test. All tests were performed before (control session) and after (10 and 60 min) drug injection. Data are means ± SEM of 6 determinations per group and were expressed as percentage of the control session. *p<0.05, **p<0.01 different from saline (RM ANOVA followed by contrast analysis and the sequentially rejective Bonferrroni's test).

DA receptor subtypes differentially modulate motor actions of NOP receptor antagonists

We previously reported that NOP receptor antagonists elevate striatal DA release in rats, suggesting that endogenous N/OFQ tonically inhibits nigro-striatal DA transmission (Marti et al., 2004a). We therefore employed selective DA receptor antagonists to unravel the contribution of endogenous DA to motor actions of NOP

receptor antagonists. The D_1/D_5 receptor antagonist SCH23390, the D_2/D_3 receptor antagonists raclopride and amisulpride, and the D_3 selective receptor antagonist S33084 were tested alone and in combination with motor facilitating or inhibiting doses of NOP receptor antagonists.

Effects of DA receptor antagonists

Raclopride dose-dependently inhibited motor performance, as shown by an increase in immobility time (Fig. 3A) and a reduction in both the number of steps (Fig. 3B) and time on rod (Fig. 3C). These effects were evoked at 0.1 and 0.3 mg/Kg and observed both 30 and 80 min after administration. Amisulpride partially replicated motor inhibiting action of raclopride, causing a prolonged increase in immobility time (Fig. 3D) and inhibition of rotarod performance (Fig. 3F) at the highest dose tested (15 mg/Kg). Delayed impairment of rotarod performance was observed also at 5 mg/Kg. Different from raclopride, amisulpiride did not affect stepping activity in the drag test (Fig. 3E).

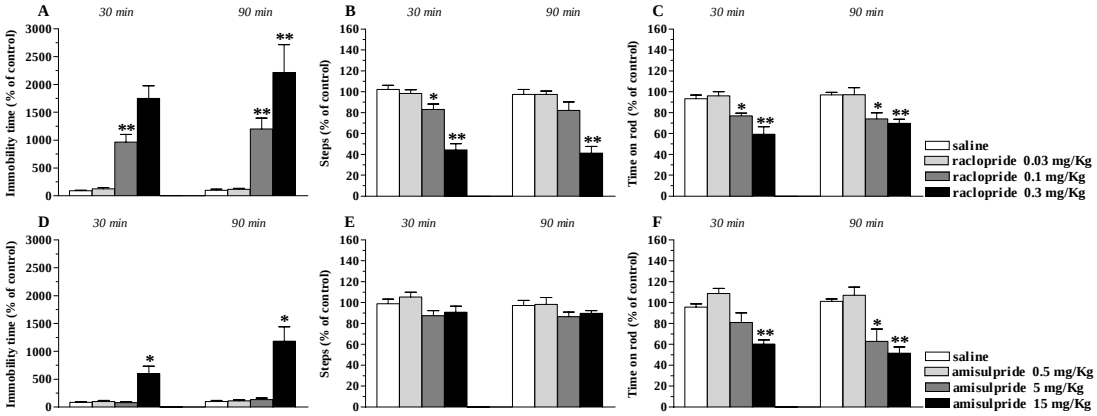

Figure 3. D_2/D_3 receptor antagonists decreased motor activity in C57BL/6J mice. Systemic administration of raclopride (0.03-0.3 mg/Kg, i.p.) and amisulpride (0.5-15 mg/Kg, i.p.) affected motor performance in the bar (**A, D**), drag (**B, E**) and rotarod (**C, F**) test. All tests were performed before (control session) and after (30 and 80 min) drug injection. Data are means ± SEM of 6 determinations per group and were calculated as percentage of the control session. *p<0.05, **p<0.01 different from saline (RM ANOVA followed by contrast analysis and the sequentially rejective Bonferrroni's test).

SCH23390 produced consistent motor inhibition in the three tests (Fig. 4). Increased immobility time (Fig. 4A), reduced stepping activity (Fig. 4B) and rotarod performance (Fig. 4C) were observed at 0.01 and 0.03 mg/Kg. The effects in the bar and drag tests were prolonged, while those in the rotarod were detected only 30 min after injection.

S33084 did not produce marked changes in motor activity (Fig. 4D-F), the only effect observed being mild inhibition of stepping at 0.64 mg/Kg (Fig. 4E).

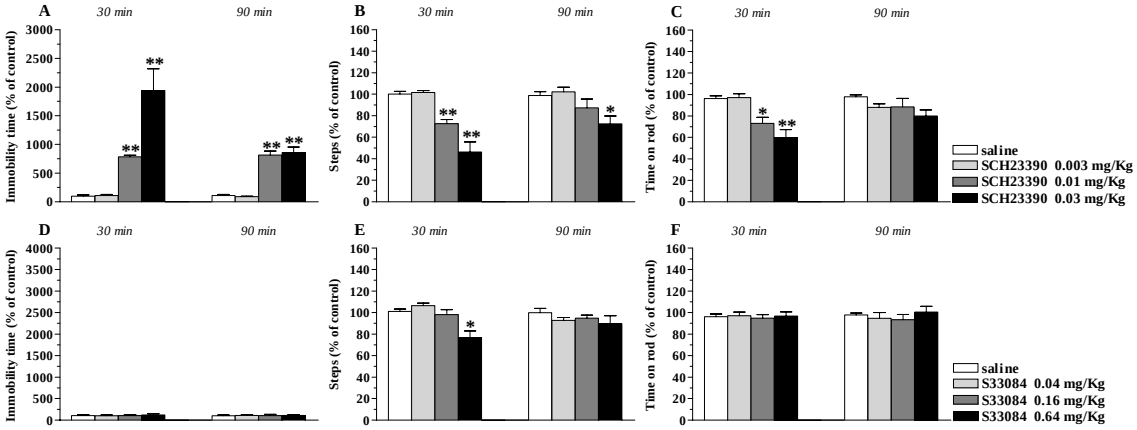

Figure 4. D_1/D_5 and D_3 receptor antagonists differentially affected motor activity in C57BL/6J mice. Systemic administration of the D_1/D_5 antagonist SCH23390 (0.003-0.03 mg/Kg, i.p.) affected motor performance in the bar (**A**), drag (**B**) and rotarod (**C**) test. Systemic administration of the D_3 receptor selective antagonist S33084 (0.04-0.64 mg/Kg, i.p.) affected motor performance in the drag (**E**) but not in the bar (**D**) and rotarod (**F**) test. All tests were performed before (control session) and after (30 and 80 min) drug injection. Data are means ± SEM of 6 determinations per group and were calculated as percentage of the control session. *p<0.05, **p<0.01 different from saline (RM ANOVA followed by contrast analysis and the sequentially rejective Bonferrroni's test).

Interaction between DA receptor antagonists and NOP receptor antagonists

To disclose the role of endogenous DA, we challenged motor facilitating or inhibiting doses of NOP receptor antagonists with doses of DA receptor antagonists per se ineffective on motor activity. Motor facilitating doses were first investigated. Raclopride (0.03 mg/Kg) prevented the increase in stepping activity (Fig. 5B) and rotarod performance (Fig. 5C) induced by J-113397 (0.3 mg/Kg), Trap-101 (0.3 mg/Kg) and UFP-101 (3 nmol). Conversely, amisulpride (0.5 mg/Kg), SCH23390 (0.003 mg/Kg) and S33084 (0.16 mg/Kg) were ineffective (Fig. 5E-F).

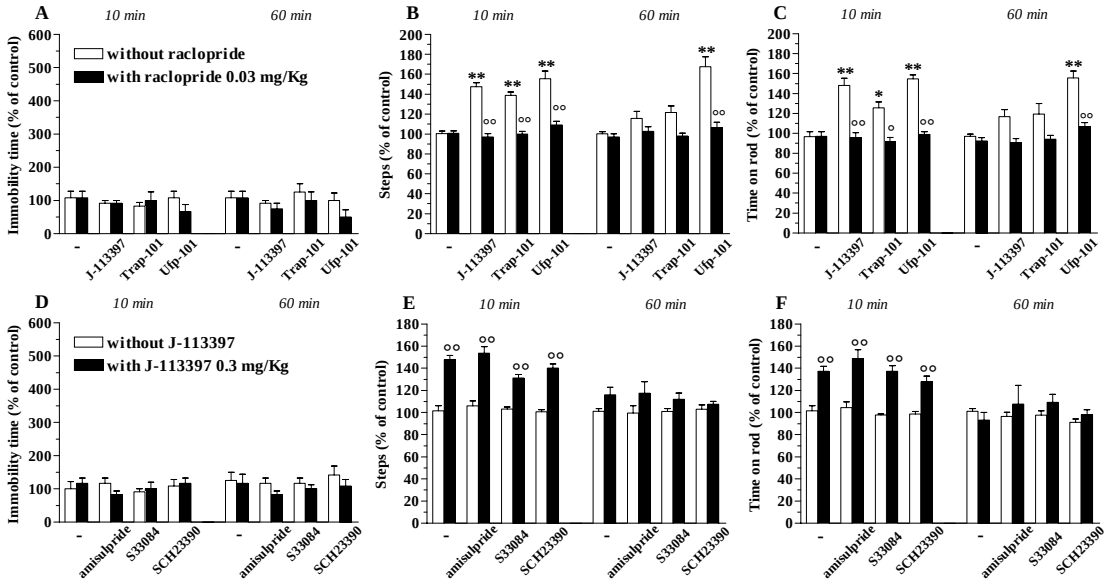

Figure 5. Facilitation of motor activity induced by NOP receptor antagonists in C57BL/6J mice was selectively prevented by the D_2/D_3 selective antagonist raclopride. Pretreatment (20 min in advance) with raclopride (0.03 mg/Kg, i.p.) prevented motor facilitation induced by low doses of J-113397 (0.3 mg/Kg, i.p.), Trap-101 (10 mg/Kg, i.p.) and UFP-101 (3 nmol, i.c.v.) in the drag (**B**) and rotarod (**C**) test. Raclopride and NOP receptor antagonists did not affect motor performance in the bar test (**A**). Pretreatment with amisulpride (0.5 mg/Kg, i.p.), S33084 (0.16 mg/Kg, i.p.) and SCH23390 (0.003 mg/Kg, i.p.) did not affect motor facilitation induced by J-113397 (0.3 mg/Kg, i.p.) in the drag (**E)** and rotarod (**F**) test. Amisulpride, S33084, SCH23390 and J-113397 (alone or in combination) did not affect motor performance in the bar test (**D**). All tests were performed before (control session) and after (10 and 60 min) NOP receptor antagonist administration. When DA receptor antagonists were tested alone, behavioral testing was performed 30 and 80 min after drug injection. Data are means ± SEM of 6 determinations per group and were calculated as percentage of the control session. *p<0.05, **p<0.01 different from saline; °p<0.05, °°p<0.01 different from the same group in the absence of raclopride or J-113397 (RM ANOVA followed by contrast analysis and the sequentially rejective Bonferrroni's test).

Differently from facilitation, motor inhibition caused by J-113397 (10 mg/Kg), Trap-101 (30 mg/Kg) and UFP-101 (30 nmol) in the bar (Fig. 6A), drag (Fig. 6B) and rotarod (Fig. 6C) test was prevented by amisulpride, raclopride being ineffective (Fig. 6D-F). It is noteworthy that individual doses of J-113397 and Trap-101 which caused inhibition of stepping activity in the drag test induced significant stimulation in the presence of amisulpride (Fig. 6B). A similar reversal of action was observed for J-113397 on rotarod performance (Fig. 6C).

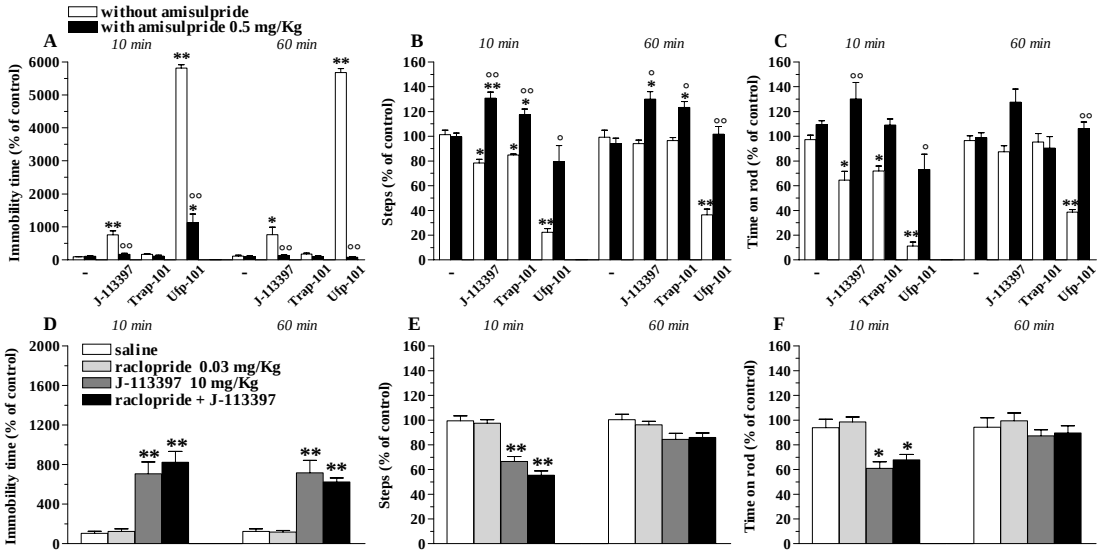

Figure 6. Inhibition of motor activity induced in C57BL/6J mice by NOP receptor antagonists was selectively prevented by the D_2/D_3 selective antagonist amisulpride. Pretreatment (20 min in advance) with amisulpride (0.5 mg/Kg, i.p.) reduced motor inhibition caused by high doses of J-113397 (10 mg/Kg, i.p.), Trap-101 (30 mg/Kg, i.p.) and UFP-101 (30 nmol, i.c.v) in the bar (**A**), drag (**B**) and rotarod (**C**) test. Conversely, pretreatment with raclopride (0.03 mg/Kg, i.p.) was ineffective (**D-F**). All tests were performed before (control session) and after (10 and 60 min) NOP receptor antagonist injection. When DA receptor antagonists were tested alone, behavioral testing was performed 30 and 80 min after drug administration. Data are means ± SEM of 6 determinations per group and were expressed as percentage of the control session. *p<0.05, **p<0.01 different from saline; °p<0.05, °°p<0.01 different from the same group in the absence of amisulpride (RM ANOVA followed by contrast analysis and the sequentially rejective Bonferrroni's test).

Raclopride prevented motor facilitation induced by N/OFQ

The data collected thus far indicate that the dual action profile of NOP antagonists is mediated by endogenous DA acting on populations of D_2 receptors differently sensitive to amisulpride and raclopride. Previous studies in mice have reported that N/OFQ given i.c.v. stimulates spontaneous locomotion through DA-dependent mechanisms (Florin et al., 1996; Kuzmin et al., 2004). We therefore investigated the role of D_2 receptors in motor facilitation induced by N/OFQ in the bar, drag and rotarod tests. N/OFQ produced different effects on motor activity depending on the dose and motor task used. In particular, N/OFQ monotonically increased immobility time (Fig. 7A) and dually regulated both stepping activity (Fig. 7B) and rotarod performance (Fig. 7C). The effects were also detected after 60 min from administration. Motor facilitation in the drag and rotarod tests was observed at 0.01 nmol while motor inhibition predominated

at higher doses (0.1-10 nmol) in all tests. Increases in stepping activity and rotarod performance induced by 0.01 nmol N/OFQ were prevented by raclopride (Fig. 7E-F).

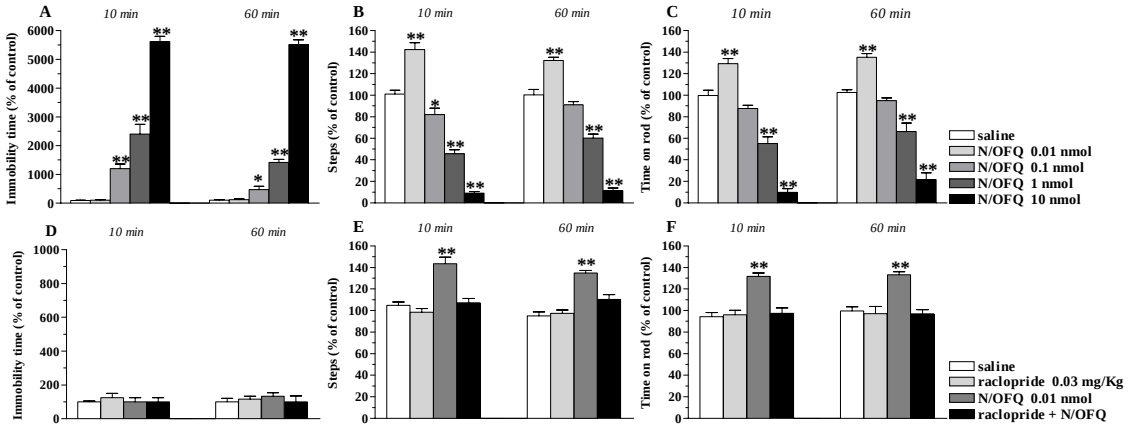

Figure 7. N/OFQ dually modulated motor activity in C57BL/6J mice. I.c.v. injections of N/OFQ (0.1-30 nmol) affected motor performance in the bar (**A**), drag (**B**) and rotarod (**C**) test. Pretreatment (20 min in advance) with raclopride (0.03 mg/Kg, i.p.) prevented motor facilitation induced by low doses of N/OFQ (0.01 nmol, i.c.v.) in the drag (**E**) and rotarod test (**F**). Low doses of N/OFQ, alone or in combination with raclopride, did not affect motor performance in the bar test (**D**). All tests were performed before (control session) and after (10 and 60 min) N/OFQ injection. When DA receptor antagonists were tested alone, behavioral testing was performed 30 and 80 min after drug injection. Data are means ± SEM of 6 determinations per group and were calculated as percentage of the control session. *p<0.05, **p<0.01 different from saline (RM ANOVA followed by contrast analysis and the sequentially rejective Bonferrroni's test).

Selectivity of NOP receptor ligands

To test the specificity of NOP receptor ligands, motor facilitating and inhibitory doses of J-113397, UFP-101 and N/OFQ were challenged in $NOP^{+/+}$ and $NOP^{-/-}$ mice.

In $NOP^{+/+}$ mice (Fig. 8A), J-113397 facilitated rotarod performance at 0.1 and 1 mg/Kg and inhibited it at 10 mg/Kg. No major difference was observed between Swiss and $NOP^{+/+}$ mice in terms of sensitivity to J-113397 or duration of the response. Conversely, J-113397 was not effective in $NOP^{-/-}$ mice at any of the doses tested (Fig. 8B), suggesting that both the facilitation and the inhibition observed in $NOP^{+/+}$ mice were due to NOP receptor blockade.

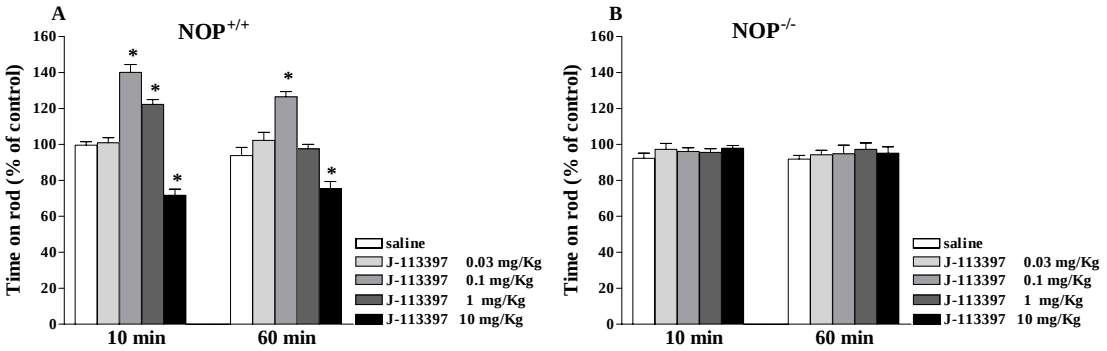

Figure 8. Selectivity of J-113397. Systemic administration of J-113397 (0.03-10 mg/Kg, i.p.) affected motor performance in the rotarod test in NOP$^{+/+}$ mice (**A**) but was ineffective in NOP$^{-/-}$ mice (**B**). The test was performed before (control session) and after (10 and 60 min) drug injection. Data are means ± SEM of 8-10 determinations per group and were calculated as percentage of the control session. *p<0.05 different from saline (RM ANOVA followed by contrast analysis and the sequentially rejective Bonferroni's test).

Low doses of UFP-101 (3 nmol) and N/OFQ (0.01 nmol) did not affect immobility time (Fig 9A) but facilitated stepping activity (Fig. 9B) and rotarod performance (Fig. 9C) in NOP$^{+/+}$ mice. Higher doses of UFP-101 (30 nmol) and N/OFQ (10 nmol) elevated immobility time and inhibited stepping and rotarod performance (Fig. 10A-C). These effects were detectable also at 60 min after treatment. No major difference was observed between C57BL/6J and NOP$^{+/+}$ mice in terms of sensitivity to N/OFQ or duration of the response. Conversely, UFP-101 and N/OFQ were not effective in NOP$^{-/-}$ mice at any of the doses tested, suggesting that the dual responses they evoked in NOP$^{+/+}$ mice relied on the interaction (blockade and stimulation, respectively) with NOP receptors.

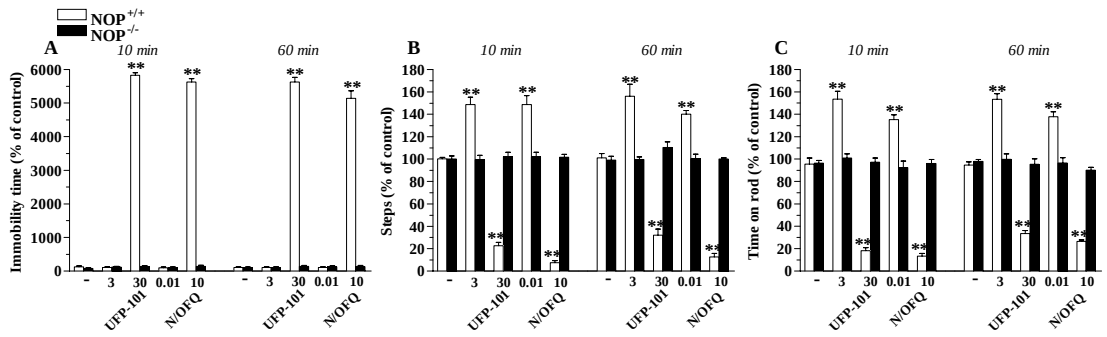

Figure 9. Selectivity of UFP-101 and N/OFQ. I.c.v. injections of motor facilitating and inhibiting doses of UFP-101 (3 and 30 nmol, respectively) and N/OFQ (0.01 and 10 nmol, respectively) affected motor performance in the bar (**A**), drag (**B**) and rotarod (**C**) test in NOP$^{+/+}$ mice, being ineffective in NOP$^{-/-}$ mice. All tests were performed before (control session) and 10 min and 60 min after drug injection. Data are means ± SEM of 6 determinations per group and were calculated as percentage of the control session.

**p<0.01 different from saline (RM ANOVA followed by contrast analysis and the sequentially rejective Bonferrroni's test).

DA receptor antagonists prevented motor inhibition induced by L-dopa and PPX

To strengthen the role of D_2 receptors in motor control, we first analyzed motor responses to the DA precursor, L-dopa (in combination with benserazide), and the D_3/D_2 agonist PPX. These compounds were tested alone or in combination with different classes of DA receptor antagonists.

L-dopa

L-dopa inhibited motor activity at the highest dose tested (100 mg/Kg), elevating immobility time (Fig. 10A) and reducing both stepping activity (Fig. 10B) and rotarod performance (Fig. 10C). Impaired rotarod performance was also detected at the lower 10 mg/Kg dose.

PPX

Similar to L-dopa, PPX evoked a marked increase in immobility time (Fig. 10D) and rotarod performance (Fig. 10F) at 0.1 and 1 mg/Kg. Stepping activity, however, was minimally and transiently reduced only at the highest PPX dose tested (1 mg/Kg; Fig. 10E). These effects were also observed at 60 min post-injections time.

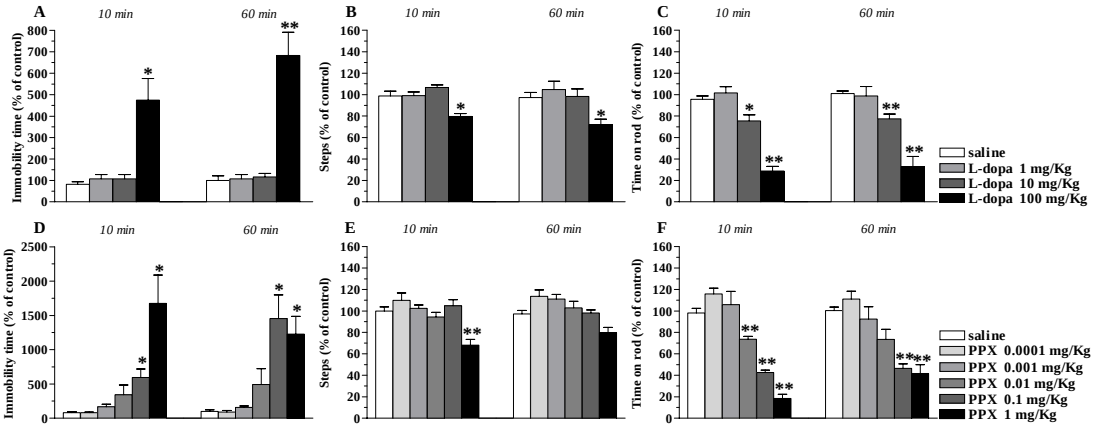

Figure 10. DA receptor agonists decreased motor activity in C57BL/6J mice. Systemic administration of L-dopa (1-100 mg/Kg plus benserazide 4:1 ratio, i.p.) and PPX (0.0001-1 mg/Kg, i.p.) affected motor performance in the bar (**A, D**), drag (**B, E**) and rotarod (**C, F**) test. All tests were performed before (control session) and after (10 and 60 min) drug administration. Data are means ± SEM of 6 determinations per group and were calculated as percentage of the control session. *p<0.05, **p<0.01

different from saline (RM ANOVA followed by contrast analysis and the sequentially rejective Bonferrroni's test).

Interaction between DA receptor antagonists and agonists

Since motor inhibition was the only effect detected following DA agonists, amisulpride and raclopride were used to demonstrate the involvement of D_2/D_3 receptors. Amisulpride consistently prevented motor inhibition induced by high doses of L-dopa (100 mg/Kg) in the bar, drag and rotarod tests (Fig. 11A-C). Conversely, it modulated the effects of PPX depending on the test and agonist dose used. Thus, amisulpride prevented the increase in immobility time induced by 0.1 mg/Kg PPX (Fig. 11A) but failed to attenuate the impairment in rotarod performance induced by the same dose (Fig. 11C). Amisulpride also did not affect motor inhibition induced by the higher PPX dose (1 mg/Kg) in the bar and drag tests (Fig. 11A-B) but slightly attenuated impairment in rotarod performance (Fig. 11C). On the other hand, raclopride did not prevent motor inhibition induced by PPX on the rotarod (Fig. 11F) and even worsened the inhibition of immobility time (Fig. 11D) and stepping activity (Fig. 11E) induced by PPX in the bar and drag tests, respectively.

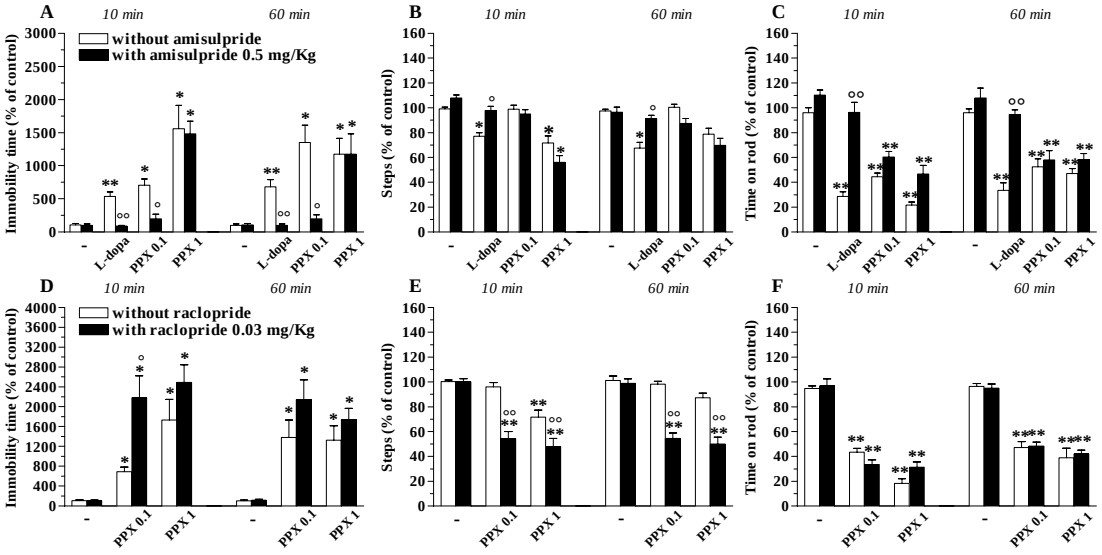

Figure 11. Motor inhibition induced by L-dopa in C57BL/6J mice was inhibited by the D_2/D_3 receptor selective antagonist amisulpride. Pretreatment (20 min in advance) with amisulpride (0.5 mg/Kg, i.p.) differentially affected motor inhibition induced by L-dopa (100 mg/Kg plus benserazide 25 mg/Kg, i.p.) and PPX (0.1 and 1 mg/Kg, i.p.) in the bar (**A**), drag (**B**) and rotarod (**C**) test. Amisulpiride prevented the inhibition induced by L-dopa but was ineffective against that induced by PPX (1 mg/Kg). Amisulpiride only prevented the inhibition induced by PPX 0.1 mg/Kg in the bar test (**A**). Pretreatment with raclopride (0.03 mg/Kg, i.p.) did not attenuate motor inhibition induced by L-dopa and PPX and even worsened it (**D-F**). All tests were performed before (control session) and after (10 and 60 min) L-dopa and PPX

administration. When DA receptor antagonists were tested alone, behavioral testing was performed 30 and 80 min after drug injection. Data are means ± SEM of 6 determinations per group and were calculated as percentage of the control session. *p<0.05, **p<0.01 different from saline; °p<0.05, °°p<0.01 different from the same group in the absence of amisulpride or raclopride (RM ANOVA followed by contrast analysis and the sequentially rejective Bonferrroni's test).

Since PPX is a potent D_3 receptor agonist, we investigated whether motor inhibition could be mediated by D_3 receptors (Fig. 12). Not only did S33084 not prevent motor inhibition induced by both doses of PPX in the three tests (Fig. 12A-C) but it even worsened impairment of stepping activity induced by PPX 1 mg/Kg in the drag test (Fig. 12B). Likewise, S33084 enhanced inhibition of stepping activity induced by 100 mg/Kg L-dopa (Fig. 12B) leaving unaffected its motor responses in the bar (Fig. 12A) and rotarod (Fig. 12C) tests. A combination of S33084, amisulpride and raclopride failed to attenuate PPX-induced inhibition (data not shown). We finally investigated whether peripheral D_2-like receptors could contribute to motor inhibition induced by PPX, e.g. by inducing hypotension. The peripheral non selective D_2 receptor antagonist domperidone (5 mg/Kg; Fig. 12D-F) did not affect motor activity alone and also failed to prevent the effect of 0.1 mg/Kg PPX.

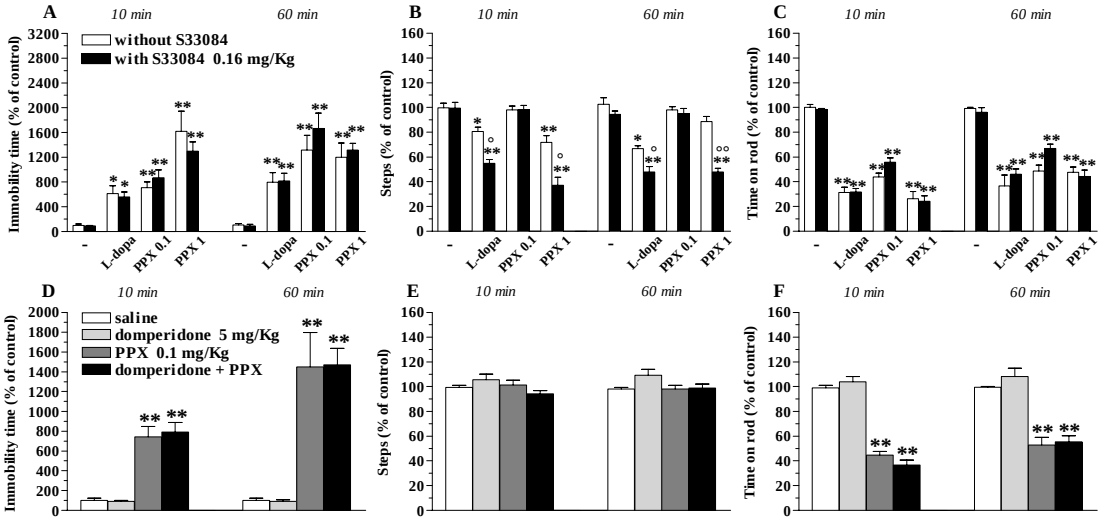

Figure 12. Motor inhibition induced by DA agonists in C57BL/6J mice was insensitive to the D_3 selective receptor antagonist S33084 or the peripheral non selective DA receptor antagonist domperidone. Pretreatment (20 min in advance) with S33084 (0.16 mg/Kg, i.p.) or domperidone (5 mg/Kg, i.p.) did not attenuate motor inhibition caused by L-dopa (100 mg/Kg plus benserazide 25 mg/Kg; i.p.) and PPX (0.1 and 1 mg/Kg) in the bar (**A, D**), drag (**B, E**) and rotarod (**C, F**) test. S33084 alone even increased the inhibition induced by both DA receptor agonists in the drag test (**B**). All tests were performed before (control session) and after (10 and 60 min) DA receptor agonist administration. When DA receptor antagonists were tested alone, behavioral testing was performed 30 and 80 min after drug injection. Data

are means ± SEM of 6 determinations per group and were calculated as percentage of the control session. *p<0.05, **p<0.01 different from saline; °p<0.05, °°p<0.01 different from the same group in the absence of S33084; #p<0.05 different from PPX 1 mg/Kg (RM ANOVA followed by contrast analysis and the sequentially rejective Bonferrroni's test).

L-dopa and PPX oppositely modulated [^{3}H]-DA release in striatal synaptosomes

Previous in vivo data suggest that motor inhibitory actions of L-dopa and PPX rely on an interaction with presynaptic D_2 autoreceptors. We therefore analyzed the effects of L-dopa (free-base) and PPX in a preparation of striatal synaptosomes preloaded with [^{3}H]-DA (Figs 13-14). This would also demonstrate whether L-dopa might have biological activity per se or if its effects are due to its conversion to DA. Basal synaptosomal [^{3}H]-DA efflux was 0.021 ± 0.001 pmol mg prot^{-1} min^{-1} (n=68) and corresponded to a fractional release of 6.79 ± 0.15 %. A 2 minute pulse of KCl 10 mM evoked a tritium overflow of 0.006 ± 0.001 pmol mg prot^{-1} min^{-1} (n=24) which was attenuated by ~70 % in the absence of Ca^{++} (Fig. 14). PPX (100 nM) decreases [^{3}H]-DA overflow (~51 %) and this effects was prevented by pre-treatment with amisulpride (100 nM), ineffective per se (Fig. 13A). Conversely, L-dopa (1 μM) doubled [^{3}H]-DA overflow (Fig. 13B). This effect was prevented by SCH23390 (100 nM) but not by the DA transporter blocker GBR12783 (300 nM; Fig 13B). Neither compound affected the K^+-evoked tritium overflow.

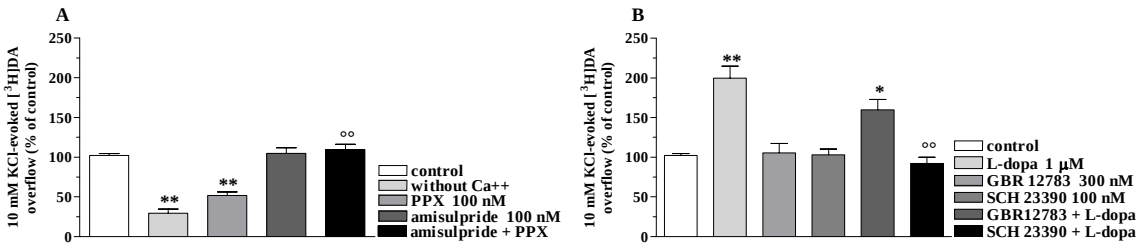

Figure 13. PPX and L-dopa oppositely modulated K^+-evoked DA release from synaptosomes. PPX (100 nM) inhibited (**A**) while L-dopa (1 μM) elevated (**B**) the [^{3}H]-DA overflow evoked by a 2 min pulse of 10 mM KCl from a preparation of striatal synaptosomes in superfusion. The inhibition induced by PPX was prevented by the D_2-like receptor antagonist amisulpride (**A**) while the stimulation induced by L-dopa was prevented by the D_1-like receptor antagonist SCH23390 (**B**). PPX and L-dopa were administered 6 min KCl whereas antagonists 3 min before agonists. Data are means ± SEM of 6 determinations per group and were expressed as percentage of control (i.e. the K^+-evoked tritium overflow). *p<0.05, **p<0.01 different from control (ANOVA followed by the Newman-Keuls test).

L-dopa (1-100 μM) also increased in a dose-dependent manner tritium efflux (Fig. 14A). GBR12783 (300 nM) prevented the response to 10 μM L-dopa (Fig. 14B) and attenuated that of 100 μM L-dopa (Fig. 14C), while SCH23390 (1 μM) was ineffective. GBR12783 and SCH23390 did not affect spontaneous tritium efflux at the doses tested.

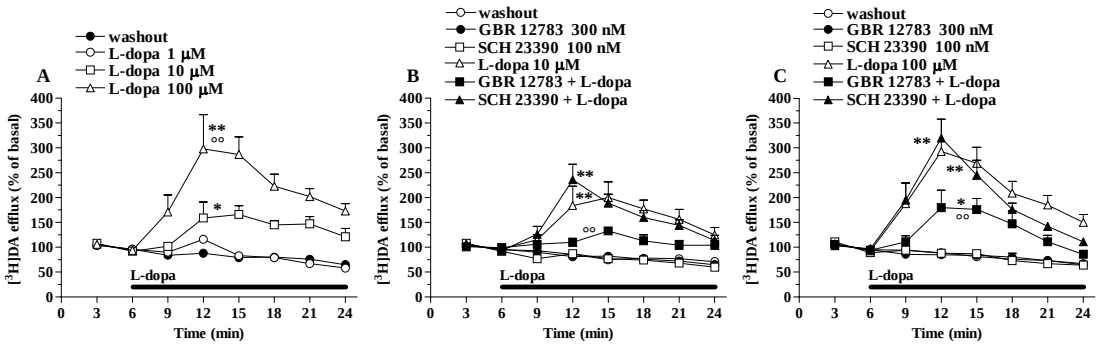

Figure 14. L-dopa increased spontaneous tritium efflux from synaptosomes. L-dopa (1-100 μM) elevated spontaneous tritium efflux from a preparation of striatal synaptosomes in superfusion pre-loaded with [^{3}H]-DA (**A**). The DA transporter blocker GBR12783 but not the D_1-like selective antagonist SCH23390 prevented the elevation induced by L-dopa (10 μM; **B**) and attenuated that induced by L-dopa (100 μM; **C**). GBR12783 and SCH23390 were given 3 min before L-dopa and maintained until the end of experiments. Data are means ± SEM of 6 determinations per group and were expressed as percentage of basal tritium efflux (calculated as the mean between the two samples before L-dopa). *p<0.05, **p<0.01 different from washout; °°p<0.01 different from L-dopa alone (ANOVA followed by the Newman-Keuls test performed on AUC values).

Part II. NOP receptor antagonists attenuate parkinsonism in MPTP-treated mice

Characterisation of the experimental model

In C57BL/6J mice, MPTP administration induced a variety of acute behavioral changes observed unsystematically, such as muscular hypotonia, piloerection, elevated bowed stiff tail (i.e. Straub tail), increased respiration (i.e. hyperpnea). These phenomena appeared immediately after the first injection and vanished within 16 hours. About 30% of MPTP-treated mice died within 24 hr after toxin administration. Body weight of surviving MPTP-treated mice did not change with respect to vehicle-injected mice over time (data not shown).

MPTP induced loss of TH staining in the striatum

Seven days after treatment, MPTP-treated mice displayed partial (~60%) bilateral loss of TH-immunoreactive DA terminals compared to vehicle-injected mice (Fig. 15A-C).

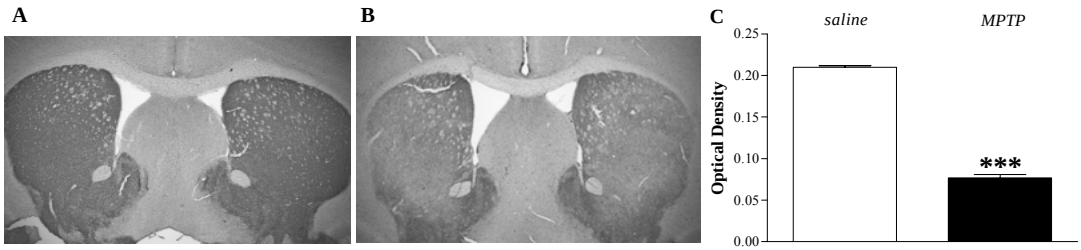

Figure 15. MPTP-treatment reduced the TH-immunoreactive fibre density in the C57BL/6J mouse striatum. Photomicrographs of TH-immunoreactive fibres in the striatum of a saline (**A**) and MPTP-treated (**B**) mouse. **C,** Optical density of TH-immunoreactive fibres in the striatum. Data are means ± SEM of 10 determinations per group. ***p<0.001 different from saline (Student's t-test).

MPTP treatment caused akinesia and bradykinesia

MPTP increased the immobility time. The effect was maximal at D1 after injection and subsided from D4 onward (Fig. 16A). At 6 days after MPTP, mice were still akinetic. MPTP caused a marked loss of reactivity (Fig. 16B), that was substantially unchanged from D1 through D6, and a decrease in stepping activity(Fig. 16C), that was maximal at D1 and D2 (~60%) and still detectable, albeit attenuated (~15%), at D6. MPTP caused a marked impairment of climbing speed (Fig. 16D) at D1 (~70%) which tended to revert back over time (~40% at D6), and a maximal reduction of pulling force (Fig. 16E) in the D1-D4 range. After 6 days, however, the pulling force was normalized. Finally, MPTP caused a maximal ~65% impairment of the rotarod performance (Fig. 16F) at D1. In the following days, attenuation of motor impairment settled to ~30%.

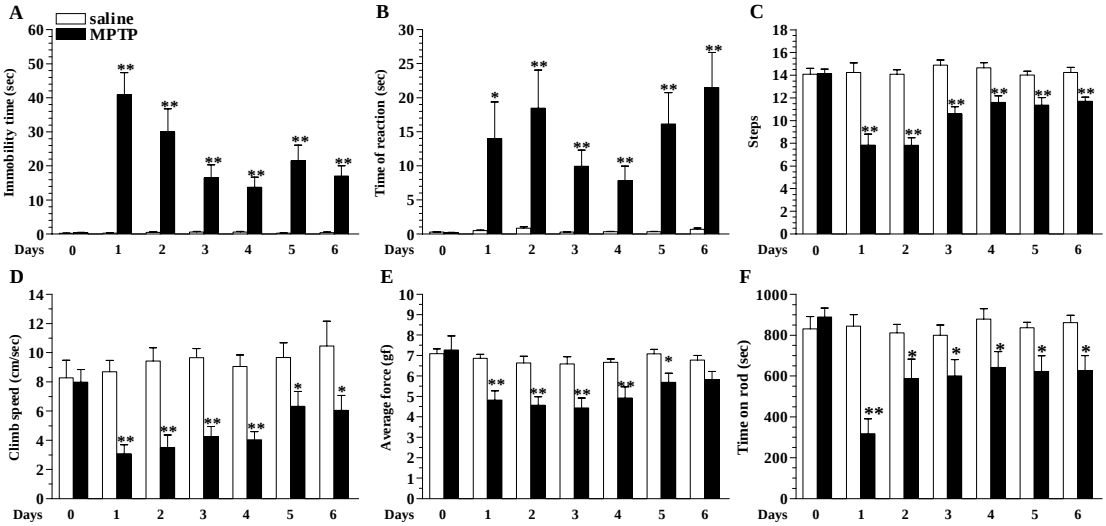

Figure 16. MPTP-treatment induced akinesia and bradykinesia in C57BL/6J mice. Systemic administration of MPTP (4x20 mg/Kg) increased the immobility time (bar test; in sec, A) and reaction time (reaction time test; in sec; B) and decreased the number of steps (drag test; **C**), the climbing speed (stair climbing test; cm/sec; **D**), the pulling force (grip test; gram force; **E**) and the time spent on the rod (in sec, rotarod test; **F**). All tests were performed before and after (daily for 6 days) MPTP-treatment. Data are means ± SEM of 10 determinations per group. *p<0.05, **p<0.01 different from saline (RM ANOVA followed by contrast analysis and the sequentially rejective Bonferroni's test).

MPTP treatment caused abnormalities in gait and posture

MPTP caused a slight reduction (~16%) of hindpaw stride length (Fig. 17A). A parallel impairment was detectable by measuring forepaw stride length (data not shown). MPTP caused a long lasting increase (~20%) of hindpaw stride width (Fig. 17B) and caused a mismatch in the overlap of the ipsilateral paw that showed a tendency to recover over time (Fig. 17C). Moreover, MPTP caused a stable increase in the angle amplitude between hindpaws and the main direction (Fig. 17D). Finally, MPTP caused an marked decrease of running speed (Fig. 17E), which was almost halved with respect to saline-treated animals.

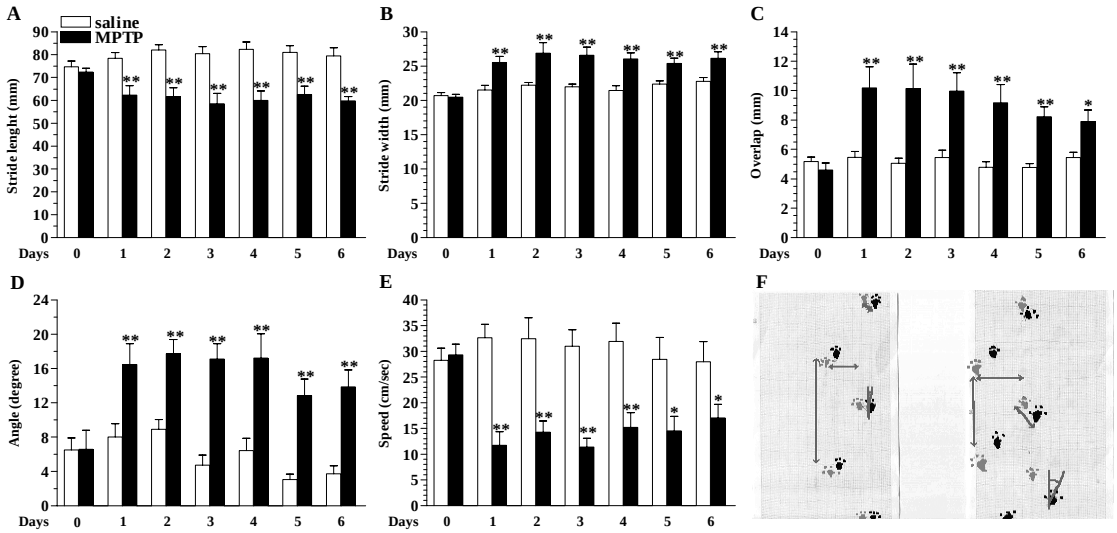

Figure 17. MPTP-treatment induced abnormalities of gait and posture in C57BL/6J mice. Systemic administration of MPTP reduced the stride length of hindlimbs (in mm; **A**), increased the stride width of hindlimbs (in mm; **B**), the distance of matching (in mm; **C**) and the angle of hindpaws (in degrees; **D**), and reduced the run speed (in cm/sec; **E**). **F.** Complete set of parameters in footprints of a saline (left) and MPTP-treated mouse (right). All tests were performed before and after (daily for 6 days) MPTP-treatment. Data are means ± SEM of 10 determinations per group. *p<0.05, **p<0.01 different from saline (RM ANOVA followed by contrast analysis and the sequentially rejective Bonferroni's test).

Responsiveness to classical antiparkinsonian compounds

To investigate whether the MPTP-induced phenotype was generated by DA deficiency, the ability of DA receptor agonists (i.e. L-dopa and PPX) to attenuate motor deficit was investigated. Animals were challenged in the bar, drag and rotarod test, performed 7 days after MPTP intoxication, when mice displayed increased immobility time (Fig 18A), reduced number of steps (Fig 18B) and impaired rotarod performance (Fig. 18C) compared to pre-treatment values.

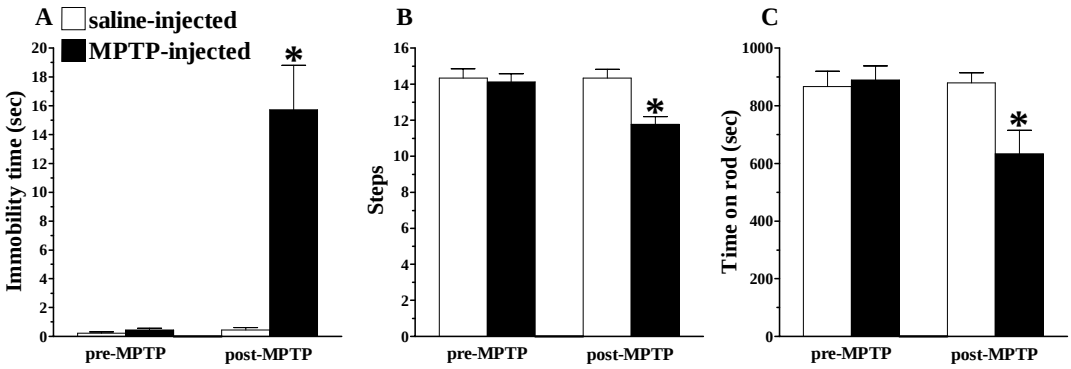

Figure 18. Motor impairment in C57BL/6J mice at 7 days after MPTP treatment. Systemic administation of MPTP (4x20 mg/Kg, i.p.) affected motor performance in the bar (in sec; **A**), drag (**B**) and rotarod test (in sec; **C**). All tests were performed before (pre-MPTP, control session) and 7 days after (post-MPTP) MPTP. Data are means ± SEM of 10 determinations per group. *p<0.05, different from saline (ANOVA followed by the Newman-Keuls test).

L-dopa

L-dopa caused dual and prolonged changes of immobility time (Fig. 19A), namely a reduction at 10 mg/Kg and an increase at 100 mg/Kg. L-dopa elevated the number of steps (Fig. 19B) at 1 and 10 mg/Kg, being ineffective at higher doses. The effect of 1 mg/Kg was transient whereas that produced by 10 mg/Kg was detected also 60 min after injection. Finally, L-dopa increased rotarod performance (Fig. 19C) at 10 mg/Kg and reduced it at 100 mg/Kg. These effects were long lasting. Since L-dopa was administered in combination with benserazide (ratio 4:1), benserazide alone was tested at the highest does (25 mg/Kg). Benserazide did not affect motor performance with respect to saline (data not shown).

PPX

PPX 0.01 and 0.1 mg/Kg increased the immobility time (Fig. 19D), although the effect of the lower dose appeared only 60 min after injection. Lower PPX doses were ineffective. PPX elevated the number of steps (Fig. 19E) in the 0.0001-0.01 mg/Kg dose range but was ineffective at higher doses (0.1 mg/Kg). Only the facilitation induced by 0.001 mg/Kg was long lasting. Finally, PPX failed to modulate rotarod performance up to 0.001 mg/Kg while impairing it at 0.01 and 0.1 mg/Kg (Fig. 19F).

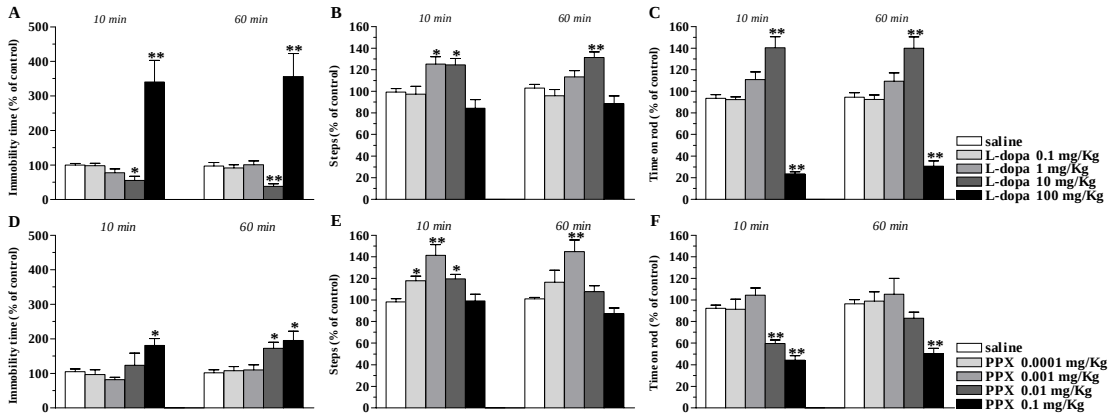

Figure 19. DA receptor agonists attenuated parkinsonian symptoms in MPTP-treated C57BL/6J mice. Systemic administration of L-Dopa (0.1-100 mg/Kg, i.p.) or PPX (0.0001-0.1 mg/Kg, i.p.) affected motor performance in the bar (**A,D**), drag (**B,E**) and rotarod test (**C,F**). All tests were performed at 7 days after MPTP administration, before (control session) and after (10 and 60 min) drug injection. Data are means ± SEM of 7-8 determinations per group and were calculated as percentage of the control session. *p<0.05, **p<0.01 different from saline (RM ANOVA followed by contrast analysis and the sequentially rejective Bonferroni's test).

Responsiveness to NOP receptors antagonists

Seven days after MPTP treatment, NOP receptor antagonists J-113397 and Trap-101 were also tested since these compounds were found effective in promoting movement in rats treated with 6-OHDA (Marti et al., 2005, 2007, 2008).

J-113397

J-113397 (0.01-0.03 mg/Kg) reduced the immobility time (Fig. 20A) the number of steps (Fig 20B) and the rotarod performance (Fig. 20C). However, higher doses of J-113397 exerted opposite effects. In fact, J-113397 (1 mg/Kg) increased the immobility time and reduced rotarod performance, being ineffective in the drag test.

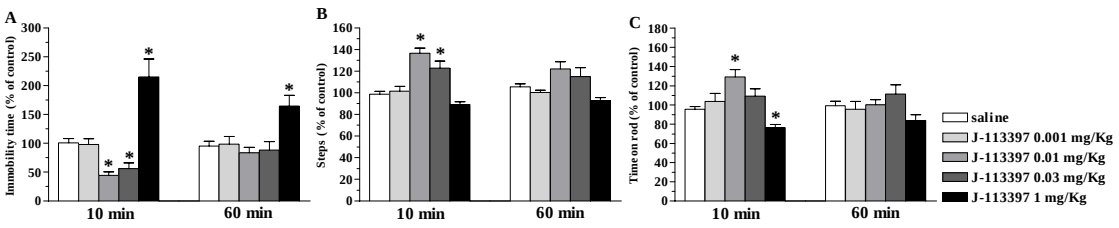

Figure 20. J-113397 attenuated parkinsonian symptoms in MPTP-treated C57BL/6J mice. Systemic administration of J-113397 (0.01-1 mg/Kg, i.p.) affected motor performance in the bar (**A**), drag (**B**) and

rotarod test (**C**). All tests were performed at 7 days after MPTP administration, before (control session) and after (10 and 60 min) drug injection. Data are means ± SEM of 8-10 determinations per group and were calculated as percentage of the control session. *p<0.05 different from saline (RM ANOVA followed by contrast analysis and the sequentially rejective Bonferroni's test).

Trap-101

Trap-101 caused a transient reduction of immobility time (Fig. 21A) at 0.01 and 0.1 mg/Kg but was ineffective at 1 mg/Kg. Moreover, Trap-101 elevated the number of steps (Fig. 21B) in the 0.001-0.1 mg/Kg dose range, being ineffective at 1 mg/Kg. Only the facilitation induced by Trap-101 0.1 mg/Kg was detected at 60 min after injection. Trap-101 failed to modulate the rotarod performance up to 0.1 mg/Kg and transiently reduced it at 1 mg/Kg (Fig. 21C).

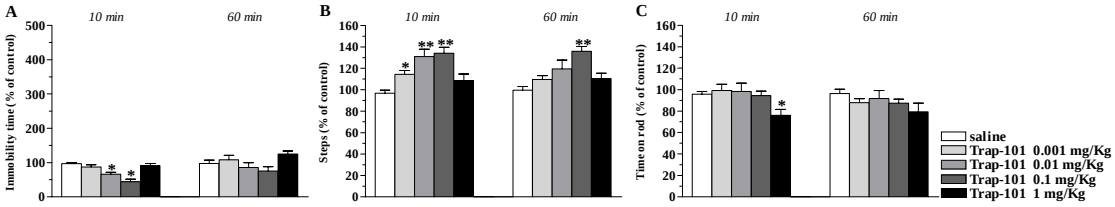

Figure 21. Trap-101 attenuated parkinsonian symptoms in MPTP-treated C57BL/6J mice. Systemic administration of Trap-101 (0.001-1 mg/Kg, i.p.) affected motor performance in the bar (**A**), drag (**B**) and rotarod test (**C**). All tests were performed at 7 days after MPTP administration, before (control session) and after (10 and 60 min) drug injection. Data are means ± SEM of 7-8 determinations per group and were calculated as percentage of the control session. *p<0.05, **p<0.01 different from saline (RM ANOVA followed by contrast analysis and the sequentially rejective Bonferroni's test).

Interaction between DA receptor agonists and NOP receptor antagonists

We previously demonstrated (Marti et al., 2007, 2008) that co-administration of L-dopa and J-113397 or Trap-101 produced additive attenuation of parkinsonism in 6-OHDA hemilesioned rats. Therefore, we first tested whether subthreshold doses (at least in two of three tests) of L-dopa (1 mg/Kg) and Trap-101 (0.001 mg/Kg) could synergize in attenuating parkinsonism in MPTP-treated mice. We then tested whether subthreshold doses of PPX (0.0001 mg/Kg) could produce additive effects with Trap-101 (0.001 mg/Kg).

L-dopa and Trap-101

L-dopa and Trap-101 alone were ineffective whereas their combination reduced the immobility time (Fig. 22A). This effect was observed only at 10 min after injection. L-dopa and Trap-101 slightly increased the number of steps in the drag test (Fig. 22B) and their combination produced an additive effect. The combination effect was even more evident at 60 min, since both compounds were ineffective alone. No change in rotarod performance (Fig. 22C) was observed after administration of subthreshold doses of L-dopa and Trap-101, either alone or in combination.

PPX and Trap-101

No change in immobility time (Fig. 22D) or in rotarod performance (Fig. 22F) was observed after administration of subthreshold doses of PPX and Trap-101, either alone or in combination. Conversly, PPX and Trap-101 transiently elevated number of steps (Fig. 22E) while their combination produced a greater (additive) and sustained improvement.

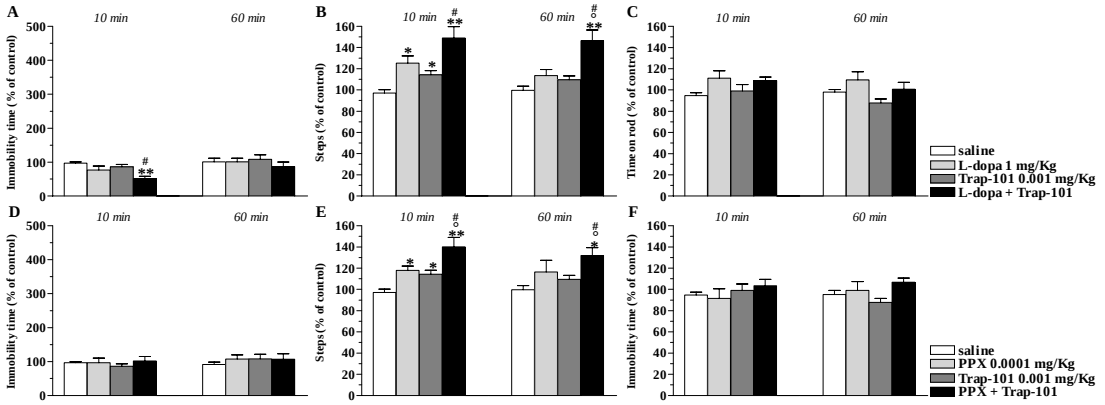

Figure 22. Combination of L-dopa and PPX with Trap-101 synergistically or additively attenuated parkinsonian symptoms in MPTP-treated C57BL/6J mice. Combined administration of L-dopa (1 mg/Kg, i.p.) and Trap-101 (0.001 mg/Kg, i.p.) affected motor performance in the bar (**A**) and drag (**B**) test but not in the rotarod test (**C**). Combined administration of PPX (0.0001 mg/Kg, i.p.) and Trap-101 (0.001 mg/Kg, i.p.) affected motor activity only in the drag test (**E**), but not in the bar (**D**) and rotarod (**F**) test. All tests were performed at 7 days after MPTP administration, before (control session) and after (10 and 60 min) drug injection. Data are means ± SEM of 7-8 determinations per group and were calculated as percentage of the control session. *$p<0.05$, **$p<0.01$ different from saline; °$p<0.05$ different from L-dopa; $^{\#}p<0.05$ different from Trap-101 (RM ANOVA followed by contrast analysis and the sequentially rejective Bonferroni's test).

D_2 receptor blockade prevented paradoxical inhibition induced by DA receptor agonists and NOP receptor antagonists

PPX is known to depress motor activity (Mierau and Schingnitz, 1992; Maj et al., 1998; Siuciak and Fujiwara, 2004), likely via stimulation of presynaptic D_{2S} (short isoform) autoreceptors (Usiello et al., 2000; Vallone et al., 2000). We therefore tested the hypothesis that motor inhibition induced by L-dopa and PPX could be reversed by the D_2/D_3 receptor antagonist amisulpride. Indeed, this antagonist preferentially bind to D_2 autoreceptors at low doses (Scatton et al., 1997; Perrault et al., 1997; Schoemaker et al., 1997). To investigate the DA-dependence of the motor inhibitory produced by NOP receptor blockade, we used J-113397. Differently from Trap-101, J-113397 caused marked motor inhibition also in the bar test (Viaro et al., 2008). The effect of amisulpride alone was first assessed in a dose-finding study.

Amisulpride

Amisulpride caused a prolonged increase of immobility time (Fig. 23A) and a prolonged reduction in stepping activity (Fig. 23B) at the highest dose tested (5 mg/Kg). Moreover, amisulpride caused sustained motor impairment on the rotarod at 0.5 and 5 mg/Kg (Fig. 23C), which could be detected also at 60 min after injection.

Interaction between amisulpride and DA receptor agonists and NOP receptor antagonists

Based on these preliminary findings we selected an ineffective dose of amisulpride (0.1 mg/Kg) and challenged it with motor inhibiting doses of L-Dopa (100 mg/Kg), PPX (0.1 mg/Kg) or J-113397 (1 mg/Kg). Motor inhibition caused by L-dopa (100 mg/Kg) and J-113397 (1 mg/Kg) in the bar test (Fig. 23D) was reversed into facilitation in the presence of amisulpride. Conversely, amisulpride did not prevent the effect of PPX. In the drag test (Fig. 23E), L-Dopa and PPX were ineffective either alone or in combination with amisulpride. However, J-113397, ineffective alone, caused a prolonged increase in stepping activity in the presence of amisulpride. Finally, motor impairment on rotarod (Fig. 23F) caused by L-dopa and J-113397 was prevented by amisulpride. However, amisulpride failed to attenuate the effect of PPX.

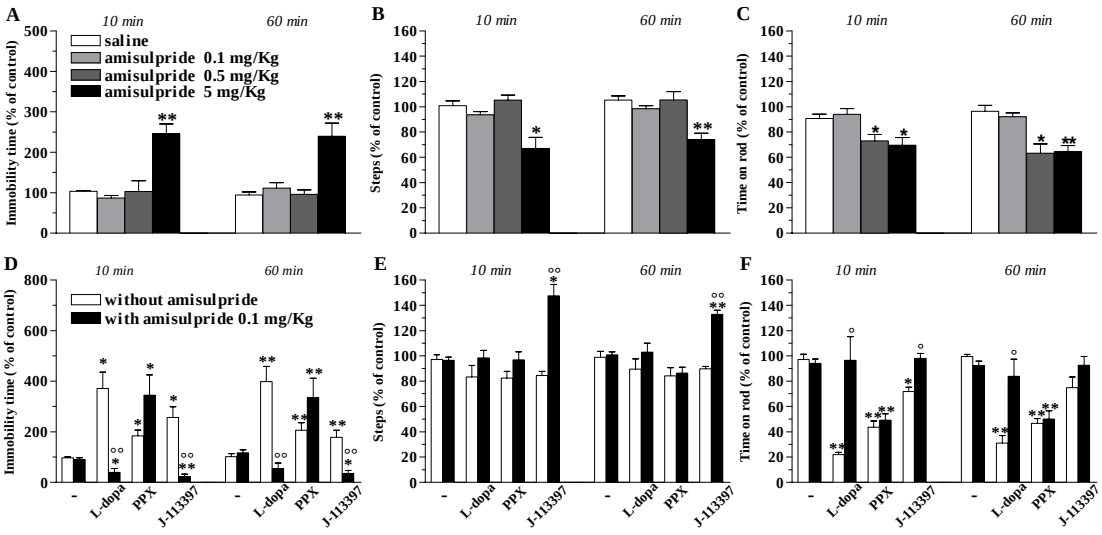

Figure 23. The D_2/D_3 receptor selective antagonist amisulpride prevented motor inhibition induced by high doses of L-dopa and J-113397 but not PPX in MPTP-treated C57BL/6J mice. Systemic administration of amisulpride alone (0.1-5 mg/Kg, i.p.) inhibited motor performance in the bar (**A**), drag (**B**) and rotarod (**C)** test. Twenty min pretreatment with amisulpride (0.5 mg/Kg, i.p.) differentially affected motor inhibition induced by L-dopa (100 mg/Kg, i.p.) and J-113397 (1 mg/Kg, i.p.) in the bar (**D**), drag (**E**) and rotarod test (**F**) but was ineffective against hypomotility induced by PPX (0.1 mg/Kg; i.p.). All tests were performed at 7 days after MPTP administration, before (control session) and after (10 and 60 min) L-dopa, PPX and J-113397 injection. When amisulpride were tested alone, behavioral testing was performed 30 and 80 min after injection. Data are means ± SEM of 6 determinations per group and were calculated as percentage of the control session. *p<0.05, **p<0.01 different from saline; °p<0.05, °°p<0.01 different from amisulpride alone (RM ANOVA followed by contrast analysis and the sequentially rejective Bonferroni's test).

Interaction between domperidone and PPX

We finally tested whether the PPX-induced hypolocomotion had a peripheral origin. The peripheral DA receptor antagonist domperidone (5 mg/Kg) alone failed to affect the immobility time (Fig. 24A), number of steps (Fig. 24B) or rotarod performance (Fig. 24C) and was not able to counteract the inhibitory effect of PPX.

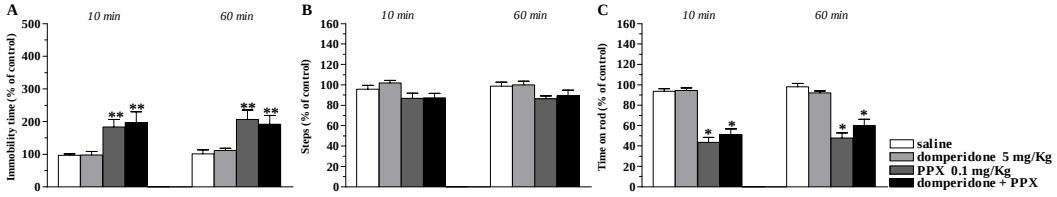

Figure 24. Motor inhibition induced by PPX was insensitive to peripheral DA antagonist domperidone in MPTP-treated mice. Twenty min pretreatment with domperidone (5 mg/Kg, i.p.) did not attenuate motor inhibition caused by PPX (0.1 mg/Kg, i.p.) in the bar (**A**), drag (**B**) and rotarod (**C**) test. All tests were

performed at 7 days after MPTP administration, before (control session) and after (10 and 60 min) PPX injection. When domperidone was tested alone, behavioral testing was performed 30 and 80 min after injection. Data are means ± SEM of 6 determinations per group and were calculated as percentage of the control session. *p<0.05, **p<0.01 different from saline (RM ANOVA followed by contrast analysis and the sequentially rejective Bonferroni's test).

Part III. NOP receptor antagonists attenuate MPTP-induced parkinsonism in nonhuman primates

J-113397 in naïve macaques

Similarly to previous experiments in mice, we first tested the efficacy of J-113397 in untreated (naïve) macaques, for an evaluation of the effective dose range. J-11397 did not affect motor performance in naïve macaques at 0.1 and 1 mg/kg (Fig. 25). At a higher dose (3 mg/kg) J-113397 induced a faster performance in the straight rod test in two of the animals (Fig. 25A), although the other two did not perform the test. Therefore we tested these animals on a simpler task (i.e. the platform task) but at this dose animals were inattentive and performance was slightly slower than normal (Fig 25B).

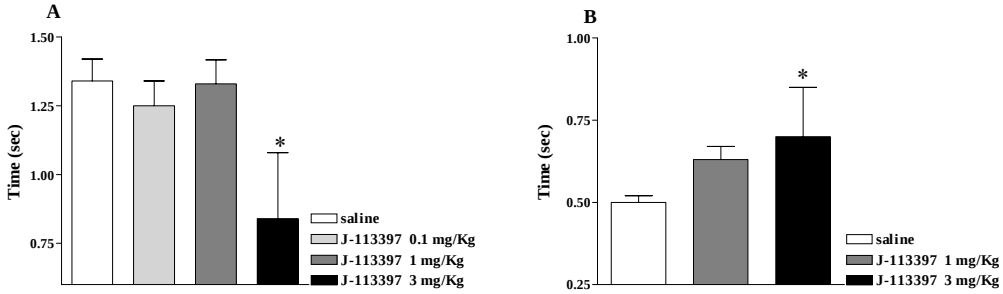

Figure 25. J-113397 modulated motor activity in nonhuman primates. Systemic administration of J-113397 (0.1-3 mg/Kg, i.m.) affected motor performance in the MAP test. Average time to retrieve a treat in the straight rod test (in sec; **A**) was significantly improved in 2 animals at the higher dose tested, but at this dose the other 2 animals showed side effects (distractibility, scratching and "wet dog" shakes) and failed to perform. These 2 animals were subsequently tested in the platform task of the MAP test (in sec; **B**) in which they performed significantly worse at the higher dose. *p<0.05 different from saline (ANOVA followed by PLSD test).

J-113397 in MPTP-treated macaques

After the study in naïve macaques, we tested the effectiveness of J-113397 in MPTP-treated-macaques. L-dopa was used as a positive control. Pharmacological tests were performed in nonhuman primates at least 3 months after the last MPTP dose (Tab. 1).

Animal	Weight (Kg)	PRS score after MPTP	PRS score 3 months after MPTP	Activity d/n (% from baseline)
Mf23	4.4	17	18.3	-76/-60
Mf25	5.4	19	21.5	-77/-62
Mf30	6.1	21	20.0	-68/-32
Mf34	5.3	18	18.5	-5/-60

Table 1. Individual characteristics of MPTP-lesioned primates.

We first examined the response to four doses of J-113397 (0.01, 0.03, 0.1 and 1 mg/kg) in two stable parkinsonian animals (data not shown). From 0.03 to 1 mg/kg we did not observe any beneficial effect on either parkinsonian score or MAP platform performance; at 1 mg/kg both animals displayed long episodes of akinesia (freezing) similar to the effect of high doses of J-113397 observed in 6-OHDA rats (30 mg/Kg, Morari and Marti, unpublished observation) and did not perform the reaching test. No major side effects were observed at 0.03 mg/kg but one animal did not test and the other did not show any improvement in the reaching task. With the lower dose (0.01 mg/kg) both animals showed an improvement in the MAP platform reaching task and therefore we selected this dose for the rest of the experiments. Both J-113397 (0.01 mg/kg) and L-dopa (30 mg/kg) induced a significant benefit in parkinsonian scores in the 4 animals (Fig 26A). The overall improvement after J-113397 administration (19±3%) was more moderate than that achieved with L-dopa (46±3%). Although as a group, the difference between L-dopa and J-113397 improvement in global PRS score did not reach significance, only in one animal (Mf25) was the response to both drugs not significantly different (Fig 26A). There was no significant effect of the baseline PRS score (i.e. severity of the parkinsonian signs) on the response to either drug. We further analyzed the therapeutic effect on parkinsonian symptoms (Fig 26B). The largest improvement induced by J-113397 (~30%) was observed on hypokinesia and the L-dopa effect on this particular symptom was not significantly different from J-113397. Other symptoms (rigidity, tremor and bradykinesia) improved significantly more with L-dopa (Fig 26B).

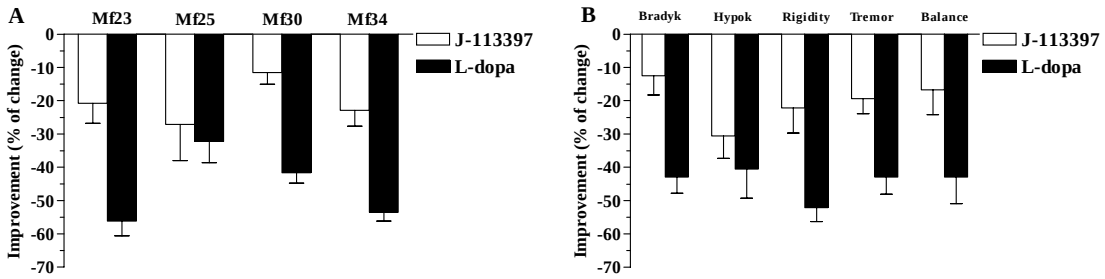

Figure 26. J-113397 attenuated parkinsonian symptoms in MPTP-treated primates. Systemic administration of J-113397 (0.01 mg/kg, i.p.) and L-dopa (30 mg/kg, i.p.) affected the global PRS score. The average improvement over the baseline score (n= 2-3 pharmacological tests for each compound) is shown for each animal (**A**). The improvement after J-113397 administration was more moderate than that achieved with L-dopa (Fisher PLSD). Comparative analysis of the pharmacological effects of L-dopa and J-113397 on parkinsonian symptoms (**B**) showed that all symptoms improved more with L-dopa except for hypokinesia. All tests were performed at least 3 months after the last MPTP dose.

Finally, we evaluated the performance of the parkinsonian animals in the MAP test (Fig 27). MPTP induced a significant increase in the time needed to complete the platform task in 3 out of 4 animals (Mf23, Mf25 and Mf30). These animals showed a significant improvement in the time to retrieve treats from the platform with L-dopa and one of them had also a significant improvement in performance after J-113397.

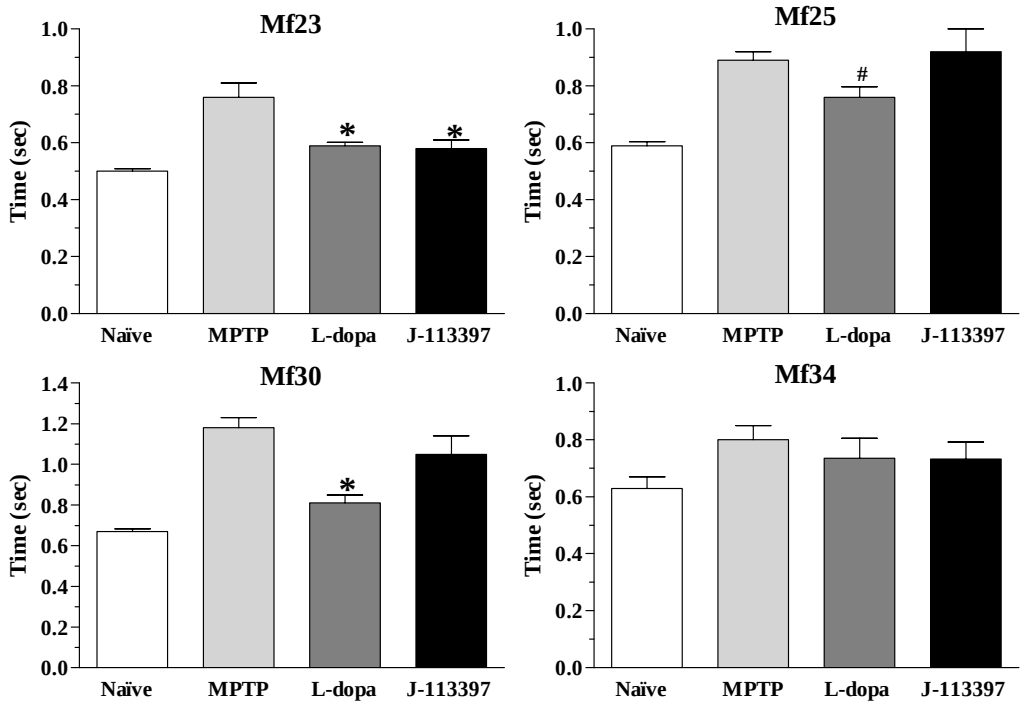

Figure 27. J-113397 attenuated parkinsonian symptoms in MPTP-treated primates. Systemic administration of J-113397 (0.01 mg/kg, i.p.) affected motor performance on the MAP test. MPTP induced a significant increase in the time needed to complete the platform task (animals were unable to

perform the straight rod task) in 3 out of 4 animals (Mf23, Mf25 and Mf30). In these animals, L-dopa improvement on task performance was significant. Only one of them (Mf23) showed a significant improvement in response to J-113397. All tests were performed at least 3 months after the last MPTP dose. *p<0.05, different from post-MPTP performance; #p<0.05, different from J-113397 (ANOVA followed by PLSD test).

Part IV. Deletion of the NOP receptor confers resistance to MPTP-induced toxicity

NOP$^{-/-}$ mice are partially resistant to MPTP-induced motor deficits

MPTP treatment caused greater fatalities in NOP$^{+/+}$ (58%) than NOP$^{-/-}$ mice (11%) at 24 hr after administration. Body weight of MPTP-treated mice did not change over time with respect to vehicle-injected mice. Treatment with saline did not change motor performance in both NOP$^{-/-}$ and NOP$^{+/+}$ mice.

Physiological motor activity in NOP$^{+/+}$ and NOP$^{-/-}$ mice

NOP$^{-/-}$ mice exhibited a different basal motor activity with respect to NOP$^{+/+}$ mice (Tab. 2). In particular, NOP$^{-/-}$ mice displayed greater number of steps, speed run, time on rod and horizontal locomotion, showing less fine movements. NOP$^{-/-}$ mice also displayed a faster preparation and iniziation time of movement and execution speed. Finally, NOP$^{-/-}$ displayed a greater average force than NOP$^{+/+}$ mice.

		NOP$^{+/+}$	**NOP$^{-/-}$**
Exercise-driven activity	Immobility time (sec)	0.3±0.1	0.1±0.1
	Number of steps	10.8±0.2	13.2±0.7 **
	Run speed (cm/sec)	48.4±2.4	63.7±4.5 **
	Time on rod (sec)	1517.8±54.6	1926.6±50.6 ***
Spontaneous activity	Movement time (sec)	119.0±1.0	119.7±0.3
	Horizontal locomotion time (sec)	48.9±2.5	111.9±6.6 ***
	Fine movements time (sec)	71.1.1±2.5	8.1±6.6 ***
	Freezing time (sec)	0.8±0.8	0.3±0.3
Step parameters	Preparation time (sec)	0.056±0.002	0.041±0.001 ***
	Initiation time (sec)	0.266±0.032	0.121±0.006 ***
	Air time (sec)	0.920±0.068	0.981±0.068
	Execution speed (cm/sec)	0.478±0.030	0.579±0.019 *
	Step length (cm)	6.720±0.169	6.259±0.177
Muscle strength	Maximal force (gf/cm)	123.0±10.1	130.2±5.5
	Average force (gf/cm)	20.2±1.5	28.2±1.5 **

Table 2. NOP$^{-/-}$ mice perform better than NOP$^{+/+}$ mice. Basal motor activity was measured by analyzing spontaneous or exercise-driven motor activity, step parameters and muscle strength. Data are means ±

SEM of 10 determinations per group. *p<0.05, **p<0.01, ***p<0.001 different from $NOP^{+/+}$ mice (Student's t-test).

Exercise-driven activity in MPTP-treated $NOP^{+/+}$ and $NOP^{-/-}$ mice

MPTP increased immobiliy time in both genotypes (Fig. 28A). However, $NOP^{-/-}$ mice displayed a lower impairment with respect to $NOP^{+/+}$ mice, which was significant from D3 onward (D6: 6.4±1.4 vs 13.1±2.8 sec). MPTP reduced the number of steps (Fig. 28B) in both genotypes at D1 and D2, although the effect was milder in $NOP^{-/-}$ mice. In the following days, motor impairment was significant only in $NOP^{+/+}$ mice, Likewise, MPTP reduced the speed of run (Fig. 28C) in both genotypes from D1 through D3. However, while speed impairment was long lasting in $NOP^{+/+}$ mice, $NOP^{-/-}$ mice were normal from D4 (D6: 95.6±7.5% vs 62.9±7.1%). Finally, MPTP decreased the rotarod performance (Fig. 28D) in both genotypes. Nevertheless, $NOP^{-/-}$ mice showed lesser impairment than $NOP^{+/+}$ mice (95.6±7.5% vs 62.9±7.1%) at D1.

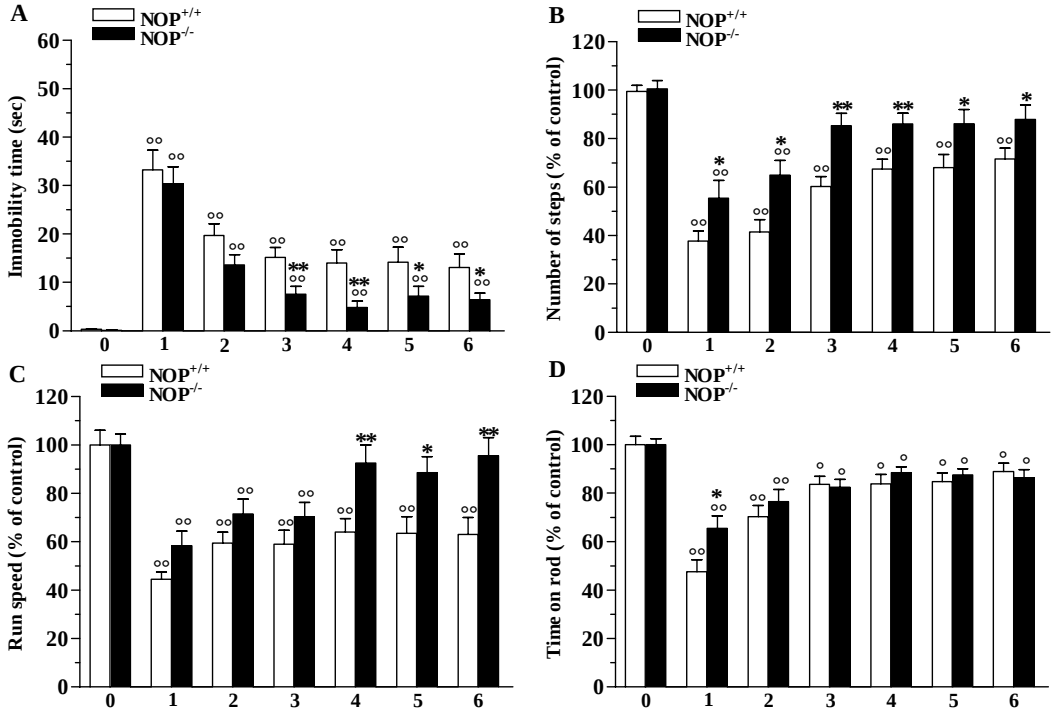

Figure 28. $NOP^{-/-}$ mice are more resistant than $NOP^{+/+}$ mice to MPTP-induced hypokinesia. Systemic administration of MPTP (4x20 mg/Kg, i.p.) affected exercise-driven activity in the bar (**A**), drag (**B**), speed (**C**) and rotarod test (**D**). All tests were performed before (control session) and after (daily for 6 days) MPTP-treatment. Data are means ± SEM of 10 determinations per group and were calculated as percentage of the control session. *p<0.05, **p<0.01 different from $NOP^{+/+}$ mice; °p<0.05, °°p<0.01 different from pre-MPTP values (day 0) (RM ANOVA followed by contrast analysis and the sequentially rejective Bonferrroni's test).

Spontaneous activity in MPTP-treated NOP$^{+/+}$ and NOP$^{-/-}$ mice

MPTP reduced global movements (Fig. 29A) in both genotypes at 6 days after treatment. This reduction was greater in NOP$^{+/+}$ than NOP$^{-/-}$ mice. MPTP also reduced horizontal movements to a greater extent in NOP$^{+/+}$ mice (Fig. 29B) . This reduction was inversely correlated to an increase in fine movements. Hypolocomotion was also related to an increase in freezing episodes that were more frequent in NOP$^{+/+}$ mice.

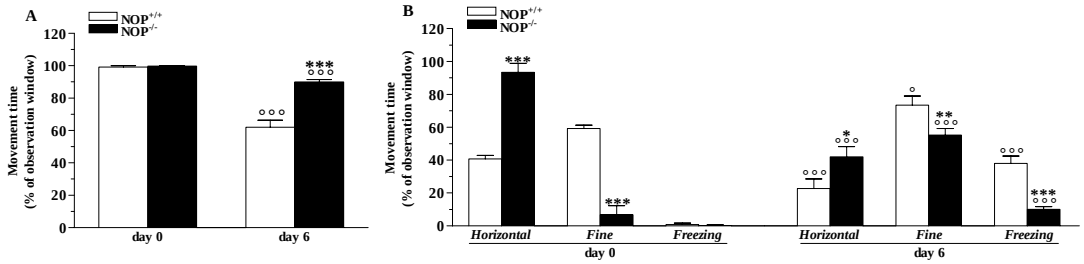

Figure 29. NOP$^{-/-}$ mice are more resistant than NOP$^{+/+}$ mice to MPTP-induced impairment of spontaneous activity. Systemic administration of MPTP (4x20 mg/Kg, i.p.) reduced total movements (**A**), horizontal locomotion and fine movements, and freezing time (**B**) All tests were performed before (control session) and 6 days after MPTP-treatment. Data are means ± SEM of 8 determinations per group and were calculated as percentage of pre-MPTP values. *p<0.05, **p<0.01, ***p<0.001 different from NOP$^{+/+}$ mice; °p<0.05, °°°p<0.001 different from day 0 (RM ANOVA followed by contrast analysis and the sequentially rejective Bonferrroni's test).

Step parameters in MPTP-treated NOP$^{+/+}$ and NOP$^{-/-}$ mice

Analysis of various step parameters(Fig. 30), performed 6 days after treatment, showed that only NOP$^{+/+}$ mice had an impairment in preparation and iniziation time, air time, execution time and step length.

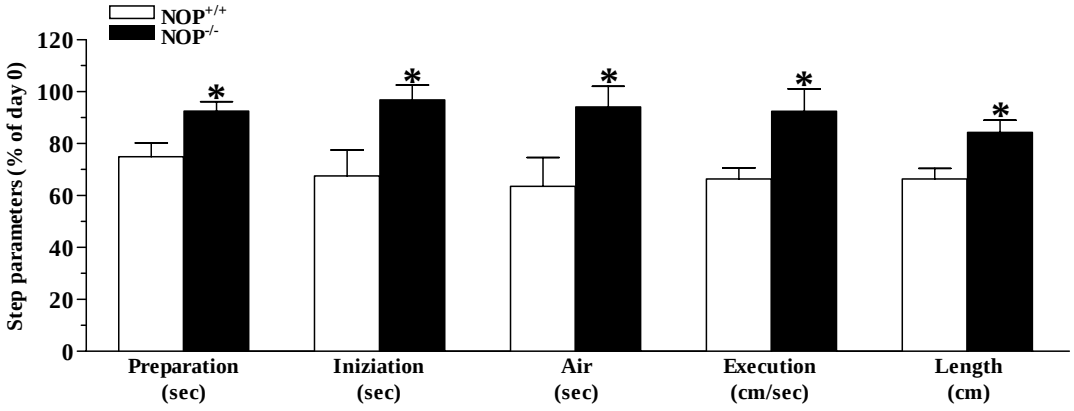

Figure 30. NOP$^{-/-}$ mice are more resistant than NOP$^{+/+}$ mice to MPTP-induced changes in step parameters. Systemic administration of MPTP (4x20 mg/Kg, i.p.) reduced preparation, iniziation and air time, execution speed and step length. Data were collected before (control session) and 6 days after

MPTP-treatment. Data are means ± SEM of 5-8 determinations per group and were calculated as percentage of the control session (pre-MPTP values). *p<0.05 different from $NOP^{+/+}$ mice (Student's t-test).

Muscle strength in MPTP-treated $NOP^{+/+}$ and $NOP^{-/-}$ mice

MPTP reduced the force peak and average force values (Fig. 31) at 6 days after treatment, both in $NOP^{-/-}$ and $NOP^{+/+}$ mice. In this case, no difference was observed between genotypes.

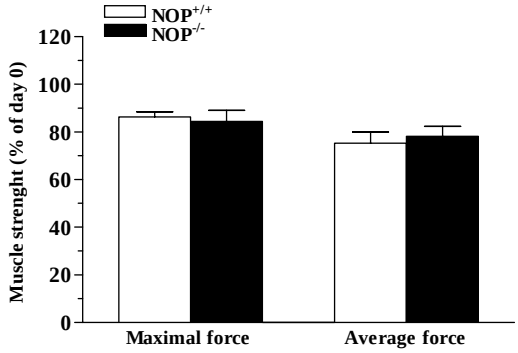

Figure 31. $NOP^{-/-}$ mice are more resistant than $NOP^{+/+}$ mice to MPTP-induced inhibition of muscle strength. Systemic administration of MPTP (4x20 mg/Kg, i.p.) reduced maximal and average force. The tests were performed before (control session) and 6 days after MPTP-treatment. Data are means ± SEM of 5-8 determinations per group and were calculated as percentage of the control session (pre-MPTP values).

$NOP^{-/-}$ mice are partially resistant to MPTP-induced neurodegeneration

Under control conditions (saline treatment Fig. 32A-D) both $NOP^{-/-}$ and $NOP^{+/+}$ mice showed similar numbers of TH-immunoreactive neurons in SNc (3973.03±426.29 vs 3917.03±403.51). MPTP treatment caused a marked loss of the number of TH-immunoreactive cells (Fig. 32E). However, the number of TH-immunoreactive cells surviving MPTP treatment was significantly higher in $NOP^{-/-}$ mice than $NOP^{+/+}$ (2347.99±304.93 vs 1044.15±152.81).

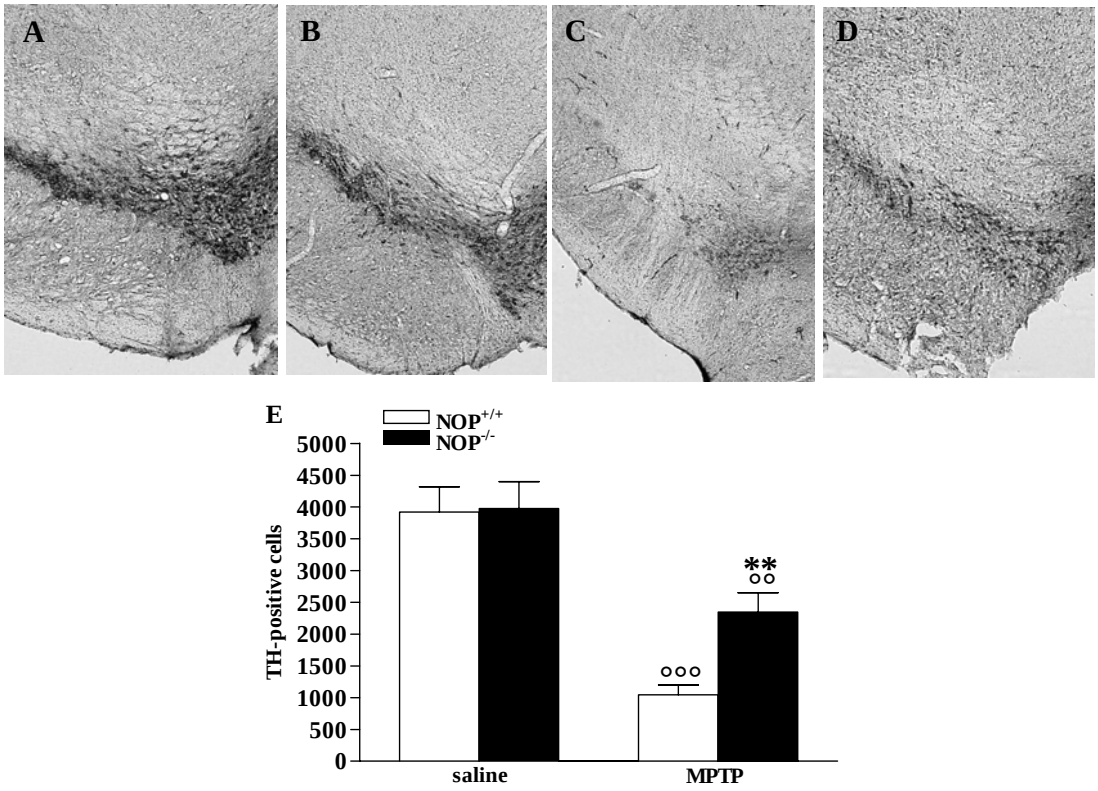

Figure 32. NOP receptor deletion partially attenuated MPTP-induced loss of DA cells in SNc. Representative microphotographs of TH-positive neurons in SNc, 7 days after saline or MPTP treatment (80 mg/Kg) in $NOP^{+/+}$ (**A, C**) and $NOP^{-/-}$ (**B, D**) mice. Stereological quantification of DA neurons (**E**). Data are means ± SEM of 5-10 determinations. **p<0.01, different from $NOP^{+/+}$ mice; °°p<0.01, °°°p<0.001 different from saline (ANOVA followed by the Newman-Keuls test).

Part V. N/OFQ modulates cortical output and motor activity in rats through nigral NOP receptors

I.c.v. injections of NOP receptor ligands affect motor activity

To investigate the role of central NOP receptors in modulation of motor activity, N/OFQ was injected i.c.v. (in LCV). UFP-101 was also administered to test the specificity of N/OFQ action and to investigate the role of endogenous N/OFQ. Saline injections did not affect motor activity. Indeed, immobility time, number of steps, speed and rotarod performance were similar in saline-injected (0.6 ± 0.2 sec, 13.2 ± 0.3, 67.4 ± 2.1 cm/sec and 1021 ± 27 sec, respectively) and control (0.8 ± 0.3 sec, 12.9 ± 0.8, 68.6 ± 6.3 cm/sec and 1064 ± 18 sec, respectively) rats. Since i.c.v. injection of saline,

N/OFQ and UFP-101 did not induce forepaw motor asymmetry, results obtained at the contralateral and the ipsilateral forepaw in the bar and drag test were pooled together.

N/OFQ

N/OFQ 0.1 nmol evoked a modest and transient elevation of immobility time compared to saline (Fig. 33A) while 1 and 10 nmol N/OFQ evoked a more robust and prolonged response, detectable 60 min after injection. No change in immobility time was elicited by 0.01 nmol. N/OFQ evoked a biphasic response in the drag test (Fig. 33B), namely facilitation at 0.01 nmol and inhibition at higher doses (0.1-10 nmol). Both facilitation and inhibition were detected after 60 min. A biphasic response was showed also in the speed test (Fig. 33C), where N/OFQ improved speed at 0.01 nmol and inhibited it at higher doses (0.1-10 nmol). Both effects were long-lasting. Finally, N/OFQ improved rotarod performance (Fig. 33D) at 0.01 nmol and impaired it at higher doses.

UFP-101

UFP-101 caused prolonged reduction of immobility time (Fig. 33E) and elevation of number of steps (Fig. 33F), speed (Fig. 33G) and rotarod performance (Fig. 33H) at 10 nmol. UFP-101 also improved rotarod performance at 1, although the effect was transient.

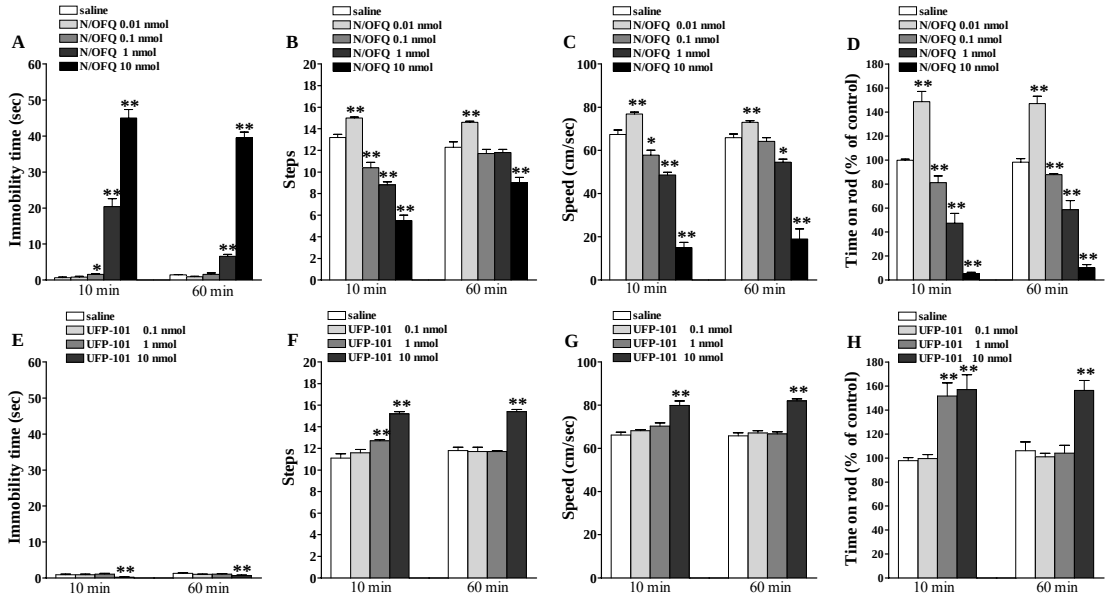

Figure 33. N/OFQ and UFP-101 modulated motor activity in naïve rats. I.c.v. injection of N/OFQ (0.01-10 nmol) or UFP-101 (0.1-10 nmol) affected motor performance in the bar (**A**, **E**), drag (**B**, **F**), speed (**C**, **G**) and rotarod (**D**, **H**) test. All tests were performed before (control session) and after (10 and 60 min)

drug injection. Data are means ± SEM of 7-9 determinations per group. *p<0.05, **p<0.01 different from saline (RM ANOVA followed by contrast analysis and the sequentially rejective Bonferrroni's test).

Co-injection of N/OFQ and UFP-101

To investigate the selectivity of N/OFQ action, co-injections of low and high N/OFQ and UFP-101 doses (1:10 ratio) were performed. LCV injection of N/OFQ or UFP-101 did not induce turning behavior in the range of doses tested. We first tested the specificity of 0.01 nmol N/OFQ by challenging it with 0.1 nmol UFP-101 (Fig. 34). N/OFQ elevations of number of steps (Fig. 34A), speed (Fig. 34B) and rotarod performance (Fig. 34C) were prevented by UFP-101 which was ineffective alone.

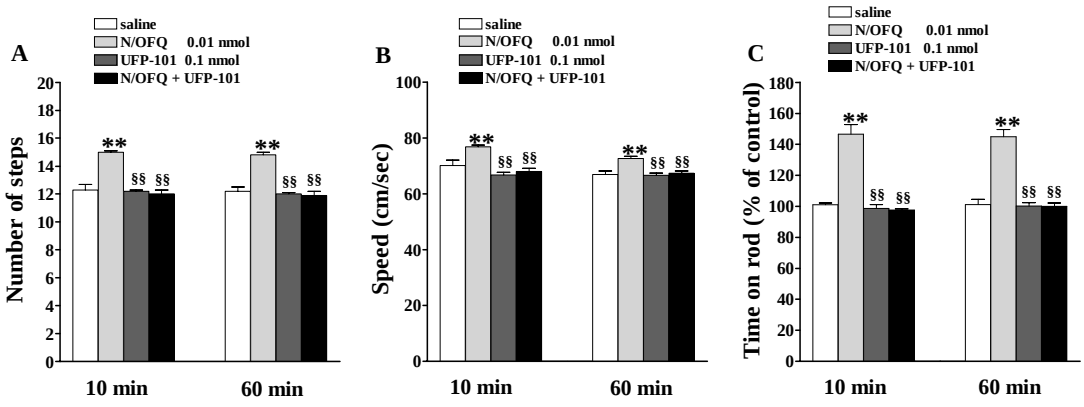

Figure 34. Motor facilitation induced by i.c.v. N/OFQ in naïve rats is NOP receptor dependent. Low doses of N/OFQ (0.01 nmol) and UFP-101 (0.1 nmol) were co-injected in the lateral cerebral ventricle and motor performance was evaluated in the drag (**A**), speed (**B**) and rotarod (**C**) test. All tests were performed before (control session) and after (10 and 60 min) drug injection. In the drag and speed test data are expressed as absolute values (steps, and cm/sec, respectively) whereas in the rotarod test as percentage of the control session Data are means ± SEM of 7 determinations per group. **p<0.01 different from saline; §§p<0.01 different from N/OFQ (RM ANOVA followed by contrast analysis and the sequentially rejective Bonferrroni's test).

We then tested the specificity of high N/OFQ doses by challenging 1 nmol N/OFQ with 10 nmol UFP-101 (Fig. 35). N/OFQ elevated immobility time (Fig. 35A) while UFP-101, ineffective alone, prevented this effect. In the drag test (Fig. 35B), N/OFQ reduced the number of steps while UFP-101 increased it. The combination of the two was the sum of their effects, i.e. no change with respect to saline-treated animals. In the speed test (Fig. 35C), N/OFQ reduced, whereas UFP-101 increased speed. Again, combination of the two caused no change in speed when compared to saline-treated animals. Finally, N/OFQ reduced rotarod performance (Fig. 35D) and UFP-101 improved it. Co-

application of N/OFQ and UFP-101 caused a slight increase in performance compared to saline-treated rats.

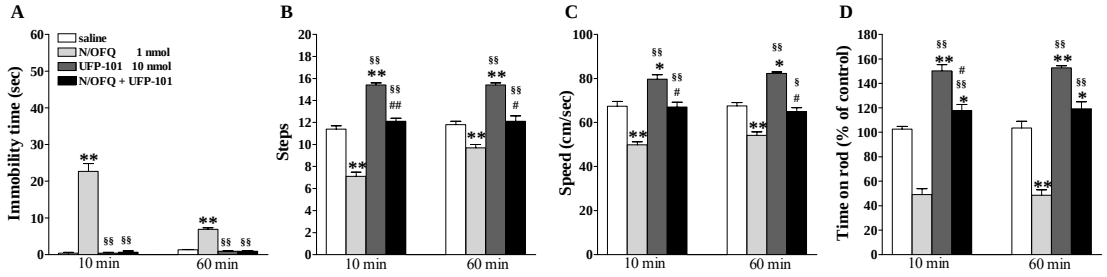

Figure 35. Motor inhibition induced by i.c.v. N/OFQ in naïve rats is NOP receptor dependent. High doses of N/OFQ (1 nmol) and UFP-101 (10 nmol) were co-injected in the lateral cerebral ventricle and motor performance evaluated in the bar (A), drag (B), speed (C) and rotarod (D) test. All tests were performed before (control session) and after (10 and 60 min) drug injection. In the bar, drag and speed test data are expressed as absolute values (sec, steps, and cm/sec, respectively) whereas in the rotarod test as percentage of the control session. Data are means ± SEM of 7 determinations per group. *p<0.05, **p<0.01 different from saline. §p<0.05, §§p<0.01 different from N/OFQ. $^{\#}$p<0.05, $^{\#\#}$p<0.01 different from UFP-101 (RM ANOVA followed by contrast analysis and the sequentially rejective Bonferrroni's test).

M1 injections of NOP receptor ligands did not affect motor activity

To investigate the localization of NOP receptors involved in motor actions elicited by i.c.v. N/OFQ and UFP-101, intracortical injections (layer V of M1) were first made. Saline, N/OFQ (0.01-10 nmol) or UFP-101 (10 nmol) failed to affect rat performance in the bar, drag, speed and rotarod test (Fig. 36A-C).

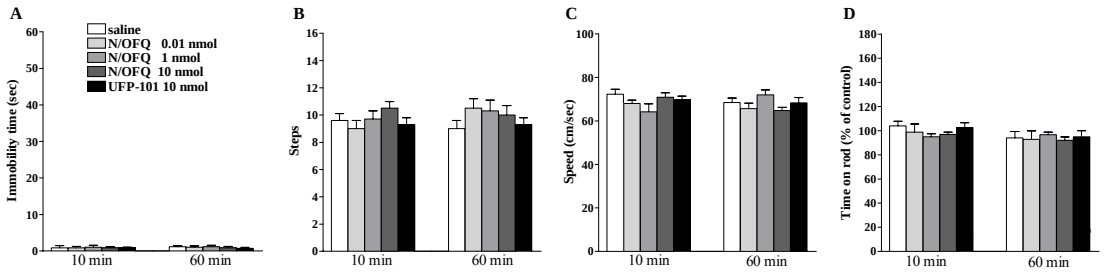

Figure 36. Intracortical injections of N/OFQ or UFP-101 did not affect motor activity. N/OFQ (0.01-10 nmol) or UFP-101 (0.1-10 nmol) were injected in M1 and motor performance evaluated in the bar (**A**), drag (**B**), speed (**C**) and rotarod (**D**) test. Motor performance in the bar and drag test was evaluated separately at the paws ipsilateral and contralateral to the injection side. All tests were performed before (control session) and after (10 and 60 min) drug injection. In the bar, drag and speed test data are expressed as absolute values (sec, steps, and cm/sec, respectively) whereas in the rotarod test as

percentages of motor activity in the control session. Data are means ± SEM of 7 determinations per group.

SNr injections of NOP receptor ligands affect motor activity

Based on our previous finding that NOP receptors located in the SNr modulate rotarod performance in rats (Marti et al, 2004a) we investigated whether motor effects induced by i.c.v. N/OFQ and UFP-101 could be reproduced by SNr injections. Since injections were made unilaterally, motor activity was evaluated separately at the ipsilateral and contralateral paw. Saline did not affect motor parameters at the contralateral and ipsilateral forepaw compared to control rats.

N/OFQ

Analysis of the immobility time at the contralateral paw in the bar test (Fig. 37A-B) showed that N/OFQ increased the immobility time dose-dependently and in a prolonged way, being active yet at 0.1 nmol. Qualitatively similar data were obtained at the ipsilateral paw. In the drag test (Fig. 37C-D), N/OFQ elevated the number of steps at the contralateral paw at 0.01 nmol but reduced them in the 0.1-10 nmol range. Conversely, N/OFQ dose-dependently reduced the number of steps at the ipsilateral paw,, the threshold inhibitory dose being 1 nmol. N/OFQ biphasically modulated rat speed (Fig. 37E), low doses (0.01 nmol) being facilitatory and higher ones (0.1–10 nmol) inhibitory.

UFP-101

Analysis of the immobility time did not reveal significant effects of UFP-101 at the contralateral and ipsilateral paws. UFP-101 (1 and 10 nmol) elevated the number of steps at the contralateral paw in the drag test (Fig. 37F-G) both at 10 and 60 min post injection time. Conversely, no changes were observed on stepping activity at the ipsilateral paw. Finally, UFP-101 (1 and 10 nmol) consistently elevated speed at 10 and 60 min after injection. (Fig. 37H).

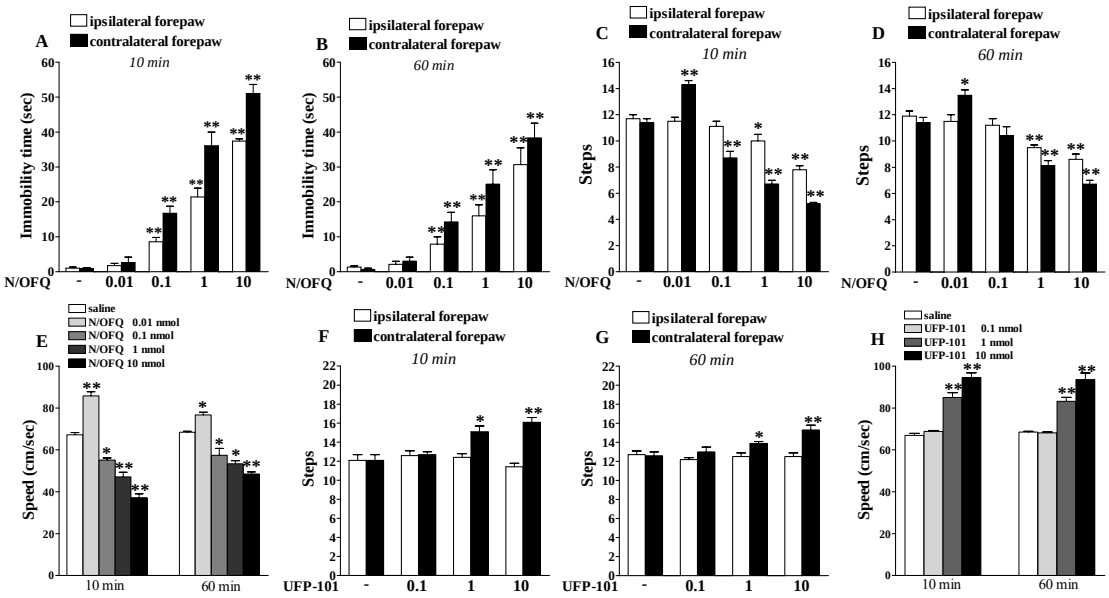

Figure 37. Intranigral injections of N/OFQ or UFP-101 modulated motor activity in naïve rats. N/OFQ (0.01-10 nmol) or UFP-101 (0.1-10 nmol) were injected in SNr and motor performance evaluated in the bar (**A-B**), drag (**C-D**, **F-G**) and speed (**E-H**) test. Motor performance in the bar and drag test was evaluated separately at the paws ipsilateral and contralateral to the injection side. All tests were performed before (control session) and after (10 and 60 min) drug injection. In the bar, drag and speed test data are expressed as absolute values (sec, steps, and cm/sec, respectively) whereas in the rotarod test as percentages of motor activity in the control session. Data are means ± SEM of 7 determinations per group. *p<0.05 and **p<0.01 different from saline (RM ANOVA followed by contrast analysis and the sequentially rejective Bonferrroni's test).

Co-injection of N/OFQ and UFP-101

To investigate the selectivity of N/OFQ action in SNr, co-injections of low and high N/OFQ and UFP-101 doses (1:10 ratio) were performed (Fig. 38). UFP-101 (0.1 nmol), ineffective alone, prevented the increase in the number of steps (Fig. 38A) and speed (Fig. 38B) induced by N/OFQ (0.01 nmol). Likewise, UFP-101 (10 nmol) ineffective alone, prevented the increase in immobility time induced by N/OFQ (1 nmol) both at the contralateral and ipsilateral (Fig. 38C) paw. In the drag test (Fig. 38D), N/OFQ reduced the number of steps made by the contralateral paw while UFP-101 increased it. The combination of the two did not result in significant changes compared to saline-treated animals. At the ipsilateral paw, N/OFQ reduced the number of steps and UFP-101, ineffective alone, prevented this effect. Finally, N/OFQ reduced speed (Fig. 38E), UFP-101 increased it and their combination resulted in a stimulation not different from that evoked by UFP-101 alone.

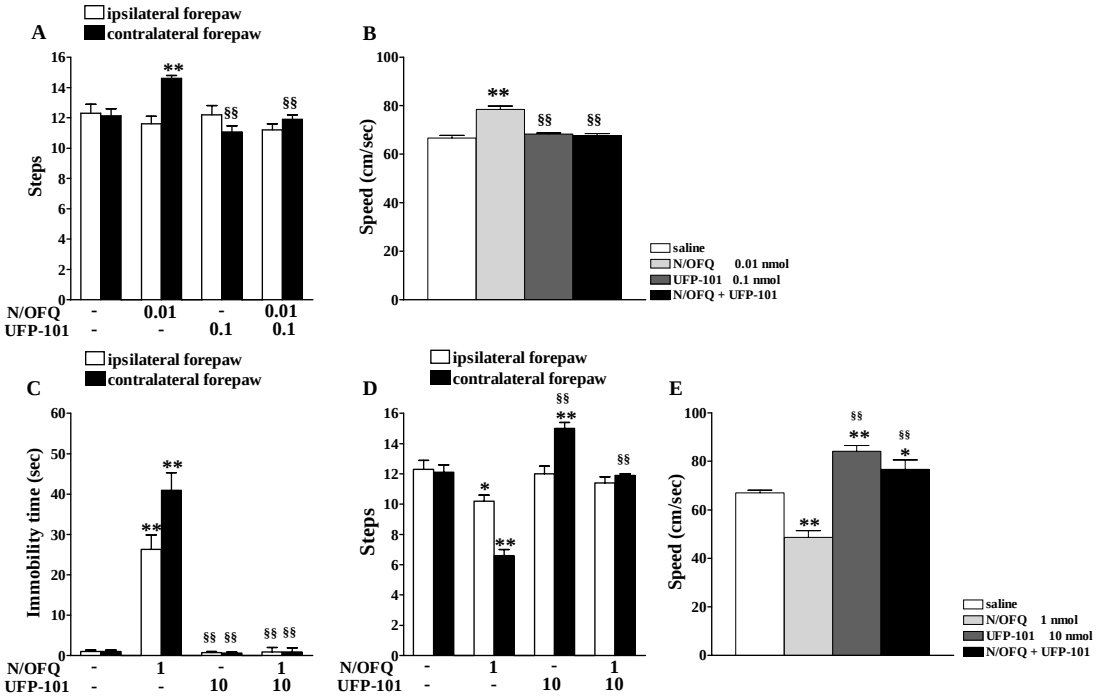

Figure 38. Motor changes induced by intranigral N/OFQ in naïve rats were NOP receptor dependent. N/OFQ and UFP-101 were co-injected at low (0.01 and 0.1 nmol, respectively; **A-B**) and high (1 and 10 nmol, respectively; **C-E**) doses in SNr and motor performance evaluated in the drag (**A, D**), speed (**B, E**) and bar (**C**) test. Motor performance in the bar and drag test was evaluated separately at the paws ipsilateral and contralateral to the injection side. All tests were performed 10 min after drug injection. In the bar, drag and speed test data are expressed as absolute values (sec, steps, and cm/sec, respectively) and are means ± SEM of 7 determinations per group. *p<0.05, **p<0.01 different from saline. §§p<0.01 different from N/OFQ (RM ANOVA followed by contrast analysis and the sequentially rejective Bonferrroni's test).

Effects of NOP receptor ligands on M1 output

Since NOP receptor stimulation or blockade affected motor activity, the hypothesis was tested that manipulation of central NOP receptors could change output from M1.

I.c.v. injections of NOP receptor ligands

Examination of M1 maps (examples are given in Fig. 39) revealed several changes in movement representation in the 10 nmol N/OFQ group (Fig. 39E). Contiguous unresponsive sites were consistently observed within M1 after i.c.v. injection of 10 nmol N/OFQ.

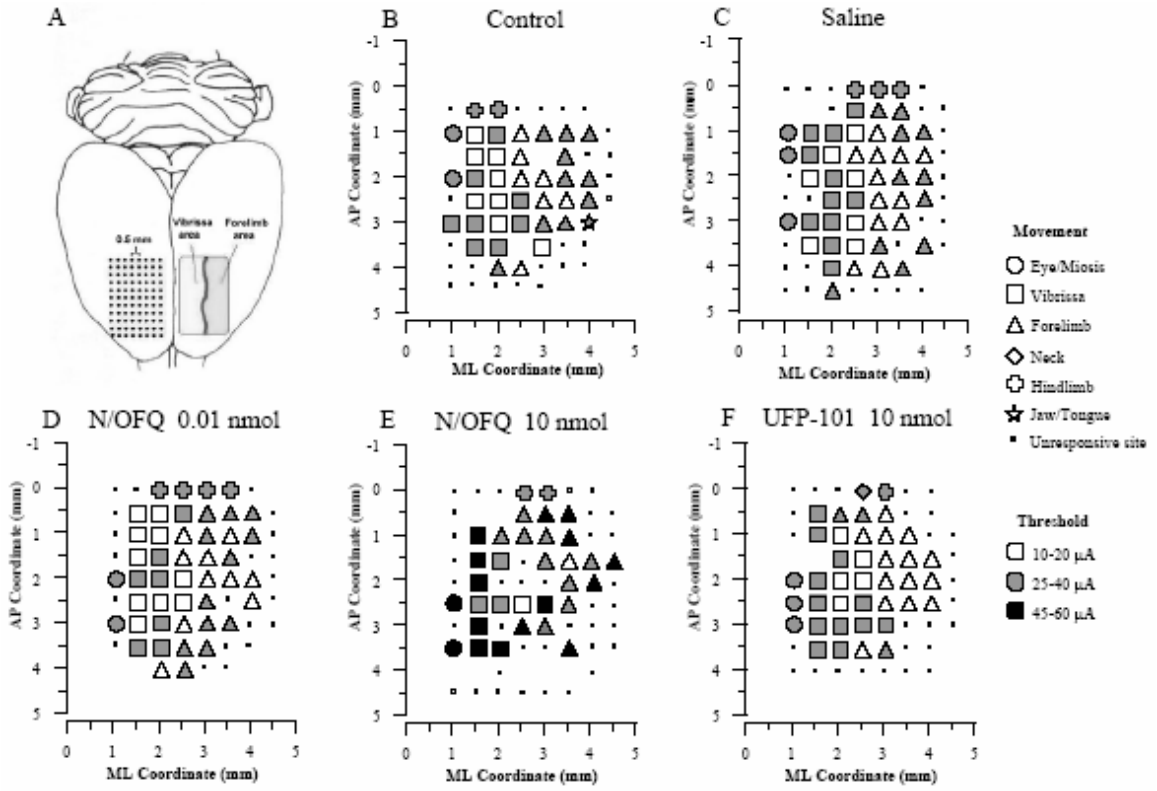

Figure 39. Effect of i.c.v. injection of N/OFQ and UFP-101 on M1 output in naïve rats. Representative M1 maps of movements evoked at threshold current levels in the vibrissa and forelimb areas. A schematic of rat brain is represented (**A**), which shows vibrissa and forelimb areas (right) and reports a coordinate grid (left). The maps relative to control rats (**B**) and rats injected with saline (**C**), N/OFQ (0.01 nmol; **D**), N/OFQ (10 nmol; **E**) and UFP-101 (10 nmol; **F**) in the lateral cerebral ventricle are also shown. The microelectrode was sequentially introduced to a depth of 1500 µm. Interpenetration distances were 500 µm. In these mapping schemes, frontal poles are at the bottom. Zero corresponds to bregma; numbers indicate rostral or caudal distance from the bregma or lateral distance from the mid-line. Movement evoked at one point is indicated by symbols and threshold range by the different grey scale. Absence of symbol (within or at the border of the maps) indicates that penetration was not performed due to presence of a large vessel.

To quantitatively assess these changes, the percentage of both unresponsive and responsive sites (movement sites in the vibrissa and forelimb areas) was calculated within the total site population (Fig. 40A). Analysis revealed changes in movement representation after injection of NOP receptor ligands. N/OFQ 10 nmol doubled the percentage of unresponsive sites. This effect was associated with a significant decrease (~49 %) in movement sites in the vibrissa representation and no change in excitable sites in forelimb representation. NOP receptor ligands significantly affected movement thresholds (Fig. 40B). N/OFQ (10 nmol) increased threshold currents in both vibrissa and forelimb representations (~55% and ~47%, respectively) whereas both N/OFQ (0.01 nmol) and UFP-101 (10 nmol) reduced them (~17 and ~33 %), although only in

forelimb representation. The differences in excitability appeared in more detail by looking at the distribution of vibrissa and forelimb movement thresholds. N/OFQ (10 nmol) caused a significant increase in the percentage of those sites where higher currents were necessary to evoke vibrissa (Fig. 40C) and forelimb (Fig. 40D) movements. Conversely, N/OFQ (0.01 nmol) and UFP-101 (10 nmol) did not change the distribution of thresholds in the vibrissa but caused a significant leftward shift of the distribution curve in the forelimb representation. In ~40 % of sites, currents lower than 20 μA were usually necessary to evoke forelimb movement.

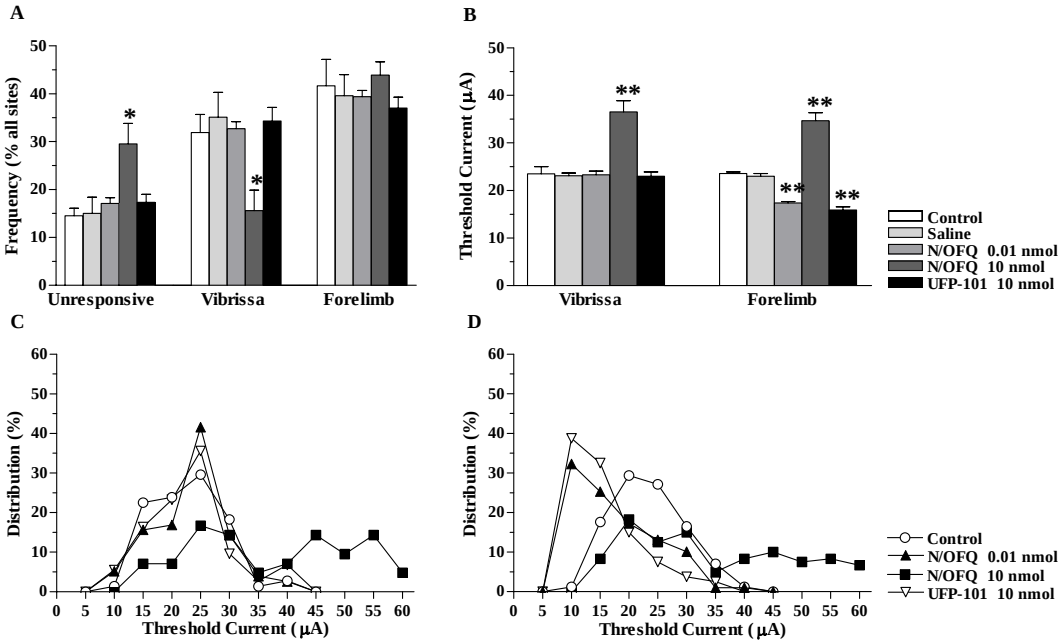

Figure 40. Effect of i.c.v. injection of N/OFQ and UFP-101 on M1 output in naïve rats. N/OFQ (0.01 and 10 nmol) and UFP-101 (10 nmol) were injected in the lateral cerebral ventricle, and the percentage of unresponsive and excitable sites in the vibrissa and forelimb areas (**A**) or average thresholds currents required to evoke vibrissa and forelimb movements (**B**) were measured. Threshold current distribution is also shown (**C-D**). The percentage of other movements sites (neck, jaw, eye and hindlimb) are not shown because these movements were not extensively explored. Data are means ± SEM of 5 determinations per group. *p<0.05, **p<0.01 different from control (ANOVA followed by the Newman-Keuls test).

Cortical injection of NOP receptor ligands

To investigate whether NOP receptors located in M1 modulated local excitability, injections of NOP receptor ligands in the layer V of M1 were made (examples are given in Fig. 41).

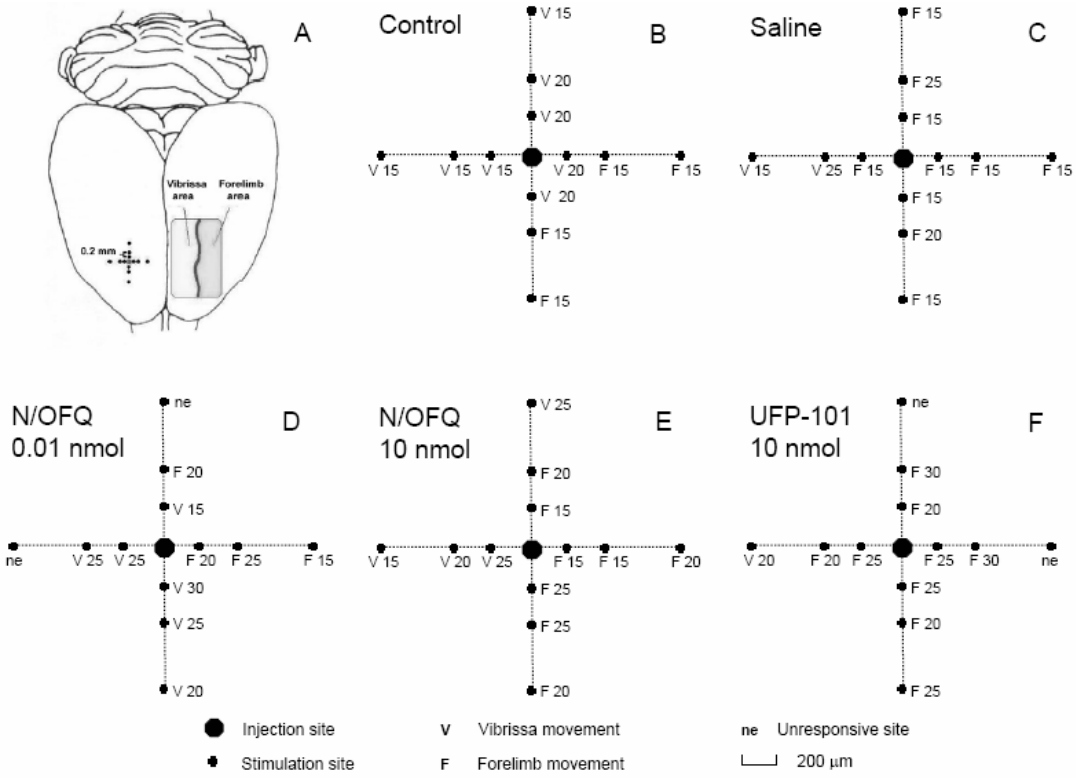

Figure 41. Intracortical injections of N/OFQ and UFP-101 in naïve rats. Examples of cross-shaped grids showing injection and stimulation sites in control rats (**B**) or rats injected with saline (**C**), N/OFQ (0.01 and 10 nmol; **D**, **E**), and UFP-101 (10 nmol; **F**) in M1. A schematic of rat brain showing vibrissa and forelimb areas (right) and reporting a coordinate grid (left) is also represented (**A**). For each stimulation site, a letter indicates the type of ICMS-evoked movement and the corresponding number the threshold current (in µA) required to evoke it.

No significant changes were observed in all treated group compared to saline at each level away from the injection site (Fig. 42).

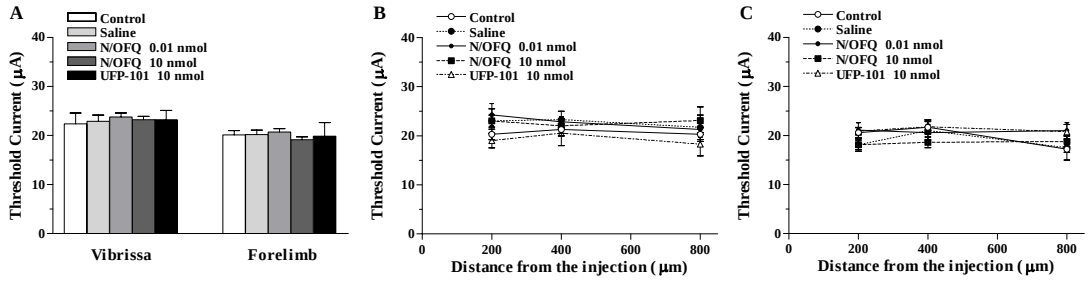

Figure 42. M1 injections of N/OFQ and UFP-101 had no effects on M1 output in naive rats. N/OFQ (0.01 and 10 nmol) and UFP-101 (10 nmol) were injected in the central M1 and the average thresholds currents required to evoke vibrissa and forelimb movements (**A**) were measured. Threshold current distribution of vibrissa (**B)** and forelimb (**C**) is also shown. The percentage of other movements sites (neck, jaw, eye and hindlimb) are not shown because these movements were not extensively explored. Data are means ± SEM of 5 determinations per group (ANOVA followed the Newman-Keuls test).

SNr injections of NOP receptor ligands

Intranigral injections of NOP receptor ligands were performed to investigate whether NOP receptors located in SNr affected motor excitability (representative examples given in Fig. 43).

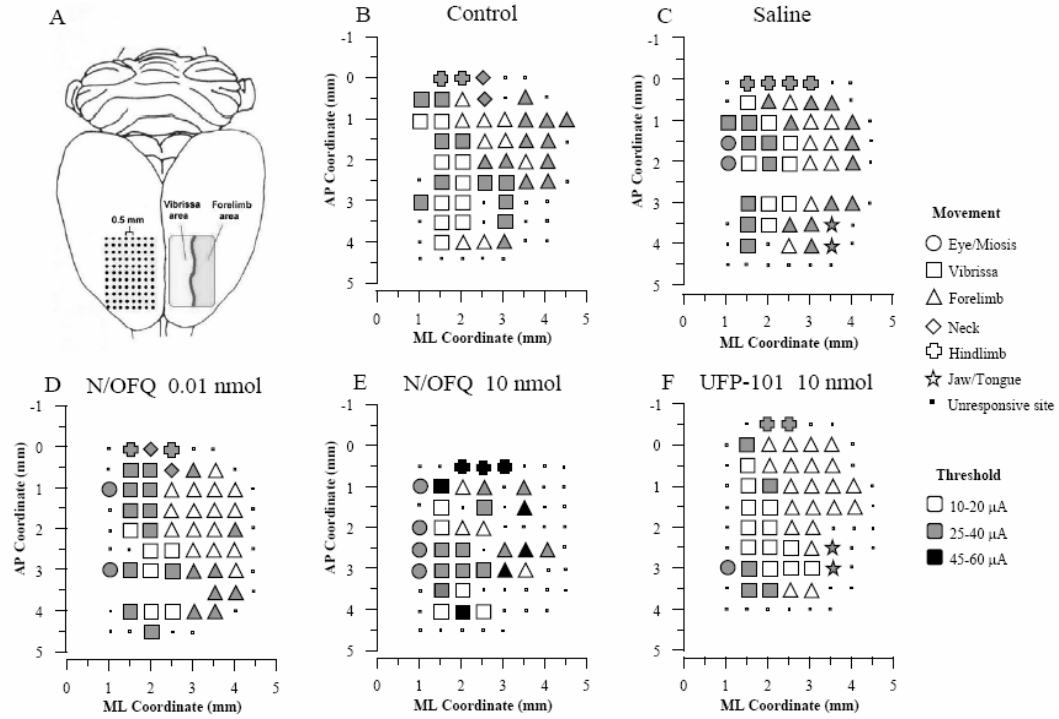

Figure 43. Effect of intranigral injection of N/OFQ and UFP-101 on M1 output in naive rats. Representative M1 maps of movements evoked at threshold current levels in the vibrissa and forelimb areas. A schematic of rat brain showing vibrissa and forelimb areas (right) and reporting a coordinate grid (left) is represented (**A**). The maps relative to control rats (**B**) and rats injected with saline (**C**), N/OFQ (0.01 nmol; **D**), N/OFQ (10 nmol; **E**) and UFP-101 (10 nmol; **F**) in substantia nigra reticulata are also shown. The microelectrode was sequentially introduced to a depth of 1500 µm. Interpenetration distances were 500 µm. In these mapping schemes, frontal poles are at the bottom. Zero corresponds to bregma; numbers indicate rostral or caudal distance from the bregma or lateral distance from the mid-line. Movement evoked at one point is indicated by symbols and threshold range by the different grey scale. Absence of symbol (within or at the border of the maps) indicates that penetration was not performed due to presence of a large vessel.

M1 maps derived in SNr revealed that NOP receptor ligands modulated the number of responsive and unresponsive sites (Fig. 44A). N/OFQ (10 nmol) was ineffective in the vibrissa area but increased (~121 %) the number of unresponsive sites and simultaneously reduced (~60 %) the number of excitable sites in the forelimb representation. NOP receptor ligands modulated threshold currents (Fig. 44B). N/OFQ (10 nmol) enhanced the mean threshold values in the vibrissa (~29 %) and forelimb (~58 %) areas. Moreover, UFP-101 (10 nmol) reduced (~44 %) threshold currents

selectively in the forelimb. A slight inhibition (~15 %) was also observed with 0.01 nmol N/OFQ in the forelimb area which, however, did not reach the level of significance. Threshold distribution showed that N/OFQ 10 nmol shifted to the right the distribution in both vibrissa (Fig. 44C) and forelimb (Fig. 44D) evoked movements. Conversely, N/OFQ (0.01 nmol) and UFP-101 (10 nmol) caused a significant leftward shift in the threshold distribution in forelimb representation.

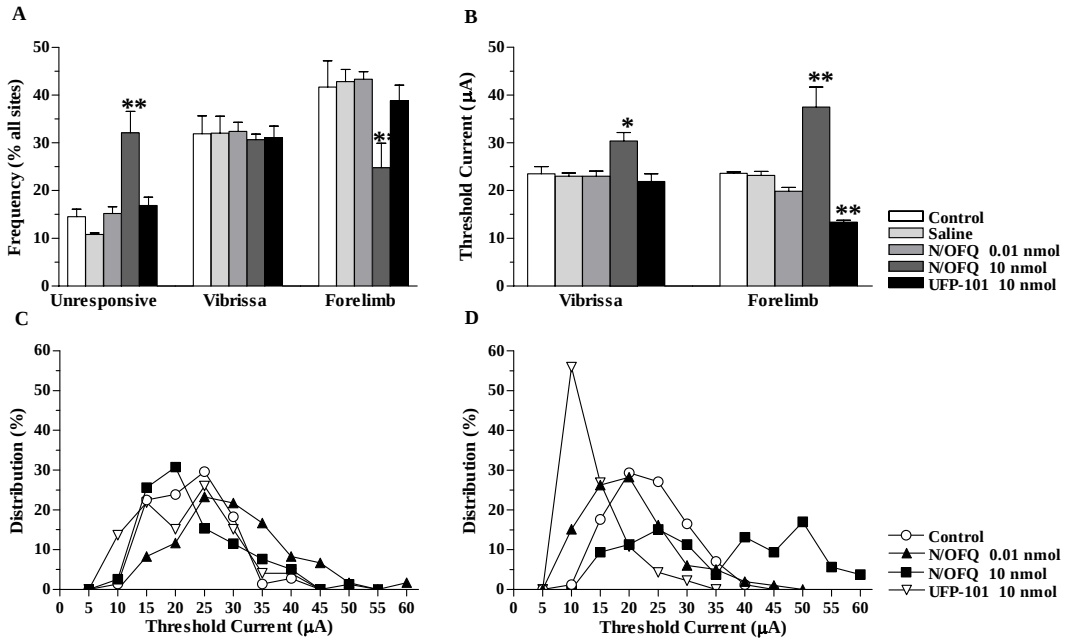

Figure 44. Effect of intranigral injection of N/OFQ and UFP-101 on M1 output in naive rats. N/OFQ (0.01 and 10 nmol) and UFP-101 (10 nmol) were injected in SNr, and the percentage of unresponsive and excitable sites in the vibrissa and forelimb areas (**A**) or the thresholds currents required to evoke vibrissa and forelimb movements (**B**) were measured. Threshold current distribution is also shown (**C-D**). The percentage of other movements sites (neck, jaw, eye and hindlimb) are not shown because these movements were not extensively explored. Data are means ± SEM of 5 determinations per group. *p<0.05, **p<0.01 significantly different from control (ANOVA followed by the Newman-Keuls test).

Part VI. Cortical progressive changes in 6-OHDA-treated rats

Time-course of the M1 reorganization in 6-OHDA-treated rats

6-OHDA treatment induced progressive loss of DA terminals

Unilateral 6-OHDA injection caused a marked loss of striatal DA terminals in the hemisphere ipsilateral to the lesion (Fig. 45A-C)., The denervation was significant in

the ventral but not dorsolateral striatum at 3 days after lesion. At later stages, both regions were almost totally denervated (Fig. 45D).

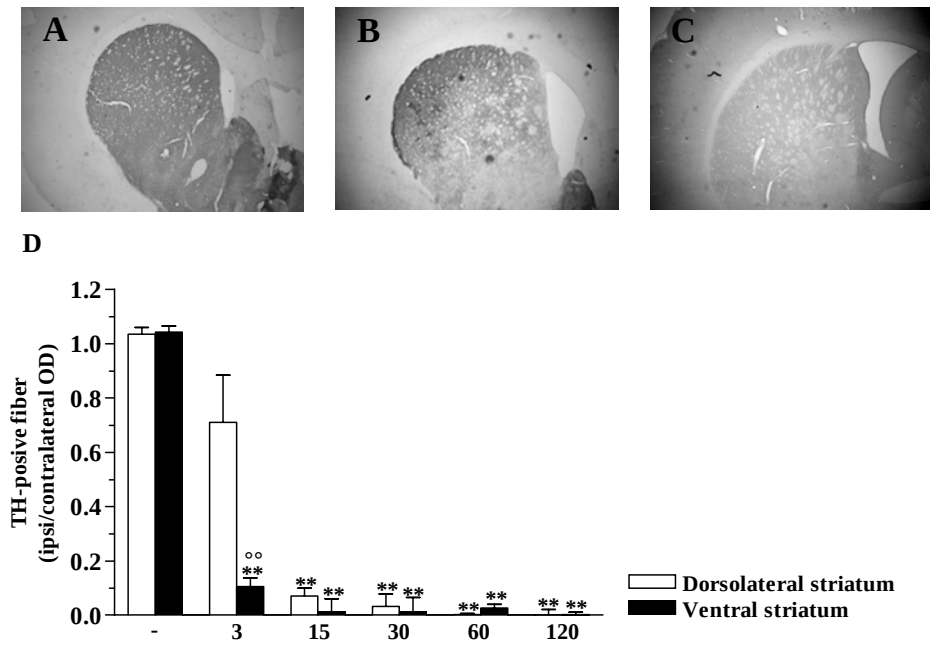

Figure 45. Unilateral 6-OHDA injection in rats destroyed TH-immunoreactive DA terminals in the ipsilateral striatum. Representative microphotographs of TH-immunoreactive fibers in the ipsilateral striatum before **(A)** and 3 **(B)** and 15 days **(C)** after 6-OHDA treatment. **(E)** Optical density of TH-immunoreactive fibers in the striatum. Data are means ± SEM of 5 determinations per group and are expressed as ratio between optical density in the denervated (ipsilateral) and intact (contralateral) side. **p<0.01 different from control; °°p<0.01 different from dorsolateral striatum (RM ANOVA followed by contrast analysis and the sequentially rejective Bonferrroni's test).

6-OHDA treatment affected motor activity

6-OHDA caused a marked and bilateral increase of immobility time in bar test (Fig. 46A), which was almost maximal already from 3 days after lesion. 6-OHDA caused a severe and prolonged decrease in stepping activity at the contralateral limb (Fig. 46B). The ipsilateral limb was quantitatively less affected, showing full recovery after 120 days. Finally, 6-OHDA caused a prolonged decrease of number of swings which selectively affected the contralateral side (Fig. 46C).

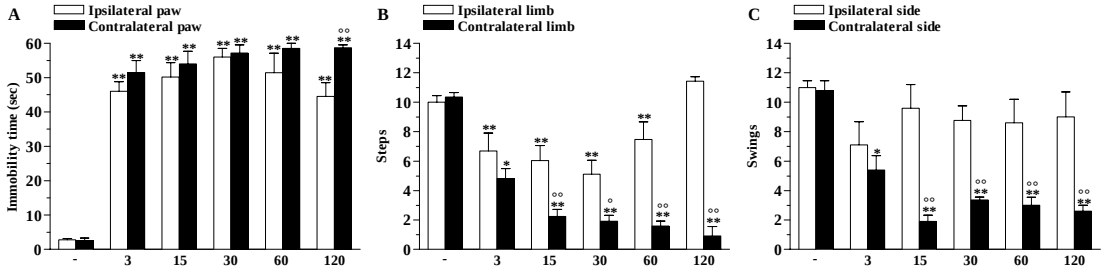

Figure 46. 6-OHDA injection affected motor activity in rats. Motor activity was evaluated in the bar (**A**), drag (**B**) and elevated body swing (**C**) test. All tests were performed before as well as 3, 15, 30, 60 and 120 days after lesion. No effect was observed after vehicle injection. Data are means ± SEM of 5 determinations per group and are expressed as absolute values (sec, steps and swings, respectively). *p<0.05, **p<0.01 different from control; °p<0.05, °°p<0.01 different from the ipsilateral side (RM ANOVA followed by contrast analysis and the sequentially rejective Bonferrroni's test).

6-OHDA treatment altered M1 excitability

In parallel with behavioural testing, ICMS was performed in 6-OHDA-lesioned rats at different time points after lesion (3, 15, 30, 60 and 120 days). Examination of M1 maps (examples are given in Fig. 47) revealed several progressive changes in movement representation. An incresase of unresponsive sites were consistently observed within M1 after 6-OHDA injection.

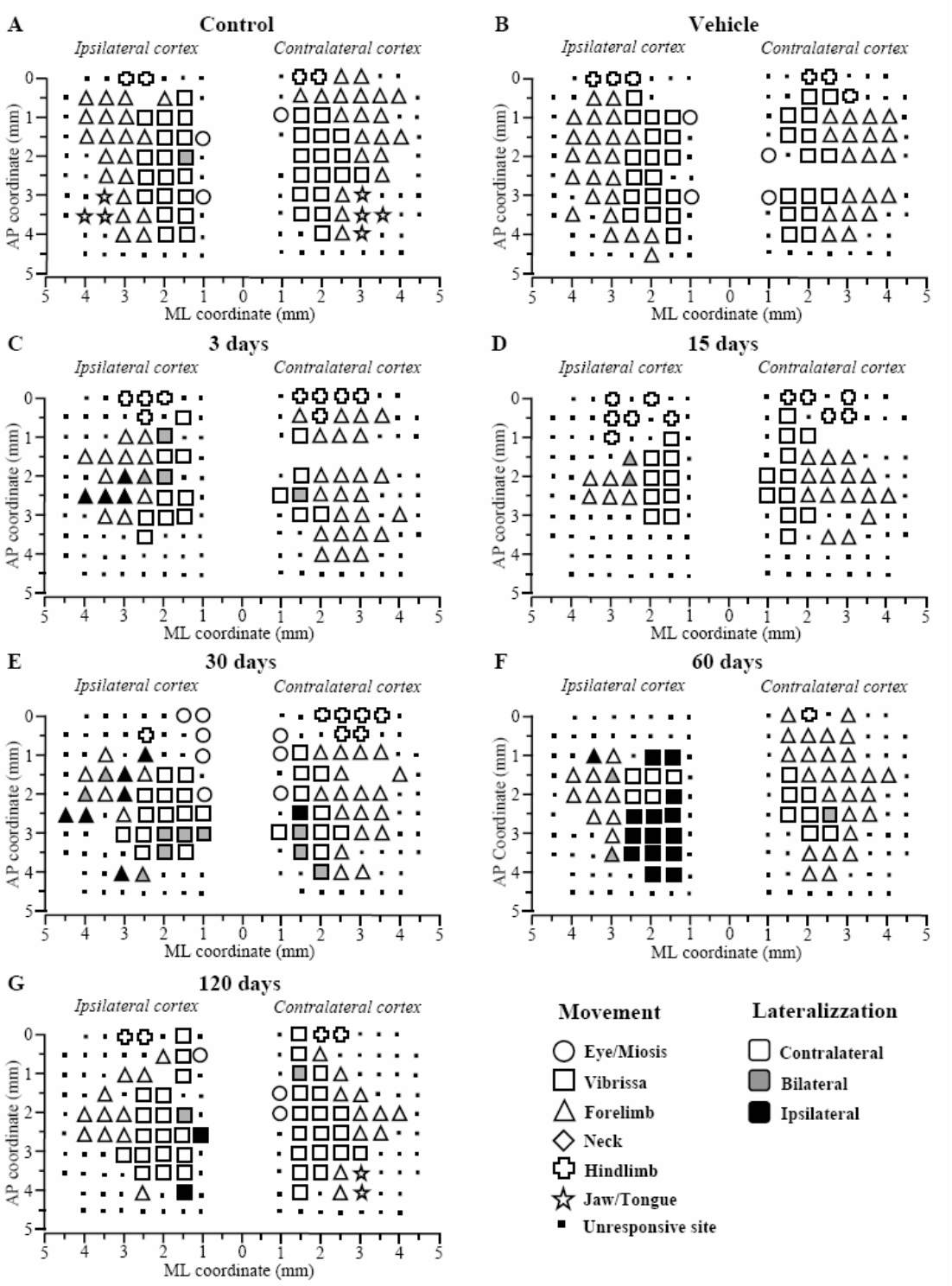

Figure 47. 6-OHDA injection in rats affected M1 output. Representative bilateral M1 maps of movements evoked at threshold current levels relative to control (**A**) and vehicle-injected **(B)** rats as well as rats at 3 **(C)**, 15 **(D)**, 30 **(E)**, 60 **(F)**, 120 **(G)** days after unilateral 6-OHDA injection. The microelectrode was sequentially introduced to a depth of 1500 µm. Interpenetration distances were 500 µm. In these mapping schemes, frontal poles are at the bottom. Zero corresponds to bregma; numbers indicate rostral or caudal distance from the bregma or lateral distance from the mid-line. Movement evoked at one point is indicated by symbols and movement type by the different grey scale. Absence of

symbol (within or at the border of the maps) indicates that penetration was not performed due to presence of a large vessel.

6-OHDA rats exhibited a marked increase in total size of not excitable area in M1 (Fig. 48A). The effect was maximal at 15 days for both the lesioned and unlesioned side and it was still evident, albeit attenuated, within the 30-120 days range. The size of unexcitable area was greater in the lesioned than unlesioned side in all groups of rats, although the difference reached significance only within the 3-15 days range. To quantitatively assess the difference in movement representation between control and 6-OHDA rats, we compared the cortical areas where vibrissa and forelimb movement were represented at threshold current. Other cortical areas (e.g. those evoking eye and neck movements) were too small, so these values were not considered for quantitative analysis. 6-OHDA caused a bilateral transient decrease in the size of the vibrissa area (Fig. 48B) both at 3 and 15 days after treatment, although only at 15 days the size of vibrissa area in the lesioned side was significantly smaller than in the unlesioned side. For the forelimb area, analysis was performed separately for the caudal and rostral regions. 6-OHDA decreased the size of caudal forelimb area (Fig. 48C) selectively in the lesioned side from 15 days onward (at 30 days only a trend to inhibition was observed, though). MPTP treatment significantly decreased the size of rostral forelimb area in the lesioned side (Fig. 48D) from 15 days on. Surprisingly, in the unlesioned side, there was a strong and transient increase in the area size at 3 days. However, area size dropped below control values at 15 days and normalized at later times. 6-OHDA treatment caused an increase of threshold currents in both the ipsilateral and contralateral vibrissa area within the 3-15 days range (Fig. 48E). The increase was significantly greater in the lesioned than unlesioned side. The ipsilateral vibrissa area displayed a slight increase of threshold values also within the 60-120 days range. An increase of threshold currents in both ipsilateral and contralateral forelimb area (Fig. 48F) was found from 15 days after 6-OHDA lesion. At this time-point, threshold values were strongly higher in the lesioned than unlesioned side. Conversely, at later points no difference was detected between hemispheres. No differences were also observed in the threshold current intensities required to elicit forelimb movements in caudal vs rostral forelimb area (data not shown).

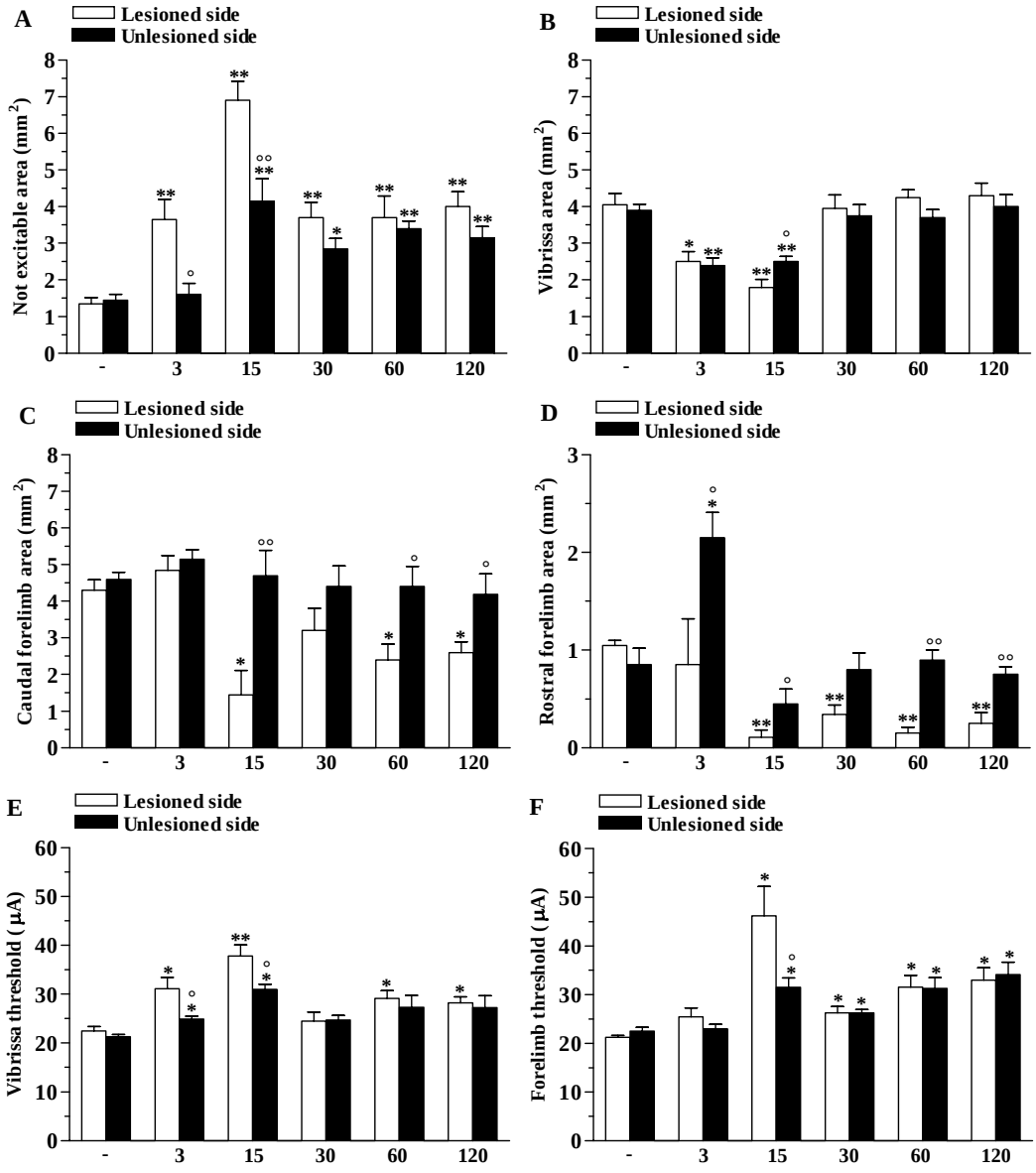

Figure 48. 6-OHDA lesion in rats changed M1 excitability. 6-OHDA treatment affected the size (in mm) of not excitable (**A**), vibrissa (**B**), caudal (**C**) and rostral forelimb (**D**) areas as well as threshold currents (in μA) in vibrissa (**E**) and forelimb (**F**) areas. All measures were performed in control and vehicle-injected rats as well as in rats at 3, 15, 30, 60 and 120 days after 6-OHDA lesion. No effect was observed after vehicle treatment. Data are means ± SEM of 5 determinations per group. *p<0.05, **p<0.01 different from control; °p<0.05, °°p<0.01 significantly different from the ipsilateral side (RM ANOVA followed by contrast analysis and the sequentially rejective Bonferrroni's test).

6-OHDA treatment affected evoked movement

To evaluate the status of the interhemispheric connections, the percentage of ipsilateral vs contralateral movements elicited by stimulation in the M1 of lesioned and unlesioned hemisperes was investigated. Under control conditions (i.e. before 6-OHDA lesion),

unilateral stimulation of M1 elicited movement only in the contralateral vibrissa. After lesion, however, the percentage of ipsilateral (mono or bilateral) movements increased to equal contralateral movements at days 30 and 60 (Fig. 49A). Stimulation in the unlesioned side resulted in a different pattern of changes. Indeed, the percentage of ipsi-bilateral vibrissa movement significantly increased only at 30 days (Fig. 49B). For forelimb movement in the lesioned side, the percent of total forelimb area eliciting ipsi-bilateral movement in all 6-OHDA rats was greater compared to control rats (Fig. 49C). This increase was significant only in the 30-day rat group, almost approaching 70% of the forelimb area value. For forelimb movements in the unlesioned side, the percentage of total forelimb area eliciting ipsi-bilateral and contralateral forelimb movements did not differ between 6-OHDA and control rats (Fig. 49D). Finally, we evaluated the changes in the typology and amplitude of forelimb movements, Under control conditions, unilateral M1stimulation elicited distal movements (~90%). In the lesioned side, distal movements in 6-OHDA rats were significantly less compared to control rats (Fig. 49E). Decrease in distal movements was greater in the 30-day group rats. In the unlesioned side, the percent of distal movements was smaller in 6-OHDA rats compared to control rats, though the decrease was significant only within the 3-30 days range (Fig. 49F).

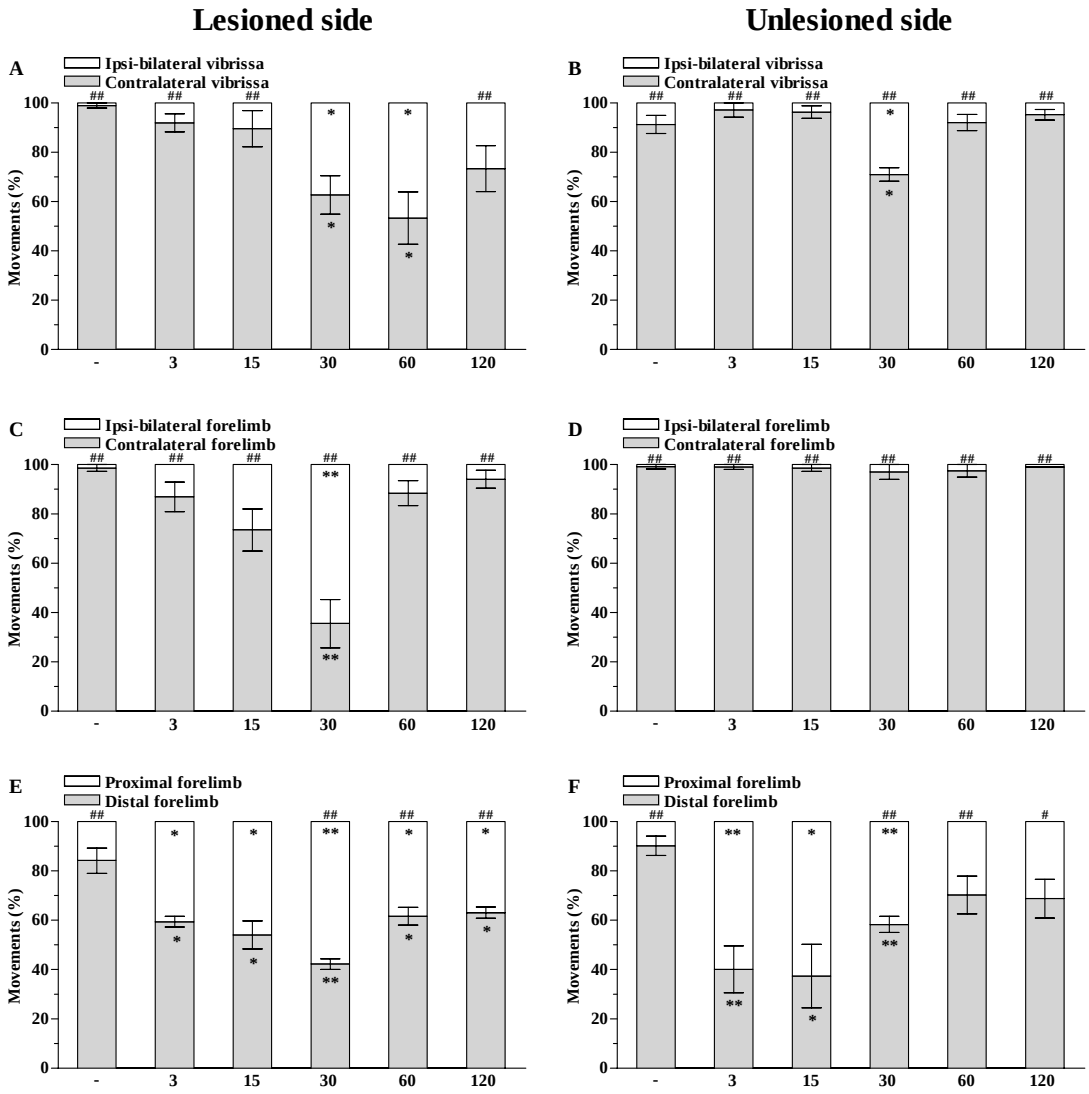

Figure 49. 6-OHDA treatment changed the type of evoked-movements in rats. In both the lesioned and unlesioned sides, 6-OHDA treatment affected the the percentage of ipsi-bilateral and contralateral vibrissa (**A, B**) and forelimb **(C-D)** movements as well as the percentage of distal and proximal forelimb movements. All measures were performed in control, vehicle-injected and 6-OHDA hemilesioned rats at 3, 15, 30, 60 and 120 days after lesion. No effect was observed after vehicle treatment. Data are means ± SEM of 5 determinations per group. *p<0.05, **p<0.01 different from control; °p<0.05, °°p<0.01 different from ipsilateral side (RM ANOVA followed by contrast analysis and the sequentially rejective Bonferrroni's test).

Biochemical mechanisms underlying M1 changes in 6-OHDA-treated rats

Mechanisms underling the short- and long-term M1 changes (evaluated at 15 and 60 days, respectively) were determined by means of three pharmacological treatments aimed at different targets: the local anesthetic lidocaine, to measure the effect of

interhemispheric (i.e. transcallosal) activity, the DA precursor L-dopa to restore the DAergic transmission, and the $GABA_A$ antagonist bicuculline to remove endogenous inhibitory activity of cortical circuits. Studies began 10 minutes after drug treatments.

Lidocaine restored lateralization of movements

To investigate if the increase of ipsi-bilateral forelimb movements in the lesioned side of 30-day rats was due to the activity in the unlesioned side (i.e. homotopic contralateral cortex), we injected lidocaine (3%) into the forelimb area of the unlesioned side (Fig. 50A). Saline injections did not produce changes. In 6-OHDA rats, the percent of total map area eliciting ipsi-bilateral and contralateral vibrissa movement (Fig. 50B) did not differ between saline and lidocaine treatment. The percentage of total map area eliciting ipsi-bilateral and contralateral forelimb movements (Fig. 50C) did not differ between control and 6-OHDA rats treated with lidocaine. We conclude that lidocaine injections into the homotopic M1 of the unlesioned side normalized the ratio between contalateral and ipsi-bilateral forelimb movements in the forelimb area of the lesioned side.

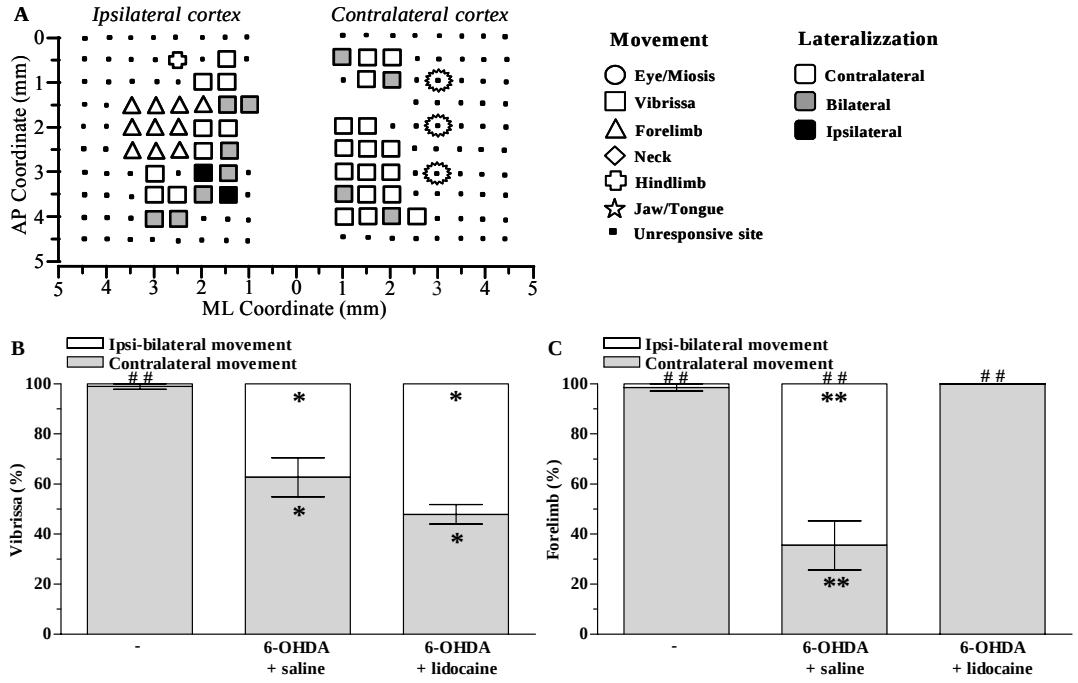

Figure 50. Lidocaine restored the type of evoked-movements in 6-OHDA-treated rats. Representative bilateral M1 maps of movements evoked at threshold current levels after intracortical injection of lidocaine (3%) at 30 days after unilateral 6-OHDA treatment (**A**). The microelectrode was sequentially introduced to a depth of 1500 μm. Interpenetration distances were 500 μm. In these mapping schemes, frontal poles are at the bottom. Zero corresponds to bregma; numbers indicate rostral or caudal distance from the bregma or lateral distance from the mid-line. Movement evoked at one point is indicated by symbols and movement type by the different grey scale. Absence of symbol (within or at the border of the

maps) indicates that penetration was not performed due to presence of a large vessel. Lidocaine, injected in forelimb area of homotopic cortex (injected sites are marked with circles), restored output in the forelimb (**C**) but not vibrissa (**B**) area. *p<0.05, **p<0.01 different from control; ##p<0.01 different from contralateral movement (RM ANOVA followed by the Newman-Keuls test).

L-dopa partially restored M1 output

To investigate if the 6-OHDA-induced effects were due to DA loss, the ability of L-dopa (6 mg/Kg; with benserazide 15 mg/Kg) to reverse 6-OHDA-induced effects on M1 was investigated at 15 and 60 days after lesion. Vehicle administration had no effect in both control and 6-OHDA rats (data not shown). Treatment with L-dopa had no effect in control rats. Conversely,, L-dopa partially reversed 6-OHDA-induced effects on ipsilateral M1 at both 15 and 60 days (Fig. 51).

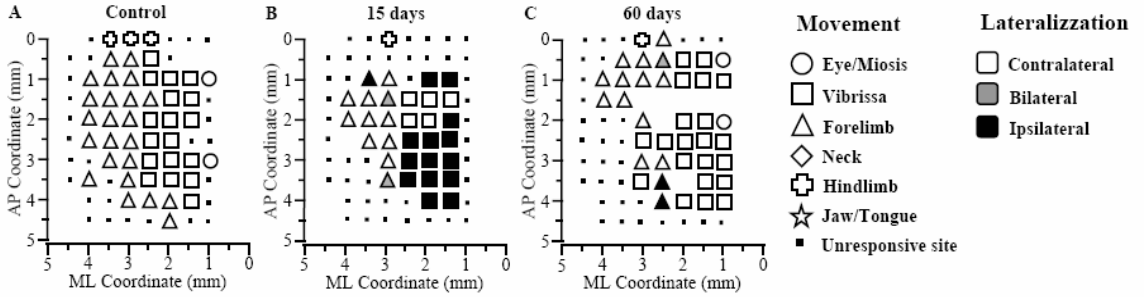

Figure 51. L-dopa treatment affected M1 output in 6-OHDA-treated rats. Representative unilateral M1 maps of movements evoked at threshold current levels after L-dopa injection (6 mg/Kg plus benserazide 15 mg/Kg, i.p) in control rats (**A**) and 6-OHDA hemilesioned rats at 15 **(B)** and 60 **(C)** days after lesion. The microelectrode was sequentially introduced to a depth of 1500 μm. Interpenetration distances were 500 μm. In these mapping schemes, frontal poles are at the bottom. Zero corresponds to bregma; numbers indicate rostral or caudal distance from the bregma or lateral distance from the mid-line. Movement evoked at one point is indicated by symbols and movement type by the different grey scale. Absence of symbol (within or at the border of maps) indicates that penetration was not performed due to presence of a large vessel.

In particular, L-dopa attenuated the increase of not excitable area induced by 6-OHDA (Fig. 52A); the effect of L-dopa was stronger at 15 than 30 days though the size remained significantly higher compared to control in both groups. L-dopa restored the size of vibrissa area in the 15-days rat group (Fig. 52B). Consistently, L-dopa restored the size of the caudal forelimb movement representation at both 15 and 60 days (Fig. 52C) although it failed to do so in the rostral forelimb area (Fig. 52D). L-dopa also normalized the number of both distal (Fig. 52E) and proximal (Fig. 52F) forelimb movements. Finally, L-dopa failed to restore the normal threshold current values in both

the vibrissa and forelimb areas(Fig. 52G) although it attenuated the increase in threshold current values in the vibrissa area at 15 days (Fig. 52H).

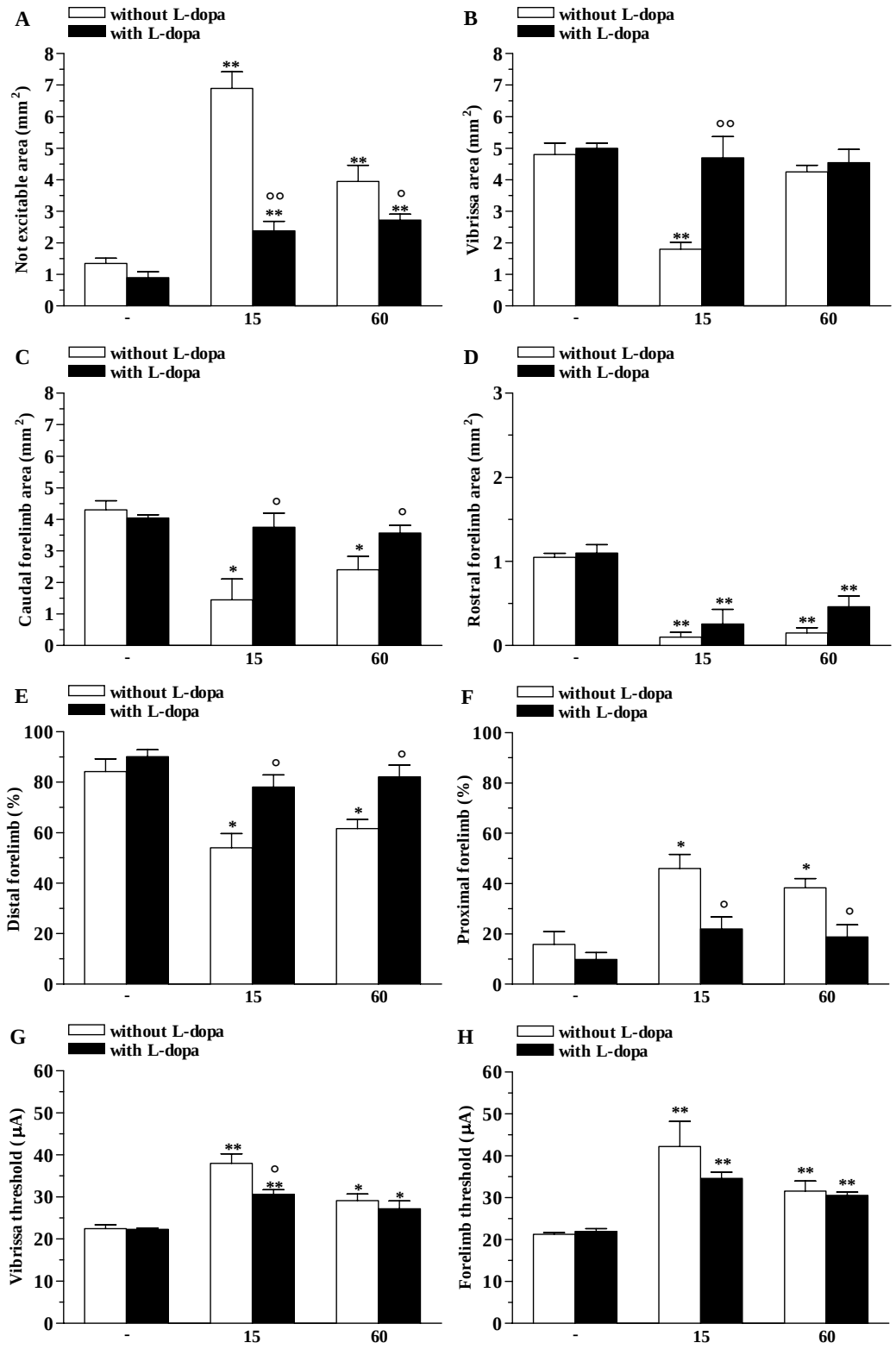

Figure 52. L-dopa treatment partially restored M1 output in 6-OHDA-treated rats. L-dopa (6 mg/Kg plus benserazide 15 mg/Kg, i.p.) affected the size (in mm) of not excitable area (**A**), vibrissa area (**B**), caudal (**C**) and rostral forelimb area (**D**) the percentage of distal (**E**) and proximal (**F**) forelimb movements and

the threshold current (in μA) of vibrissa (**G**) and forelimb area (**H**). All measures were performed on the cortex ipsilateral to the 6-OHDA injection in control, sham and 6-OHDA hemilesioned rats at 15 and 60 days after lesion. No effect was observed after vehicle treatment. Data are means ± SEM of 5 determinations per group. *p<0.05, **p<0.01 different from control; °p<0.05 and °°p<0.01 significantly different from vehicle ("without L-dopa"; RM ANOVA followed by contrast analysis and the sequentially rejective Bonferrroni's test).

Bicuculline partially restored M1 output

To investigate if the 6-OHDA-induced changes in M1 output are due to an increased influence of inhibitory pathways, mediated by cortical $GABA_A$ receptor activation), the ability of bicuculline (50 μM) to attenuate cortical depression was investigated. Treatment with vehicle did not produce changes in both control and 6-OHDA treated rats (Fig. 53).

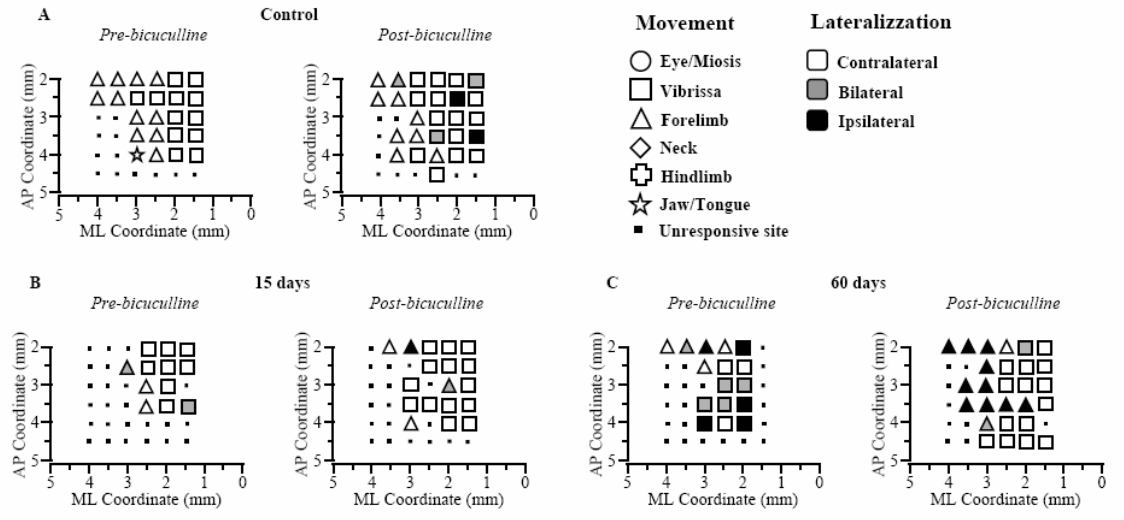

Figure 53. Bicuculline treatment affected M1 output in 6-OHDA-treated rats. Representative unilateral motor cortex maps of movements evoked at threshold current levels after cortical application of bicuculline (50μM) in control (**A**) and 6-OHDA hemilesioned rats at 15 **(B)** and 60 **(C)** days after lesion. The microelectrode was sequentially introduced to a depth of 1500 μm. Interpenetration distances were 500 μm. In these mapping schemes, frontal poles are at the bottom. Zero corresponds to bregma; numbers indicate rostral or caudal distance from the bregma or lateral distance from the mid-line. Movement evoked at one point is indicated by symbols and movement type by the different grey scale. Absence of symbol (within or at the border of the maps) indicates that penetration was not performed due to presence of a large vessel.

Bicuculline decreased not excitable area in both control and 6-OHDA-treated rats (Fig. 54A). Consistently, bicuculline increased the size of vibrissa area in control rats and 6-OHDA lesioned rats (Fig. 54B). In these animals, the area size was normalized compared to control animals (without bicuculline). Analysis on caudal forelimb area

values (Fig. 54C) showed that bicuculline caused a marked decrease in control rats, without changing the effects of 6-OHDA. Conversely, bicuculline restores the size of rostral forelimb area both at 15 and 60 days after 6-OHDA (Fig. 54D). Bicuculline decreased the number of distal forelimb movements (Fig. 54E) and increased the number of proximal forelimb movements (Fig. 54F) in control rats, although it failed to modulate movements in 6-OHDA-treated rats. Finally, bicuculline produced a mild reduction of vibrissa (Fig. 54G) and forelimb (Fig. 54H) threshold currents in control rats, without changing them in 6-OHDA. It is worthy of mention, however, that 60 days after 6-OHDA lesion, threshold currents after bicuculline did not differ from pre-bicuculline levels.

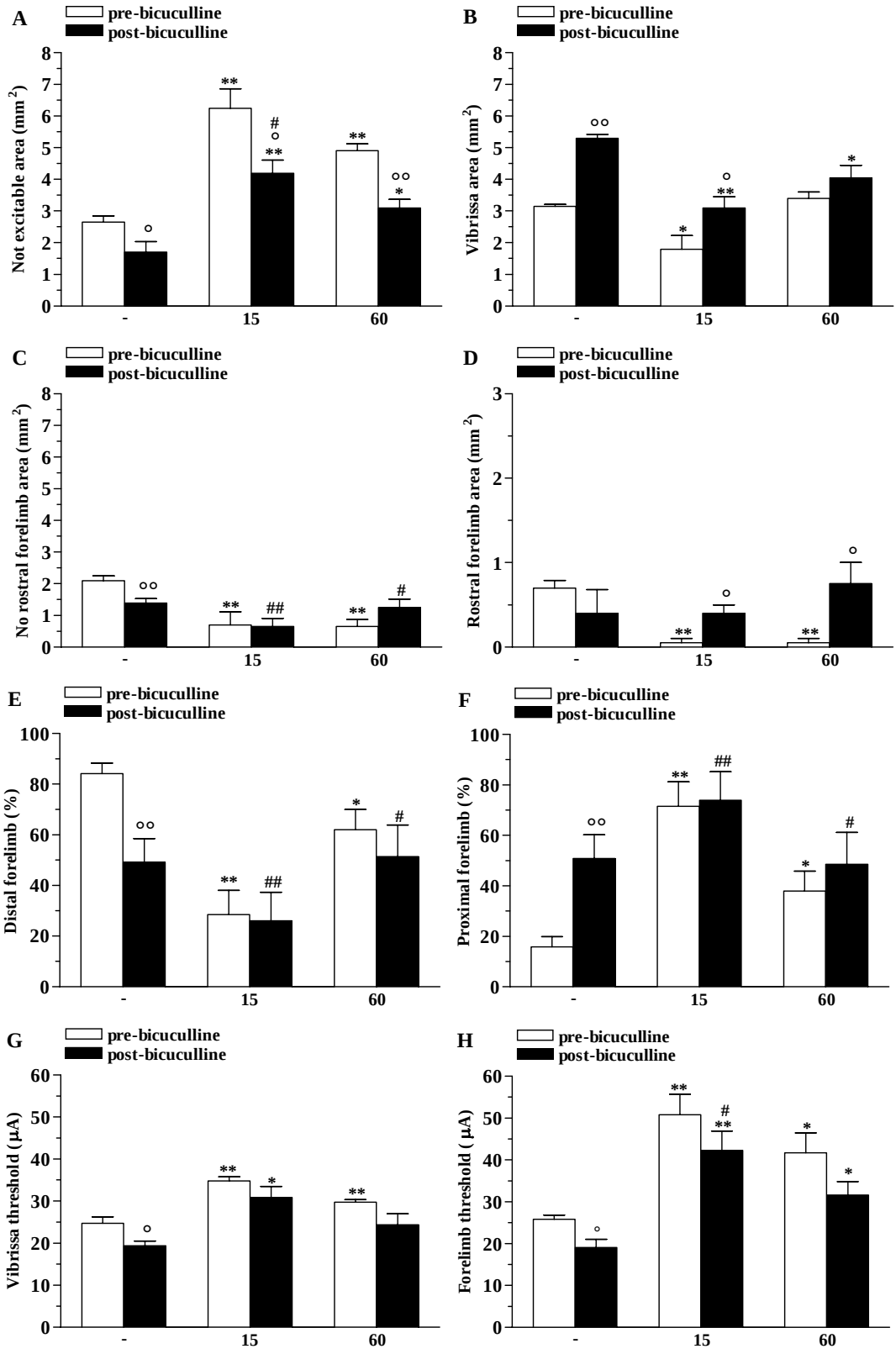

Figure 54. Bicuculline partially restored M1 output in 6-OHDA-treated rats. Cortical application of bicuculline (50 µM) affected the size (in mm) of not excitable area (**A**), vibrissa area (**B**), caudal (**C**) and rostral forelimb area (**D**), the percentage of distal (**E**) and proximal (**F**) forelimb movements and the threshold current (in µA) of vibrissa (**G**) and forelimb area (**H**). All measures were performed in the

cortex of control, sham and 6-OHDA hemilesioned rats (ipsilateral M1) at 15 and 60 days after lesion. No effect was observed after vehicle treatment. Data are means ± SEM of 5 determinations per group. *$p<0.05$, **$p<0.01$ from control; °$p<0.05$ and °°$p<0.01$ different from pre-bicuculline; $^{\#}p<0.05$ and $^{\#\#}p<0.01$ different from control pre-bicuculline (RM ANOVA followed by contrast analysis and the sequentially rejective Bonferrroni's test).

General discussion

Part I. Endogenous DA mediates motor responses of NOP receptor antagonists

The role of endogenous DA in the modulation of motor activity has been largely investigated using DA selective antagonists, DA lesioning techniques and DA receptor knockout mice (Clark and White, 1997; Millan et al., 2004; Scatton et al., 1997; Vallone et al., 2000). In keeping with these studies, raclopride and amisulpride dose-dependently increased akinesia (bar test) and bradykinesia (drag test), and impaired overall gait abilities (rotarod test), likely through the blockade of striatal D_{2L} (long isoform) postsynaptic receptors (Wang et al., 2000). D_3 receptors appear to be minimally involved in tonic regulation of motor activity since S33084 alone did not produce marked changes in motor performance. Mimicking D_2/D_3 receptor antagonists, SCH23390 induced dose-dependent motor impairment (Clark and White, 1997). L-dopa and PPX caused monotonic motor inhibition. Hypomotility is mediated by central (domperidone-insensitive) DA receptors, possibly presynaptic D_{2S} (short isoform) receptors, via reduced striatal DA release (Carter and Müller, 1991). Indeed, L-dopa and PPX-induced motor inhibition was counteracted by amisulpride supporting the role of D_2 autoreceptors (Scatton et al., 1997). However, PPX effects appeared poorly sensitive to amisulpride. This may be due to the different levels of DA receptor occupancy required to induce the biological response and/or to the different spectrum of DA receptors activated by the two agonists. Additional mechanisms not involving classical D_2 receptors may also be recruited by PPX to inhibit motor performance. Interestingly, although D_3 receptors appear not to be tonically activated, they markedly contributed to motor responses to PPX and L-dopa. Indeed, S33084 worsened inhibition of stepping activity induced by both agonists in the drag test, suggesting that D3 receptors play a specific role in facilitation of movement initiation and execution. The worsening of PPX-induced motor inhibition observed in the presence of raclopride may also rely on the high affinity of this compound for the D_3 receptor. Alternatively, the opposite modulation of the PPX response exerted by raclopride (enhancement) and amisulpride (attenuation) may be due to blockade of different D_2 receptor subpopulations, namely post- and presynaptic. In fact, amisulpride given systemically was reported to inhibit D_2 autoreceptors at low doses and block postsynaptic D_2 receptors, thereby causing

akinesia and catalepsy, at higher ones (Scatton et al., 1997). UFP-101 microinjections in SNr or systemic administrations of J-113397 and Trap-101 in mice facilitated motor activity at low doses and inhibited it at higher ones. Motor facilitation induced by NOP receptor antagonists was raclopride-sensitive but amisulpride-insensitive, suggesting that NOP receptor blockade can ultimately lead to postsynaptic D_{2L} receptor activation. Motor facilitation induced by low N/OFQ doses was also raclopride-sensitive. This extends previous findings that N/OFQ-induced facilitation was prevented by haloperidol (Florin et al., 1996) or by lesioning the DA system (Kuzmin et al., 2004), further suggesting that low doses of N/OFQ and NOP antagonists activate common pathways. Contrary to facilitation, motor inhibition induced by NOP antagonists was amisulpride-sensitive and raclopride-insensitive, suggesting that high doses of NOP receptor antagonists cause excessive DA release leading to stimulation of negative feedback mechanisms via D_2 autoreceptors. Indeed, motor inhibition was reversed into facilitation in the presence of amisulpride. D_1/D_5 and D_3 receptors do not contribute to motor responses to NOP receptor ligands. An important finding of the release studies, is that D_1/D_5 receptors mediate presynaptic facilitatory actions of L-dopa on DA release occurring prior to its conversion to DA. This finding may be clinically relevant as D_1/D_5 receptor stimulation underlie L-dopa-induced dyskinesia during PD therapy (Obeso et al., 2000).

For a more detailed discussion, see original paper VI reported in appendix II.

Part II. NOP receptor blockade attenuates parkinsonism in mice

The use of a broad range of motor tasks allowed for the collection of information on different motor parameters in MPTP-treated mice such as the time required to initiate (akinesia) and execute (bradykinesia) a movement, muscle strength, gait patterns and coordinated motor performance in freely moving or exercise-driven conditions. These tests showed that the MPTP-induced bilateral partial (~60%) lesions of striatal DA terminals was associated with an increase of immobility and reaction time, a reduction of stepping activity, climbing speed, time on rod and muscle strength, as well as gait abnormalities such as reduced stride length and increased stride width. Motor deficits were maximal the day following MPTP administration and subsided 3-4 days afterward, being still detectable a week later. The evidence of a parkinsonian-like phenotype at 7

days after intoxication was further confirmed by positive response to DA agonists. L-dopa (1-10 mg/Kg) attenuated MPTP-induced motor impairment in the bar, drag and rotarod tests. Motor testing however disclosed a paradoxical effects of L-dopa, high doses causing exacerbation of parkinsonism. Reports that L-dopa can exacerbate symptoms in patients have been published (Wiener et al., 1978; Jenkins and Pearce, 1992; Merello and Lees, 1992; Cicarelli et al., 2002), but this is the first evidence for a dual motor response to L-dopa in a model of parkinsonism. PPX exerted symptomatic antiparkinsonian effects in MPTP-treated mice by promoting stepping in the drag test. This effect was observed at very low doses but vanished at higher ones. In fact, overt motor inhibition in the bar and rotarod tests emerged at this dose. As for L-dopa, this dual response has not been previously reported for PPX. J-113397 and Trap-101 attenuated parkinsonism in MPTP-treated mice. In addition, Trap-101 synergistically or additively (depending on test) attenuated MPTP-induced akinesia/bradykinesia when combined with L-dopa and PPX. Both antiparkinsonian and pro-akinetic actions of NOP receptor antagonists appeared at much lower doses than those effective in promoting movement naïve mice. This leftward shift of the dose-response curve may be related to up-regulation of N/OFQ transmission following DA depletion (Marti et al., 2005; Di Benedetto et al., 2009). A possible explanation of the dual motor responses of tested drugs calls for a different contribution of D_2 pre- and postsynaptic receptors. The main result of the present study suggests that low doses of a D_2/D_3 receptor antagonist, possibly acting on D_2 (auto)receptors, can reverse it. Indeed, under parkinsonian conditions, DA deafferentation causes compensatory supersensitvity in striatal postsynaptic D_2 receptors, which allows DA agonists to promote movement (Seeman, 2007) outweighing the negative contribution of D_2 autoreceptors. This possibility may be further underpinned by experiments with amisulpride that inhibit D_2 autoreceptors at low doses and block postsynaptic D_2 receptors at higher ones (Scatton et al., 1997; Perrault et al., 1997; Schoemaker et al., 1997). High L-dopa doses not only activate D_2 postsynaptic receptors but also D_2 autoreceptors, leading to a reduction of neurosecretion and firing activity at DA pathways. In this context, reversal of L-dopa motor inhibition into facilitation (bar test) by amisulpride may be explained on the basis of a removal of D_2 autoreceptor inhibition leading to disclosure of a D_2 postsynaptic facilitation. D_3 receptors have been shown to inhibit locomotion (Sautel et al., 1995; Pritchard et al., 2007; Mela et al., 2010). The failure of amisulpride in preventing PPX-induced hypolocomotion remains puzzling. One possible reason could be a suboptimal

antagonist/agonist dose ratio, in view of the poor brain penetrability of amisulpride (Assiè et al., 2006) and the different mechanisms of action of L-dopa and PPX. A major concern regarding possible clinical use of NOP receptor antagonists was that high doses of these compounds caused motor inhibition in MPTP-treated mice. As for L-dopa, amisulpride reversed the pro-akinetic effect of J-113397 and prevented its inhibition of rotarod performance. In addition, it disclosed a J-113397-mediated facilitation in the drag test. This suggests that motor inhibition induced by NOP receptor antagonists is mediated by endogenous DA.

For a more detailed discussion, see original paper V reported in appendix II.

Part III. NOP receptor blockade attenuates parkinsonism in nonhuman primates

The most important finding of the present study is that the NOP receptor antagonist J-113397 reversed motor disabilities in MPTP-treated nonhuman primates. In line with a previous study (Ko et al, 2006), J-113397 did not exert motor effects in naïve macaques up to 1 mg/Kg. However, higher doses (3 mg/Kg) improved arm speed (straight rod test) in two animals while the remaining two could not perform the test, looking distracted and slightly "hallucinated". Although the inconsistency of response prevents from drawing firm conclusions on the role of endogenous N/OFQ, the data obtained in two animals are in line with the view that the peptide plays an inhibitory role on motor activity. Nevertheless, high doses of J-113397 may also activate sigma receptors (Chiou et al., 2007), causing loss of attention and hallucinations (Okuyama et al., 1994). The MPTP-lesioned nonhuman primate (macaque) model reproduces many PD motor symptoms faithfully and is used to assess the therapeutic potential of novel antiparkinsonian drugs (Dauer and Przedborski, 2003). J-113397 was effective, not only in the rodents models of PD, but also in the parkinsonian macaques, overall suggesting that endogenous N/OFQ plays a role in experimental parkinsonism independent of the species and models used. Interestingly, not only did DA loss not prevent the antiparkinsonian action of J-113397 but it also enhanced sensitivity to J-113397, resulting in a leftward shift of the dose-response curve. In parkinsonian macaques, J-113397 was less effective than L-dopa, although it improved hypokinesia comparably to L-dopa, indicating a general depressive effect of endogenous N/OFQ on movement. From a clinical perspective, however, the narrow therapeutic range is quite

disappointing, as the antiparkinsonian effects of 0.01 mg/Kg J-113397 vanished at higher doses, turning into motor inhibition at 1 mg/Kg. It can be proposed that the antiparkinsonian action of J-113397 is mediated by blockade of inhibitory NOP receptors expressed on residual nigral DA cells resulting in increased DA transmission. However, NOP receptor antagonists are effective also under conditions of DA depletion and DA receptor blockade (Marti et al., 2004b; Marti et al., 2005) suggesting that endogenous N/OFQ causes motor depressant responses also via non-DA mechanisms. our data reinforce the view that endogenous N/OFQ plays a role in motor symptoms in parkinsonism across species. Moreover, the efficacy of J-113397 in some MPTP-treated primates raises the possibility of a therapeutic effect of NOP receptor antagonists in PD patients, although the dual action of J-113397 in parkinsonian primates needs to be further characterized (i.e. presynaptic D_2 blockade).
For a more detailed discussion, see original paper II reported in appendix II.

Part IV. NOP receptor deletion protects against MPTP-induced toxicity.

$NOP^{-/-}$ mice had a different motor phenotype than $NOP^{+/+}$ mice. Indeed, at variance with previous studies (Nishi et al., 1997; Murphy et al., 2002; Gavioli et al., 2003; Koizumi et al., 2004), we found that $NOP^{-/-}$ mice had greater exploratory activity, involving movement of the limbs, head and other body muscles. Moreover, $NOP^{-/-}$ mice displayed an increased speed of movement execution and muscle strength. Therefore, NOP receptors tonically activated by endogenous N/OFQ appear to inhibit both spontaneous and exercise-driven motor activity. Endogenous N/OFQ also contributes to symptoms associated with experimental parkinsonism. In fact deletion of the NOP receptor attenuates the MPTP-induced motor impairment. This protective effect was observed in a dynamic context (exercise-driven motor activity) as well as by analyzing spontaneous activity and steps parameters. In these last years, we collected compelling pharmacological (Marti et al., 2004, 2005, 2007, 2008; Viaro et al., 2008, 2010; Mabrouk et al. 2010) and genetic (Marti et al., 2005; Mabrouk et al., 2010) evidence that N/OFQ sustains motor deficit associated with experimental parkinsonism. The role of N/OFQ in parkinsonism, however, may go beyond phenotype modulation. Mice with deletion of the N/OFQ precursor (ppN/OFQ) were found to be partially resistant to MPTP toxicity as shown by less severe loss of nigral DA cells and striatal DA terminals

observed following MPTP in comparison with wild-type controls (Marti et al.,. 2005; Brown et al., 2006). However, different peptides (i.e. N/OFQ, N/OFQ II and nocistatin) are generated by cleavage of the ppN/OFQ precursor (Okuda-Ashitaka and Ito, 2000). These peptides do not bind to the NOP receptor but exert biological activity (Reinscheid et al., 2000), questioning the view that endogenous N/OFQ is the culprit for MPTP-induced neurotoxicity. The stereological cell counting technique has unequivocally demonstrated that endogenous N/OFQ contributes to MPTP toxicity because the deletion of the NOP receptor conferred (partial) resistance to MPTP-induced cells loss. This finding suggests that N/OFQ is involved in the MPTP-induced neurodegeneration, possibly playing a pathogenic role in PD. Therefore, NOP receptor antagonists may be used not only in the symptomatic but also in the neuroprotective treatment of PD.

Part V. Nigral NOP receptors modulate M1 excitability and motor activity

Exogenous N/OFQ produced a dose-dependent, biphasic regulation of motor performance in rats. Inhibition was predominant since it was quantitatively larger and detected in a wider dose-range than facilitation. Conversely, UFP-101 monotonically facilitated motor activity suggesting an inhibitory role for endogenous N/OFQ in motor control. NOP receptor ligands produced changes in M1 output which were consistent with their motor effects. ICMS in layer V of M1 elicits movement via direct stimulation of corticofugal and/or intracortical neurons (Jankowska et al, 1975), resulting in summation of excitatory synaptic potentials in motoneurons and muscle activity. Thus, exogenous N/OFQ biphasically regulated motor cortex excitability, low doses being facilitatory and higher ones inhibitory. Conversely, UFP-101 increased motor cortex excitability (in the forelimb area), suggesting that endogenous N/OFQ tonically inhibits forelimb movement. Both behavioral and electrophysiological effects were evoked by i.c.v. and intranigral, but not intracortical, drug injections, overall suggesting that subcortical NOP receptors regulate motor behavior and motor cortex output via modulation of cortical afferents. Indeed, neither motor output nor behavior was affected by M1 injections of NOP receptor ligands. This indicates that cortical NOP receptors were not involved in local modulation of cortico-fugal neurons and motor activity. Motor impairment has been consistently reported as one of the main biological effects induced by central NOP receptor stimulation in rodents (Nishi et al., 1997; Noda et al.,

1998; Higgins et al., 2001). This study reveals that motor inhibition is associated with a reduction in cortical activity. Inhibition of locomotion was not the only effect induced by central NOP receptor stimulation since very low doses of N/OFQ (0.01 nmol) produced mild but significant facilitation. This facilitation was previously related to the well-known anxiolytic effect of NOP receptor agonists (Jenck et al, 1997). However, the present study points out that the 0.01 nmol N/OFQ-induced facilitation is a specific motor effect. Indeed, i.c.v. N/OFQ enhanced not only motor performance, but also M1 excitability. Moreover, both facilitation in motor performance and increase in M1 excitability was replicated by stimulation of NOP receptors in the SNr, suggesting activation of motor pathways. Despite the fact that exogenous N/OFQ evoked both motor facilitation and inhibition, the latter effect appeared predominant. This is in line with the finding that endogenous N/OFQ physiologically inhibits movement. Indeed, UFP-101, given i.c.v. or injected in SNr, facilitated motor performance and increased M1 excitability. Therefore, the present study suggests that changes in cortical output and behavior are mainly operated by subcortical NOP receptors located in SNr, possibly through modulation of the "cortico-basal ganglia-thalamo-cortical" loop.
For a more detailed discussion, see original paper IV reported in appendix II.

Part VI. Cortical progressive changes in parkinsonian conditions

In recent years, many works have attempted to investigate the relationship between the activity of motor cortex and the progression of PD, although the results have been controversial. The purpose of the present study was to investigate the time-course of changes in the motor cortex following DA depletion induced by unilateral MFB 6-OHDA injection. Knowledge of the rate of M1 changes, particularly during the early phases, is essential for the understanding of the neurobiological mechanisms as well as for the design of experimental trials to evaluate potential treatment strategies. Histological evaluation showed that, beginning 15 days after 6-OHDA lesion, DA loss was complete and stable. Detection of behavioral impairment in hemiparkinsonian rats revealed an important and bilateral akinesia at rest (bar test). Forelimb, trunk and neck were impaired prevalently at the contralateral side (drag and elevated body swings test). To study the short and long term motor cortex reorganization in hemiparkinsonian rats we performed bilateral mapping of M1. ICMS-derived maps of movement

representation in M1 are essentially static and reflect the strength of corticospinal connections. In hemiparkinsonian rats, global cortical excitability was decreased after 6-OHDA lesioning. M1 changes were evident in both the ipsilateral and contralateral hemispheres. M1 reorganization was time-dependent but not in a linear fashion. We found an initial progressive depression (3-15 days) followed by a compensation with a transient increase of excitability (30 days) and a stabilization phase (60-120 days). Moreover, 6-OHDA treatment increased the number of proximal limb movements, demonstrating that M1 loses the ability to evoke fine movements (paw, finger). Several mechanisms may account for the reduction in excitability and movement representations in the motor cortex. First, an altered pattern of neuronal discharge in the basal ganglia may led to abnormalities in M1 preventing the facilitation of cortical excitability required to induce ICMS-evoked movements. Since lidocaine normalized the ratio between contralateral and ipsi-bilateral forelimb movements in the lesioned side, we can conclude that the increase of ipsi-bilateral forelimb movements in the lesioned side is due to a transcallosal activity. This aspect underpinned the importance of the compensatory role of the homotopic contralateral cortex (Maggiolini et al., 2008). In humans, interhemispheric connections are thought to play a crucial role in motor control by ensuring a spatially and temporally coordinated recruitment of a set of muscles (Devanne et al, 2006). Under parkinsonian conditions the role of interhemispheric connections may thus be altered. Response to L-dopa revealed that cortical changes induced by 6-OHDA lesioning were, at least partially, generated by DA deficiency. Indeed, systemic L-dopa totally restored the size in the vibrissa and caudal forelimb area, but was ineffective in promoting similar changes at the rostral forelimb area. Previous studies (Marti et al., 2005, 2007) demonstrated that 6 mg/Kg L-dopa was effective in increasing the motor performance in 6-OHDA-treated rats. Consistently, a recent study revealed a modulatory role for DA upon the rostral forelimb region excitability (Hosp et al., 2009). Pyramidal neurons of the motor areas are considered to be under the control of thalamo-cortical afferents (Kuramoto et al., 2009). After DA depletion, a loss of the normal thalamic modulation on pyramidal cells is observed due to an increase in nigro-thalamic GABAergic pathway discharge. This may the probability of pyramidal cells to reach ICMS-induced activity. In the present model of PD, 6-OHDA injection may also affect DA tegmental neurons causing a reduction of the facilitatory action of DA on M1 pyramidal neurons. Indeed, the motor cortex receives DA projections arising from the ventral tegmental region (i.e. the mesocortical

pathway; Seamans and Yang, 2004). Finally, experiments with bicuculline showed that M1 changes are also due to an increase in intracortical GABAergic inhibition. In fact, intracortical application of bicuculline at a subconvulsive concentration ensuring full GABA receptor blockade (Stojic et al., 2008), increased the number of excitable sites in the rostral forelimb area, a region were L-dopa was ineffective. In normal conditions, endogenous cortical GABA is critically placed to maintain the form of motor representations (Benali et al., 2008). In 6-OHDA rats, endogenous GABAergic transmission in this area gets stronger than in other regions of M1 and this cortical GABAergic influence may account for dysruptions of cortical activity. Overall, this study provides evidence that dynamic remodelling of movement representation occurs in the motor cortex of hemi-parkinsonian rats. For the first time, ICMS technique could be proved useful to predict the effectiveness of classical and potential antiparkinsonian therapeutics.

Acknowledgments

I gratefully thank Michele Morari and his collaborator Matteo Marti for their teachings during studies. I am grateful to Gianfranco Franchi and his collaborator Emma Maggiolini for his assistance in the electrophysiological experiments. I am also grateful to Erwan Bezard and Pierre-Olivier Fernagut for their help in the learning the stereological counting. Finally, I gratefully acknowledge the contribution of Stefania Carretta, Anna Secchiero, Laura Cioni and Riccardo Libralesso in the acquisition of experimental data.

References

Agid Y, Bonnet AM, Ruberg M, Javoy-Agid F (1985). Pathophysiology of L-dopa-induced abnormal involuntary movements. Psychopharmacology 2: 145-159.

Albin RA, Young AB, Penney B (1989). The functional anatomy of the basal ganglia disorders. Trends Neurosci 12: 366-375.

Alexander GE, DeLong MR, Strick PL (1986). Parallel organization of functionally segregated circuits linking basal ganglia and cortex. Annu Rev Neurosci 9: 357-381.

Alexander GE, Crutcher MD (1990). Functional architecture of basal ganglia circuits: neural substrates of parallel processing. Trends Neurosci 13: 266-271.

Ashkan K,Wallace B, Bell BA,Benabid AL (2004). Deep brain stimulation of the subthalamic nucleus in Parkinson's disease 1993-2003: where are we 10 years on? Br J Neurosurg 18: 19-34.

Assié MB, Dominguez H, Consul-Denjean N, Newman-Tancredi A (2006). In vivo occupancy of dopamine D2 receptors by antipsychotic drugs and novel compounds in the mouse striatum and olfactory tubercles. Naunyn Schmiedebergs Arch Pharmacol 373: 441-450.

Barcia C, Bautista V, Sanchez-Bahillo A, Fernandez-Villalba E, Navarro-Ruis JM, Barreiro AF, Poza YP, Herrero MT (2003). Circadian determinations of cortisol, prolactin and melatonin in chronic methyl-phenyl-tetrahydropyridine-treated monkeys. Neuroendocrin 78: 118-128.

Benali A, Weiler E, Benali Y, Dinse HR, Eysel UT (2008). Excitation and inhibition jointly regulate cortical reorganization in adult rats. J Neurosci 28: 12284-12293.

Bezard E, Dovero S, Belin D, Duconger S, Jackson-Lewis V, Przedborski S, Piazza PV, Gross CE, Jaber M (2003). Enriched environment confers resistance to 1-methyl-4-phenyl-1,2,3,6- tetrahydropyridine and cocaine: involvement of dopamine transporter and trophic factors. J Neurosci 23: 10999–11007.

Birkmayer W, Riederer P, Youdim MB, Linauer W (1975). The potentiation of the anti akinetic effect after L-dopa treatment by an inhibitor of MAO-B, Deprenil. J Neural Transm 36: 303-326.

Bouwman BM, van Lier H, Nitert HE, Drinkenburg WH, Coenen AM, van Rijn CM (2005). The relationship between hippocampal EEG theta activity and locomotor behaviour in freely moving rats: effects of vigabatrin. Brain Res Bull 64: 505-509.

Braak H, Del Tredici K, Rüb U, de Vos RA, Jansen Steur EN, Braak E (2003). Staging of brain phatology related to sporadic Parkinson's disease. Neurobiol Aging 24: 197-210.

Brecht M, Krauss A, Muhammad S, Sinai-Esfahani L, Bellanca S, Margrie TW (2004). Organization of rat vibrissa motor cortex and adjacent areas according to cytoarchitectonics, microstimulation, and intracellular stimulation of identified cells. J Comp Neurol 479: 360-373.

Brown JM, Gouty S, Iyer V, Rosenberger J, Cox BM (2006). Differential protection against MPTP or methamphetamine toxicity in dopamine neurons by deletion of ppN/OFQ expression. J Neurochem 98: 495-505.

Brown AR, Hu B, Antle MC, Teskey GC (2009). Neocortical movement representations are reduced and reorganized following bilateral intrastriatal 6-hydroxydopamine infusion and dopamine type-2 receptor antagonism. Exp Neurol 220: 162-170.

Buhmann C, Glauche V, Stürenburg HJ, Oechsner M, Weiller C, Büchel C (2003). Pharmacologically modulated fMRI--cortical responsiveness to levodopa in drug-naive hemiparkinsonian patients. Brain 126: 451-461.

Calne DB (1993). Treatment of Parkinson's disease. N Engl J Med 329: 1021-1027.

Calo' G, Rizzi A, Rizzi D, Bigoni R, Guerrini R, Marzola G, Marti M, McDonald J, Morari M, Lambert DG, Salvadori S, Regoli D (2002). [Nphe1,Arg14,Lys15] nociceptin-NH2, a novel potent and selective antagonist of the nociceptin/orphanin FQ receptor. Br J Pharmacol 136: 303-311.

Calo' G, Rizzi A, Cifani C, Micioni Di Bonaventura MV, Regoli D, Massi M, Salvatori S, Lambert DG, Guerrini R (2010). UFP-112 a potent and long-lasting agonist selective for the nociceptin/orphanin FQ receptor. CNS Neurosci Ther, in press.

Carlsson A (2002). Treatment of Parkinson's with L-DOPA. The early discovery phase, and a comment on current problems. J Neural Transm 109: 777-787.

Carter AJ, Müller RE (1991). Pramipexole, a dopamine D2 autoreceptor agonist, decreases the extracellular concentration of dopamine in vivo. Eur J Pharmacol 200: 65-72.

Chia LG, Ni DR, Cheng LJ, Kuo JS, Cheng FC, Dryhurst G (1996). Effects of 1-methyl-4-phenyl-1,2,3,6-tetrahydropyridine and 5,7 dihydroxytryptamine on the locomotor activity and striatal amines in C57BL/6 mice. Neurosci Lett 218: 67-71.

Chiou LC, Liao YY, Fan PC, Kuo PH, Wang CH, Riemer C, Prinssen EP (2007). Nociceptin/orphanin FQ peptide receptors: pharmacology and clinical implications. Curr Drug Targets 8: 117-135.

Cicarelli G, Pellecchia MT, De Michele G, Pizzolato G, Barone P (2002). Paradoxical response to apomorphine in a case of atypical parkinsonism. Mov Disord 17: 604-606.

Clark D, White FJ (1997). D1 dopamine receptor--the search for a function: a critical evaluation of the D1/D2 dopamine receptor classification and its functional implications. Synapse 1: 347-388.

Colotla VA, Flores E, Oscos A, Meneses A, Tapia R (1990). Effects of MPTP on locomotor activity in mice. Neurotoxicol Teratol 4: 405-407.

Cox BM, Cavkin C, Christie MJ, Civelli O, Evans C, Hamon MD, Hoellt V, Kieffer B, Kitchen I, McNight AT, Meunier JC, Portoghese PS (2000). In the IUPHAR Compendium of Receptor Characterization and Classification. Ed. Girdlestone, D London: IUPHAR Media Ltd.

Darland T, Heinricher MM, Grandy DK (1998). Orphanin FQ/nociceptin: a role in pain and analgesia, but so much more. Trend Neurosci 21: 215-221.

Dauer W, Przedborski S (2003). Parkinson's disease: mechanisms and models. Neuron 39: 889-909.

DeLong MR (1990). Primate models of movement disorders of basal ganglia origin. Trends Neurosci 13: 281-285.

Devanne H, Cassim F, Ethier C, Brizzi L, Thevenon A, Capaday C (2006). The comparable size and overlapping nature of upper limb distal and proximal muscle representations in the human motor cortex. Eur J Neurosci 23: 2467-2476.

Devine DP, Taylor L, Reinscheid RK, Monsma FJ Jr, Civelli O, Akil H (1996). Rats rapidly develop tollerance to the locomotor-inhibiting effects of the novel neuropeptide orphanin FQ. Neurochem Res 21: 1387-1396.

Di Benedetto M, Cavina C, D'Addario C, Leoni G, Candeletti S, Cox BM, Romualdi P (2009). Alterations of N/OFQ and NOP receptor gene expression in the substantia nigra and caudate putamen of MPP+ and 6-OHDA lesioned rats. Neuropharmacology 56: 761-767.

Dick JP, Cowan JM, Day BL, Berardelli A, Kachi T, Rothwell JC, Marsden CD (1984). The corticomotoneurone connection is normal in Parkinson's disease. Nature 310: 407-409.

Donoghue JP, Wise SP (1982). The motor cortex of the rat: cytoarchitecture and microstimulation mapping. J Comp Neurol 212: 76-88.

Donoghue JP (1995). Plasticity of adult sensorimotor representations. Curr Opin Neurobiol 5: 749-754.

Duvoisin RC (1967). Cholinergic-anticholinergic antagonism in parkinsonism. Arch Neurol 17: 124-136.

Emborg ME (2007). Nonhuman Primate Models of Parkinson's Disease ILAR J 48: 339-355.

Escola L, Michelet T, Douillard G, Guehl D, Bioulac B, Burbaud P (2002). Disruption of the proprioceptive mapping in the medial wall of parkinsonian monkeys. Ann Neurol 52: 581-587.

Escola L, Michelet T, Macia F, Guehl D, Bioulac B, Burbaud P (2003). Disruption of information processing in the supplementary motor area of the MPTP-treated monkey: a clue to the pathophysiology of akinesia? Brain 126: 95-114.

Factor SA (2008). Current status of symptomatic medical therapy in Parkinson's disease. Neurotherapeutics 5: 164-180.

Florin S, Suaudeau C, Meunier JC, Costentin J (1996). Nociceptin stimulates locomotion and exploratory behaviour in mice. Eur J Pharmacol 317: 9-13.

Franchi G (2000). Reorganization of vibrissal motor representation following severing and repair of the facial nerve in adult rats. Exp Brain Res 131: 33-43.

Fredriksson A, Plaznik A, Sundström E, Archer T (1994). Effects of D1 and D2 agonists on spontaneous motor activity in MPTP treated mice. Pharmacol Toxicol 75: 36-41.

Galvan A, Wichmann T (2008). Pathophysiology of parkinsonism. Clin Neurophysiol 119: 1459-1474.

Gavioli EC, Marzola G, Guerrini R, Bertorelli R, Zucchini S, De Lima TC, Rae GA, Salvadori S, Regoli D, Calo G. 2003 Blockade of nociceptin/orphanin FQ-NOP receptor signalling produces antidepressant-like effects: pharmacological and genetic evidences from the mouse forced swimming test. Eur J Neurosci17: 1987-1990.

George JL, Mok S, Moses D, Wilkins S, Bush AI, Cherny RA, Finkelstein DI (2009). Targeting the progression of Parkinson’s disease. Curr Neuropharmacol 7: 9-36.

Gerfen CR, Engber TM, Mahan LC, Susel Z, Chase TN, Monsma FJ Jr, Sibley DR (1990). D1 and D2 dopamine receptor-regulated gene expression of striatonigral and striatopallidal neurons. Science 250: 1429-1432.

Glinka Y, Gassen M, Youdim MB (1997). Mechanism of 6-hydroxydopamine neurotoxicity. J Neural Transm 50: 55-66.

Glinka Y, Tipton KF, Youdim MB (1996). Nature of inhibition of mitochondrial respiratory complex I by 6-Hydroxydopamine. J Neurochem 66: 2004-2010.

Glinka Y, Youdim MB (1995). Inhibition of mitochondrial complexes I and IV by 6-hydroxydopamine. Eur J Pharmacol 292. 329-332.

Goldstein DS, Li ST, Holmes C, Bankiewicz K (2003). Sympathetic innervation in the 1-methyl-4-phenyl-1,2,3,6-tetrahydropyridine primate model of Parkinson's disease. J Pharmacol Exp Ther 306: 855-860.

Graziano MSA, Taylor CSR, Moore T, Cooke DF (2002). The cortical control of movement revisited. Neuron 36: 349-362.

Gross CE, Ravenscroft P, Dovero S, Jaber M, Bioulac B, Bezard E (2003). Pattern of levodopa-induced striatal changes is different in normal and MPTP-lesioned mice. J Neurochem 84: 1246–1255.

Haobam R, Sindhu KM, Chandra G, Mohanakumar KP (2005). Swim-test as a function of motor impairment in MPTP model of Parkinson's disease: a comparative study in two mouse strains. Behav Brain Res 163: 159-167.

Henderson JM, Stanic D, Tomas D, Patch J, Horne MK, Bourke D, Finkelstein DI (2005). Postural changes after lesions of the substantia nigra pars reticulata in hemiparkinsonian monkeys. Behav Brain Res 160: 267-276.

Higgins GA, Grottick AJ, Ballard TM, Richards JG, Messer J, Takeshima H, Pauly-Evers M, Jenck F, Adam G, Wichmann J (2001). Influence of the selective ORL1 receptor agonist, Ro64-6198, on rodent neurological function. Neuropharmacology 41: 97-107.

Homberg JR, Mul JD, de Wit E, Cuppen E (2009). Complete knockout of the nociceptin/orphanin FQ receptor in the rat does not induce compensatory changes in mu, delta and kappa opioid receptors. Neuroscience 163: 308-315.

Hornykiewicz O (2002). L-DOPA: from a biologically inactive amino acid to a successful therapeutic agent. Amino Acids 23: 65-70.

Hosp JA, Molina-Luna K, Hertler B, Atiemo CO, Luft AR (2009). Dopaminergic modulation of motor maps in rat motor cortex: an in vivo study. Neuroscience 159: 692-700.

Huang C, Tang C, Feigin A, Lesser M, Ma Y, Pourfar M, Dhawan V, Eidelberg D (2007). Changes in network activity with the progression of Parkinson's disease. Brain 130: 1834-1846.

Irizarry MC, Growdon W, Gomez-Isla T, Newell K, George JM, Clayton DF, Hyman BT (1998). Nigral and cortical Lewy bodies and dystrophic nigral neurites in Parkinson's disease and cortical Lewy body disease contain alpha-synuclein immunoreactivity. J Neuropathol Exp Neurol 57: 334-337.

Itzhak Y, Martin JL, Black MD, Ali SF (1999). Effect of the dopaminergic neurotoxin MPTP on cocaine-induced locomotor sensitization. Pharmacol Biochem Behav 63: 101-107.

Jackson-Lewis V, Przedborski S (2007). Protocol for the MPTP mouse model of Parkinson’s disease. Nat Protoc 1: 141-151.

Jankowska E, Padel Y, Tanaka R (1975). The mode of activation of pyramidal tract cells by intracortical stimuli. J Physiol 249: 617-636.

Jenck F, Moreau J, Martin J, Kilpatrick G, Reinschied RK, Monsma FJ Jr, Nothaker H., Civelli O (1997). Orphanin FQ acts as an anxiolitic to attenuate behavioural responses to stress. Proc Natl Acad Sci 94: 14854-14858.

Jenkins JR, Pearce JM (1992). Paradoxical akinetic response to apomorphine in parkinsonism. J Neurol Neurosurg Psychiatry 55: 414-415.

Jenkins BG, Sanchez-Pernaute R, Brownell AL (2004). Mapping dopamine function in primates using pharmacologic magnetic resonance imaging. J Neurosci 24: 9553-9560.

Jenner P, Mori A, Hauser R, Morelli M, Fredholm BB, Chen JF (2009). Adenosine, adenosine A 2A antagonists, and Parkinson's disease. Parkinsonism Relat Disord 15: 406-413.

Kawamoto H, Ozaki S, Itoh Y, Miyaji M, Arai S, Nakashima H, Kato T, Ohta H, Iwasawa Y (1999). Discovery of the fist potent and selective small molecule opioid receptor-like (ORL-1) antagonist: 1-[(3R,4R)-1-cyclooctymethyl-3-hydroxymethyl-4-piperidyl]-3-ethyl-1,3-diydro-2H-benzimidazol-2-one (J-113397). J Med Chem 42: 5061-5063.

Kirik D, Rosenblad C, Björklund A. 1998. Characterization of behavioral and neurodegenerative changes following partial lesions of the nigrostriatal dopamine system induced by intrastriatal 6-hydroxydopamine in the rat. Exp Neurol 152: 259-277.

Klapdor K, Dulfer BG, Hamman A, Van der Staay FJ (1997). A low-cost method to analise footprints patterns. J. Neurosci. Methods 75. 49-54.

Ko MC, Wie H, Woods JH, Kennedy RT (2006). Effects of intrathecally administered nociceptin/orphanin FQ in monkeys: behavioral and mass spectrometric studies. J Pharmacol Exp Ther 318. 1257-1264.

Koizumi M, Sakoori K, Midorikawa N, Murphy NP (2004). The NOP (ORL1) receptor antagonist Compound B stimulates mesolimbic dopamine release and is rewarding in mice by a non-NOP-receptor-mediated mechanism. Br J Pharmacol 143: 53-62.

Köster A, Montkowski A, Schulz S, Stübe EM, Knaudt K, Jenck F, Moreau JL, Nothacker HP, Civelli O, Reinscheid RK (1999). Targeted disruption of the orphanin FQ/nociceptin gene increases stress susceptibility and impairs stress adaptation in mice. Proc Natl Acad Sci USA 96: 10444-10449.

Kumar VL, Sehgal R (2007). Calotropis procera latex-induced inflammatory hyperalgesia - effect of bradyzide and morphine. Auton Autacoid Pharmacol 27: 143-149.

Kuramoto E, Furuta T, Nakamura KC, Unzai T, Hioki H, Kaneko T (2009). Two types of thalamocortical projections from the motor thalamic nuclei of the rat: a single neuron-tracing study using viral vectors. Cereb Cortex 19: 2065-2077.

Kuzmin A, Sandin J, Terenius L, Ogren SO (2004). Evidence in locomotion test for the functional heterogeneity of ORL-1 receptors. Br J Pharmacol 141: 132-140.

Lambert DG (2008). The nociceptin/orphanin FQ receptor: a target with broad therapeutic potential. Nat Rev Drug Discov 7: 694-710.

Langston JW, Ballard P, Tetrud JW, Irwin I (1983). Chronic Parkinsonism in humans due to a product of meperidine-analog synthesis. Science 219: 979-980.

Laursen SE, Belknap JK (1986). Intracerebroventricular injections in mice. Some methodological refinements. J Pharmacol Methods 16: 355-357.

Lee J, Zhu WM, Stanic D, Finkelstein DI, Horne MH, Henderson J, Lawrence AJ, O'Connor L, Tomas D, Drago J, Horne MK (2008). Sprouting of dopamine terminals and altered dopamine release and uptake in Parkinsonian dyskinaesia. Brain 131: 1574-1587.

Lefaucheur JP (2005). Motor cortex dysfunction revealed by cortical excitability studies in Parkinson's disease: influence of antiparkinsonian treatment and cortical stimulation. Clin Neurophysiol 116: 244-253.

Mabrouk OS, Marti M, Morari M (2010). Endogenous nociceptin/orphanin FQ (N/OFQ) contributes to haloperidol-induced changes of nigral amino acid transmission and parkinsonism: a combined microdialysis and behavioral study in naïve and nociceptin/orphanin FQ receptor knockout mice. Neuroscience 166: 40-48.

Maggiolini E, Viaro R, Franchi G (2008). Suppression of activity in the forelimb motor cortex temporarily enlarges forelimb representation in the homotopic cortex in adult rats. Eur J Neurosci 27: 2733-2746.

Maj J, Rogóz Z, Skuza G, Kołodziejczyk K (1997). The behavioural effects of pramipexole, a novel dopamine receptor agonist. Eur J Pharmacol 324: 31-37.

Marti M, Mela F, Bianchi C, Beani L, Morari M (2002). Striatal dopamine-NMDA receptor interactions in the modulation of glutamate release in the substantia nigra pars reticulata in vivo: opposite role for D1 and D2 receptors. J Neurochem 83: 635-644.

Marti M, Mela F, Veronesi C, Mela F, Veronesi C, Guerrini R, Salvadori S, Federici M, Mercuri NB, Rizzi A, Franchi G, Beani L, Bianchi C, Morari M (2004a). Blockade of nociceptin/orphanin FQ receptor signalling in rat substantia nigra pars reticulata stimulates nigrostriatal dopaminergic transmission and motor behaviour. J Neurosci 24: 6659-6666.

Marti M, Mela F, Guerrini R, Calo' G, Bianchi C, Morari M (2004b). Blockade of nociceptin/orphanin FQ transmission in rat substantia nigra reverses haloperidol-induced akinesia and normalizes nigral glutamate release. J Neurochem 91: 1501–1504.

Marti M, Mela F, Fantin M, Zucchini S, Brown JM, Witta J, Di Benedetto M, Buzas B, Reinscheid RK, Salvadori S, Guerrini R, Romualdi P, Candeletti S, Simonato M, Cox BM, Morari M (2005). Blockade of nociceptin/orphanin FQ transmission attenuates symptoms and neurodegeneration associated with Parkinson's disease. J Neurosci 95: 9591-9601.

Marti M, Trapella C, Viaro R, Morari M (2007). The Nociceptin/Orphanin FQ Receptor antagonist J-113397 and L-Dopa additively attenuate experimental parkinsonism through overinhibition of the nigrothalamic pathway. J Neurosci 27: 1297-1307.

Marti M, Trapella C, Morari M (2008). The novel nociceptin/orphanin FQ receptor antagonist Trap-101 alleviates experimental parkinsonism through overinhibition of

the nigro-thalamic pathway: positive interaction with L-DOPA. J Neurochem 107: 1683-1696.

Marti M, Viaro R, Guerrini R, Franchi G, Morari M (2009). Nociceptin/orphanin FQ modulates motor behavior and primary motor cortex output through receptors located in substantia nigra reticulata. Neuropsychopharmacology 34: 341-355.

Mela F, Millan MJ, Brocco M, Morari M (2010). The selective D(3) receptor antagonist, S33084, improves parkinsonian-like motor dysfunction but does not affect L-DOPA-induced dyskinesia in 6-hydroxydopamine hemi-lesioned rats. Neuropharmacology 58: 528-536.

Merello M, Lees AJ (1992). Beginning-of-dose motor deterioration following the acute administration of levodopa and apomorphine in Parkinson's disease. J Neurol Neurosurg Psychiatry 55. 1024-1026.

Metz GA, Piecharka DM, Kleim JA, Whishaw IQ (2004). Preserved ipsilateral-to-lesion motor map organization in the unilateral 6-OHDA-treated rat model of Parkinson's disease. Brain Res 1026: 126-135.

Meunier JC, Mollerau C, Toll L, Saudeau C, Moisand C, Alvinerie P, Butour J, Guillemont JC, Ferrara P, Monsarrat B, Mazaguil H, Vassart G, Parmentier M, Constentin J (1995). Isolation and structure of the endogenus agonist of opioid receptor-like ORL1 receptor. Nature 377: 532-535.

Meyer OA, Tilson HA, Byrd WC, Riley MT (1979). A method for the routine assessment of fore- and hindlimb grip strength of rats and mice. Neurobehav Toxicol 1: 233-236.

Mierau J, Schingnitz G (1992). Biochemical and pharmacological studies on Pramipexole, a potent and selective dopamine D_2 receptor agonist. Eur J Pharmacol 215: 161-170.

Millan MJ, Seguin L, Gobert A, Cussac D, Brocco M (2004). The role of dopamine D3 compared with D2 receptors in the control of locomotor activity: a combined behavioural and neurochemical analysis with novel, selective antagonists in rats. Psychopharmacology (Berl) 174: 341-357.

Miller DB, Reinhard JF Jr, Daniels AJ, O'Callaghan JP (1991). Diethyldithiocarbamate potentiates the nuerotoxicity of in vivo 1-methyl-4-phenyl-1,2,3,6-tetrahydropyridine and of in vitro 1-methyl-4-phenylpyridinium. J Neurochem 57: 541-549.

Mogil JS, Pasternak GW (2001). The molecular and behavioral pharmacology of the orphanin FQ/nociceptin peptide and receptor family. Pharmacological Reviews 53: 381-415.

Mollereau C, Parmentier M, Mailleux P, Butour JL, Moisand C, Chalon P, Caput D, Vassart G, Meunier JC (1994). ORL1, a novel member of the opioid receptor family. Cloning, functional expression and localization. FEBS Lett 341: 33-38.

Morari M, Sbrenna S, Marti M, Caliari C, Bianchi C, Beani L (1998). NMDA and non-NMDA ionotropic glutamate receptors modulate striatal acetylcholine release via pre- and postsynaptic mechanisms. J Neurochem 71: 2006-2017.

Murphy NP, Maidment NT (1999). Orphanin FQ/nociceptin modulation of mesolimbic dopamine transmission determined by microdialisis. J Neurochem 73: 179-186.

Murphy NP, Lam HA, Chen Z, Pintar JE, Maidment NT (2002). Heroin-induced locomotion and mesolimbic dopamine release is unchanged in mice lacking the ORL.1 receptor gene. Brain Res. 953:276-280.

Narayanan S, Lam H, Carroll FI, Lutfy K (2004). Orphanin FQ/nociceptin suppresses motor activity through an action along the mesoaccumbens axis in rats. J Psychiatry Neurosci 29: 116-123.

Neal CR Jr, Mansour A, Reinscheid R, Nothacker HP, Civelli O, Akil H, Watson SJ Jr (1999). Opioid receptor-like (ORL1) receptor distribution in the rat central nervous system: comparison of ORL1 receptor mRNA expression with (125)I-[(14)Tyr]-orphanin FQ binding. J Comp Neurol 412: 563-605.

Nishi K, Kondo T, Narabayashi H (1991). Destruction of norephinephrine terminals in 1-methyl-4-phenyl-1,2,3,6-tetrahydropyridine (MPTP)-treated mice reduces locomotor activity induced by L-Dopa. Neurosci Lett 123: 244-247.

Nishi M, Houtani T, Noda Y, Mamiya T, Sato K, Doi T, Kuno J, Takeshima H, Nukada T, Nabeshima T, Yamashita T, Noda T, Sugimoto T (1997). Unrestrained nociceptive response and disregulation of hearing ability in mice lacking the nociceptin/orphaninFQ receptor. EMBO J 16: 1858-1864.

Noda Y, Mamiya T, Nabeshima T, Nishi M, Higashioka M, Takeshima H (1998). Loss of antinociception induced by naloxone benzoylhydrazone in nociceptin receptor-knockout mice. J Biol Chem 273: 18047-18051.

Obeso JA, Rodríguez-Oroz MC, Rodríguez M, Lanciego JL, Artieda J, Gonzalo N, Olanow CW (2000). Pathophysiology of the basal ganglia in Parkinson's disease. Trends Neurosci 23: 8-19.

Obeso JA, Rodriguez-Oroz M, Marin C, Alonso F, Zamarbide I, Lanciego JL, Rodriguez-Diaz M (2004). The origin of motor fluctuations in Parkinson's disease: importance of dopaminergic innervation and basal ganglia circuits. Neurology 62: 17-30.

Okuda-Ashitaka E, Ito S (2000). Nocistatin: a novel neuropeptide encoded by the gene for the nociceptin/orphanin FQ precursor. Peptides 21: 1101-1109.

Okuyama S, Imagawa Y, Sakagawa T, Nakazato A, Yamaguchi K, Katoh M, Yamada S, Araki H, Otomo S (1994). NE-100, a novel sigma receptor ligand: effect on phencyclidine-induced behaviors in rats, dogs and monkeys. Life Sci 55: 133-138.

Olanow CW (1993). A radical hypothesis for neurodegeneration. Trends Neurosci, 16, 439-444.

Olanow CW, McNaught KS (2006). Ubiquitin-proteasome system and Parkinson's disease. Mov Disord 21: 1806-1823.

Parr-Brownlie LC, Hyland BI (2005). Bradykinesia induced by dopamine D2 receptor blockade is associated with reduced motor cortex activity in the rat. J Neurosci 25: 5700-5709.

Paxinos G, Watson C (1982). The rat brain in stereotaxic coordinates. Sydney: Academic Press.

Paxinos G, Franklin K (2003). The mouse brain in stereotaxic coordinates. Elsevier San Diego Academic Press.

Pelled G, Bergman H, Goelman G (2002). Bilateral overactivation of the sensorimotor cortex in the unilateral rodent model of Parkinson's disease - a functional magnetic resonance imaging study. Eur J Neurosci 15: 389-394.

Perrault GH,. Scatton B, Sanger DJ, Morel E, and Depoortere R (1997) Psychopharmacological profile of amisulpride: an antipsychotic drug with presynaptic D_2/D_3 dopamine receptor antagonist activity and limbic selectivity. J Pharmacol Exp Ther 280: 73-82.

Polymeropoulos MH, Higgins JJ, Golbe LI, Johnson WG, Ide SE, Di Iorio G, Sanges G, Stenroos ES, Pho LT, Schaffer AA, Lazzarini AM, Nussbaum RL, Duvoisin RC (1996). Mapping of a gene for Parkinson's disease to chromosome 4q21-q23. Science 274: 1197-1199.

Pritchard LM, Newman AH, McNamara RK, Logue AD, Taylor B, Welge JA, Xu M, Zhang J, Richtand NM (2007). The dopamine D3 receptor antagonist NGB 2904

increases spontaneous and amphetamine-stimulated locomotion. Pharmacol Biochem Behav 86. 718-726.

Przedborski S, Jackson-Lewis V, Djaldetti R, Liberatore G, Vila M, Vukosavic S, Almer G (2000). The parkinsonian toxin MPTP: action and mechanism. Restor Neurol Neurosci 16: 135-142.

Radad K, Gille G, Rausch WD (2005). Short review on dopamine agonists: insight into clinical and research studies relevant to Parkinson's disease. Pharmacol Rep 57: 701-712.

Reischeid RK, Nothacker HP, Burson A, Adati A, Henningens RA, Bunzow JR, Grandy DK, Langen H, Monsma FJ Jr, Civelli O (1995). Orphanin FQ: a neuropeptide that activates an opioid-like G protein-coupled receptor. Science 270: 792-794.

Reinscheid RK, Nothacker H, Civelli O (2000). The orphanin FQ/nociceptin gene: structure, tissue distribution of expression and functional implications obtained from knockout mice. Peptides 21: 901-906.

Rizzi A, Marzola G, Bigoni R, Guerrini R, Salvadori S, Mogil JS, Regoli D, Calo' G (2001). Endogenous nociceptin signaling and stress-induced analgesia. Neuroreport 12: 3009-3013.

Rozas G, Guerra MJ, Labandeira-Garcia JL (1997). An automated rotarod method for quantitative drug-free evaluation of overall motor deficits in rat models of parkinsonism. Brain Res Brain Res Protoc 2: 75-84.

Ruottinen HM, Rinne UK (1998). COMT inhibition in the treatment of Parkinson's disease. J Neurol 245: 25-34.

Sabatini U, Boulanouar K, Fabre N, Martin F, Carel C, Colonnese C, Bozzao L, Berry I, Montastruc JL, Chollet F, Rascol O (2000). Cortical motor reorganization in akinetic patients with Parkinson's disease: a functional MRI study. Brain 123: 394-403.

Sanberg PR, Bunsey MD, Giordano M, Norman AB (1988). The catalepsy test: its ups and downs. Behav Neurosci 102: 748-759.

Sanchez-Pernaute R, Jenkins BG, Choi JK, Iris Chen YG, Isacson O (2007). In vivo evidence of D3 dopamine receptor sensitization in parkinsonian primates and rodents with l-DOPA-induced dyskinesias. Neurobiol Dis 27 : 220-227.

Sanes JN, Suner S, Donoghue JP (1990). Dynamic organization of primary motor cortex output to target muscles in adult rats. I. Long-term pattern of reorganization following motor or mixed peripheral nerve lesion. Exp Brain Res 79: 479-491.

Sautel F, Griffon N, Sokoloff P, Schwartz JC, Launay C, Simon P, Costentin J, Schoenfelder A, Garrido F, Mann A, Wermuth CG (1995). Nafadotride, a potent preferential dopamine D3 receptor antagonist, activates locomotion in rodents. J Pharmacol Exp Ther 275: 1239–1246.

Scatton B, Claustre Y, Cudennec A, Oblin A, Perrault G, Sanger DJ, et al. (1997). Amisulpride: From Animal Pharmacology To Therapeutic Action. International Clinical Psychopharmacology 12: 29-36.

Schallert T, De Ryck M, Whishaw IQ, Ramirez VD, Teitelbaum P (1979). Excessive bracing reactions and their control by atropine and L-DOPA in an animal analog of Parkinsonism. Exp Neurol 64: 33-43.

Schieber MH (2001). Constraints on somatotopic organization in the primary motor cortex. J Neurophysiol 86: 2125-2143.

Sedelis M, Hofele K, Auburger GW, Morgan S, Huston JP, Schwarting RKW (2000). Evidence for resistance to MPTP in C57BL/6 × BALB/c F1 hybrids as compared with their progenitor strains. Neuroport 11: 1093-1096.

Seiss E, Praamstra P (2004). The basal ganglia and inhibitory mechanisms in response selection: evidence from subliminal priming of motor responses in Parkinson's disease. Brain 127: 330-339.

Schoemaker H, Claustre Y, Fage D, Rouquier L, Chergui K, Curet O, Oblin A, Gonon F, Carter C, Benavides J, Scatton B (1997). Neurochemical characteristics of amisulpride, an atypical dopamine D2/D3 receptor antagonist with both presynaptic and limbic selectivity. J Pharmacol Exp Ther 280: 83-97.

Sedelis M, Schwarting RKW, Huston JP (2001). Behavioral phenotyping of the MPTP mouse model of Parkinson's disease. Behav. Brain Res 125: 109-125.

Seamans JK, Yang CR (2004). The principal features and mechanisms of dopamine modulation in the prefrontal cortex. Prog Neurobiol 74: 1-58.

Seeman P (2007). Antiparkinson therapeutic potencies correlate with their affinities at dopamine D2(High) receptors. Synapse 61: 1013-1018.

Siuciak JA, Fujiawara RA (2004). The activity of pramipexole in the mouse forced swim test is mediated by D_2 rather than D_3 receptors. Psychopharmacology 175: 163-169.

Smeyne RJ, Jackson-Lewis V (2005). The MPTP model of Parkinson's disease. Brain Res Mol Brain Res 134: 57-66.

Stephenson DT, Meglasson MD, Connell MA, Childs MA, Hajos-Korcsok E, Emborg ME (2005). The effects of a selective dopamine D_2 receptor agonist on behavioral and pathological outcome in 1-methyl-4-phyenyl-1,2,3,6-tetrahydropyridine-treated squirrel monkeys. J Pharm Exp Ther 314: 1-10.

Stojic AS, Lane RD, Killackey HP, Rhoades RW (2000). Suppression of hindlimb inputs to S-I forelimb-stump representation of rats with neonatal forelimb removal: GABA receptor blockade and single-cell responses. J Neurophysiol 83: 3377-3387.

Taylor JR, Elsworth JD, Lawrence MS, Sladek JR Jr, Roth RH, Redmond DE Jr (1999). Spontaneous blink rates correlate with dopamine levels in the caudate nucleus of MPTP-treated monkeys. Exp Neurol 158: 214-220.

Theoret H, Boire D, Herbin M, Ptito M (1999). Stereological evaluation of substantia nigra cell number in normal and hemispherectomized monkeys. Brain Res 835: 354–359.

Thickbroom GW, Byrnes ML, Walters S, Stell R, Mastaglia FL (2006). Motor cortex reorganisation in Parkinson's disease. J Clin Neurosci 13: 639-642.

Trapella C, Guerrini R, Piccagli L, Calo’ G, Carra' G, Spagnolo B, Rubini S, Fanton G, Hebbes C, McDonald J, Lambert DG, Regoli D, Salvadori S (2006). Identification of an achiral analogue of J-113397 as potent nociceptin/orphanin FQ receptor antagonist. Bioorg Med Chem 14: 692-704.

Ungerstedt U (1968). 6-Hydroxy-dopamine induced degeneration of central monoamine neurons. Eur J Pharmacol 5: 107-110.

Ungerstedt U, Arbuthnott GW (1970) Quantitative recording of rotational behaviour in rats after 6-hydroxydopamine lesions of the nigrostriatal dopamine system. Brain Res 24: 485-493.

Ungerstedt U (1971). Adipsia and aphagia after 6-hydroxydopamine induced degeneration of the nigro-striatal dopamine system. Acta Physiol Scand Suppl 367: 95-122.

Usiello A, Baik JH, Rougé-Pont F, Picetti R, Dierich A, LeMeur M, Piazza PV, Borrelli E (2000). Distinct functions of the two isoforms of dopamine D2 receptors. Nature 408: 199-203.

Vallone D, Picetti R, Borrelli E (2000). Structure and function of dopamine receptors. Neurosci Biobehav Rev 24: 125-132.

Viaro R, Sanchez-Pernaute R, Marti M, Trapella C, Isacson O, Morari M (2008). Nociceptin/orphanin FQ receptor blockade attenuates MPTP-induced parkinsonism. Neurobiol Dis 30: 430-438.

Viaro R, Marti M, Morari M (2010). Dual motor response to L-dopa and nociceptin/orphanin FQ receptor antagonists in 1-methyl-4-phenyl-1,2,5,6-tetrahydropyridine (MPTP) treated mice: Paradoxical inhibition is relieved by D_2/D_3 receptor blockade. Exp Neurol, in press.

Visanji NP, de Bie RM, Johnston TH, McCreary AC, Brotchie JM, Fox SH (2008). The nociceptin/orphanin FQ (NOP) receptor antagonist J-113397 enhances the effects of levodopa in the MPTP-lesioned nonhuman primate model of Parkinson's disease. Mov Disord 23: 1922-1925.

Wang Y, Xu R, Sasaoka T, Tonegawa S, Kung MP, Sankoorikal EB (2000). Dopamine D2 long receptor-deficient mice display alterations in striatum-dependent functions. J Neurosci 20: 305-314.

West MJ, Gundersen HJ (1990). Unbiased stereological estimation of the number of neurons in the human hippocampus. J Comp Neurol 296: 1–22.

Wichmann T, DeLong MR (1996). Functional and pathophysiological models of the basal ganglia. Curr Opin Neurobiol 6: 751-758.

Wiener WJ, Kramer J, Nausieda PA, Klawans HL (1978). Paradoxial response to dopaminergic agents in parkinsonism. Arch Neurol 35: 453-455.

Zigmond MJ, Stricker EM (1972). Deficits in feeding behavior after intraventricular injection of 6-hydroxydopamine in rats. Science 177: 1211-1214.

Appendix I. Statistical analysis

Tab. 1

Analysis not required.

Tab. 2

Stimulated activity (immobility time, $p=0.07$; number of steps, $p=0.0012$; run speed, $p=0.0080$, time on rod, $p<0.0001$).

Spontaneous activity (movement time, $p=0.44$; horizontal locomotion time, $p<0.0001$; fine movements time, $p<0.0001$; freezing time, $p=0.44$).

Step parameters (preparation time; $p<0.0001$; iniziation time, $p=0.0002$; air time, $p=0.56$; execution speed $p=0.0121$; step length, $p=0.11$).

Muscular activity (maximal force, $p=0.55$; average force, $p=0.0044$).

Fig. 1

A) Effect of treatment ($F_{4,20}=23.95$, $p<0.0001$), time ($F_{1,4}=0.16$, $p=0.68$) and time x treatment interaction ($F_{4,25}=0.13$, $p=0.97$).

B) Effect of treatment ($F_{4,20}=31.97$, $p<0.0001$), time ($F_{1,4}=16.33$, $p=0.0004$) and time x treatment interaction ($F_{4,25}=12.88$, $p<0.0001$).

C) Effect of treatment ($F_{4,20}=11.62$, $p<0.0001$) time ($F_{1,4}=20.64$, $p=0.0001$) and time x treatment interaction ($F_{4,25}=17.15$, $p<0.0001$).

Fig. 2

A) Effects of treatment ($F_{4,20}=0.79$, $p=0.54$), time ($F_{1,4}=0.23$, $p=0.63$) and time x treatment interaction ($F_{4,25}=0.26$, $p=0.89$).

B) Effect of treatment ($F_{4,20}=12.27$, $p<0.0001$), time ($F_{1,4}=0.51$, $p=0.48$) and time x treatment interaction ($F_{4,25}=4.81$, $p=0.0051$).

C) Effect of treatment ($F_{4,20}=11.39$, $p<0.0001$), time ($F_{1,4}=0.15$, $p=0.70$) and time x treatment interaction ($F_{4,25}=1.44$, $p=0.25$).

D) Effect of treatment ($F_{5,25}=2918.82$, $p<0.0001$), time ($F_{1,5}=4.03$, $p=0.05$) and time x treatment interaction ($F_{5,30}=3.45$, $p=0.0139$).

E) Effect of treatment ($F_{5,25}=68.00$, $p<0.0001$), time ($F_{1,5}=0.22$, $p=0.63$) and time x treatment interaction ($F_{5,30}=7.15$, $p=0.0002$).

F) Effect of treatment ($F_{5,25}$=182.58, p<0.0001), time ($F_{1,5}$=1.57, p=0.22) and time x treatment interaction ($F_{5,30}$=3.67, p=0.0103).

Fig. 3

A) Effect of treatment ($F_{3,15}$=42.92, p<0.0001), time ($F_{1,3}$=1.19, p=0.29) and time x treatment interaction ($F_{3,20}$=0.49, p=0.70).

B) Effect of treatment ($F_{3,15}$=28.19, p<0.0001), time ($F_{1,3}$=0.83, p=0.37) and time x treatment interaction ($F_{3,20}$=0.12, p=0.95).

C) Effect of treatment ($F_{3,15}$=14.53, p=0.0001), time ($F_{1,3}$=1.10, p=0.31) and time x treatment interaction ($F_{3,20}$=0.91, p=0.45).

D) Effect of treatment ($F_{3,15}$=17.26, p<0.0001), time ($F_{1,3}$=12.43, p=0.0021) and time x treatment interaction ($F_{3,20}$=8.83, p=0.0006).

E) Effect of treatment ($F_{3,15}$=2.66, p=0.06), time ($F_{1,3}$=1.40, p=0.25) and time x treatment interaction ($F_{3,20}$=0.43, p=0.74).

F) Effect of treatment ($F_{3,15}$=11.83, p=0.0003), time ($F_{1,3}$=3.94, p=0.06) and time x treatment interaction ($F_{3,20}$=2.95, p=0.06).

Fig. 4

A) Effect of treatment ($F_{3,15}$=29.84, p<0.0001), time ($F_{1,3}$=12.28, p=0.0022) and time x treatment interaction ($F_{3,20}$=13.08, p=0.0001).

B) Effect of treatment ($F_{3,15}$=14.15, p=0.0001), time ($F_{1,3}$=15.56, p=0.0008) and time x treatment interaction ($F_{3,20}$=6.21, p=0.0037).

C) Effect of treatment ($F_{3,15}$=6.68, p=0.0044), time ($F_{1,3}$=9.59, p=0.0057) and time x treatment interaction ($F_{3,20}$=8.96, p=0.0006).

D) Effect of treatment ($F_{3,15}$=0.08, p=0.97), time ($F_{1,3}$=0.02, p0.89) and time x treatment interaction ($F_{3,20}$=0.09, p=0.96).

E) Effect of treatment ($F_{3,15}$=3.99, p=0.0283), time ($F_{1,3}$=0.59, p=0.45) and time x treatment interaction ($F_{3,20}$=9.36, p=0.0005).

F) Effect of treatment ($F_{3,15}$=0.22, p=0.87), time ($F_{1,3}$=0.05, p=0.83) and time x treatment interaction ($F_{3,20}$=0.69, p=0.57).

Fig. 5

A) Effect of treatment ($F_{7,35}$=1.32, p=0.27), time ($F_{1,7}$=0.01, p=1.00) and time x treatment interaction ($F_{7,40}$=0.54, p=0.80).

B) Effect of treatment ($F_{7,35}$=26.79, p<0.0001), time ($F_{1,7}$=13.89, p=0.0006) and time x treatment interaction ($F_{7,40}$=12.61, p<0.0001).

C) Effect of treatment ($F_{7,35}$=34.90, p<0.0001), time ($F_{1,7}$=2.97, p=0.09) and time x treatment interaction ($F_{7,40}$=2.62, p=0.0252).

D) Effect of treatment ($F_{7,35}$=0.90, p=0.52), time ($F_{1,7}$=1.27, p=0.27) and time x treatment interaction ($F_{7,40}$=0.45, p=0.87).

E) Effect of treatment ($F_{7,35}$=12.42, p<0.0001), time ($F_{1,7}$=91.79, p<0.0001) and time x treatment interaction ($F_{7,40}$=11.75, p<0.0001).

F) Effect of treatment ($F_{7,35}$=5.65, p=0.0002), time ($F_{1,7}$=59.43, p<0.0001) and time x treatment interaction ($F_{7,40}$=6.07, p=0.0001).

Fig. 6

A) Effect of treatment ($F_{7,35}$=514.87, p<0.0001), time ($F_{1,7}$=12.34, p=0.0011) and time x treatment interaction ($F_{7,40}$=9.39, p<0.0001).

B) Effect of treatment ($F_{7,35}$=42.86, p<0.0001), time ($F_{1,7}$=13.50, p=0.0007) and time x treatment interaction ($F_{7,40}$=3.12, p=0.0101).

C) Effect of treatment ($F_{7,35}$=34.92, p<0.0001), time ($F_{1,7}$=6.05, p=0.0183) and time x treatment interaction ($F_{7,40}$=8.26, p<0.0001).

D) Effect of treatment ($F_{3,15}$=34.80, p<0.0001), time ($F_{1,3}$=1.20, p=0.29) and time x treatment interaction ($F_{3,20}$=1.52, p=0.24).

E) Effect of treatment ($F_{3,15}$=57.83, p<0.0001), time ($F_{1,3}$=23.35, p=0.0001) and time x treatment interaction ($F_{3,20}$=9.37, p=0.0005).

F) Effect of treatment ($F_{3,15}$=4.59, p=0.0180), time ($F_{1,3}$=30.16, p<0.0001) and time x treatment interaction ($F_{3,20}$=9.10, p=0.0005).

Fig. 7

A) Effect of treatment ($F_{4,20}$=490.48, p<0.0001), time ($F_{1,4}$=13.44, p=0.0012) and time x treatment interaction ($F_{4,25}$=4.57, p=0.0066).

B) Effect of treatment ($F_{4,20}$=220.49, p<0.0001), time ($F_{1,4}$=1.71, p=0.20) and time x treatment interaction ($F_{4,25}$=3.34, p=0.0253).

C) Effect of treatment ($F_{4,20}$=170.50, p<0.0001), time ($F_{1,4}$=7.66, p=0.0105) and time x treatment interaction ($F_{4,25}$=0.36, p=0.83).

D) Effect of treatment ($F_{3,15}$=0.41, p=0.75), time ($F_{1,3}$=0.16, p=0.70) and time x treatment interaction ($F_{3,20}$=0.34, p=0.80).

E) Effect of treatment ($F_{3,15}$=57.83, p<0.0001), time ($F_{1,3}$=2.51, p=0.13) and time x treatment interaction ($F_{3,20}$=1.44, p=0.26).

F) Effect of treatment ($F_{3,15}$=18.92, p<0.0001), time ($F_{1,3}$=0.77, p=0.39) and time x treatment interaction ($F_{3,20}$=0.36, p=0.78).

Fig. 8

See original paper II reported on appendix II.

Fig. 9

A) Effect of treatment ($F_{4,20}$=2194.47, p<0.0001), time ($F_{1,4}$=4.82, p=0.0376) and time x treatment interaction ($F_{4,25}$=2.27, p=0.09).

B) Effect of treatment ($F_{4,20}$=200.43, p<0.0001), time ($F_{1,4}$=1.42, p=0.24) and time x treatment interaction ($F_{4,25}$=1.67, p=0.19).

C) Effect of treatment ($F_{4,20}$=393.10, p<0.0001), time ($F_{1,4}$=5.88, p=0.0229) and time x treatment interaction ($F_{4,25}$=1.92, p=0.14).

Fig. 10

A) Effect of treatment ($F_{3,15}$=28.28, p<0.0001), time ($F_{1,3}$=2.80, p=0.11) and time x treatment interaction ($F_{3,20}$=2.07, p=0.14).

B) Effect of treatment ($F_{3,15}$=32.23, p<0.0001), time ($F_{1,3}$=0.85, p=0.37) and time x treatment interaction ($F_{3,20}$=1.08, p=0.38).

C) Effect of treatment ($F_{3,15}$=36.80, p<0.0001), time ($F_{1,3}$=0.65, p=0.43) and time x treatment interaction ($F_{3,20}$=0.45, p=0.72).

D) Effect of treatment ($F_{5,25}$=11.59, p<0.0001), time ($F_{1,5}$=1.47, p=0.26) and time x treatment interaction ($F_{5,30}$=4.84, p=0.0023).

E) Effect of treatment ($F_{5,25}$=8.22, p=0.0001), time ($F_{1,5}$=4.54, p=0.0414) and time x treatment interaction ($F_{5,30}$=2.77, p=0.0360).

F) Effect of treatment ($F_{5,25}$=27.42, p<0.0001), time ($F_{1,5}$=0.76, p=0.39) and time x treatment interaction ($F_{5,30}$=3.02, p=0.0251).

Fig. 11

A) Effect of treatment ($F_{7,35}$=18.96, p<0.0001), time ($F_{1,7}$=0.04, p=0.84) and time x treatment interaction ($F_{7,40}$=3.15, p=0.0095).

B) Effect of treatment ($F_{7,35}$=26.39, p<0.0001), time ($F_{1,7}$=0.96, p=0.33) and time x treatment interaction ($F_{7,40}$=2.99, p=0.0128).

C) Effect of treatment ($F_{7,35}$=48.11, p<0.0001), time ($F_{1,7}$=5.19, p=0.0281) and time x treatment interaction ($F_{7,40}$=2.05, p=0.07).

D) Effect of treatment ($F_{5,25}$=16.19, p<0.0001), time ($F_{1,5}$=0.44, p=0.51) and time x treatment interaction ($F_{5,30}$=2.48, p=0.05).

E) Effect of treatment ($F_{5,25}$=44.81, p<0.0001), time ($F_{1,5}$=2.93, p=0.10) and time x treatment interaction ($F_{5,30}$=1.70, p=0.17).

F) Effect of treatment ($F_{5,25}$=64.86, p<0.0001), time ($F_{1,5}$=20.52, p=0.0001) and time x treatment interaction ($F_{5,30}$=3.72, p=0.0098).

Fig. 12

A) Effect of treatment ($F_{7,35}$=16.12, p<0.0001), time ($F_{1,7}$=9.16, p=0.0043) and time x treatment interaction ($F_{7,40}$=5.03, p=0.0004).

B) Effect of treatment ($F_{7,35}$=41.59, p<0.0001), time ($F_{1,7}$=0.01, p=0.91) and time x treatment interaction ($F_{7,40}$=5.72, p=0.0001).

C) Effect of treatment ($F_{7,35}$=59.90, p<0.0001), time ($F_{1,7}$=29.81, p<0.0001) and time x treatment interaction ($F_{7,40}$=3.55, p=0.0046).

D) Effect of treatment ($F_{3,15}$=23.27, p<0.0001), time ($F_{1,3}$=16.54, p=0.0006) and time x treatment interaction ($F_{3,20}$=5.52, p=0.0063).

E) Effect of treatment ($F_{3,15}$=3.13, p00.06), time ($F_{1,3}$=0.32, p=0.58) and time x treatment interaction ($F_{3,20}$=1.51, p=0.24).

F) Effect of treatment ($F_{3,15}$=64.81, p<0.0001), time ($F_{1,3}$=13.39, p=0.0016) and time x treatment interaction ($F_{3,20}$=3.44, p=0.0365).

Fig. 13

A) Effect of treatment ($F_{4,35}$=44.24, p<0.0001).

B) Effect of treatment ($F_{5,43}$=14.80, p<0.0001).

Fig. 14

A) Effect of treatment ($F_{3,22}$=19.62, p<0.0001).

B) Effect of treatment ($F_{5,32}$=13.73, p<0.0001).

C) Effect of treatment ($F_{3,22}$=18.57, p<0.0001).

Figs. 15–17

See original paper V reported on appendix II.

Fig. 18

A) Effect of treatment ($F_{3,35}$=24.52, p<0.0001).

B) Effect of treatment ($F_{3,35}$=7.21, p=0.0008).

C) Treatment ($F_{3,35}$=7.54, p=0.0002).

Fig. 19

See original paper V reported on appendix II.

Fig. 20

See original paper II reported on appendix II.

Figs. 21–24

See original paper V reported on appendix II.

Figs. 25–27

See original paper II reported on appendix II.

Fig. 28

A) Effect of genotype ($F_{1,9}$=6.21, p=0.0343), time ($F_{6,6}$=34.51, p=0.00002) and time x genotype interaction ($F_{6,108}$=1.31, p=0.3760).

B) Effect of genotype ($F_{1,9}$=13.35, p=0.0053), time ($F_{6,6}$=20.73, p=0.0009) and time x genotype interaction ($F_{6,108}$=2.07, p=0.20).

C) Effect of genotype ($F_{1,9}$=13.22, p=0.0054), time ($F_{6,6}$=7.04, p=0.0158) and time x genotype interaction ($F_{6,108}$=2.47, p=0.15).

D) Effect of genotype ($F_{1,9}$=0.94, p=0.3573), time ($F_{6,6}$=15.41, p=0.0021) and time x genotype interaction ($F_{6,108}$=2.23, p=0.18).

Fig. 29

A) Effect of genotype ($F_{1,7}$=165.41, p<0.0001), time ($F_{1,1}$=3.12, p=0.08) and time x genotype interaction ($F_{1,14}$=82.59, p=0.07).

B) Effect of genotype ($F_{5,35}$=16.43, p=0.0009), time ($F_{1,42}$=0.19, p=0.68) and time x genotype interaction ($F_{5,42}$=50.16, p=0.0003).

Fig. 30

Effect of treatment (preparation time, p=0.0166; iniziation time, p=0.0256; air time, p=0.0416; execution speed, p=0.0442; step length, p=0.0211).

Fig. 31

A) Effect of genotype ($F_{1,7}$=0.02, p=0.88), time ($F_{1,1}$=12281.25, p=0.0057) and time x genotype interaction ($F_{1,14}$=0.01, p=0.97).

B) Effect of genotype ($F_{1,7}$=0.06, p=0.82), time ($F_{1,1}$=199.19, p=0.0450) and time x genotype interaction ($F_{1,14}$=0.19, p=0.74).

Fig. 32

Effect of treatment ($F_{3,26}$=16.84, p<0.0001).

Figs. 33–44

See original paper IV reported on appendix II.

Fig 45

Effect of striatal region ($F_{1,6}$=12.29, p=0.0016), time ($F_{6,24}$=106.86, p<0.0001) and time x striatal region interaction ($F_{6,28}$=10.45, p<0.0001).

Fig. 46

A) Effect of treatment ($F_{1,6}$=17.87, p=0.0002), time ($F_{6,24}$=25.83, p<0.0001) and time x treatment interaction ($F_{6,28}$=3.18, p=0.0166).

B) Effect of treatment ($F_{1,6}$=138.28, p<0.0001), time ($F_{6,24}$=25.56, p<0.0001) and time x treatment interaction ($F_{6,28}$=20.12, p<0.0001).

C) Effect of treatment ($F_{1,6}$=50.11, p<0.0001), time ($F_{6,24}$=10.28, p<0.0001) and time x treatment interaction ($F_{6,28}$=4.59, p=0.0023).

Fig. 47

Analysis not required.

Fig. 48

A) Effect of treatment ($F_{1,6}$=23.99, p<0.0001), time ($F_{6,24}$=25.83, p<0.0001) and time x treatment interaction ($F_{6,28}$=4.43, p=0.003).

B) Effect of treatment ($F_{1,6}$=1.12, p=0.30), time ($F_{6,24}$=15.04, p<0.0001), and time x treatment interaction ($F_{6,28}$=1.46, p=0.23).

C) Effect of treatment ($F_{1,6}$=29.64, p<0.0001), time ($F_{6,24}$=4.29, p=0.0045) and time x treatment interaction ($F_{6,28}$=3.54, p=0.0099).

D) Effect of treatment ($F_{1,6}$=25.06, p<0.0001), time ($F_{6,24}$=9.27, p<0.0001) and time x treatment interaction ($F_{6,28}$=4.56, p=0.0024).

E) Effect of treatment ($F_{1,6}$=12.38, p=0.0015), time ($F_{6,24}$=10.70, p<0.0001) and time x treatment interaction ($F_{6,28}$=2.15, p=0.08).

F) Effect of treatment ($F_{1,6}$=3.67, p=0.06), time ($F_{6,24}$=18.02, p<0.0001) and time x treatment interaction ($F_{6,28}$=3.19, p=0.0162).

Fig. 49

A) Effect of movement ($F_{1,6}$=133.53, p<0.0001), time ($F_{6,24}$=1.00, p=0.45) and time x movement interaction ($F_{6,28}$=6.29, p=0.0002).

B) Effect of movement ($F_{1,6}$=1368.37, p<0.0001), time ($F_{6,24}$=1.00, p=0.45) and time x movement interaction ($F_{6,28}$=9.56, p<0.0001).

C) Effect of movement ($F_{1,6}$=202.13, p<0.0001), time ($F_{6,24}$=1.00, p=0.45) and time x movement interaction ($F_{6,28}$=13.85, p<0.0001).

D) Effect of movement ($F_{1,6}$=855.11, p<0.0001), time ($F_{6,24}$=1.00, p=0.45) and time x movement interaction ($F_{6,28}$=0.36, p=0.90).

E) Effect of movement ($F_{1,6}$=93.38, p<0.0001), time ($F_{6,24}$=1.10, p=0.39) and time x movement interaction ($F_{6,28}$=15.69, p<0.0001).

F) Effect of movement ($F_{1,6}$=24.98, p<0.0001), time ($F_{6,24}$=1.00, p=0.49) and time x movement interaction ($F_{6,28}$=7.25, p<0.0001).

Fig. 50

A) Analysis not required.

B) Effect of treatment ($F_{5,29}$=34.02, p<0.0001).

C) Effect of treatment ($F_{5,29}$=62.15, p<0.0001).

Fig. 51

Analysis not required.

Fig. 52

A) Effect of treatment ($F_{1,4}$=28.34, p=0.0060), time ($F_{2,2}$=53.07, p<0.0001) and time x treatment interaction ($F_{2,16}$=19.61, p<0.0001).

B) Effect of treatment ($F_{1,4}$=11.88, p=0.0261), time ($F_{2,2}$=11.42, p=0.0008) and time x treatment interaction ($F_{2,16}$=9.56, p<0.0019).

C) Effect of treatment ($F_{1,4}$=7.89, p=0.0483), time ($F_{2,2}$=7.57, p<0.0049) and time x treatment interaction ($F_{2,16}$=4.58, p=0.0267).

D) Effect of treatment ($F_{1,4}$=2.57, p=0.18), time ($F_{2,2}$=46.81, p<0.0001) and time x treatment interaction ($F_{2,16}$=0.85, p=0.45).

E) Effect of treatment ($F_{1,4}$=36.05, p=0.0039), time ($F_{2,2}$=9.65, p<0.0018) and time x treatment interaction ($F_{2,16}$=1.85, p=0.19).

F) Effect of treatment ($F_{1,4}$=36.06, p=0.0039), time ($F_{2,2}$=9.64, p<0.0018) and time x treatment interaction ($F_{2,16}$=1.85, p=0.19).

G) Effect of treatment ($F_{1,4}$=5.34, p=0.08), time ($F_{2,2}$=33.35, p<0.0001) and time x treatment interaction ($F_{2,16}$=3.26, p=0.06).

H) Effect of treatment ($F_{1,4}$=1.67, p=0.27), time ($F_{2,2}$=28.16, p<0.0001) and time x treatment interaction ($F_{2,16}$=3.53, p=0.05).

Fig. 53

Analysis not required.

Fig. 54

A) Effect of treatment ($F_{1,4}$=27.23, p=0.0064), time ($F_{2,2}$=27.97, p<0.0001) and time x treatment interaction ($F_{2,16}$=0.99, p=0.39).

B) Effect of treatment ($F_{1,4}$=45.90, p=0.0025), time ($F_{2,2}$=18.17, p=0.0001) and time x treatment interaction ($F_{2,16}$=3.07, p=0.07).

C) Effect of treatment ($F_{1,4}$=0.31, p=0.61), time ($F_{2,2}$=8.01, p=0.0039) and time x treatment interaction ($F_{2,16}$=2.71, p=0.10).

D) Effect of treatment ($F_{1,4}$=4.09, p=0.11), time ($F_{2,2}$=1.71, p=0.21) and time x treatment interaction ($F_{2,16}$=4.16, p=0.0351).

E) Effect of treatment ($F_{1,4}$=2.55, p=0.19), time ($F_{2,2}$=9.49, p<0.0019) and time x treatment interaction ($F_{2,16}$=1.62, p=0.23).

F) Effect of treatment ($F_{1,4}$=2.55, p=0.19), time ($F_{2,2}$=9.49, p<0.0019) and time x treatment interaction ($F_{2,16}$=1.62, p=0.23).

G) Effect of treatment ($F_{1,4}$=25.21, p=0.0074), time ($F_{2,2}$=15.02, p=0.0002) and time x treatment interaction ($F_{2,16}$=0.09, p=0.92).

H) Effect of treatment ($F_{1,4}$=37.69, p=0.0036), time ($F_{2,2}$=15.18, p=0.0002) and time x treatment interaction ($F_{2,16}$=0.07, p=0.93).

Appendix II. Original papers

I) Marti M, Trapella C, **Viaro R**, Morari M (2007). The nociceptin/orphanin FQ receptor antagonist J-113397 and L-DOPA additively attenuate experimental parkinsonism through overinhibition of the nigrothalamic pathway. J Neurosci 27: 1297-1307.

II) Viaro R, Sanchez-Pernaute R, Marti M, Trapella C, Isacson O, Morari M (2008). Nociceptin/orphanin FQ receptor blockade attenuates MPTP-induced parkinsonism. Neurobiol Dis 30: 430-438.

III) Maggiolini E, **Viaro R**, Franchi G (2008). Suppression of activity in the forelimb motor cortex temporarily enlarges forelimb representation in the homotopic cortex in adult rats. Eur J Neurosci 27: 2733-2746.

IV) *Marti M, ***Viaro R**, Guerrini R, Franchi G, Morari M (2009). Nociceptin/orphanin FQ modulates motor behavior and primary motor cortex output through receptors located in substantia nigra reticulate. Neuropsychopharmacology 34: 341-355. *Marti M and *Viaro R equally contributed to this work.

V) Viaro R, Marti M, Morari M (2010). Dual motor response to L-dopa and nociceptin/orphanin FQ receptor antagonists in 1-methyl-4-phenyl-1,2,5,6-tetrahydropyridine (MPTP) treated mice: paradoxical inhibition is relieved by D_2/D_3 receptor blockade. Exp Neurol in press.

VI) Viaro R, Marti M, Morari M (submitted for publication). Different subpopulations of D_2 receptors mediate dual motor responses of nociceptin/orphanin FQ receptor antagonists in mice.

Neurobiology of Disease

The Nociceptin/Orphanin FQ Receptor Antagonist J-113397 and L-DOPA Additively Attenuate Experimental Parkinsonism through Overinhibition of the Nigrothalamic Pathway

Matteo Marti,[1] Claudio Trapella,[2] Riccardo Viaro,[1] and Michele Morari[1]

[1]Department of Experimental and Clinical Medicine, Section of Pharmacology, and Neuroscience Center, and [2]Department of Pharmaceutical Sciences and Biotechnology Center, University of Ferrara, 44100 Ferrara, Italy

By using a battery of behavioral tests, we showed that nociceptin/orphanin FQ receptor (NOP receptor) antagonists attenuated parkinsonian-like symptoms in 6-hydroxydopamine hemilesioned rats (Marti et al., 2005). We now present evidence that coadministration of the NOP receptor antagonist 1-[(3*R*,4*R*)-1-cyclooctylmethyl-3-hydroxymethyl-4-piperidyl]-3-ethyl-1,3-dihydro-2*H* benzimidazol-2-one (J-113397) and L-DOPA to 6-hydroxydopamine hemilesioned rats produced an additive attenuation of parkinsonism. To investigate the neurobiological substrates underlying this interaction, *in vivo* microdialysis was used in combination with behavioral measurements (bar test). J-113397 and L-DOPA alone reduced the time on bars (i.e., attenuated akinesia) and elevated GABA release selectively in the lesioned substantia nigra reticulata. J-113397 also reduced nigral glutamate levels, whereas L-DOPA was ineffective. J-113397 and L-DOPA coadministration produced additive antiakinetic effect, which was associated with additive increase in nigral GABA release but no additional reductions in glutamate levels. To investigate whether the increase in nigral GABA release could translate to changes in nigrothalamic transmission, GABA release was monitored in the ventromedial thalamus (one of the main target areas of the nigrothalamic projections). J-113397 and L-DOPA decreased thalamic GABA release and attenuated akinesia, their combination resulting in a more profound effect. These actions were prevented by perfusing the voltage-dependent Na^+ channel blocker tetrodotoxin or the $GABA_A$ receptor antagonist bicuculline in the substantia nigra reticulata. These data demonstrate that J-113397 and L-DOPA exert their antiparkinsonian action through overinhibition of nigrothalamic transmission and suggest that NOP receptor antagonists may be useful as an adjunct to L-DOPA therapy for Parkinson's disease.

Key words: **J-113397; L-DOPA; microdialysis; nociceptin; 6-OHDA; Parkinson's disease**

Introduction

Nociceptin/orphanin FQ (N/OFQ) and its receptor (NOP) are expressed in cortical and subcortical motor areas and, particularly, in the substantia nigra (SN), which contains dopamine (DA) neurons that degenerate in Parkinson's disease (PD). N/OFQ inhibits the activity of DA neurons located in the SN compacta (SNc) (Marti et al., 2004a) and impairs spontaneous (Reinscheid et al., 1995; Devine et al., 1996) and exercise-induced locomotion (Marti et al., 2004a). More recently, we presented evidence that endogenous N/OFQ sustains symptoms and neurodegeneration associated with PD. Indeed, upregulation of N/OFQergic transmission was found in the DA-depleted SN reticulata (SNr) of 6-hydroxydopamine (6-OHDA) hemilesioned (hemiparkinsonian) rats (Marti et al., 2005). Moreover, systemic or intranigral injections of NOP receptor antagonists attenuated akinesia both in hemiparkinsonian and haloperidol-treated rats (Marti et al., 2004b, 2005). Finally, deletion of the NOP receptor or the preproN/OFQ gene conferred mice partial resistance to the cataleptic action of haloperidol and protection against MPTP-induced loss of SNc DA neurons, respectively (Marti et al., 2005). Reduction of glutamate (GLU) release in the SNr may represent the mechanism by which NOP receptor antagonists reverse parkinsonism, because this class of compounds normalized haloperidol-evoked GLU levels in the SNr, an effect that correlated with attenuation of akinesia (Marti et al., 2004b, 2005). To further strengthen the view that NOP receptor antagonists may be useful in PD therapy, we undertook the present study to investigate the ability of the nonpeptide NOP receptor antagonist 1-[(3*R*,4*R*)-1-cyclooctylmethyl-3-hydroxymethyl-4-piperidyl]-3-ethyl-1,3-dihydro-2*H* benzimidazol-2-one (J-113397) (Kawamoto et al., 1999) to synergize with L-DOPA. L-DOPA still represents the most effective treatment of PD, although chronic treatment almost invariably produces motor fluctuations and

Received May 25, 2006; revised Dec. 19, 2006; accepted Dec. 24, 2006.

This work was supported by grants from the University of Ferrara (ex-60%), the Italian Ministry of the University (FIRB 2001), and the CARIFE Foundation. We gratefully acknowledge Dr. Antonio Berti (University of Padua, Padua, Italy) for assistance in statistical analysis.

Correspondence should be addressed to Dr. Michele Morari, Department of Experimental and Clinical Medicine, Section of Pharmacology, and Neuroscience Center, University of Ferrara, via Fossato di Mortara 17-19, 44100 Ferrara, Italy. E-mail: m.morari@unife.it.

DOI:10.1523/JNEUROSCI.4346-06.2007

 0270-6474/07/271297-11$15.00/0

dyskinesias (Obeso et al., 2000) that cause reduction in the clinical response over time. From a clinical point of view, combining L-DOPA with other antiparkinsonian drugs may allow a reduction in L-DOPA dosage, thereby delaying the onset of L-DOPA side effects.

In the present study, we evaluated L-DOPA action in a full dose range (experiment 1), further testing whether subthreshold (experiment 2) and submaximal (experiment 3) doses of J-113397 and L-DOPA produced additive antiparkinsonian effects. To investigate the mechanisms underlying this interaction, GLU and GABA release was analyzed by microdialysis in the SNr of rats undergoing behavioral testing (bar test; experiment 4). To determine whether changes in SNr neurotransmitter release correlated with changes of activity of nigrothalamic GABAergic neurons (i.e., the basal ganglia motor output), GABA release was also measured in the ventromedial thalamus (VMTh) (experiment 5), one of the main targets of nigrothalamic GABAergic neurons (Di Chiara et al., 1979; MacLeod et al., 1980). Finally, to confirm that both antiakinetic action and the changes in thalamic GABA release after J-113397 and L-DOPA coadministration were attributable to inhibition of nigrothalamic GABAergic transmission, neurochemical and behavioral analysis were performed during reverse dialysis of the voltage-dependent Na^+ channel blocker tetrodotoxin (TTX) (experiment 6) or the $GABA_A$ receptor antagonist bicuculline (experiment 7) in the SNr.

Materials and Methods

Rats used in the study (see below) were kept under regular lighting conditions (12 h light/dark cycle) and given food and water *ad libitum*. The experimental protocols performed in the present study were approved by the Italian Ministry of Health (license number 71-2004-B) and by the Ethics Committee of the University of Ferrara.

Measurement of antiakinetic effects of levodopa and J-113397 in hemiparkinsonian rats

6-OHDA lesion

Unilateral lesion of DA neurons (Marti et al., 2005) was induced in isoflurane-anesthetized male Sprague Dawley rats (150 g; Harlan Italy, S. Pietro al Natisone, Italy). Eight micrograms of 6-OHDA (in 4 μl of saline containing 0.02% ascorbic acid) were stereotaxically injected according to the following coordinates from bregma: anteroposterior (AP), −4.4 mm; mediolateral (ML), −1.2 mm; ventrodorsal (VD), −7.8 mm below dura (Paxinos and Watson, 1982). The rotational model (Ungerstedt and Arbuthnott, 1970) was used to select the rats that had been successfully lesioned. Two weeks after surgery, rats were injected with amphetamine (5 mg/kg, i.p., dissolved in saline) and only those rats performing more than seven ipsilateral turns per minute were enrolled in the study. This behavior has been associated with >95% loss of striatal extracellular DA levels (Marti et al., 2002b). Experiments were performed 6–8 weeks after lesion.

Histological evaluation

The animals were deeply anesthetized with Zoletil 100 (10 mg/kg, i.m.; Virbac Laboratories, Carros, France), transcardially perfused with 20 mM potassium PBS (KPBS) and fixed with 4% paraformaldehyde in KPBS, pH 7.4. The brains were removed, fixed in the fixative overnight, and transferred to 25% sucrose solution in KPBS for cryoprotection. Serial coronal sections of 40 μm thickness were made using a freezing microtome. Every second section in the striatum was selected from the region spanning from bregma −0.5 to +1.5 and processed for tyrosine hydroxylase (TH) immunohistochemistry.

Sections were rinsed three times in KPBS and incubated for 15 min in 3% H_2O_2 and 10% methanol in KPBS to block the endogenous peroxidase activity. After washing in KPBS, the sections were preincubated in blocking serum (5% normal horse serum and 0.3% Triton X-100 in KPBS) for 60 min, followed by incubation in anti-TH mouse monoclonal antibody solution (1:2000; Millipore, Billerica, MA) for 16 h at room temperature. The sections were then rinsed in KPBS and incubated for 1 h in biotinylated horse anti-mouse IgG secondary antibody (1:200; Vector Laboratories, Burlingame, CA). After rinsing, sections were incubated with avidin–biotin peroxidase complex (Vector Laboratories) for 30 min at room temperature. After rinsing with KPBS, immunoreactivity was visualized by incubating the sections in a solution containing 0.05% 3,3-diaminobenzidine (DAB) in 0.013% H_2O_2 in KPBS for ~1 min. The sections were rinsed in KPBS, mounted on gelatin-coated slides, dried with ethanol and xylene, and coverslipped with mounting medium. Every section was viewed with a Zeiss Axioskop (Zeiss, Oberkochen, Germany), acquired with Polaroid (Waltham, MA) DMC camera and TH-immunoreactive fiber density analyzed using ImageJ software (Wayne Rasband, National Institutes of Health, Bethesda, MD). To estimate the TH-density staining, the optical densities were corrected for nonspecific background density, which was measured in the corpus callosum. TH-positive fiber density was calculated as the ratio between optical density in the denervated (ipsilateral) and intact (contralateral) side (Fig. 1).

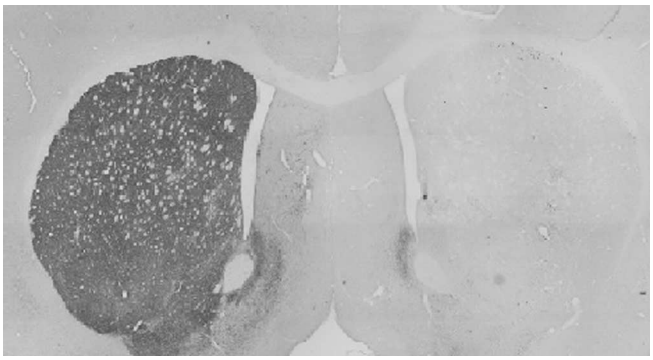

Figure 1. Effect of 6-OHDA injections on the TH-positive fiber density in the striatum. Photomicrograph of TH-positive fibers in the striata of a hemiparkinsonian rat.

Behavioral studies in rats

Motor activity in rats was evaluated by means of three behavioral tests specific for different motor abilities, as previously described (Marti et al., 2005): (1) the bar test (Sanberg et al., 1988), which measures rat ability to respond to an externally imposed static posture; (2) the drag test [modification of the postural adjustment test (Lindner et al., 1999)], which measures rat ability to balance body posture using forelimbs in response to an externally imposed dynamic stimulus (backward dragging); and (3) the rotarod test, which measures rat ability to run on a rotating cylinder (Rozas et al., 1997). The different tests are useful to evaluate akinesia and motor asymmetry under static conditions (bar test), akinesia, bradykinesia, and asymmetry under dynamic conditions (drag test), and overall motor performance (rotarod test) as an integration of coordination, gait, balance, muscle tone, and motivation to run. The bar and the drag tests were performed 10 min after intraperitoneal injections of J-113397, L-DOPA, or their combination, whereas the rotarod test was performed 10 and 60 min after drug injection.

Bar test. Each rat was placed gently on a table, and the contralateral and ipsilateral forepaws were placed alternatively on blocks of increasing heights (3, 6, and 9 cm). Total time (in seconds) spent by each paw on the blocks was recorded (cutoff time, 20 s).

Drag test. Each rat was gently lifted from the tail (allowing forepaws on the table) and dragged backwards at a constant speed (~20 cm/s) for a fixed distance (100 cm). The number of steps made by each paw was counted by two separate observers.

Rotarod test. The fixed-speed rotarod test (Rozas et al., 1997) was used according to a previously described protocol (Marti et al., 2004a). Briefly, rats were trained for 10 d to a specific motor task on the rotarod until their motor performance became reproducible. Rats were tested in a control session at four increasing speeds (10, 15, 20, 25 rpm for hemiparkinsonian rats and 30, 35, 40, and 45 rpm for sham-operated rats; 180 s each), causing a progressive decrement of performance to ~40% of the maximal response (i.e., the experimental cutoff time). Such a protocol

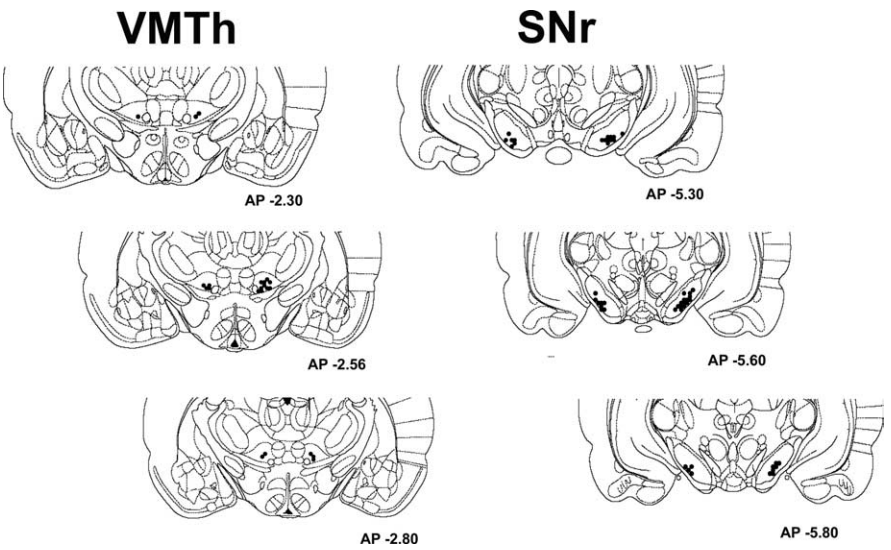

Figure 2. Schematic representation of coronal sections indicating microdialysis probe location in the SNr (AP −5.30, −5.60, and −5.80 from bregma) and VMTh (AP −2.30, −2.56, and −2.80 from bregma). The filled circles represent the location of the tip of the probe (data obtained from 45 animals).

was set to detect both facilitatory and inhibitory drug effects. Two other sessions were repeated 10 and 60 min after drug injection, and drug effect was expressed as total time spent on the rod.

Measurement of GLU and GABA levels in hemiparkinsonian rats by microdialysis

Two microdialysis probes (1 mm dialyzing membrane; AN69; Hospal, Bologna, Italy) were implanted bilaterally in the lesioned and unlesioned SNr (AP, −5.5; ML, ± 2.2; VD, −8.3) or ipsilateral and contralateral VMTh (AP, −2.3; ML, ± 1.4; VD, −7.4) of isoflurane-anesthetized hemiparkinsonsian rats. Twenty-four hours after implantation, probes were perfused (3 μl/min) with a modified Ringer's solution (in mM: 1.2 $CaCl_2$, 2.7 KCl, 148 NaCl, and 0.85 $MgCl_2$) and sample collection (every 15 min) started after a 6–7 h washout. L-DOPA and J-113397 were administered systemically (intraperitoneally) alone or in combination, and GLU and GABA levels were monitored every 15 min up to 3 h. In a separate set of experiments, two microdialysis probes were implanted in the lesioned SNr and ipsilateral VMTh, and GABA was measured in the VMTh. In these experiments, to correlate changes of amino acid dialysate levels with motor activity, rats undergoing microdialysis were challenged in the bar test every 15 min (Marti et al., 2004b, 2005). Routinely, experiments were repeated for 3 d after surgery, and treatments were randomized between groups, because preliminary testing showed that drug effect did not change depending on the day of experiment or treatment received in the preceding days. A notable exception was, however, represented by experiments using TTX because the toxin produced long-lasting effects that prevented additional testing. At the end of the experiments, rats were killed and probe location verified by microscopic examination (Fig. 2).

GLU and GABA levels in the dialysate were measured by HPLC coupled to fluorimetric detection, with minor modifications of the method described previously (Marti et al., 2003). Briefly, 40 μl samples were pipetted into glass microvials and placed in a thermostated (4°C) Triathlon autosampler (Spark Holland, Emmen, The Netherlands). Thirty-five microliters of *o*-pthaldialdheyde/boric acid solution were added to each sample, and 50 μl of the solution was injected onto a Chromsep analytical column (3 mm inner diameter, 10 cm length; Chrompack, Middelburg, The Netherlands). The column was eluted at a flow rate of 0.48 ml/min with a mobile phase containing 0.1 M sodium acetate, 10% ethanol, and 2.5% tetrahydrofuran, pH 6.5; to achieve a good separation, a two-step linear gradient of methanol in aqueous sodium acetate buffer was provided by a Beckman 125 pump (Beckman Instruments, Fullerton, CA). GLU and GABA were detected by means of a fluorescence spectrophotometer RF-551 (Shimadzu, Kyoto, Japan). GLU and GABA retention times were ~4 and ~17 min, respectively, and the sensitivity of the method for both amino acids was 150 fmol/sample.

Data presentation and statistical analysis

Motor performance has been expressed as time on bar or on rod (in seconds) and number of steps (drag test). In microdialysis studies, GLU and GABA release has been expressed as percentage ± SEM of basal values (calculated as mean of the two samples before the treatment). In Figure legends (and in Results), amino acid dialysate levels for each group of rats are also given in absolute values (in nanomolar concentration).

To analyze behavior, statistical analysis was performed (CoStat 6.3; CoHort Software, Monterey, CA) on absolute data by one-way or two-way ANOVA followed by the Newman–Keuls test for multiple comparisons. Drug interaction was studied experimentally according to a 2 × 2 factorial design, and data were analyzed with conventional two-way ANOVA, factor one being L-DOPA and factor two being J-113397. Whenever behavior was analyzed at different time points (e.g., during the rotarod test), repeated-measure ANOVA was performed on absolute data, "within" factor being time and "between" factor being treatment. In the case that ANOVA yielded to a significant *F* score, *post hoc* analysis was performed in contrast analysis to determine group differences. In the case that a significant time × treatment interaction was found, the sequentially rejective Bonferroni test was used (implemented on an Excel spreadsheet) to determine specific differences (i.e., at the single time-point level) between groups. Two-way ANOVA with repeated measures on percentage data was used in neurochemical experiments, within factor being time and between factor being treatment. For each group, two pretreatment and six post-treatment samples were considered. Contrast *post hoc* analysis was used to determine group differences, and the sequentially rejective Bonferroni test was used to determine differences at the single time-point level, as described above. p values <0.05 were considered to be statistically significant.

Materials

Amphetamine, 6-OHDA bromide, methyl L-DOPA hydrochloride, and benserazide were purchased from Sigma (St. Louis, MO), TTX from Alomone Labs (Jerusalem, Israel), and bicuculline from Tocris Neuramin (Bristol, UK). J-113397 was synthesized in our laboratories as reported previously (Marti et al., 2004a). All drugs were freshly dissolved in isoosmotic saline solution just before use.

Results

L-DOPA relieved akinesia in hemiparkinsonian rats (experiment 1)

Hemiparkinsonian rats displayed severe (~98%) loss of TH-positive DA terminals in the striatum ipsilateral to the 6-OHDA injection side (0.02 ± 0.03 ipsilateral/contralateral ratio, $n = 6$) (Fig. 1), whereas sham-operated rats showed no depletion at all (0.99 ± 0.02 ipsilateral/contralateral ratio, $n = 5$). Hemiparkinsonian rats also displayed overall marked akinesia/bradykinesia and motor asymmetry compared with vehicle-injected sham-operated rats (Table 1). L-DOPA (in combination with 15 mg/kg benserazide, i.p.) attenuated akinesia/bradykinesia and normalized motor asymmetry within the 0.1–6 mg/kg dose range, inducing a clear contralateral bias at higher doses (25 mg/kg) (Fig. 3). Lower L-DOPA doses reduced the time spent on the blocks

Table 1. Characterization of motor activity in vehicle-injected (sham-operated) and 6-OHDA-injected (hemiparkinsonian) rats

	Sham-operated		Hemiparkinsonian	
	Ipsilateral	Contralateral	Ipsilateral	Contralateral
Bar test (s)	0.7 ± 0.2 ($n = 12$)	0.8 ± 0.2 ($n = 12$)	41.6 ± 2.0* ($n = 22$)	50.0 ± 1.5*,** ($n = 22$)
Drag test (steps)	12.3 ± 0.3 ($n = 12$)	12.4 ± 0.5 ($n = 12$)	10.4 ± 0.4 ($n = 17$)	3.8 ± 0.3*,** ($n = 17$)
Rotarod (s)	1044 ± 93 ($n = 11$)		428 ± 30* ($n = 19$)	

Hemiparkinsonian rats displayed an increase in the total time spent on the blocks in the bar test, reduction in the number of steps made by the contralateral forepaw in the drag test, and reduced rotarod performance, compared with sham-operated animals. Data (mean ± SEM) have been obtained from 11 vehicle-injected and 19 hemiparkinsonian rats. *$p < 0.05$ versus sham-operated rats (Student's *t* test or ANOVA followed by the Newman–Keuls *post hoc* test, when appropriate). **$p < 0.05$ versus the ipsilateral forepaw.

($F_{(9,64)} = 54.74$; $p < 0.001$) (Fig. 3*A*), increased the number of steps ($F_{(9,72)} = 45.96$; $p < 0.001$) (Fig. 3*B*), and affected rotarod performance (Fig. 3*C*). In this respect, repeated-measure ANOVA revealed a significant effect of treatment ($F_{(5,22)} = 11.25$; $p < 0.001$), time ($F_{(2,68)} = 6.59$; $p = 0.002$), and time × treatment ($F_{(10,68)} = 50.81$; $p < 0.001$). *Post hoc* analysis revealed that L-DOPA stimulated motor performance in the 0.3–6 mg/kg dose range and inhibited it at 25 mg/kg. Overall, the most sensitive test was the bar test, with L-DOPA significantly attenuating akinesia at 0.1 mg/kg and normalizing motor asymmetry at 6 mg/kg. When L-DOPA was injected at high doses (25 mg/kg), it induced contralateral turning and reversal of motor asymmetry, the contralateral side of the body being more active than the ipsilateral one. Contralateral turning was, however, associated with hampered rotarod performance (see also Rozas et al., 1997; Marti et al., 2004a).

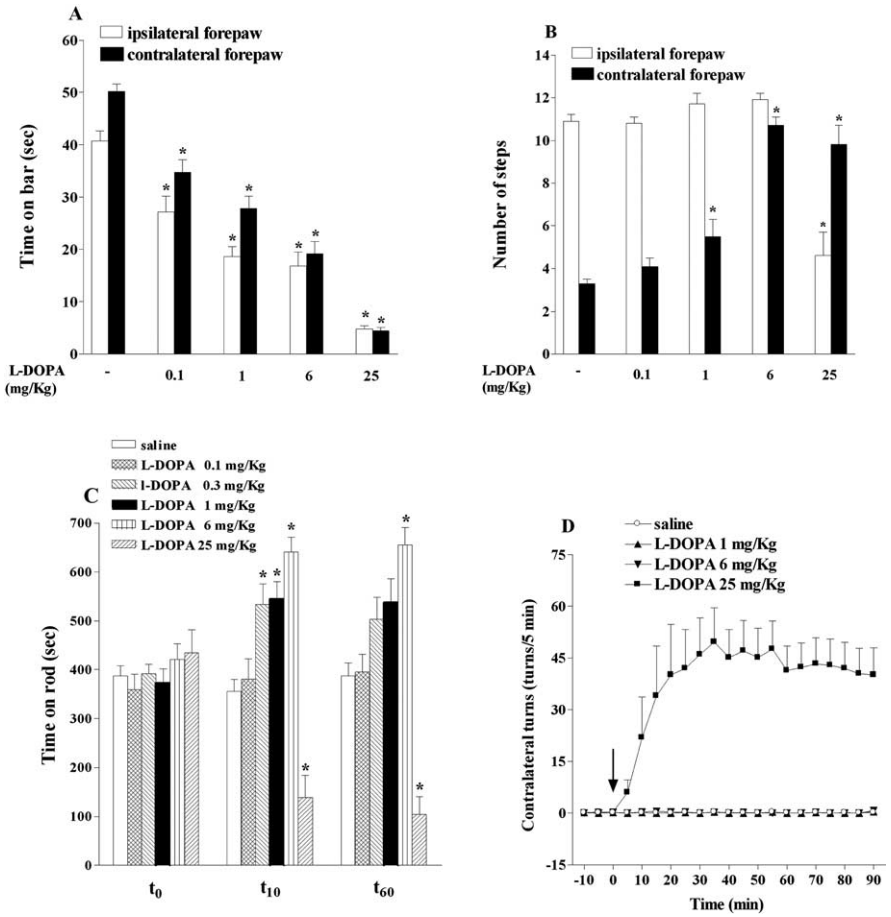

Figure 3. L-DOPA relieved akinesia/bradykinesia in hemiparkinsonian rats. ***A–D***, Systemic administration (intraperitoneal; arrow) of L-DOPA (0.1–25 mg/kg, in combination with 15 mg/kg benserazide) reduced the time spent on the blocks in the bar test (***A***), increased the number of steps of the contralateral forepaw in the drag test (***B***), improved overall motor performance in the rotarod test (***C***), and induced contralateral rotations (***D***). The bar and drag tests were performed 10 min after injection; the rotarod test was performed 10 and 60 min after injection. Motor asymmetry was evaluated by separately measuring activity of the paws ipsilateral and contralateral (parkinsonian) to the lesioned side. Turning behavior (***D***) was assessed by counting the number of rotations in the direction opposite to the injection side (i.e., contralateral) in 90 min. Data are mean ± SEM (6–14 rats per group). Statistical analysis was performed by one-way ANOVA followed by the Newman–Keuls test (***A***, ***B***) or ANOVA with repeated measures followed by contrast analysis and the sequentially rejective Bonferroni test (***C***). *$p < 0.05$ versus saline-treated rats.

Combination of L-DOPA and J-113397 attenuated parkinsonian-like symptoms in an additive way (experiments 2 and 3)

By using the bar, drag, and rotarod tests, we reported previously (Marti et al., 2005) that systemic (intraperitoneal) injections of J-113397 attenuated akinesia/bradykinesia and attenuated motor asymmetry in hemiparkinsonian rats. Its action fully developed within the 0.1–3 mg/kg range, with 0.1 and 1 mg/kg being the subthreshold and submaximal doses in two of three tests, respectively. We therefore selected subthreshold (0.1 mg/kg) and submaximal (1 mg/kg) doses of J-113397 and L-DOPA to test whether their combination could produce additive effects.

Interaction between subthreshold doses (experiment 2)

In the bar test (Fig. 4*A*), two-way ANOVA revealed the main effect of L-DOPA ($F_{(1,32)} = 11.89$; $p = 0.0016$), but not J-113397 ($F_{(1,32)} = 0.71$; $p = 0.40$), and a significant L-DOPA × J-113397 interaction ($F_{(1,32)} = 14.08$; $p = 0.0007$) at the ipsilateral side. At the contralateral side, two-way ANOVA revealed the main effect of L-DOPA ($F_{(1,30)} = 26.06$; $p < 0.0001$) and J-113397 ($F_{(1,30)} = 26.06$; $p = 0.057$) and a significant L-DOPA × J-113397 interaction ($F_{(1,30)} = 5.41$; $p = 0.0269$). *Post hoc* analysis revealed that L-DOPA and J-113397 reduced the time spent on the bar at both forepaws, the effect of the combination being no greater than that evoked by each compound alone. In the drag test (Fig. 4*B*), no effect was detected, either when compounds were administered alone or together. In the rotarod test (Fig. 4*C*), no main effect of treatment was found ($F_{(3,15)} = 1.84$; $p = 0.18$). Instead, a main effect of time ($F_{(2,42)} = 8.0$; $p < 0.001$) and a significant time × treatment interaction ($F_{(6,42)} = 9.28$; $p < 0.001$) was evident. *Post hoc* analysis revealed that L-DOPA and J-113397 were ineffective, whereas their combination elevated rotarod performance at 60 min after injection.

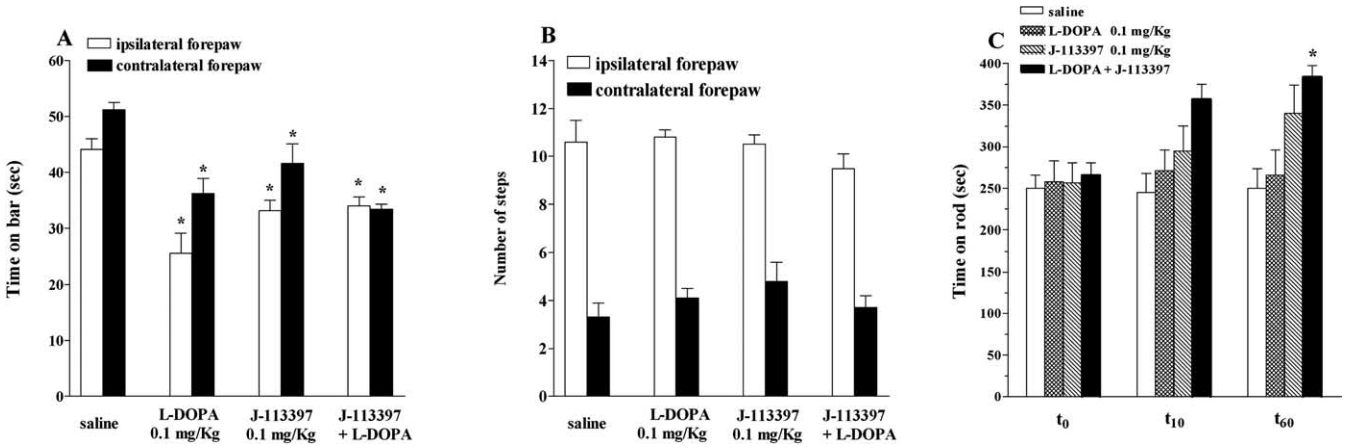

Figure 4. Combination of low (subthreshold) doses of J-113397 and L-DOPA relieved akinesia/hypokinesia in hemiparkinsonian rats. ***A***, Systemic (intraperitoneal) administration of J-113397 (0.1 mg/kg), L-DOPA (0.1 mg/kg plus 15 mg/kg benserazide), or their combination reduced the time spent on the blocks in the bar test. ***B***, No effect was observed in the drag test. ***C***, In the rotarod test, improvement of motor performance was detected only when J-113397 and L-DOPA were combined. Motor asymmetry was evaluated by separate measures at the paws ipsilateral and contralateral (parkinsonian) to the lesioned side. The bar and drag tests were performed 10 min after injection; the rotarod test was performed 10 and 60 min after injection. Data are mean ± SEM (6–14 rats per group). Statistical analysis was performed by conventional two-way ANOVA followed by the Newman–Keuls test (***A***, ***B***) or by two-way ANOVA with repeated measures followed in contrast analysis and the sequentially rejective Bonferroni test (***C***). $^{*}p < 0.05$ versus saline-treated rats.

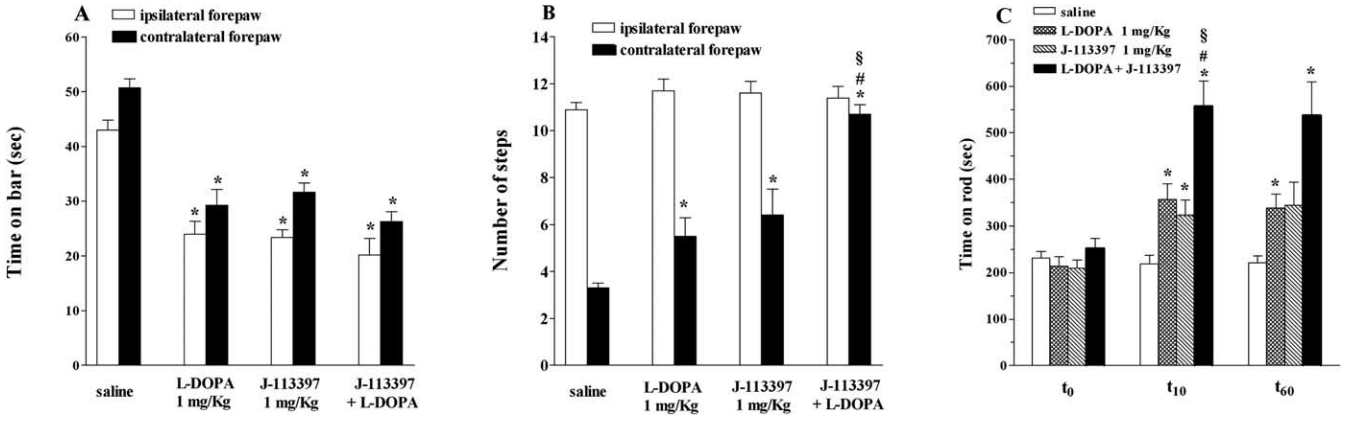

Figure 5. Combination of high (submaximal) doses of J-113397 and L-DOPA relieved akinesia/hypokinesia in hemiparkinsonian rats. ***A–C***, Systemic (intraperitoneal) administration of J-113397 (1 mg/kg), L-DOPA (1 mg/kg plus 15 mg/kg benserazide), or their combination reduced the time spent on the blocks in the bar test (***A***), increased the number of steps made by the contralateral paw in the drag test (***B***), and improved overall motor performance in the rotarod test (***C***). In the drag and rotarod tests, a greater effect (additive) was detected when J-113397 and L-DOPA were combined together. Motor activity was evaluated by separate measures at the paws ipsilateral and contralateral (parkinsonian) to the lesioned side. The bar and drag tests were performed 10 min after injection; the rotarod test was performed 10 and 60 min after injection. Data are mean ± SEM (6–10 rats per group). Statistical analysis was performed by conventional two-way ANOVA followed by the Newman–Keuls test (***A***, ***B***) or by two-way ANOVA with repeated measures followed by contrast analysis and the sequentially rejective Bonferroni test (***C***). $^{*}p < 0.05$ versus saline-treated rats. $^{\#}p < 0.05$ versus L-DOPA alone. $^{\S}p < 0.05$ versus J-113397 alone.

Interaction between submaximal doses (experiment 3)

In the bar test (Fig. 5*A*), the main effect of L-DOPA ($F_{(1,26)} = 29.00$; $p < 0.0001$) and J-113397 ($F_{(1,26)} = 26.77$; $p < 0.0001$) were found together with a significant L-DOPA × J-113397 interaction ($F_{(1,26)} = 15.03$; $p = 0.0006$) at the ipsilateral paw. Main effects of L-DOPA ($F_{(1,23)} = 43.30$; $p = 0.0001$) and J-113397 ($F_{(1,23)} = 21.33$; $p < 0.0001$) and a significant L-DOPA × J-113397 interaction ($F_{(1,23)} = 17.42$; $p = 0.0004$) were also observed at the contralateral paw. At both forepaws, the effects of each compound alone did not differ from that induced by their coadministration.

In the drag test (Fig. 5*B*), neither compound affected motor activity at the side of the body ipsilateral to the lesion. Conversely, two-way ANOVA revealed the main effect of L-DOPA ($F_{(1,29)} = 23.70$; $p < 0.0001$) and J-113397 ($F_{(1,29)} = 13.25$; $p = 0.0011$), although not a significant L-DOPA × J-113397 interaction ($F_{(1,29)} = 0.09$; $p = 0.76$), at the contralateral forepaw. *Post hoc* analysis showed that the coapplication induced a greater effect than each compound alone, leading to restoration of motor activity at the parkinsonian forepaw.

In the rotarod test (Fig. 5*C*), main effects of treatment ($F_{(3,16)} = 9.53$; $p = 0.0007$) and time ($F_{(2,57)} = 32.24$; $p < 0.0001$) and a significant time × treatment interaction ($F_{(10,57)} = 6.91$; $p < 0.0001$) were found. *Post hoc* analysis at 10 min after injection revealed that L-DOPA and J-113397 elevated rotarod performance, and the coapplication produced greater (additive) improvement.

L-DOPA and J-113397 differentially modulated GLU and GABA release in the SNr (experiment 4)

In previous studies, we showed that NOP receptor antagonists inhibited spontaneous (Marti et al., 2002a, 2005) and haloperidol-evoked (Marti et al., 2004b, 2005) GLU release in the SNr and that this effect correlated with relief from akinesia. We

therefore first investigated whether additive antiparkinsonian effects produced by coadministration of submaximal L-DOPA and J-113397 doses were associated with greater reduction of SNr GLU release (Fig. 6*A*,*B*). GLU levels did not differ in the unlesioned (96.1 ± 6.9 nM, $n = 30$) and lesioned (94.4 ± 6.9 nM, $n = 30$) SNr. Neither compounds affected GLU outflow in the unlesioned SNr (Fig. 6*A*). However, repeated-measure ANOVA revealed a main effect of treatment ($F_{(3,18)} = 33.15$; $p < 0.0001$) and time ($F_{(7,168)} = 9.53$; p=<0.0001), as well as a significant time × treatment interaction ($F_{(21,168)} = 3.27$; $p = 0.0045$) in the lesioned SNr (Fig. 6*B*). *Post hoc* analysis showed that L-DOPA did not affect GLU levels, whereas J-113397 reduced them, the combination of the two being no more effective than J-113397 alone. Because these findings did not indicate that changes in GLU levels underlie the additive effect on behavior, we next measured GABA release in the same area (Fig. 6*C*,*D*). GABA levels did not differ in the unlesioned (10.5 ± 0.4 nM, $n = 26$) and lesioned (10.0 ± 0.5 nM, $n = 26$) SNr. Neither compounds affected GABA outflow in the unlesioned SNr (Fig. 6*C*). Conversely, repeated-measure ANOVA showed main effects of treatment ($F_{(3,15)} = 26.46$; $p < 0.0001$) and time ($F_{(7,147)} = 23.42$; $p < 0.0001$) and a significant time × treatment interaction in the lesioned SNr (Fig. 6*D*). *Post hoc* analysis revealed that L-DOPA and J-113397 elevated GABA levels compared with saline, the effect of the combination being greater than that of each compound alone (Fig. 6*D*).

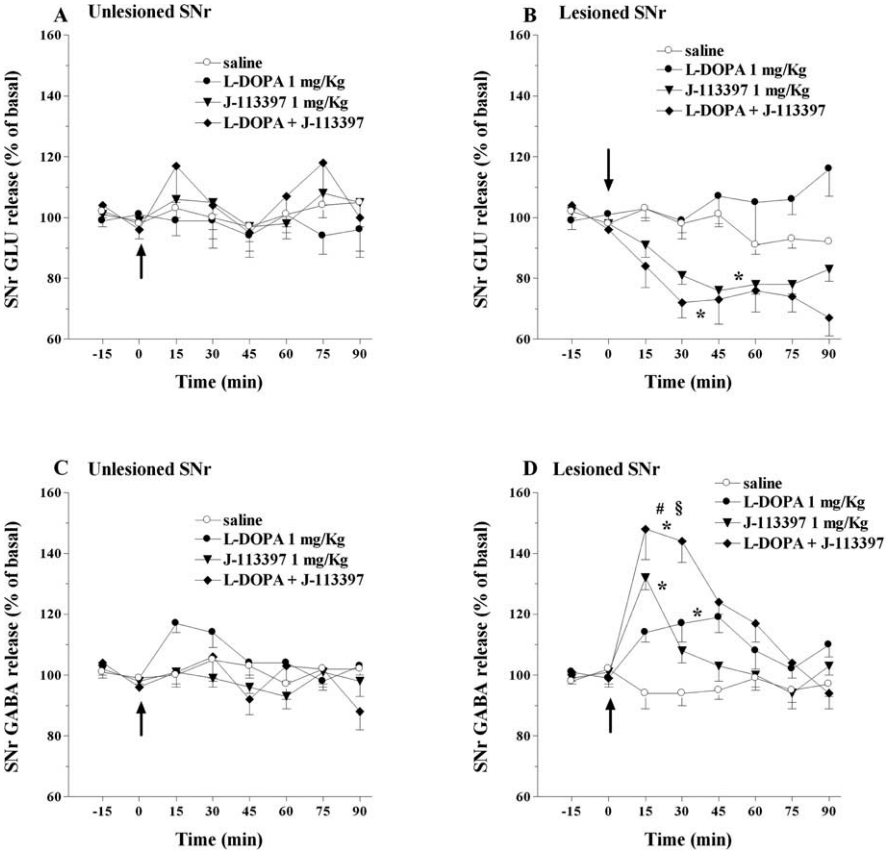

Figure 6. J-113397 and L-DOPA regulated GLU and GABA release in the lesioned SNr. ***A–D***, Two microdialysis probes were bilaterally implanted in the unlesioned (***A***, ***C***) and lesioned (***B***, ***D***) SNr of hemiparkinsonian rats. Rats were treated systemically (intraperitoneally; arrow) with J-113397 (1 mg/kg), L-DOPA (1 mg/kg plus benserazide 15 mg/kg), or their combination. Data are expressed as means ± SEM of *n* experiments. Basal GLU levels (in nanomolar concentration) in the dialysate from the unlesioned and lesioned SNr were, respectively, as follows: 100.2 ± 15.8, 103.7 ± 19.5 (saline, $n = 6$ both); 76.8 ± 15.2, 73.2 ± 14.7 (L-DOPA, $n = 6$ both); 112.4 ± 12.4, 100.9 ± 12.1 (J-113397, $n = 11$ and 12, respectively); 83.4 ± 9.5, 94.7 ± 9.9 (L-DOPA + J-113397, $n = 7$ both). Basal GABA levels (in nanomolar concentration) in the dialysate from the unlesioned and lesioned SNr were, respectively, as follows: 9.4 ± 0.6, 9.2 ± 0.9 (saline, $n = 6$ both); 10.9 ± 0.9, 9.5 ± 1.0 (L-DOPA, $n = 6$ both); 10.5 ± 1.2, 11.6 ± 0.9 (J-113397, $n = 7$ both); 11.0 ± 0.7, 9.6 ± 1.3 (L-DOPA + J-113397, $n = 7$ both). Statistical analysis was performed by two-way ANOVA with repeated measures followed by contrast analysis and the sequentially rejective Bonferroni test. $^{*}p <$ 0.05 versus saline-treated rats. $^{\S}p < 0.05$ versus J-113397 alone. $^{\#}p < 0.05$ versus L-DOPA alone.

L-DOPA and J-113397 reduced GABA release in the VMTh (experiment 5)

SNr is known to send GABAergic projections to the VMTh (Di Chiara et al., 1979; MacLeod et al., 1980), which represents the motor output of the basal ganglia. Thus, we hypothesized that the attenuation of motor disabilities could be associated with inhibition of nigrothalamic transmission. To this purpose, we first investigated whether J-113397 and L-DOPA administration evoked changes in thalamic GABA release (Fig. 7*A*,*B*). GABA levels in the dialysate from the VMTh ipsilateral to the lesioned SNr (18.9 ± 1.0 nM; $n = 27$) were ~23% higher compared with those collected from the contralateral one (14.6 ± 1.0 nM; $n = 25$; $p <$ 0.05, Student's *t* test). Neither L-DOPA or J-113397 affected GABA release in the VMTh contralateral to the lesioned SNr (Fig. 7*A*). However, repeated-measure ANOVA revealed main effects of treatment ($F_{(3,15)} = 18.48$; $p < 0.0001$) and time ($F_{(7,132)} = 13.55$; $p < 0.0001$) and a significant time × treatment interaction ($F_{(21,132)} = 2.24$; $p = 0.003$) in the VMTh ipsilateral to the lesioned SNr (Fig. 7*B*). *Post hoc* analysis revealed that L-DOPA and J-113397 inhibited thalamic GABA release compared with saline, and the combination produced greater inhibition compared with that evoked by each compound alone.

Simultaneous behavioral testing was performed in animals subjected to microdialysis, and motor activity was assessed separately at the contralateral and ipsilateral forepaw by using the bar test (Fig. 7*C*,*D*). At the contralateral paw, the main effects of treatment ($F_{(3,32)} = 34.23$; $p < 0.0001$) and time ($F_{(7,300)} = 95.22$; $p < 0.0001$) and a significant time × treatment interaction ($F_{(21,300)} = 14.06$; $p < 0.0001$) were found (Fig. 7*C*). The main effects of treatment ($F_{(3,32)} = 8.44$; $p < 0.0001$) and time ($F_{(7,300)} = 51.07$; $p < 0.0001$) and a significant time × treatment interaction ($F_{(21,300)} = 8.50$; $p < 0.0001$) were also observed at the ipsilateral paw (Fig. 7*D*). *Post hoc* analysis showed that L-DOPA and J-113397 reduced to the same extent the time spent on the blocks at both the contralateral and ipsilateral forepaw, although only at the contralateral paw the combined administration of L-DOPA and J-113397 produced greater effect than each compound alone.

Reverse dialysis of TTX in the SNr prevented changes in thalamic GABA release and motor behavior by L-DOPA and J-113397 combination (experiment 6)

To demonstrate that ongoing neuronal activity in the SNr was essential for both the reduction of GABA release in the VMTh

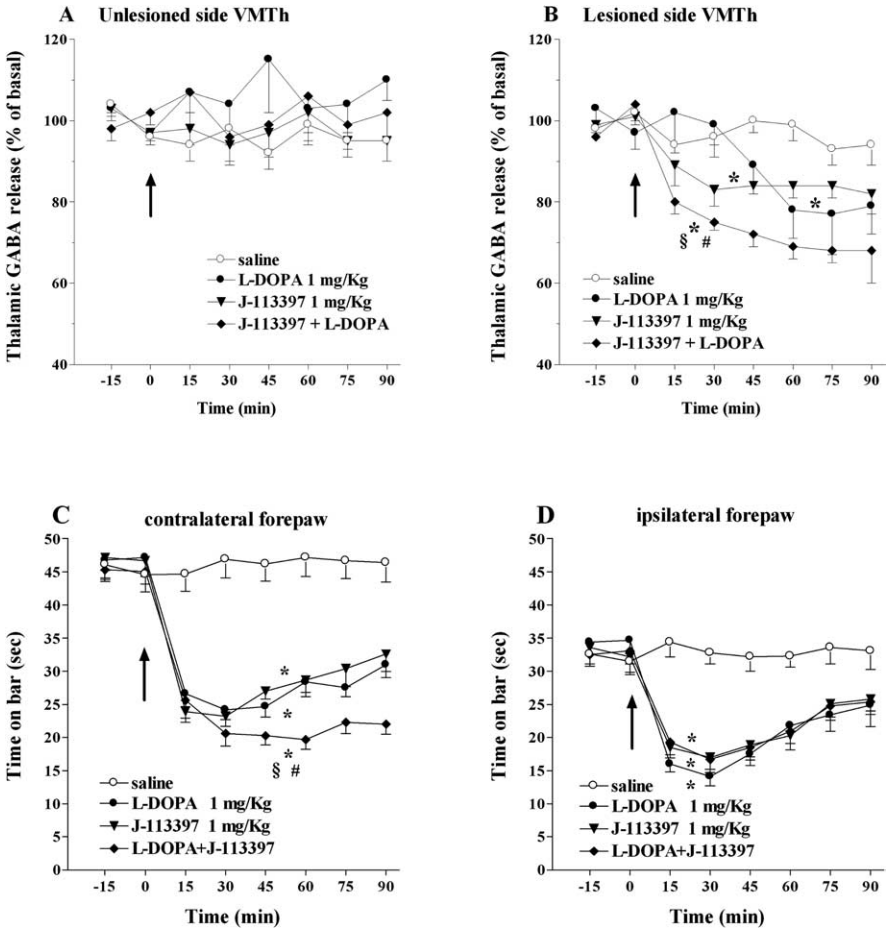

Figure 7. J-113397 and L-DOPA produced inhibition of GABA release in the VMTh and reduction of the time spent on the blocks. ***A***, ***B***, Two microdialysis probes were bilaterally implanted in the VMTh contralateral (unlesioned side; ***A***) and ipsilateral (lesioned side; ***B***) to the lesioned SNr of hemiparkinsonian rats. Rats were treated systemically (intraperitoneally; arrow) with J-113397 (1 mg/kg), L-DOPA (1 mg/kg plus 15 mg/kg benserazide), or their combination. Data are expressed as means ± SEM of *n* experiments. Basal GABA levels (in nanomolar concentration) in the dialysate from the VMTh at the unlesioned and lesioned side were, respectively, as follows: 12.5 ± 1.0, 15.8 ± 2.3 (saline, $n = 6$ both); 16.4 ± 1.9, 20.4 ± 0.4 (L-DOPA, $n = 6$ both); 15.4 ± 1.2, 20.9 ± 1.7 (J-113397, $n = 6$ both); 15.3 ± 3.2, 22.7 ± 1.4 (L-DOPA + J-113397, $n = 6$ both). ***C***, ***D***, Hemiparkinsonian rats implanted in the SNr (Fig. 6) or VMTh were challenged in the bar test. Akinesia was evaluated (every 15 min for up to 90 min) by using the bar test separately at the contralateral (***C***) and ipsilateral (***D***) paws (described in Materials and Methods). L-DOPA and J-113397 attenuated akinesia at both paws although greater effect was observed at the contralateral paw when both compounds were applied together. Data are means ± SEM of *n* experiments (8–12 per group). Statistical analysis was performed by two-way ANOVA with repeated measures followed by contrast analysis and the sequentially rejective Bonferroni test. $^{*}p < 0.05$ versus saline-treated rats. $^{\#}p < 0.05$ versus L-DOPA alone. $^{\S}p < 0.05$ versus J-113397 alone.

and the antiakinetic action, L-DOPA and J-113397 were coadministered systemically while perfusing the voltage-operated Na^+ channel blocker TTX in the lesioned SNr (Fig. 8).

Repeated-measure ANOVA on GABA levels in the lesioned SNr (Fig. 8*A*) revealed a main effect of treatment ($F_{(3,14)} = 46.40$; $p < 0.0001$) and time ($F_{(7,125)} = 9.50$; $p < 0.0001$) and a significant time × treatment interaction ($F_{(21,125)} = 7.52$; $p < 0.0001$). *Post hoc* analysis showed that SNr perfusion with TTX did not affect spontaneous SNr GABA levels and prevented the elevation of GABA release induced by combined administration of J-113397 and L-DOPA. Repeated-measure ANOVA on ipsilateral VMTh GABA levels (Fig. 8*B*) revealed main effect of treatment ($F_{(3,14)} = 77.50$; $p < 0.0001$) and time ($F_{(7,125)} = 2.55$; $p = 0.017$) and a significant time × treatment interaction ($F_{(21,125)} = 4.63$; $p < 0.0001$). *Post hoc* analysis showed that SNr perfusion with TTX reduced VMTh GABA release and prevented the inhibitory effect induced by coapplication of J-113397 and L-DOPA.

From a behavioral point of view, repeated-measure ANOVA analysis at the contralateral paw revealed a main effect of treatment ($F_{(3,12)} = 15.40$; $p = 0.0002$) and time ($F_{(7,120)} = 13.61$; $p < 0.0001$), as well as a significant time × treatment interaction ($F_{(21,120)} = 6.92$; $p < 0.0001$) (Fig. 8*C*). A similar response was observed at the ipsilateral paw (Fig. 8*D*). *Post hoc* analysis showed that TTX significantly reduced the time spent on the bar and prevented the inhibition induced by coapplication of J-113397 and L-DOPA.

Reverse dialysis of bicuculline in the SNr prevented changes in thalamic GABA release and motor behavior by L-DOPA and J-113397 combination (experiment 7)

To demonstrate that activation of $GABA_A$ receptors in the SNr was responsible for overinhibition of nigrothalamic neurons and antiparkinsonian action associated with it, L-DOPA and J-113397 were coadministered systemically while perfusing the $GABA_A$ receptor blocker bicuculline in the lesioned SNr (Fig. 9).

Repeated-measure ANOVA on GABA levels in the lesioned SNr (Fig. 9*A*) revealed a main effect of treatment ($F_{(3,14)} = 27.75$; $p < 0.0001$) and time ($F_{(7,125)} = 11.05$; $p < 0.0001$) and a significant time × treatment interaction ($F_{(21,125)} = 5.17$; $p < 0.0001$). *Post hoc* analysis showed that perfusion with bicuculline in the SNr did not affect basal GABA levels and left unchanged the elevation of GABA release induced by combined administration of J-113397 and L-DOPA. In the VMTh (Fig. 9*B*), main effects of treatment ($F_{(3,14)} = 10.10$; $p = 0.0008$), but not time ($F_{(7,125)} = 1.58$; $p = 0.14$), and a significant time × treatment interaction ($F_{(21,125)} = 2.29$; $p = 0.0025$) were found. *Post hoc* analysis revealed that bicuculline did not affect spontaneous GABA release and prevented the inhibitory influence induced by J-113397 and L-DOPA combination.

From a behavioral point of view, repeated-measure ANOVA at the contralateral paw (Fig. 9*C*) revealed a main effect of treatment ($F_{(3,12)} = 36.33$; $p < 0.0001$) and time ($F_{(7,112)} = 8.12$; $p < 0.0001$), as well as a significant time × treatment interaction ($F_{(21,112)} = 8.93$; $p < 0.0001$). At the ipsilateral paw (Fig. 9*D*), repeated-measure ANOVA revealed a main effect of treatment ($F_{(3,12)} = 4.51$; $p = 0.024$) and time ($F_{(7,112)} = 2.16$; $p = 0.043$) and a significant time × treatment interaction ($F_{(7,112)} = 2.82$; $p < 0.0001$). *Post hoc* analysis revealed that bicuculline did not affect the time spent on the bar but prevented the inhibitory effect induced by J-113397 and L-DOPA combination.

To study the relevance of GLU release inhibition in the antiakinetic response to combined application of L-DOPA and J-113397, GLU levels were analyzed in the lesioned SNr during perfusion of bicuculline (Fig. 10). Repeated-measure ANOVA

revealed a main effect of treatment ($F_{(3,14)} = 18.80$; $p < 0.0001$) and time ($F_{(7,125)} = 15.46$; $p < 0.0001$) and a significant time × treatment interaction ($F_{(21,125)} = 5.47$; $p < 0.0001$). *Post hoc* analysis showed that perfusion with bicuculline in the SNr did not affect basal GLU levels. However, it delayed the reduction in GLU release induced by combined administration of J-113397 and L-DOPA.

Discussion

Systemic administration of an NOP receptor antagonist (J-113397) or L-DOPA alone dose-dependently attenuated parkinsonian-like symptoms in hemiparkinsonian rats, whereas their combination evoked additive effects depending on the dose and the test used. Both compounds exerted their antiakinetic actions through a common "effector" as they produced additive elevation of SNr GABA and inhibition of VMTh GABA release. This effect was dependent on ongoing neuronal activity in the SNr (TTX sensitive) and activation of SNr $GABA_A$ receptors (bicuculline sensitive), suggesting that J-113397 and L-DOPA acted through overinhibition of nigrothalamic GABAergic neurons.

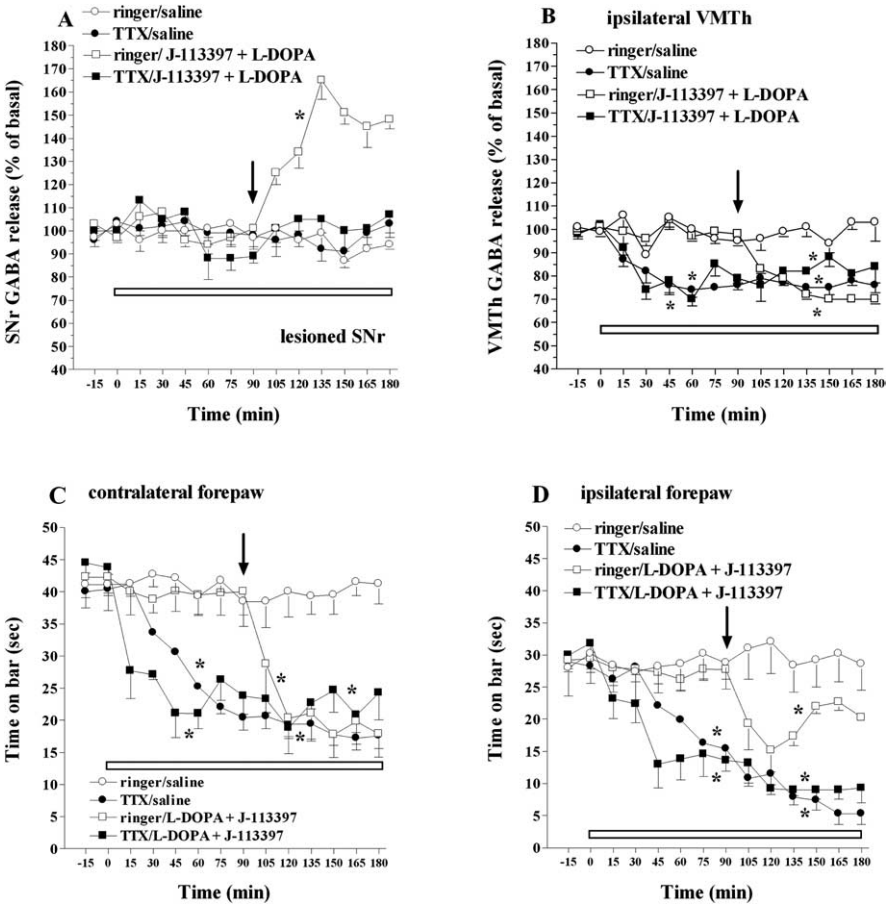

Figure 8. TTX prevented the reduction in VMTh GABA release and immobility time induced by L-DOPA and J-113397 coadministration. Two microdialysis probes were implanted in the lesioned SNr and ipsilateral VMTh of hemiparkinsonian rats. Perfusion with TTX (1 μM; open bar) in the SNr started 90 min before systemic (intraperitoneal) coadministration (arrow) of J-113397 (1 mg/kg) and L-DOPA (1 mg/kg plus 15 mg/kg benserazide) and continued until the end of experiment. ***C***, ***D***, In the same rats, akinesia was evaluated (every 15 min for up to 180 min) by using the bar test separately at the contralateral (***C***) and ipsilateral (***D***) paws (described in Materials and Methods). Statistical analysis was performed by two-way ANOVA with repeated measures followed by contrast analysis and the sequentially rejective Bonferroni test. Data are means ± SEM of *n* experiments. ***A***, ***B***, Basal GABA levels (in nanomolar concentration) in the dialysate from the lesioned SNr (***A***) and ipsilateral VMTh (***B***) were, respectively, as follows: 9.1 ± 0.6 and 9.7 ± 1.1 (washout/saline, $n = 5$); 7.0 ± 0.5 and 11.6 ± 0.8 (TTX/saline, $n = 6$); 7.3 ± 0.7 and 13.5 ± 0.9 (washout/J-113397 + L-DOPA, $n = 5$); 9.0 ± 0.5 and 10.9 ± 2.1 (TTX/J-113397 + L-DOPA, $n = 5$). *$p < 0.05$ versus saline-treated rats.

J-113397/L-DOPA interaction on behavior

Unilateral lesion of SNc DA neurons caused dramatic bilateral increase in the immobility time, with the contralateral ("parkinsonian") forepaw being more severely affected than the ipsilateral ("good") one. Although puzzling, this observation is consistent with reports that unilateral DA depletion also affected posture (Whishaw et al., 2003), stepping time, and stepping length (Olsson et al., 1995) at the ipsilateral paw. Interestingly, when the animal was forced to move (drag test), motor activity at the ipsilateral paw was only slightly impaired, suggesting that the bar and drag test provide information on different aspects of motor program. The bar test essentially measures the time to initiate a movement (akinesia), whereas the drag test measures both the time to initiate and to execute it (bradykinesia). The degree of motor asymmetry in the drag test (~65%) was consistent with that reported by Wessell et al. (2004) (~75%) and in line with that found with the stepping [~90% (Olsson et al., 1995); 80–90% (Winkler et al., 2002); ~70% (Tillerson et al., 2001); ~75% (Tseng et al., 2005); 50–90% (Kelsey et al., 2004)] or the postural adjustment [~75% (Lindner et al., 1996); >95% (Chang et al., 1999)] tests. Powerful, dose-dependent attenuation of parkinsonism was produced by increasing L-DOPA doses: reduction of akinesia at both the ipsilateral and the contralateral forepaw (0.1 mg/kg), improvement of exercise-induced motor performance (0.3 mg/kg), and reversal of motor asymmetry both under resting (bar test) and dynamic (drag test) conditions (6 mg/kg). Similar findings were reported by using the stepping (Olsson et al., 1995; Chang et al., 1999; Winkler et al., 2002; Kelsey et al., 2004), postural adjustment (Lindner et al., 1996), and "wheelbarrow" [i.e., forward dragging (Schallert et al., 1979)] tests. It is noteworthy that L-DOPA exerted an antiparkinsonian action at doses (0.1–6 mg/kg) lower than those eliciting contralateral rotations (25 mg/kg), strengthening the view that ethological tests may be more sensitive than analysis of pharmacologically induced (e.g., by dopamine agonists) turning behavior in screening for antiparkinsonian drugs.

The NOP receptor antagonist J-113397 reproduced L-DOPA action, although less effectively because it did not reverse fully motor asymmetry in the drag test (Marti et al., 2005). However, combination of subthreshold doses (0.1 mg/kg) of J-113397 and L-DOPA (ineffective per se) stimulated rotarod performance to the same extent as L-DOPA 0.3 mg/kg, whereas combination of submaximal doses (1 mg/kg) was as effective as L-DOPA 6 mg/kg in the drag test (i.e., it fully reversed asymmetry) and evoked a sustained antiakinetic response in the bar test (see Results). Most interestingly, combination of submaximal doses evoked supramaximal rotarod performance, suggesting that L-DOPA and

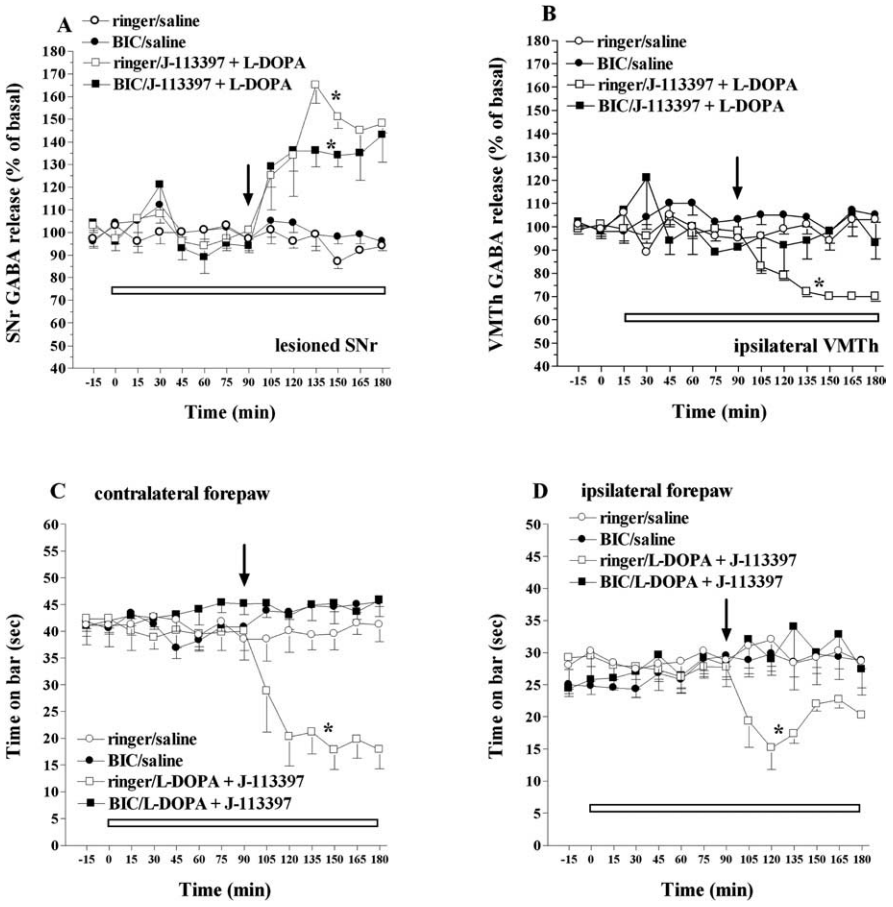

Figure 9. Bicuculline (BIC) prevented the reduction in VMTh GABA release and immobility time induced by L-DOPA and J-113397 coadministration. Two microdialysis probes were implanted in the lesioned SNr and ipsilateral VMTh of hemiparkinsonian rats. Perfusion with BIC (10 μM; open bar) in the SNr started 90 min before systemic (intraperitoneal) coadministration (arrow) of J-113397 (1 mg/kg) and L-DOPA (1 mg/kg plus 15 mg/kg benserazide) and continued until the end of experiment. ***C***, ***D***, In the same rats, akinesia was evaluated (every 15 min for up to 180 min) by using the bar test separately at the contralateral (***C***) and ipsilateral (***D***) paws (described in Materials and Methods). Statistical analysis was performed by two-way ANOVA with repeated measures followed by contrast analysis and the sequentially rejective Bonferroni test. Data are means ± SEM of *n* experiments. ***A***, ***B***, Basal GABA levels (in nanomolar concentration) in the dialysate from the lesioned SNr (***A***) and ipsilateral VMTh (***B***) were, respectively, as follows: 9.1 ± 0.6 and 9.7 ± 1.1 (washout/saline, $n = 5$); 7.8 ± 0.9 and 11.9 ± 1.8 (BIC/saline, $n = 5$); 7.3 ± 0.7 and 13.5 ± 0.9 (washout/J-113397 + L-DOPA, $n = 5$); 9.2 ± 1.5 and 12.1 ± 2.3 (BIC/J-113397 + L-DOPA, $n = 5$). *$p < 0.05$ versus saline-treated rats.

J-113397 activated independent neuronal pathways rather than a common, "saturable" mechanism. These data suggest that an NOP receptor antagonist may be a good candidate for a combination therapy. From a clinical point of view, combination therapy may benefit early PD patients by lowering L-DOPA dosage and delaying dyskinesia onset, or it may benefit advanced PD patients who require more than one medication to adequately control PD symptoms.

Neurobiological substrates underlying J-113397/L-DOPA interaction

Massive GLUergic innervation to the SNr is provided by the subthalamic nucleus, which becomes overactive under parkinsonian conditions (DeLong, 1990). Consistently, haloperidol evoked catalepsy and elevated SNr GLU release (Marti et al., 2004b, 2005). NOP receptor antagonists attenuated haloperidol-induced akinesia and normalized SNr GLU levels (Marti et al., 2004b, 2005), prompting us to suggest that inhibition of SNr GLU release underlies their antiparkinsonian action. SNr injections of UFP-101 [[Nphe^1,Arg^{14},Lys^{15}]N/OFQ-NH$_2$] (Marti et al., 2004b) reproduced the effects of systemic injections of J-113397 (Marti et al., 2005), further pointing to the SNr as their site of action. Reverse dialysis of N/OFQ in the SNr elevated local GLU release via GABA- and DA-mediated mechanisms (Marti et al., 2002a). Thus, NOP receptor antagonists may reduce SNr GLU release in the DA-depleted SNr by blocking tonic inhibition of DA and GABA neurons by endogenous N/OFQ. Indeed, N/OFQ inhibits DA and GABA transmission in mesencephalic areas (Zheng et al., 2002; Marti et al., 2004a), whereas NOP receptor antagonists elevate SNr GABA release (present study) and nigrostriatal DA transmission (Marti et al., 2004a). However, bicuculline did not affect the increase in SNr GABA and only delayed the reduction in GLU release evoked by L-DOPA and J-113397, suggesting that GABAergic inhibition is minimally involved in this phenomenon. In the same animals, bicuculline prevented the motor effects of combined L-DOPA and J-113397, further indicating that inhibition of GLU release may not be sufficient to explain the antiakinetic action of J-113397. In this respect, J-113397 also increased GABA release in the lesioned SNr and lowered GABA release in the ipsilateral VMTh. L-DOPA shared this action, although it did not affect SNr GLU levels. This suggests that DA receptor stimulation and NOP receptor blockade activated independent neuronal pathways, converging on a common "effector". According to the current model of basal ganglia functional organization (DeLong et al., 1990), reduction of the subthalamonigral GLUergic excitatory drive and/or increase of the GABAergic inhibitory influence on nigrothalamic GABAergic neurons leads to disinhibition of thalamocortical GLUergic projections and movement initiation (Deniau and Chevalier, 1985). Thus, this "effector" is likely represented by nigrothalamic GABAergic neurons. More evidence endorses this view. TTX perfusion in the SNr produced per se a rapid decline in VMTh GABA release. This indicates that spontaneous VMTh GABA release partly reflects impulse-dependent neuronal activity and is consistent with the fact that nigrothalamic GABA neurons provide a tonic input to the thalamus (Guyenet and Aghajanian 1978; Waszczak et al., 1980). This input is enhanced after DA lesion (Burbaud et al., 1995), which may explain why GABA levels were higher in the VMTh ipsilateral to the lesioned side. Interestingly, reduction of VMTh GABA release induced by TTX was associated with attenuation of akinesia. This is consistent with our previous finding that SNr perfusion of higher TTX concentrations (10 μM) evoked contralateral rotations in naive rats (Morari et al., 1996) and strengthens the view that inhibition of nigrothalamic GABAergic neurons results in disinhibition of locomotion (Starr et al., 1983; Deniau and Chevalier, 1985). Nigrothalamic GABAergic neurons express $GABA_A$ receptors (Nicholson et al., 1995), which drive both tonic (Rick

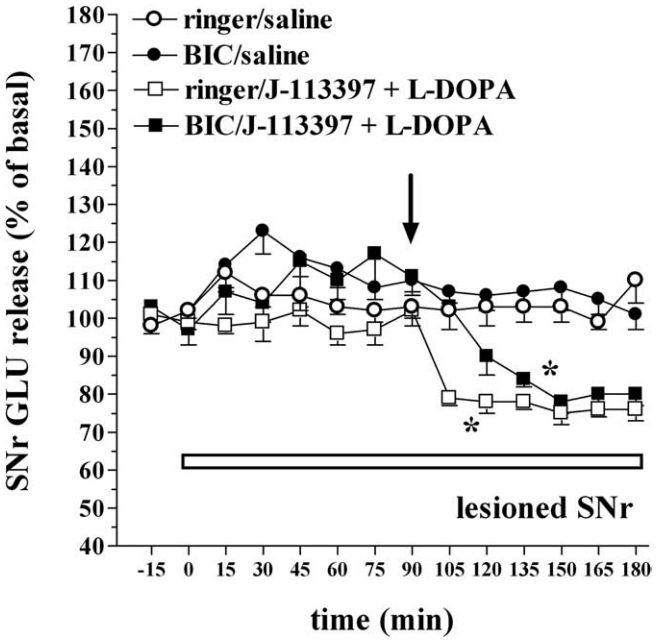

Figure 10. Bicuculline (BIC) delayed the reduction in SNr GLU release induced by L-DOPA and J-113397 coadministration. Perfusion with BIC (10 μM; open bar) in the SNr started 90 min before systemic (intraperitoneal) coadministration (arrow) of J-113397 (1 mg/kg) and L-DOPA (1 mg/kg plus 15 mg/kg benserazide) and continued until the end of experiment. Statistical analysis was performed by two-way ANOVA with repeated measures followed by contrast analysis and the sequentially rejective Bonferroni test. Basal GLU levels (in nanomolar concentration) in the dialysate from the lesioned SNr were, respectively, as follows: 115.3 $\pm$ 6.1 (washout/saline, $n = 5$); 104.2 $\pm$ 7.4 (BIC/saline, $n = 6$); 105.3 $\pm$ 6.7 (washout/J-113397 + L-DOPA, $n = 5$); 129.9 $\pm$ 14.8 (BIC/J-113397 + L-DOPA, $n = 5$). *$p < 0.05$ versus saline-treated rats.

and Lacey, 1994) and phasic (*in vivo*) (Deniau and Chevalier, 1985) inhibition. Thus, bicuculline may prevent both the attenuation of akinesia and the decrease in VMTh GABA release by blocking those postsynaptic $GABA_A$ receptors. Likewise, bicuculline prevented the reduction in VMTh GABA release induced by systemic methamphetamine (Mark et al., 2004). Alternatively, blockade of inhibitory $GABA_A$ receptors on (residual) nigral DA cells may lead to increased DA release (Westerink et al., 1992) and attenuation of the inhibitory control driven by $GABA_A$ receptors onto nigrothalamic GABAergic neurons (Waszczak and Walters, 1986), which may also result in attenuation of the antiakinetic effect of L-DOPA.

The mechanisms through which systemic L-DOPA increased SNr GABA release also remain to be investigated. L-DOPA could stimulate D_1 receptors on striatonigral neurons (Gerfen et al., 1990), so to activate the "direct" pathway (Robertson and Robertson, 1989; Carta et al., 2005), or D_1 receptors on striatonigral nerve terminals (Starr, 1987; Aceves et al., 1991). The fact that TTX prevented the L-DOPA effect rules out this latter hypothesis, although it does not exclude an intranigral action of L-DOPA because this agent could stimulate GABAergic interneurons [dendritic location of D_1 receptors has been detected in the SNr (Huang et al., 1992)]. Finally, the possibility that L-DOPA increases SNr GABA release by modulating the subthalamonigral GLUergic projection cannot be discarded because L-DOPA elevated SNr GLU levels. However, this possibility appears remote in view of the mismatch between the dynamics of GABA and GLU levels.

Concluding remarks

Combined administration of an NOP receptor antagonist (J-113397) and L-DOPA produced additive attenuation of parkinsonian-like symptoms through an increase in SNr GABA release and consequent overinhibition of SNr GABAergic neurons projecting to the VMTh. These data strengthen the role of the VMTh in the modulation of parkinsonism (Wolfarth et al., 1985; Kolasiewicz et al., 1988), emphasizing its role as a relay nucleus for impulses ascending from the SNr to the cortex (Klockgether et al., 1986). This appears relevant also in humans, in which motor improvement induced by deep brain stimulation in the subthalamic nucleus was associated with lowered GABA release in the motor thalamus (Stefani et al., 2006). Overall, the present study provides novel insights into the mechanisms underlying the antiparkinsonian action of J-113397 and L-DOPA and suggests that an NOP receptor antagonist may be used alone or as an adjunct to L-DOPA in the therapy of PD.

References

Aceves J, Floran B, Martinez-Fong D, Sierra A, Hernandez S, Mariscal S (1991) L-dopa stimulates the release of [3H]gamma-aminobutyric acid in the basal ganglia of 6-hydroxydopamine lesioned rats. Neurosci Lett 121:223–226.

Burbaud P, Gross C, Benazzouz A, Coussemacq M, Bioulac B (1995) Reduction of apomorphine-induced rotational behaviour by subthalamic lesion in 6-OHDA lesioned rats is associated with a normalization of firing rate and discharge pattern of pars reticulata neurons. Exp Brain Res 105:48–58.

Carta AR, Tronci E, Pinna A, Morelli M (2005) Different responsiveness of striatonigral and striatopallidal neurons to L-DOPA after a subchronic intermittent L-DOPA treatment. Eur J Neurosci 21:1196–1204.

Chang JW, Wachtel SR, Young D, Kang UJ (1999) Biochemical and anatomical characterization of forepaw adjusting steps in rat models of Parkinson's disease: studies on medial forebrain bundle and striatal lesions. Neuroscience 88:617–628.

DeLong MR (1990) Primate models of movement disorders of basal ganglia origin. Trends Neurosci 13:281–285.

Deniau JM, Chevalier G (1985) Disinhibition as a basic process in the expression of striatal functions. II. The striato-nigral influence on thalamocortical cells of the ventromedial thalamic nucleus. Brain Res 334:227–233.

Devine DP, Taylor L, Reinscheid RK, Monsma Jr FJ, Civelli O, Akil H (1996) Rats rapidly develop tolerance to the locomotor-inhibiting effects of the novel neuropeptide orphanin FQ. Neurochem Res 21:1387–1396.

Di Chiara G, Porceddu ML, Morelli M, Mulas ML, Gessa GL (1979) Evidence for a GABAergic projection from the substantia nigra to the ventromedial thalamus and to the superior colliculus of the rat. Brain Res 176:273–284.

Gerfen CR, Engber TM, Mahan LC, Susel Z, Chase TN, Monsma Jr FJ, Sibley DR (1990) D1 and D2 dopamine receptor-regulated gene expression of striatonigral and striatopallidal neurons. Science 250:1429–1432.

Guyenet PG, Aghajanian GK (1978) Antidromic identification of dopaminergic and other output neurons of the rat substantia nigra. Brain Res 150:69–84.

Huang Q, Zhou D, Chase K, Gusella JF, Aronin N, Di Figlia M (1992) Immunohistochemical localization of the D1 dopamine receptor in rat brain reveals its axonal transport, pre- and postsynaptic localization, and prevalence in the basal ganglia, limbic system, and thalamic reticular nucleus. Proc Natl Acad Sci USA 89:11988–11992.

Kawamoto H, Ozaki S, Itoh Y, Miyaji M, Arai S, Nakashima H, Kato T, Ohta H, Iwasawa Y (1999) Discovery of the first potent and selective small molecule opioid receptor-like (ORL1) antagonist: 1-[(3R,4R)-1-cyclooctylmethyl-3-hydroxymethyl-4-piperidyl]-3-ethyl-1,3-dihydro-2H-benzimidazol-2-one (J-113397). J Med Chem 42:5061–5063.

Kelsey JE, Mague SD, Pijanowski RS, Harris RC, Kleckner NW, Matthews RT (2004) NMDA receptor antagonists ameliorate the stepping deficits produced by unilateral medial forebrain bundle injections of 6-OHDA in rats. Psychopharmacology 175:179–188.

Klockgether T, Schwarz M, Turski L, Sontag KH (1986) The rat ventromedial thalamic nucleus and motor control: role of *N*-methyl-D-aspartate-

mediated excitation, GABAergic inhibition, and muscarinic transmission. J Neurosci 6:1702–1711.
Kolasiewicz W, Wolfarth S, Ossowska K (1988) The role of the ventromedial thalamic nucleus in the catalepsy evoked from the substantia nigra pars reticulata in rats. Neurosci Lett 90:219–223.
Lindner MD, Plone MA, Francis JM, Emerich DF (1996) Validation of a rodent model of Parkinson's disease: evidence of a therapeutic window of oral Sinemet. Brain Res Bull 39:367–372.
Lindner MD, Cain CK, Plone MA, Frydel BR, Blaney TJ, Emerich DF, Hoane MR (1999) Incomplete nigrostriatal dopaminergic cell loss and partial reductions in striatal dopamine produce akinesia, rigidity, tremor and cognitive deficits in middle-aged rats. Behav Brain Res 102:1–16.
MacLeod NK, James TA, Kilpatrick IC, Starr MS (1980) Evidence for a GABAergic nigrothalamic pathway in the rat. II. Electrophysiological studies. Exp Brain Res 40:55–61.
Mark KA, Soghomonian JJ, Yamamoto BK (2004) High-dose methamphetamine acutely activates the striatonigral pathway to increase striatal glutamate and mediate long-term dopamine toxicity. J Neurosci 24:11449–11456.
Marti M, Guerrini R, Beani L, Bianchi C, Morari M (2002a) Nociceptin/orphanin FQ receptors modulate glutamate extracellular levels in the substantia nigra pars reticulata. A microdialysis study in the awake freely moving rat. Neuroscience 112:153–160.
Marti M, Mela F, Bianchi C, Beani L, Morari M (2002b) Striatal dopamine-NMDA receptor interactions in the modulation of glutamate release in the substantia nigra pars reticulata in vivo: opposite role for D1 and D2 receptors. J Neurochem 83:635–644.
Marti M, Mela F, Ulazzi L, Hanau S, Stocchi S, Paganini F, Beani L, Bianchi C, Morari M (2003) Differential responsiveness of rat striatal nerve endings to the mitochondrial toxin 3-nitropropionic acid: implications for Huntington's disease. Eur J Neurosci 18:759–767.
Marti M, Mela F, Veronesi C, Guerrini R, Salvadori S, Federici M, Mercuri NB, Rizzi A, Franchi G, Beani L, Bianchi C, Morari M (2004a) Blockade of nociceptin/orphanin FQ receptor signaling in rat substantia nigra pars reticulata stimulates nigrostriatal dopaminergic transmission and motor behavior. J Neurosci 24:6659–6666.
Marti M, Mela F, Guerrini R, Calo G, Bianchi C, Morari M (2004b) Blockade of nociceptin/orphanin FQ transmission in rat substantia nigra reverses haloperidol-induced akinesia and normalizes nigral glutamate release. J Neurochem 91:1501–1504.
Marti M, Mela F, Fantin M, Zucchini S, Brown JM Witta J, Di Benedetto M, Buzas B, Reinscheid RK, Salvadori S, Guerrini R, Romualdi P, Candeletti S, Simonato M, Cox BM, Morari M (2005) Blockade of nociceptin/orphanin FQ transmission attenuates symptoms and neurodegeneration associated with Parkinson's disease. J Neurosci 95:9591–9601.
Morari M, O'Connor WT, Darvelid M, Ungerstedt U, Bianchi C, Fuxe K (1996) Functional neuroanatomy of the nigrostriatal and the striatonigral pathways as studied with dual probe microdialysis in the awake rat. I. Effects of perfusion with tetrodotoxin and low calcium medium. Neuroscience 72:79–87.
Nicholson LF, Faull RL, Waldvogel HJ, Dragunow M (1995) GABA and GABAA receptor changes in the substantia nigra of the rat following quinolinic acid lesions in the striatum closely resemble Huntington's disease. Neuroscience 66:507–521.
Obeso JA, Olanow CW, Nutt JG (2000) Levodopa motor complication in Parkinson's disease. Trends Neurosci 23:S2–S7.
Olsson M, Nikkhah G, Bentlage C, Bjorklund A (1995) Forelimb akinesia in the rat Parkinson model: differential effects of dopamine agonists and nigral transplants as assessed by a new stepping test. J Neurosci 15:3863–3875.
Paxinos G, Watson C (1982) The rat brain in stereotaxic coordinates. Sydney: Academic.
Reinscheid RK, Nothacker HP, Bourson A, Ardati A, Henningsen RA, Bunzow JR, Grandy DK, Langen H, Monsma Jr FJ, Civelli O (1995) Orphanin FQ: a neuropeptide that activates an opioid-like G protein-coupled receptor. Science 270:792–794.
Rick CE, Lacey MG (1994) Rat substantia nigra pars reticulata neurones are tonically inhibited via GABAA, but not GABAB, receptors in vitro. Brain Res 659:133–137.
Robertson GS, Robertson HA (1989) Evidence that L-dopa-induced rotational behavior is dependent on both striatal and nigral mechanisms. J Neurosci 9:3326–3331.
Rozas G, Guerra MJ, Labandeira-Garcia JL (1997) An automated rotarod method for quantitative drug-free evaluation of overall motor deficits in rat models of parkinsonism. Brain Res Brain Res Protoc 2:75–84.
Sanberg PR, Bunsey MD, Giordano M, Norman AB (1988) The catalepsy test: its ups and downs. Behav Neurosci 102:748–759.
Schallert T, De Ryck M, Wishaw IQ, Ramirez VD, Teitelbaum P (1979) Excessive bracing reactions and their control by atropine and L-DOPA in an animal analog of parkinsonism. Exp Neurol 64:33–43.
Starr M (1987) Opposing roles of dopamine D1 and D2 receptors in nigral gamma-[3H]aminobutyric acid release? J Neurochem 49:1042–1049.
Starr MS, Summerhayes M, Kilpatrick IC (1983) Interactions between dopamine and gamma-aminobutyrate in the substantia nigra: implications for the striatonigral output hypothesis. Neuroscience 8:543–557.
Stefani A, Fedele E, Mazzone P, Galati S, Tropepi P, Stanzione P (2006) In vivo microdialysis in parkinsonian patients undergoing stereotactic neurosurgery: key insights on DBS mechanisms of actions. In: Proceedings of the 11th International Conference of In Vivo Methods (Valentini V, Di Chiara G, eds), pp 74–76. Sardinia, Italy: University of Cagliari.
Tillerson JL, Cohen AD, Philhower J, Miller GW, Zigmond MJ, Schallert T (2001) Forced limb-use effects on the behavioural and neurochemical effects of 6-hydroxydopamine. J Neurosci 21:4427–4435.
Tseng KY, Kargieman L, Gacio S, Riquelme LA, Murer G (2005) Consequences of partial and severe dopaminergic lesion on basal ganglia oscillatory activity and akinesia. Eur J Neurosci 22:2579–2586.
Ungerstedt U, Arbuthnott GW (1970) Quantitative recording of rotational behaviour in rats after 6-hydroxydopamine lesions of the nigrostriatal dopamine system. Brain Res 24:485–493.
Waszczak BL, Walters JR (1986) Endogenous dopamine can modulate inhibition of substantia nigra pars reticulate neurons elicited by GABA iontophoresis or striatal stimulation. J Neurosci 6:120–126.
Waszczak BL, Eng N, Walters JR (1980) Effects of muscimol and picrotoxin on single unit activity of substantia nigra neurons. Brain Res 188:185–197.
Wessell RH, Ahmed SM, Menniti FS, Dunbar GL, Chase TN, Oh JD (2004) NR2B selective NMDA receptor antagonist CP-101,606 prevents levodopa-induced motor response alterations in hemi-parkinsonian rats. Neuropharmacology 47:184–194.
Westerink BH, Santiago M, De Vries JB (1992) In vivo evidence for a concordant response of terminal and dendritic dopamine release during intranigral infusion of drugs. Naunyn Schmiedebergs Arch Pharmacol 346:637–643.
Whishaw IQ, Li K, Whishaw PA, Gorny B, Metz GA (2003) Distinct forelimb and hind limb stepping impairments in unilateral dopamine-depleted rats: use of the rotorod as a method for the qualitative analysis of skilled walking. J Neurosci Methods 126:13–23.
Winkler C, Kirik D, Bjorklund A, Cenci MA (2002) L-DOPA-induced dyskinesia in the intrastriatal 6-hydroxydopamine model of parkinson's disease: relation to motor and cellular parameters of nigrostriatal function. Neurobiol Dis 10:165–186.
Wolfarth S, Kolasiewicz W, Ossowska K (1985) Thalamus as a relay station for catalepsy and rigidity. Behav Brain Res 18:261–268.
Zheng F, Grandy DK, Johnson SW (2002) Actions of orphanin FQ/nociceptin on rat ventral tegmental area neurons in vitro. Br J Pharmacol 136: 1065–1071.

ELSEVIER

Neurobiology of Disease

www.elsevier.com/locate/ynbdi
Neurobiology of Disease 30 (2008) 430–438

Nociceptin/orphanin FQ receptor blockade attenuates MPTP-induced parkinsonism

Riccardo Viaro,[a,c,1] Rosario Sanchez-Pernaute,[d,e,1] Matteo Marti,[a,c] Claudio Trapella,[b] Ole Isacson,[d,e] and Michele Morari[a,c,*]

[a]*Department of Experimental and Clinical Medicine, Section of Pharmacology, University of Ferrara, Ferrara, Italy*
[b]*Department of Pharmaceutical Sciences and Biotechnology Center, University of Ferrara, Ferrara, Italy*
[c]*Neuroscience Center and Istituto Nazionale di Neuroscienze, University of Ferrara, Ferrara, Italy*
[d]*Neuroregeneration Laboratories, Center for Neuroregeneration Research, McLean Hospital, Belmont, Massachusetts, USA*
[e]*Harvard Medical School, Belmont, Massachusetts, USA*

Received 5 January 2008; revised 14 February 2008; accepted 23 February 2008
Available online 8 March 2008

Endogenous nociceptin/orphanin FQ (N/OFQ) inhibits the activity of dopamine neurons in the substantia nigra and affects motor behavior. In this study we investigated whether a N/OFQ receptor (NOP) antagonist, J-113397, can modify movement in naive mice and nonhuman primates and attenuate motor deficits in MPTP-treated parkinsonian animals. J-113397 facilitated motor activity in naïve mice at low doses (0.1–1 mg/kg) and inhibited it at higher ones (10 mg/kg). Likewise, in MPTP-treated mice, J-113397 reversed motor deficit at 0.01 mg/kg but worsened hypokinesia at higher doses (1 mg/kg). In naïve nonhuman primates, J-113397, ineffective up to 1 mg/kg, produced inconsistent motor improvements at 3 mg/kg. Conversely, in parkinsonian primates J-113397 (0.01 mg/kg) reversed parkinsonism, being most effective against hypokinesia. We conclude that endogenous N/OFQ modulates motor activity in mice and nonhuman primates and contributes to parkinsonian symptoms in MPTP-treated animals. NOP receptor antagonists may represent a novel approach to Parkinson's disease.

Keywords: J-113397; L-DOPA; MPTP; Nociceptin/orphanin FQ; NOP$^{-/-}$ mice; NOP receptor; Parkinson's disease

Introduction

Nociceptin/orphanin FQ (N/OFQ) is an opioid-like neuropeptide (Meunier et al., 1995; Reinscheid et al., 1995) which activates the NOP receptor (Cox et al., 2000). The N/OFQ-NOP receptor system is expressed in motor areas of the rodent (Neal et al., 2001) and primate brain (Bridge et al., 2003) and, particularly, in the substantia nigra (SN), which contains dopamine (DA) neurons that degenerate in Parkinson's disease (PD). N/OFQ inhibits the activity of DA neurons located in the SN compacta (SNc; Marti et al., 2004a) and impairs spontaneous (Reinscheid et al., 1995; Devine et al., 1996) and exercise-induced locomotion (Marti et al., 2004a) in rodents. Conversely, selective NOP receptor antagonists, such as [Nphe^{1}, Arg^{14}, Lys^{15}]N/OFQ-NH$_2$ (UFP-101; Calò et al., 2002) and 1-[(3R,4R)-1-cyclooctylmethyl-3-hydroxymethyl-4-piperidyl]-3-ethyl-1,3-dihydro-2H benzimidazol-2-one (J-113397 or compound B; Kawamoto et al., 1999) increase striatal DA release and rotarod performance (Marti et al., 2004a), indicating that endogenous N/OFQ exerts an inhibitory control on physiologically-stimulated locomotion. We have proposed that endogenous N/OFQ plays a pathogenic role in PD (Marti et al., 2005). Indeed, N/OFQ transmission was found to be up-regulated in the DA-depleted SN of 6-hydroxydopamine (6-OHDA) hemi-lesioned rats (Marti et al., 2005). Moreover, NOP receptor antagonists alleviated akinesia/bradykinesia induced by haloperidol administration (Marti et al., 2004b) and 6-OHDA lesion (Marti et al., 2005), and enhanced the antiparkinsonian effect of L-DOPA when co-administered to rats (Marti et al., 2007). Finally, NOP receptor and ppN/OFQ knockout mice were found to be more resistant than wild-type to haloperidol-induced akinesia and 1-methyl-4-phenyl 1,2,3,6 tetrahydropyridine (MPTP) induced toxicity, respectively (Marti et al., 2005). Here we explored the hypothesis that the NOP antagonist J-113397 alleviates motor deficit in MPTP-treated mice and nonhuman primates. The advantage of the MPTP models is that systemic administration produces a bilateral DA denervation and, in nonhuman primates, MPTP induces symptoms that closely resemble those observed in parkinsonian patients. We used NOP receptor

* Corresponding author. Department of Experimental and Clinical Medicine, Section of Pharmacology, University of Ferrara, via Fossato di Mortara 17-19, 44100 Ferrara, Italy. Fax: +39 0532 455205.
E-mail address: m.morari@unife.it (M. Morari).
[1] These authors contributed equally to this work.
Available online on ScienceDirect (www.sciencedirect.com).

0969-9961/$ - see front matter © 2008 Elsevier Inc. All rights reserved.
doi:10.1016/j.nbd.2008.02.011

Table 1
Individual characteristics of MPTP-lesioned primates

Animal #	Weight (kg)	PRS score after MPTP	PRS score 3rd month post-MPTP	Activity *d*/*n* (% from baseline)
Mf23	4.4	17	18.25	−76/−60
Mf25	5.4	19	21.5	−77/−62
Mf30	6.1	21	20	−68/−32
Mf34	5.3	18	18.5	−5/−60

knockout ($NOP^{-/-}$) mice to confirm the specificity of the in vivo action of J-113397.

Materials and methods

Subjects

Mice

Male Swiss, C57BL/6J (20–25 g; 12 week old, Harlan Italy, S. Pietro al Natisone, Italy), CD1/C57BL6J/129 $NOP^{+/+}$ and $NOP^{-/-}$ mice (20–25 g; 12–15 week old; Nishi et al., 1997) were used. Mice were kept under standard conditions (12 h dark:12 h light cycle, free access to food and water) and the experimental protocols were approved by the Italian Ministry of Health (licence n° 71-2004-B).

Mice were trained for a week in order to obtain a stable performance in the three behavioral tests used to assess motor performance. Mice were then treated acutely with MPTP (4×20 mg/kg, 90 min apart). Pharmacological tests were performed 7 days after MPTP treatment, i.e. when DA cell loss stabilizes (Jackson-Lewis and Przedborski, 2007). Mice were later sacrificed for tyrosine hydroxylase (TH) immunohistochemistry (7th day post-MPTP).

Nonhuman primates

Four young adult male macaques (*Macaca fascicularis*) were included in the study. Animals were housed individually at the New England Primate Research Center. All the studies were done following NIH guidelines for animal welfare and were approved by the IACUC at Harvard Medical Area and the New England Regional Primate Research Center. After completion of experiments in the naïve state, animals were rendered parkinsonian by systemic administration of MPTP (0.3 mg/kg/week i.v. for 7.5±2.5 weeks) as described (Jenkins et al., 2004; Sanchez-Pernaute et al., 2007). Pharmacological tests were performed at least 3 months after the last MPTP dose.

Behavioral assessment

Mice

Motor activity was evaluated blindly using a battery of previously validated behavioral tests specific for different motor abilities under static (bar test; Sanberg et al., 1988) and dynamic (drag test and fixed-speed rotarod test; Rozas et al., 1997; Marti et al., 2004a, 2005) conditions. On the day of experiment, the tests were performed before (control session) and 10 and 60 min after drug or vehicle injection. Each animal was taken as its own control.

Bar test. Each mouse was placed on a table and the contralateral and ipsilateral forepaws were placed alternatively on blocks of increasing heights (1.5, 3 and 6 cm). Total time (in seconds) spent by each paw on the blocks was recorded (cut-off time of 20 s).

Drag test. Each mouse was lifted by the tail (allowing forepaws on the table) and dragged backwards at a constant speed (~20 cm/s)

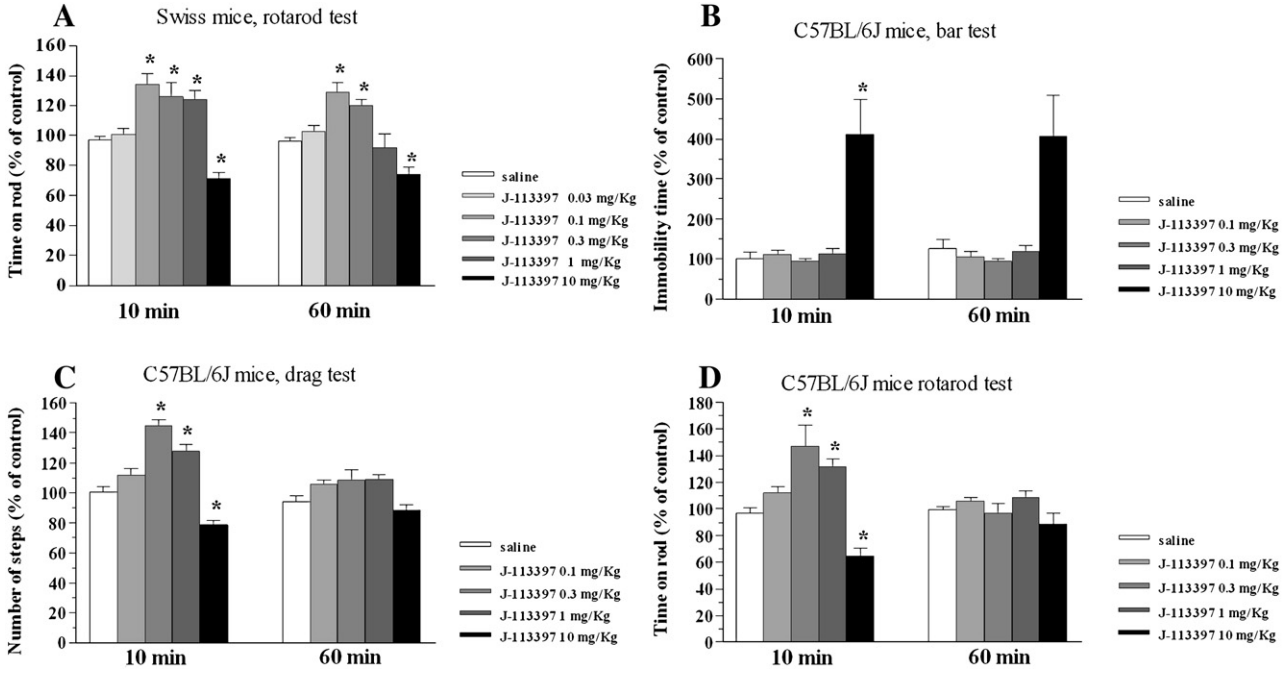

Fig. 1. J-113397 (0.03–10 mg/kg, i.p.) dually modulated rotarod performance in naïve Swiss and C57BL/6J mice. Mice were trained daily on the rotarod until their motor performance was reproducible (see Materials and methods). On the day of the experiment, three behavioral sessions were carried out, before (control session) and after (10 and 60 min) drug administration. The time spent on the rod was calculated (in seconds). Data are expressed as percent of the performance in the control session and represent the mean±SEM of 8–10 determinations for each group. *$p<0.05$; different from saline (RM ANOVA followed by contrast analysis and the sequentially rejective Bonferroni's test).

for a fixed distance (100 cm). The number of steps made by each paw was counted by two separate observers.

Rotarod test. A protocol that allowed to detect both facilitatory and inhibitory drug effects was used (Marti et al., 2004a). Mice were tested at increasing speeds (usually from 5 to 45 rpm for naïve and from 5 to 35 rpm for MPTP-treated mice; 180 s each) and motor activity was calculated by comparing the performance over a speed range (usually 30–45 rpm for naïve and 20–35 rpm for MPTP-treated mice) causing a progressive decrement of performance to ~40% of the maximal response (i.e. the experimental cut-off time).

Nonhuman primates

Animals were trained to perform a computerized timed reaching task that measures the speed of arm movements (MAP test; Jenkins et al., 2004). Training was carried out for an average of 6 days for the platform task and 8–12 days for the straight rod task, until the performance (time to retrieve the treats) was stable. For pharmacological evaluation, animals were tested 30 min after the administration of vehicle (saline) for 2 days and then with either saline or the active drugs. In addition, global motor activity data was obtained using activity monitors (Actiwatch) for a week at the naïve and parkinsonian stages (Table 1). These tests provide objective measures of bradykinesia and hypokinesia, respectively. For motor evaluation, animals were transferred to a Plexiglas observation cage where they were videotaped. Motor behavior was rated according to a scale based on the motor subscale of the UPDRS (Unified Parkinson's Disease Rating Scale), as described (Jenkins et al., 2004; Sanchez-Pernaute et al., 2007). The following signs were scored from 0 to 3: bradykinesia in the left and right arms (L/R), tremor L/R, rigidity L/R, hypokinesia, posture/balance (for a total score from 0 to 24). Scores were obtained at 30–45 min after each drug or vehicle administration.

Histological evaluation in mice

Mice were anaesthetised with ketamine 85 mg/kg and xylazine 15 mg/kg (i.p.), transcardially perfused with 20 mM phosphate-buffered saline (PBS) and fixed with 4% paraformaldehyde in PBS at pH 7.4. The brains were removed, post-fixed overnight and cryoprotected in 20% sucrose (solution in PBS). Serial coronal sections of 30 μm thickness were made in the striatum (−0.8 to +1.3 from bregma) and every second section processed for TH immunohistochemistry, as described (Marti et al., 2007). Briefly, sections were preincubated in blocking serum (5% normal horse serum and 0.3% Triton X 100 in PBS), incubated overnight in anti-TH mouse monoclonal antibody solution (1:2000, Chemicon, Temcula, CA), then in biotinylated horse anti-mouse IgG secondary antibody (1:200; Vector Laboratories, Burlingame, CA) for 1 h and finally treated with avidin–biotin-peroxidase complex (Vector Laboratories). Immunoreactivity was visualized by incubating the sections in a solution containing 0.05% 3,3-diaminobenzidine (DAB) in 0.013% H_2O_2. Images from every section were acquired with a Polaroid DMC camera mounted in a Zeiss Axioskop (Carl Zeiss, Oberkochen, Germany) and the optical density of TH-immunoreactive fibres in the striatum was analysed at five AP levels for each animal (−0.10,+ 0.20,+ 0.50,+ 0.80,+ 1.10) using ImageJ software (Wayne Rasband; NIH, USA). Region of interest for estimation of optical density was performed in the dorsolateral area of the caudate-putamen. Optical density (corrected for non-specific background measured in the corpus callosum) was first calculated for each animal as the mean of the 5 striatal levels. Group means (as presented in figure) were then obtained by averaging each individual value.

Data presentation and statistical analysis

Mice

Motor performance was calculated as time on bar or on rod (in seconds) and number of steps (drag test). Data are expressed as a percent ± SEM of the control session. Statistical analysis was performed (CoStat 6.3, CoHort Software, Monterey, CA, USA) on percent data by repeated measure (RM) analysis of variance (ANOVA) followed by contrast analysis and the sequentially rejective Bonferroni's test.

Nonhuman primates

Statistical analysis was performed (StatView Software, SAS, CA), using *t* tests and ANOVA (followed by the PLSD test) to determine

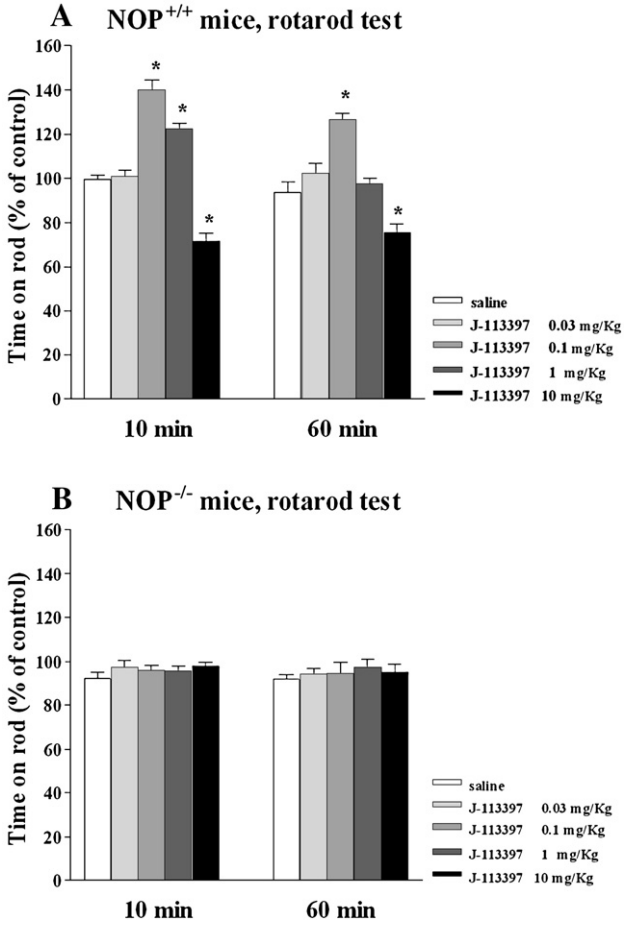

Fig. 2. Motor effects of J-113397 were dependent on NOP receptor. J-113397 (0.03–10 mg/kg, i.p.) dually modulated rotarod performance in wild-type mice ($NOP^{+/+}$; panel A) but was ineffective in NOP receptor knockout mice ($NOP^{-/-}$; panel B). Mice were trained daily on the rotarod until their motor performance was reproducible (see Materials and methods). On the day of the experiment, three behavioral sessions were carried out, before (control session) and after (10 and 60 min) drug administration. The time (in seconds) spent on the rod was calculated. Data are expressed as percent of the performance in the control session and are mean ± SEM of 8–10 determinations for each group. *$p < 0.05$; different from saline (RM ANOVA followed by contrast analysis and the sequentially rejective Bonferroni's test).

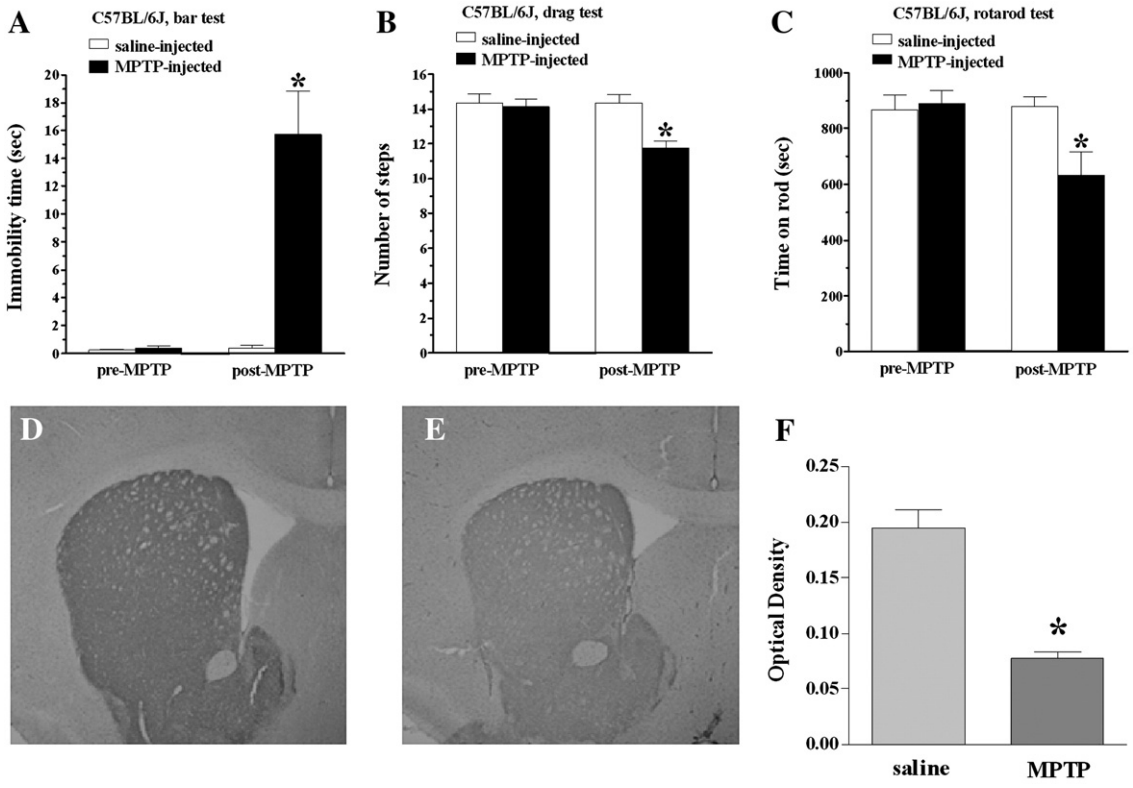

Fig. 3. MPTP administration produced motor impairment and loss of striatal DA terminals in C57BL/6J mice. Motor activity was evaluated by three behavioral tests: the bar (panel A), drag (panel B) and rotarod (panel C) test. Mice were trained daily for a week until their motor activity was reproducible (see Materials and methods). Before MPTP (20 mg/kg) or saline administration (4 injections, 90 min apart), motor activity was evaluated, and the time spent (seconds) on the blocks (bar test), the number of steps made by the forelimbs (drag test) and the time spent on the rod (rotarod test) were calculated. Another session was repeated 7 days after MPTP administration. Tyrosine hydroxylase (TH) immunohistochemistry was then performed in striatal slices (panels D–F). Photomicrograph of TH-positive fibres in the striata of saline (panel D) and MPTP-injected (panel E) mice. Optical density of TH-positive fibres in the striatum (panel F). Values are presented as means ± SEM, obtained from 4 saline- and 6 MPTP-treated mice. Data are expressed in absolute values and are mean ± SEM of 9 determinations for each group. *$p < 0.05$; different from saline-injected mice (panels A–C, ANOVA followed by the Newman–Keuls test; panel F, Student's *t*-test).

the effect of the drugs on motor performance as indicated in the text. Data are shown as mean values ± SEM.

Materials

L-DOPA methylester, benserazide and MPTP were purchased from Sigma Chemical Company (St Louis, MO, USA). J-113397 was synthesized as a racemic mixture in our laboratories (Marti et al., 2004a). All drugs were freshly dissolved in isoosmotic saline solution prior to use.

Results

Studies in mice

Naïve Swiss and C57BL/6J mice

To investigate the role of endogenous N/OFQ in the regulation of motor activity, J-113397 was administered systemically in Swiss mice (Fig. 1A). RM ANOVA showed a significant effect of treatment ($F_{5,40} = 20.90$, $p < 0.0001$), time ($F_{1,5} = 4.80$, $p = 0.033$) and a significant time × treatment interaction ($F_{5,48} = 3.51$, $p = 0.0087$). Post-hoc analysis showed that J-113397 facilitated rotarod performance in the 0.1–1 mg/kg dose range (maximal increase ~34%) while inhibited it at 10 mg/kg (~29%). Both effects were evident up to 60 min after administration. The complete battery of behavioral tests was then used to characterize J-113397 action in C57BL/6J mice (Figs. 1B–D). RM ANOVA on the immobility time as in the bar test (Fig. 1B), revealed a main effect of treatment ($F_{4,28} = 12.49$, $p < 0.0001$) but not time ($F_{1,4} = 0.04$, $p = 0.85$) and a non significant time × treatment interaction ($F_{4,39} = 0.09$, $p = 0.98$). J-113397 increased the immobility time at 10 mg/kg, lower doses being ineffective. RM ANOVA on the number of steps as in the drag test (Fig. 1C) revealed a main effect of treatment ($F_{4,28} = 23.81$, $p < 0.0001$), time ($F_{1,4} = 27.65$, $p < 0.0001$) and a significant time × treatment interaction ($F_{4,39} = 14.00$, $p < 0.0001$). Likewise, RM ANOVA on the rotarod performance (Fig. 1D) showed a main effect of treatment ($F_{4,28} = 9.81$, $p < 0.0001$), time ($F_{1,4} = 9.02$, $p = 0.0046$) and a significant time × treatment interaction ($F_{4,39} = 15.23$, $p < 0.0001$). Post-hoc analysis revealed that J-113397 enhanced the number of steps (Fig. 1C) and the exercise-stimulated locomotion (Fig. 1D) at 0.3 and 1 mg/kg while reducing them at 10 mg/kg. No effects were observed 60 min after drug administration.

Naïve NOP$^{-/-}$ mice

Since high doses of J-113397 (10 mg/kg) have been reported to exert effects independent of NOP receptors (Koizumi et al., 2004), we investigated the specificity of the J-113397 action (Fig. 2). RM

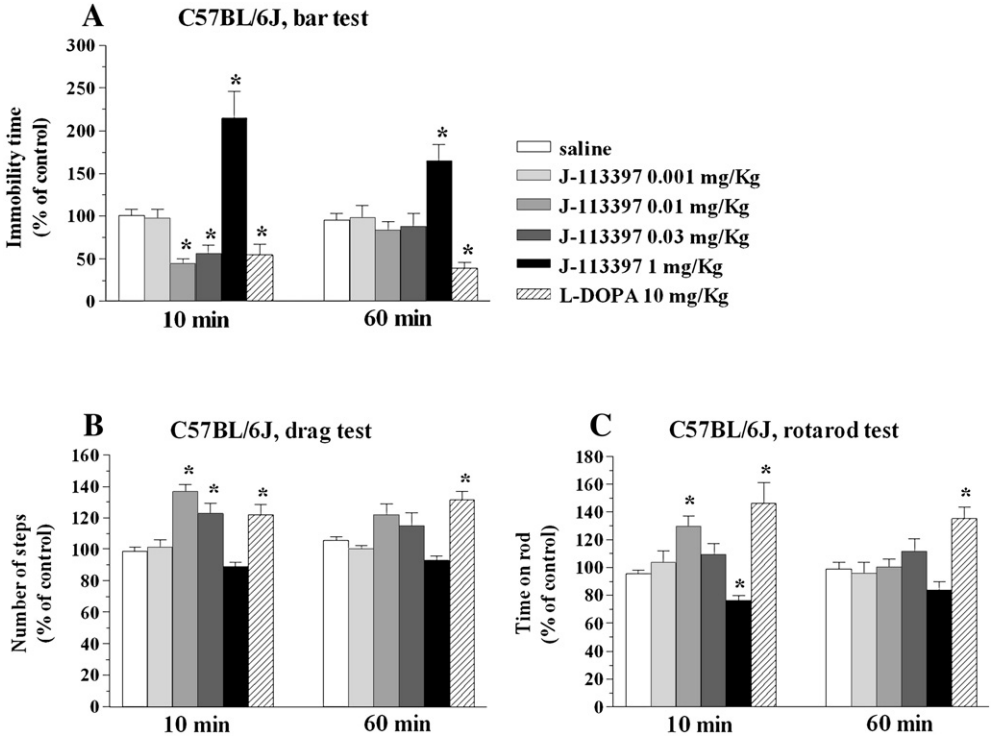

Fig. 4. J-113397 attenuated motor deficits in MPTP-treated C57BL/6J mice. Motor activity was evaluated by three behavioral tests: the bar (panel A), drag (panel B) and rotarod (panel C) test. Mice were trained daily until their motor activity was reproducible (see Materials and methods), then they were treated with MPTP. Seven days after MPTP mice were challenged with saline, J-113397 (0.01–1 mg/kg, i.p.) or L-DOPA (10 mg/kg plus benserazide 2.5 mg/kg, i.p.). Three behavioral sessions were carried out, before (control session) and after (10 and 60 min) drug or saline administration. The time spent (seconds) on the blocks (bar test), the number of steps made by the forelimbs (drag test) and the time spent on the rod (rotarod test) were calculated. Data are expressed as percent of the performance in the control session and are mean ± SEM of 8–10 determinations for each group. *$p < 0.05$; different from saline (RM ANOVA followed by contrast analysis and the sequentially rejective Bonferroni's test).

ANOVA in NOP$^{+/+}$ mice (Fig. 2A) revealed a significant effect of treatment ($F_{4,28} = 72.24$, $p < 0.0001$), time ($F_{1,4} = 15.66$, $p = 0.0003$) and a significant time × treatment interaction ($F_{4,39} = 7.42$, $p = 0.0002$). J-113397 facilitated rotarod performance at 0.1 and 1 mg/kg and inhibited it at 10 mg/kg. No major difference was observed between Swiss and NOP$^{+/+}$ mice in terms of sensitivity to J-113397 or duration of the response. Conversely, J-113397 was not effective in NOP$^{-/-}$ mice at any of the doses tested (Fig. 2B), suggesting that both the facilitation and the inhibition observed in NOP$^{+/+}$ mice were due to NOP receptor blockade.

MPTP-treated C57BL/6J mice

Seven days after MPTP intoxication, mice displayed increased immobility time (Fig. 3A), reduced number of steps (Fig. 3B) and impaired rotarod performance (Fig. 3C) compared to pre-treatment values. This behavior was associated with a ~60% loss of striatal TH-positive nerve terminals (Figs. 3D–F). Motor deficit induced by MPTP was reversed by L-DOPA and J-113397 (Fig. 4). Thus, RM ANOVA on immobility time (Fig. 4A) revealed a significant effect of treatment ($F_{5,40} = 19.92$, $p < 0.0001$) but not time ($F_{1,5} = 0.01$, $p = 0.92$), and a significant time × treatment interaction ($F_{5,48} = 4.15$, $p = 0.0032$). L-DOPA (10 mg/kg) and J-113397 (0.01–0.03 mg/kg) reduced the immobility time. However, J-113397 increased it at 1 mg/kg. RM ANOVA on the number of steps (Fig. 4B) revealed a significant effect of treatment ($F_{5,40} = 13.32$, $p < 0.0001$) but not time ($F_{1,5} = 0.12$, $p = 0.73$), and a significant time × treatment interaction ($F_{5,48} = 3.73$, $p = 0.0062$). L-DOPA and J-113397 (0.01–0.03 mg/kg) increased the number of steps. Higher doses of J-113397 (1 mg/kg) were found ineffective. Finally, RM ANOVA on the rotarod performance (Fig. 4C) showed a significant effect of treatment ($F_{5,40} = 13.07$, $p < 0.0001$) but not time ($F_{1,5} = 2.54$, $p = 0.11$), and a time × treatment interaction at the limit of significance ($F_{5,48} = 2.40$, $p = 0.05$). L-DOPA and J-113397 (0.01 mg/kg) increased the rotarod performance. However, J-113397 (1 mg/kg) inhibited it. Differently from L-DOPA, J-113397 was no longer effective after 60 min in all tests.

Studies in nonhuman primates

Naïve macaques

The NOP receptor antagonist, J-113397 did not affect motor performance in naïve macaques at 0.1 and 1 mg/kg (Fig. 5). At a higher dose (3 mg/kg) J-113397 induced a faster performance in the straight rod test in two of the animals (Fig. 5A), although the other two did not perform the test. Therefore we tested these animals on a simpler task (i.e. the platform task) but at this dose animals were inattentive and performance was slightly slower than normal (Fig. 5B).

MPTP-treated macaques

We first examined the response to four doses of J-113397 (0.01, 0.03, 0.1 and 1 mg/kg) in two stable parkinsonian animals (data not shown). From 0.03 to 1 mg/kg we did not observe any beneficial effect on either parkinsonian score or MAP platform performance; at

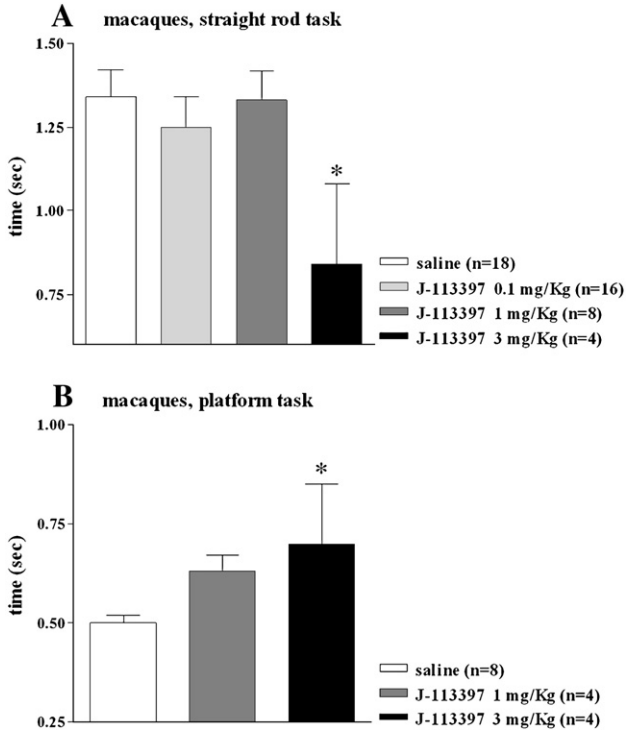

Fig. 5. J-113397 (0.1–3 mg/kg, i.m.) modulated motor activity in naïve nonhuman primates. Motor performance was evaluated in the Movement Analysis Panel (MAP) test. Average time in seconds to retrieve a treat in the straight rod (panel A) test was significantly improved in 2 animals at the higher dose of J-113397 tested, but at this dose the other 2 animals showed side effects (distractibility, scratching and "wet dog" shakes) and failed to perform. These 2 animals were subsequently tested in the platform (easier) task (panel B) of the MAP test in which they performed significantly worse at the high dose. *$p<0.05$; different from saline (ANOVA followed by PLSD test).

1 mg/kg both animals displayed long episodes of akinesia (freezing) similar to the effect of high doses of J-113397 observed in 6-OHDA rats (30 mg/kg, Morari and Marti, unpublished observation) and did not perform the reaching test. No major side effects were observed at 0.03 mg/kg but one animal did not test and the other did not show any improvement in the reaching task. With the lower dose (0.01 mg/kg) both animals showed an improvement in the MAP platform reaching task and therefore we selected this dose for the rest of the experiments.

Both J-113397 (0.01 mg/kg) and L-DOPA (30 mg/kg) induced a significant benefit in parkinsonian scores in the 4 animals ($F_{2,9}$ = 13.5, $p<0.01$; Fig. 6A). The overall improvement after J-113397 administration (~19±3%, p = 0.015) was more moderate than that achieved with L-DOPA (~46±3%, p = 0.001). Although as a group, the difference between L-DOPA and J-113397 improvement in global PRS score did not reach significance (p = 0.07), only in one animal (Mf25) was the response to both drugs not significantly different (Fig. 6A). There was no significant effect of the baseline PRS score (i.e. severity of the parkinsonian signs) on the response to either drug. We further analysed the therapeutic effect on parkinsonian symptoms (Fig. 6B). The largest improvement induced by J-113397 (~30%) was observed on hypokinesia and the L-DOPA effect on this particular symptom was not significantly different from J-113397. All other symptoms (rigidity, tremor and bradykinesia) improved significantly more with L-DOPA (Fig. 6B).

Finally, we evaluated the performance of the parkinsonian animals in the MAP test (Fig. 7). MPTP induced a significant increase in the time needed to complete the platform task in 3 out of 4 animals (Mf23, Mf25 and Mf30). These animals showed a significant improvement in the time to retrieve treats from the platform with L-DOPA and one of them had also a significant improvement in performance after J-113397 (Fig. 7).

Discussion

The most important finding of the present study is that the NOP receptor antagonist J-113397 reversed motor disabilities in MPTP-treated mice and nonhuman primates. These data reinforce the view that endogenous N/OFQ plays a role in motor symptoms in parkinsonism across species. Moreover, the efficacy of J-113397 in some MPTP-treated primates raises the possibility of a therapeutic effect of NOP receptor antagonists in PD patients, although the unusual dual action of J-113397 calls for evaluation of other (more selective?) NOP antagonists.

Role of endogenous N/OFQ in modulation of locomotion under physiological conditions

Motor impairment has been one of the main biological effects observed after intracerebroventricular injection of N/OFQ in rodents.

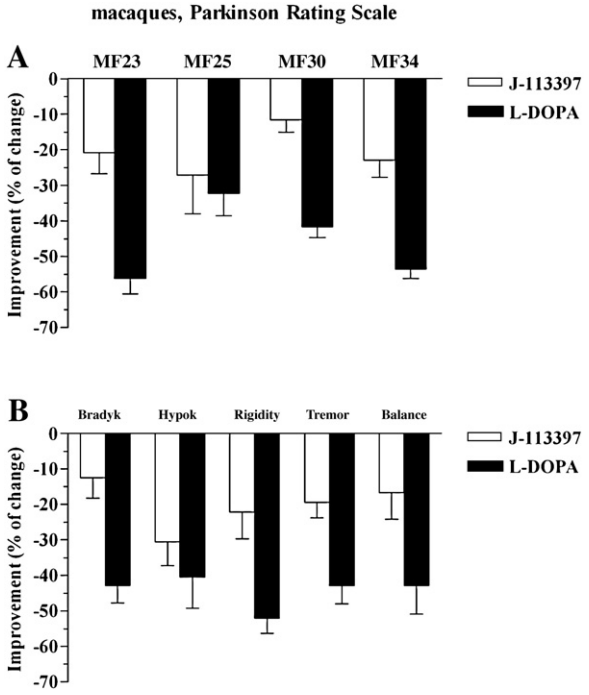

Fig. 6. Effect of J-113397 on motor symptoms in MPTP-treated primates. Panel A. Effect of J-113397 (0.01 mg/kg) and L-DOPA (30 mg/kg) on the global PRS score. The average improvement over the baseline score (n=2–3 pharmacological tests for each compound) is shown for each animal. The improvement after J-113397 administration (~19±3%) was more moderate than that achieved with L-DOPA (~46±3%, Fisher PLSD p=0.001). Comparative analysis of the pharmacological effects of L-DOPA and J-113397 on parkinsonian symptoms (panel B) showed that all symptoms improved more with L-DOPA except for hypokinesia.

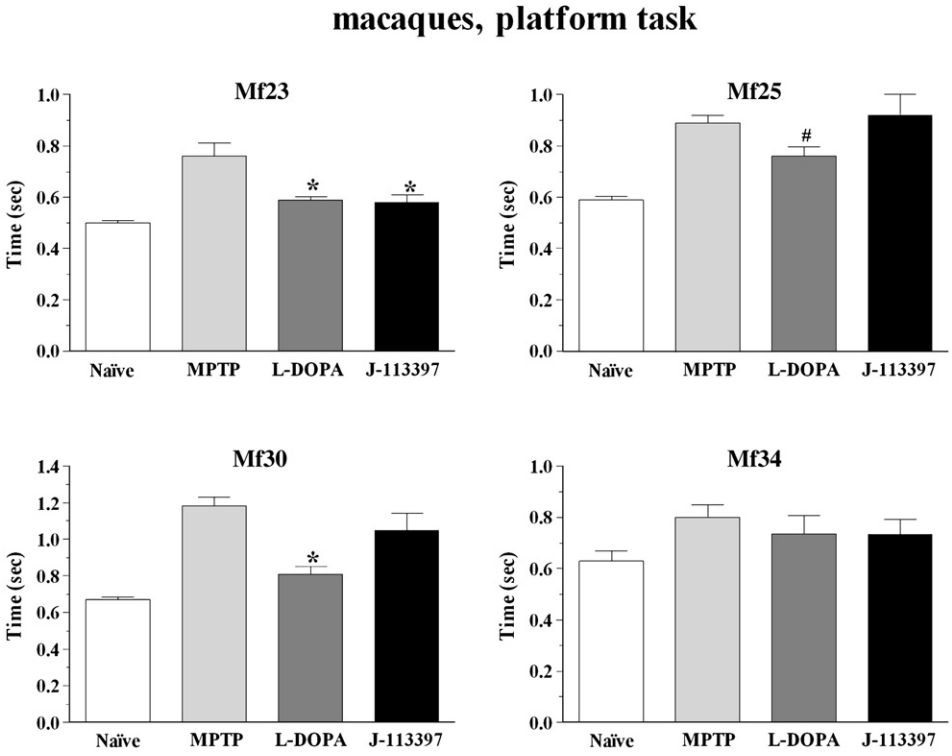

Fig. 7. Effect of J-113397 on the MAP test in MPTP-treated primates. MPTP induced a significant increase in the time needed to complete the platform task (animals were unable to perform the straight rod task) in 3 out of 4 animals (Mf23, Mf25 and Mf30). In these animals L-DOPA improvement on task performance was significant. Only one of them (Mf23) showed a significant improvement in response to J-113397. $^{*}p<0.05$; different from post-MPTP performance (ANOVA followed by PLSD test). $^{\#}p<0.05$; different from J-113397 (ANOVA followed by PLSD test).

It was observed at high N/OFQ doses (nmol) and replicated by systemic administration of nonpeptide NOP receptor agonists. (Jenck et al., 2000; Varty et al., 2005). Reports that lower N/OFQ doses (pmol) facilitate motor performance in rats (Florin et al., 1996; Kuzmin et al., 2004) and mice (Sakoori and Murphy, 2004) have also been published. Although this effect is much milder than the inhibitory one, and observed in a narrower dose range, it confers to the N/OFQ dose-response curve a biphasic profile. The finding that J-113397 dually modulated exercise-induced locomotion in Swiss, C57BL/6J and $NOP^{+/+}$ but not $NOP^{-/-}$ mice suggests that endogenous N/OFQ can both facilitate and inhibit motor activity through NOP receptor activation. These effects, however, do not appear to be physiologically equivalent, motor inhibition being predominant (Marti et al., 2004a). Systemic injection of NOP receptor antagonists or deletion of the NOP receptor gene failed to affect spontaneous locomotion (Gavioli et al., 2003; Kuzmin et al., 2004; Marti et al., 2004a; Rizzi et al., 2007). In line with this view, we did not detect motor facilitation by J-113397 in the bar test (a static test), while there was a prominent effect in tests engaging the animals in repetitive and prolonged movements (i.e. the drag and rotarod test). These data reinforce the hypothesis that endogenous N/OFQ produces a functional inhibition during induced motor activity and not at rest. Indeed, extracellular N/OFQ levels rise during rotarod performance (Marti et al., 2005).

In line with a previous study (Ko et al., 2006), J-113397 did not exert motor effects in naïve macaques up to 1 mg/kg. However, higher doses (3 mg/kg) improved arm speed (straight rod test) in two animals while the remaining two could not perform the test, looking distracted and slightly "hallucinated". Although the inconsistency of response prevents from drawing firm conclusions on the role of endogenous N/OFQ, the data obtained in two animals are in line with the view that the peptide plays an inhibitory role on motor activity. Nevertheless, high doses of J-113397 may also activate sigma receptors (Chiou et al., 2007), causing loss of attention and hallucinations (Okuyama et al., 1994).

Role of endogenous N/OFQ in modulation of MPTP-induced parkinsonism

The MPTP-lesioned nonhuman primate (macaque) model reproduces many PD motor symptoms faithfully and is used to assess the therapeutic potential of novel antiparkinsonian drugs (Dauer and Przedborski, 2003). Conversely, the neurochemical and behavioral outcomes of MPTP administration in mice are highly variable, mainly depending on strain, age, gender, route and protocol of administration (Sedelis et al., 2001; Meredith and Kang, 2006). Thus, a direct comparison with data obtained in our model is quite difficult. Nevertheless, we found that mice displayed increased immobility time (likely reflecting increased akinesia), reduced number of steps (possibly reflecting increased akinesia, bradykinesia and rigidity) and overall impaired motor performance (possibly reflecting loss of coordination and overall gait ability) at 7 days after MPTP intoxication. These data are consistent with that reported by other authors using the bar (Kato et al., 2004; Watanabe et al., 2008) and the treadmill (Petzinger et al., 2007) test at 7 days after MPTP administration (4×20 mg/kg). In the same study, no differences in rotarod performance after MPTP intoxication were observed. The discrepancy may be explained on the basis of technical issues such as rod diameter

(3 cm vs 8 cm in our model) and exercise protocol, which appear more challenging for mice in our study (from 5 to 35 rpm, for a total of 21 min) compared to the previous one (30 rpm for 200 s; Petzinger et al., 2007). Actually, the difficulty and duration of motor task appear crucial to detect changes in rotarod performance. Indeed, Sedelis et al. (2000) did not find difference in rotarod performance 4 days after MPTP intoxication (4×15 mg/kg) using a less strenuous protocol (fixed speed of 12 rpm for 120 s; rod 2.5 cm). It is noteworthy that motor impairment in our study was DA-dependent since it was associated with significant (~60%) loss of striatal DA terminals and was reversed by L-DOPA. In these tests, J-113397 reproduced the antiparkinsonian action of L-DOPA. Thus, in addition to reversing the neuroleptic and 6-OHDA-induced parkinsonism (Marti et al., 2004b, 2005, 2007), J-113397 was effective both in acute (mice) and chronic (macaques) paradigms of MPTP administration, overall suggesting that endogenous N/OFQ plays a role in experimental parkinsonism independent of the species and models used. Interestingly, not only DA loss did not prevent the antiparkinsonian action of J-113397 but it enhanced sensitivity to J-113397, resulting in a leftward shift of the dose-response curve. In 6-OHDA hemi-lesioned rats, this phenomenon was associated with up-regulation of N/OFQ expression and release (Marti et al., 2005). In parkinsonian macaques, J-113397 was less effective than L-DOPA, although it improved hypokinesia comparably to L-DOPA, indicating a general depressive effect of endogenous N/OFQ on movement. In keeping with this notion, we reported that exogenous N/OFQ depressed motor cortex excitability and motor output in vivo via activation of nigral NOP receptors (Viaro et al., 2006). From a clinical perspective, however, the narrow therapeutic range is quite disappointing, as the antiparkinsonian effects of 0.01 mg/kg J-113397 vanished at higher doses, turning into motor inhibition at 1 mg/kg. The fact that this phenomenon was observed in mice (in the same dose range) suggests that it is mediated by NOP receptors. Nevertheless, we cannot elucidate whether this is a peculiarity of the compound (e.g. kinetics of interaction with the NOP receptor, brain penetrability) or a "class effect" until other NOP receptor antagonists, preferably chemically unrelated, have been tested.

Neurobiological substrates of J-113397 action

Systemic administration of J-113397 in naïve rats increased rotarod performance and elevated striatal DA release, suggesting that endogenous DA tonically inhibits nigrostriatal DA transmission (Marti et al., 2004a). This is in line with the findings that exogenous N/OFQ inhibited activity of nigral DA cells, an effect associated with hypolocomotion (Marti et al., 2004a). Thus, it can be proposed that the antiparkinsonian action of J-113397 is mediated by blockade of inhibitory NOP receptors expressed on residual nigral DA cells resulting in increased DA transmission. However, NOP receptor antagonists are effective also under conditions of DA depletion and DA receptor blockade (Marti et al., 2004b; Marti et al., 2005) suggesting that endogenous N/OFQ causes motor depressant responses also via non-DA mechanisms. Indeed, NOP receptors are also present on serotonergic, GABAergic and glutamatergic terminals in SN (M. Morari and M. Marti, personal communication). In particular, we found that the antiakinetic effect of J-113397 was associated with increased GABA and reduced GLU release in the SNr, leading to an impairment of nigrothalamic GABAergic transmission and, possibly, thalamic disinhibition (Marti et al., 2007). Within this frame, motor inhibitory actions of J-113397 could be attributed to an excessive or more prolonged degree of NOP receptor blockade or to blockade of different subsets of NOP receptors (Kuzmin et al., 2004) (facilitating or inhibiting motor activity) located either along the same or different motor pathways. The fact that motor facilitation induced by exogenous N/OFQ was blocked by haloperidol or DA depletion (Florin et al., 1996; Kuzmin et al., 2004) suggests the involvement of the same mesencephalic DA areas that mediate locomotion.

Concluding remarks

The NOP receptor antagonist J-113397 produced a dose-dependent effect (facilitation at low doses and inhibition at high) of motor activity in naïve and MPTP-induced parkinsonian mice and nonhuman primates. This is consistent with the notion that endogenous N/OFQ is predominantly involved in motor inhibition, particularly during exercise-induced activity. Although the dual action of J-113397 in parkinsonian primates needs to be further characterized, our data support the view that NOP receptor is a new target in the therapy of PD.

Acknowledgments

This work has been supported by a grant from the Michael J. Fox Foundation for Parkinson's Research (Fast Track 2004) to M. Morari, and by grants from NINDS Parkinson's Disease Research Center of Excellence (P50 NS39793), the Michael Stern Foundation, and N.E.P.R.C. Center (Grant P51RR00168) to O. Isacson. We gratefully acknowledge the contribution of Jennifer Pagel and Jack McDowell in the acquisition of primate data.

References

Bridge, K.E., Wainwright, A., Reilly, K., Oliver, K.R., 2003. Autoradiographic localization of (125)i[Tyr(14)] nociceptin/orphanin FQ binding sites in macaque primate CNS. Neuroscience 118, 513–523.

Calò, G., Rizzi, A., Rizzi, D., Bigoni, R., Guerrini, R., Marzola, G., Marti, M., McDonald, J., Morari, M., Lambert, D.G., Salvatori, S., Regoli, D., 2002. [Nphe^{1}, Arg^{14}, Lys^{15}]Nociceptin-NH_2, a novel potent and selective antagonist of the nociceptin/orphanin FQ receptor. Br. J. Pharmacol. 136, 303–311.

Chiou, L.C., Liao, Y.Y., Fan, P.C., Kuo, P.H., Wang, C.H., Riemer, C., Prinssen, E.P., 2007. Nociceptin/orphanin FQ peptide receptors: pharmacology and clinical implications. Curr. Drug Targets 8, 117–135.

Cox, B.M., Chavkin, C., Christie, M.J., Civelli, O., Evans, C., Hamon, M.D., Hoellt, V., Kieffer, B., Kitchen, I., Mcknight, A.T., Meunier, J.C., Portoghese, P.S., 2000. Opioid receptors. In: Girdlestone, D. (Ed.), The IUPHAR Compendium of Receptor Characterization and Classification. IUPHAR Media Ltd, London.

Dauer, W., Przedborski, S., 2003. Parkinson's disease: mechanisms and models. Neuron 39, 889–909.

Devine, D.P., Taylor, L., Reinscheid, R.K., Monsma, F.J.J., Civelli, O., Akil, H., 1996. Rats rapidly develop tolerance to the locomotor-inhibiting effects of the novel neuropeptide orphanin FQ. Neurochem. Res. 21, 1387–1396.

Florin, S., Suaudeau, C., Meunier, J.C., Costentin, J., 1996. Nociceptin stimulates locomotion and exploratory behaviour in mice. Eur. J. Pharmacol. 317, 9–13.

Gavioli, E.C., Marzola, G., Guerrini, R., Bertorelli, R., Zucchini, S., De Lima, T.C., Rae, G.A., Salvadori, S., Regoli, D., Calò, G., 2003. Blockade of nociceptin/orphanin FQ-NOP receptor signalling produces antidepressant-like effect: pharmacological and genetic evidences from the mouse forced swimming test. Eur. J. Neurosci. 17, 1987–1990.

Jackson-Lewis, V., Przedborski, S., 2007. Protocol for the MPTP mouse model of Parkinson's disease. Nat. Protoc. 2, 141–151.

Jenck, F., Wichmann, J., Dautzenberg, F.M., Moreau, J.L., Ouagazzal, A.M., Martin, J.R., Lundstrom, K., Cesura, A.M., Poli, S.M., Roever, S., Kolczewski, S., Adam, G., Kilpatrick, G., 2000. A synthetic agonist at the orphanin FQ/nociceptin receptor ORL1: anxiolytic profile in the rat. Proc. Natl. Acad. Sci. U. S. A. 97, 4938–4943.

Jenkins, B.G., Sanchez-Pernaute, R., Brownell, A.L., Chen, Y.C., Isacson, O., 2004. Mapping dopamine function in primates using pharmacologic magnetic resonance imaging. J. Neurosci. 24, 9553–9560.

Kato, H., Kurosaki, R., Oki, C., Araki, T., 2004. Arundic acid, an astrocyte-modulating agent, protects dopaminergic neurons against MPTP neurotoxicity in mice. Brain Res. 1030, 66–73.

Kawamoto, H., Ozaki, S., Itoh, Y., Miyaji, M., Arai, S., Nakashima, H., Kato, T., Ohta, H., Iwasawa, Y., 1999. Discovery of the first potent and selective small molecule opioid receptor-like (ORL1) antagonist: 1-[3R, 4R)-1-cyclooctylmethyl-3-hydroxymethyl-4-piperidyl]-3-ethyl-1,3-dihydro-2H benzimidazol-2-one (J-113397). J. Med. Chem. 42, 5061–5063.

Ko, M.C., Wie, H., Woods, J.H., Kennedy, R.T., 2006. Effects of intrathecally administered nociceptin/orphanin FQ in monkeys: behavioral and mass spectrometric studies. J. Pharmacol. Exp. Ther. 318, 1257–1264.

Koizumi, M., Sakoori, K., Midorikawa, N., Murphy, N.P., 2004. The NOP (ORL1) receptor antagonist Compound B stimulates mesolimbic dopamine release and is rewarding in mice by a non-NOP-receptor-mediated mechanism. Br. J. Pharmacol. 143, 53–62.

Kuzmin, A., Sandin, J., Terenius, L., Ogren, S.O., 2004. Evidence in locomotion test for the functional heterogeneity of ORL-1 receptors. Br. J. Pharmacol. 141, 132–140.

Marti, M., Mela, F., Veronesi, C., Guerrini, R., Salvadori, S., Federici, M., Mercuri, N.B., Rizzi, A., Franchi, G., Beani, L., Bianchi, C., Morari, M., 2004a. Blockade of nociceptin/orphanin FQ receptor signaling in rat substantia nigra pars reticulata stimulates nigrostriatal dopaminergic transmission and motor behavior. J. Neurosci. 24, 6659–6666.

Marti, M., Mela, F., Guerrini, R., Calò, G., Bianchi, C., Morari, M., 2004b. Blockade of nociceptin/orphanin FQ transmission in rat substantia nigra reverses haloperidol-induced akinesia and normalizes nigral glutamate release. J. Neurochem. 91, 1501–1504.

Marti, M., Mela, F., Fantin, M., Zucchini, S., Brown, J.M., Witta, J., Di Benedetto, M., Buzas, B., Reinscheid, R.K., Salvadori, S., Guerrini, R., Romualdi, P., Candeletti, S., Simonato, M., Cox, B.M., Morari, M., 2005. Blockade of nociceptin/orphanin FQ transmission attenuates symptoms and neurodegeneration associated with Parkinson's disease. J. Neurosci. 95, 9591–9601.

Marti, M., Trapella, C., Viaro, R., Morari, M., 2007. The nociceptin/orphanin FQ receptor antagonist J-113397 and L-Dopa additively attenuate experimental parkinsonism through overinhibition of the nigrothalamic pathway. J. Neurosci. 27, 1297–1307.

Meredith, G.E., Kang, U.J., 2006. Behavioral models of Parkinson's disease in rodents: a new look at an old problem. Mov. Disord. 21, 1595–1606.

Meunier, J.C., Mollereau, C., Toll, L., Suaudeau, C., Moisand, C., Alvinerie, P., Butour, J.L., Guillemot, J.C., Ferrara, P., Monsarrat, B., Mazarguil, H., Vassart, G., Parmentier, M., Costentin, J., 1995. Isolation and structure of the endogenus agonist of opioid receptor-like ORL1 receptor. Nature 377, 532–535.

Neal, C.R.J., Akil, H., Watson, S.J., 2001. Expression of orphanin FQ and the opioid receptor-like (ORL1) receptor in the developing human and rat brain. J. Chem. Neuroanat. 22, 219–249.

Nishi, M., Houtani, T., Noda, Y., Mamiya, T., Sato, K., Doi, T., Kuno, J., Takeshima, H., Nukada, T., Nabeshima, T., Yamashita, T., Noda, T., Sugimoto, T., 1997. Unrestrained nociceptive response and disregulation of hearing ability in mice lacking the nociceptin/orphanin FQ receptor. EMBO J. 16, 1858–1864.

Okuyama, S., Imagawa, Y., Sakagawa, T., Nakazato, A., Yamaguchi, K., Katoh, M., Yamada, S., Araki, H., Otomo, S., 1994. NE-100, a novel sigma receptor ligand: effect on phencyclidine-induced behaviors in rats, dogs and monkeys. Life Sci. 55, PL133–PL138.

Petzinger, G.M., Walsh, J.P., Akopian, G., Hogg, E., Abernathy, A., Arevalo, P., Turnquist, P., Vucković, M., Fisher, B.E., Togasaki, D.M., Jakowec, M.W., 2007. Effects of treadmill exercise on dopaminergic transmission in the 1-methyl-4-phenyl-1,2,3,6-tetrahydropyridine-lesioned mouse model of basal ganglia injury. J. Neurosci. 27, 5291–5300.

Reinscheid, R.K., Nothacker, H.P., Bourson, A., Ardati, A., Henningsen, R.A., Bunzow, J.R., Grandy, D.K., Langen, H., Monsma, Jr. F.J., Civelli, O., 1995. Orphanin FQ: a neuropeptide that activates an opioid-like G protein-coupled receptor. Science 270, 792–794.

Rizzi, A., Gavioli, E.C., Marzola, G., Spagnolo, B., Zucchini, S., Ciccocioppo, R., Trapella, C., Regoli, D., Calò, G., 2007. Pharmacological characterization of the nociceptin/orphanin FQ receptor antagonist SB-612111 [(−)-*cis*-1-methyl-7-[[4-(2,6-dichlorophenyl)piperidin-1-yl] methyl]-6,7,8,9-tetrahydro-5H benzocyclohepten-5-ol]: in vivo studies. J. Pharmacol. Exp. Ther. 32, 968–974.

Rozas, G., Guerra, M.J., Labandeira-Garcia, J.L., 1997. An automated rotarod method for quantitative drug-free evaluation of overall motor deficits in rat models of parkinsonism. Brain Res. Protoc. 2, 75–84.

Sakoori, K., Murphy, N.P., 2004. Central administration of nociceptin/orphanin FQ blocks the acquisition of conditioned place preference to morphine and cocaine, but not conditioned place aversion to naloxone in mice. Psychopharmacology 172, 129–136.

Sanberg, P.R., Bunsey, M.D., Giordano, M., Norman, A.B., 1988. The catalepsy test: its ups and downs. Behav. Neurosci. 102, 748–759.

Sanchez-Pernaute, R., Jenkins, B.G., Choi, J.K., Iris Chen, Y.G., Isacson, O., 2007. In vivo evidence of D3 dopamine receptor sensitization in parkinsonian primates and rodents with l-DOPA-induced dyskinesias. Neurobiol. Dis. 27, 220–227.

Sedelis, M., Hofele, K., Auburger, G.W., Morgan, S., Huston, J.P., Schwarting, R.K.W., 2000. MPTP susceptibility in the mouse: behavioural, neurochemical and histological analysis of gender and strain differences. Behav. Genet. 30, 171–182.

Sedelis, M., Schwarting, R.K.W., Huston, J.P., 2001. Behavioral phenotyping of the MPTP mouse model of Parkinson's disease. Behav. Brain Res. 125, 109–125.

Varty, G.B., Hyde, L.A., Hodgson, R.A., Lu, S.X., McCool, M.F., Kazdoba, T.M., Del Vecchio, R.A., Guthrie, D.H., Pond, A.J., Grzelak, M.E., Xu, X., Korfmacher, W.A., Tulshian, D., Parker, E.M., Higgins, G.A., 2005. Characterization of the nociceptin receptor (ORL-1) agonist, Ro64-6198, in tests of anxiety across multiple species. Psycopharmacology (Berl.) 182, 132–143.

Viaro, R., Marti, M., Morari, M., Franchi, G., 2006. Nociceptin/orphanin FQ receptors modulate locomotion and motor cortex excitability in adult rats. Acta Physiol. 188, 5.

Watanabe, Y., Kato, H., Araki, T., 2008. Protective action of neuronal nitric oxide synthase inhibitor in the MPTP mouse model of Parkinson's disease. Metab. Brain Dis. 23, 51–69.

EJN
European Journal of Neuroscience

European Journal of Neuroscience, Vol. 27, pp. 2733–2746, 2008 doi:10.1111/j.1460-9568.2008.06248.x

Suppression of activity in the forelimb motor cortex temporarily enlarges forelimb representation in the homotopic cortex in adult rats

Emma Maggiolini, Riccardo Viaro and Gianfranco Franchi
Dipartimento di Scienze Biomediche e Terapie Avanzate, Sezione di Fisiologia umana e Istituto Nazionale di Neuroscienze, Università di Ferrara, 44100 Ferrara, Italy

Keywords: forelimb motor cortex, ICMS, rat, recovery, short-term diaschisis

Abstract

After forelimb motor cortex (FMC) damage, the unaffected homotopic motor cortex showed plastic changes. The present experiments were designed to clarify the electrophysiological nature of these interhemispheric effects. To this end, the output reorganization of the FMC was investigated after homotopic area activity was suppressed in adult rats. FMC output was compared after lidocaine-induced inactivation (L-group) or quinolinic acid-induced lesion (Q-group) of the contralateral homotopic cortex. In the Q-group of animals, FMC mapping was performed, respectively, 3 days (Q3D group) and 2 weeks (Q2W group) after cortical lesion. In each animal, FMC output was assessed by mapping movements induced by intracortical microstimulation (ICMS) in both hemispheres (hemisphere ipsilateral and contralateral to injections). The findings demonstrated that in the L-group, the size of forelimb representation was 42.2% higher than in the control group ($P < 0.0001$). The percentage of dual forelimb–vibrissa movement sites significantly increased over the controls ($P < 0.0005$). The dual-movement sites occupied a strip of the map along the rostrocaudal border between the forelimb and vibrissa representations. This form of interhemispheric diaschisis had completely reversed, with the recovery of the baseline map, 3 days after the lesion in the contralateral FMC. This restored forelimb map showed no ICMS-induced changes 2 weeks after the lesion in the contralateral FMC. The present results suggest that the FMCs in the two hemispheres interact continuously through predominantly inhibitory influences that preserve the forelimb representation and the border vs. vibrissa representation.

Introduction

The mammal primary motor cortex contains a somatotopic representation of the major subdivision of the body musculature, and predominantly controls the limb muscles on the contralateral side of the body (Porter & Lemon, 1993). However, increasing evidence suggests that the primary motor cortex is also involved in controlling the ipsilateral upper limb movements (Tanji *et al.*, 1988; Wassermann *et al.*, 1994; Chen *et al.*, 1997, 2003; Donchin *et al.*, 1998; Ziemann *et al.*, 1999; Steinberg *et al.*, 2002; Cisek *et al.*, 2003). More specifically, it controls the timing of ipsilateral upper limb muscle recruitment in goal-directed and precision grip movements (Yarosh *et al.*, 2004; Davare *et al.*, 2007).

Studies using focal ischemic or cortical injury within the forelimb motor cortex (FMC) in rats have reported substantial plastic time-related events within the undamaged contralateral forelimb motor cortex (cFMC). These studies have reported dendritic and synaptic growth within the undamaged motor cortex (Jones & Schallert, 1992, 1994; Biernaskie & Corbett, 2001) as well as axonal sprouting that runs from the undamaged motor cortex to subcortical motor structures (Kartje-Tillotson *et al.*, 1985, 1986; Napieralski *et al.*, 1996; Papadopoulos *et al.*, 2002; Emerick *et al.*, 2003). The reorganized cFMC in the undamaged hemisphere (i.e. ipsilateral to the affected forelimb) substantially contributes to recovery of skilled forelimb movement (Biernaskie *et al.*, 2005).

Although all these studies corroborate the view that the ipsilateral forelimb motor cortex (iFMC) participates in the control of forelimb movement under normal conditions as well as after cortical injury, its precise involvement in preserving the baseline map in the homotopic cortex of the contralateral hemisphere is still poorly understood.

A previous study in the rat has proposed that the ipsilateral vibrissa motor cortex (VMC) plays a crucial role in preserving the baseline map through either a facilitatory or an inhibitory transcallosal influence on the contralateral VMC (Maggiolini *et al.*, 2007). In particular, this paper supports the view that facilitatory transcallosal input preserves the normal size, shape and excitability of the VMC, whereas callosal-driven inhibition plays a crucial role in defining the boundary between vibrissa and forelimb representations.

The present study was designed to measure the effects that iFMC inactivation and lesion have on the cFMC. The final aim of the present and previous experiments (Maggiolini *et al.*, 2007) was to compare the interhemispheric diaschisis and its recovery in time between the forelimb and vibrissa motor systems. This comparison is important, because it could shed light on differences in the mechanisms of interhemispheric interaction between these two motor systems, which present different degrees of lateralization (Brosamle & Schwab, 1997; Hattox *et al.*, 2002).

Correspondence: Gianfranco Franchi, as above.
E-mail:fhg@dns.unife.it

Received 29 November 2007, revised 3 April 2008, accepted 6 April 2008

For the experiments described here, unilateral FMC inactivation and lesion were performed in one hemisphere, and intracortical microstimulation (ICMS)-induced maps of both hemispheres were used to quantitatively evaluate plastic changes in the FMC following motor disconnection. This assumes that, after iFMC disconnection, changes in the shaping and size of the forelimb representation, and in its current threshold, reflect the adaptive changes in cortical circuits within the disconnected cFMC.

Materials and methods

Overview of the experimental plan

Experiments were carried out on 27 Wistar albino rats, weighing 270–300 g. Animals were reared in a 12-h light/dark cycle, with food and water available *ad libitum*. The experimental plan was designed in compliance with Italian law regarding the care and use of experimental animals (DL116/92) and was approved by the Italian Ministry of Health. For all experimental procedures, rats were anaesthetized initially with intraperitoneal ketamine-HCl (50 mg/kg). For the duration of the experiment, anesthesia was maintained by supplementary ketamine injections so as to achieve long-latency and sluggish hindlimb withdrawal upon pinching of the hindfoot. Under anesthesia, the body temperature was maintained at 36–38 °C with a heat lamp. All animals were maintained with unlimited access to food and water presurgery and postsurgery.

The general procedures were as follows. First, seven animals underwent FMC inactivation by lidocaine injection (L-group) in one hemisphere followed by mapping of M1 movement in both hemispheres (ipsilateral and contralateral hemispheres: hemispheres ipsilateral and contralateral to the injection, respectively). Second, another group of 10 animals underwent FMC lesion by quinolinic acid injection (Q-group) in one hemisphere followed by mapping of M1 movement in both hemispheres (ipsilateral and contralateral hemispheres: hemispheres ipsilateral and contralateral to the lesion, respectively). In the Q-group of animals, M1 mapping was performed 3 days (Q3D group, five rats) or 2 weeks (Q2W group, five rats) after cortical lesion. Third, five animals (sham group) underwent three injections of saline into the FMC in one hemisphere followed by mapping of M1 movement in both hemispheres (ipsilateral and contralateral hemispheres: hemispheres ipsilateral and contralateral to the saline injections, respectively). Finally, in five animals, both hemispheres were mapped as reference for normal M1 mapping (control group: right and left hemispheres).

The control and experimental groups were matched for gender (three males and two females), age (13–17 weeks), weight (270–300 g at the time of the mapping procedure), and housing condition.

Lidocaine inactivation of the FMC

In these experiments, before M1 mapping, using a Hamilton syringe, a total of 12 μL of 3% lidocaine was injected at three sites within the FMC of one hemisphere [stereotaxic coordinates vs. the bregma: (1) anteroposterior (AP) +1, lateral (L) 3 mm; (2) AP +2, L 3.5 mm; (3) AP +3, L 3.5 mm]. Under surgical stereomicroscopy, the microsyringe needle was lowered into the selected site 1 mm below the pial surface, the lidocaine was slowly injected (4 μL/min) and, to prevent it from oozing out, the needle was only withdrawn 3–4 min later. For the duration of the experiment, cortical inactivation was maintained by supplementary injections of lidocaine (one or two times for each animal) at the same sites when the forelimb movement at these sites was ICMS-evoked at the highest current used under the present experimental condition (60 μA). The injected sites were remapped every 30 min to confirm that sites were inactivated, and ICMS began 10 min after injections.

Quinolinic lesion of the FMC

For the M1 lesion, two holes were drilled into the skull over the frontal cortex of one hemisphere at the stereotaxic coordinate relative to the bregma: AP +1.5, L 3.5 mm, and AP +3, L 3.5 mm. Injection of 1 μL of 60 mM quinolinic acid (Cambridge Research Biochemical, Billingham, UK) dissolved in saline were delivered through a 1-μL Hamilton syringe into each site at a depth of 1 mm below the top of the cortex. Each injection was made gradually over a 4-min period, and the needle was left *in situ* for another 4 min before being withdrawn. After injections, the skin was closed using 6-0 surgical sutures, and the wound was cleansed with an antibiotic solution (Rifamicina SV, Lepetit, Milan, Italy).

Intracortical stimulation mapping

In each animal, the movements evoked by ICMS in the frontal agranular cortex were mapped in both hemispheres. In the sham group, L-group and Q-group, the contralateral hemisphere M1 was mapped first, and then the ipsilateral hemisphere M1. The anesthetized animal was placed in a Kopf stereotaxic apparatus, and a large craniotomy was performed over the frontal cortex of both hemispheres. The mapping procedure was similar to the one described by Donoghue & Wise (1982) and Sanes *et al.* (1990), and detailed elsewhere (Franchi, 2000). Briefly, the dura remained intact and was kept moist with a 0.9% saline solution. The electrode penetrations were regularly spaced out over a 500-μm grid. Alteration in the coordinate grid, up to 50 μm, was sometimes necessary to prevent the electrode from penetrating the surface blood vessels. These adjustments in the coordinate grid were not reported in the reconstructing maps. When the adjustment was over 50 μm, the penetration at this site was not performed. Glass-insulated tungsten electrodes (0.6–1 MΩ impedance at 1 kHz) were used for stimulation. The electrode was lowered perpendicularly into the cortex to a depth of 1.5 mm below the cortical surface, and adjusted by ±200 μm so as to evoke movement at the lowest threshold. In preliminary experiments, this depth was found to correspond to layer V of the frontal agranular cortex (Franchi, 2000).

Monophasic cathodal pulses (30-ms train duration at 300 Hz, 200-μs pulse duration) of a maximum of 60 μA were passed through the electrode with a minimum interval of 2.5 s. Two observers were required to detect movement and determine threshold. One observed the movement without knowledge of the actual current intensity and was unaware of which group the particular rat belonged to. The other observer changed the level of the current. Starting with a 60-μA current, intensity was decreased in 5-μA steps until the movement was no longer evoked; then the intensity was increased to a level at which approximately 50% of the stimulations elicited movement. This level defined the current threshold. If no movements or twitches were evoked with 60 μA, the site was recorded as negative (ineffective site). Mapping was initiated at a high current because the initial polysynaptic recruitment of remote neurons optimizes the detection of movements in this 500-μm-step grid mapping. Body parts activated by ICMS were identified by visual inspection and/or muscle palpation. When eye movement was observed, the current threshold was determined under an optical microscope. A normal component of the output organization of rat M1 is the presence of some sites along the border region between the forelimb and vibrissa representations

from which movement of both body parts can be evoked simultaneously. At such sites, both movements were recorded for that position regardless of the individual thresholds (which were determined separately for each). Hereafter, such movements are indicated as 'threshold movement' and 'over-threshold movement', respectively, according to the value of the individual threshold. In some sites along the border region between the forelimb and vibrissa representations, both movements can be evoked simultaneously at the current threshold level (dual forelimb–vibrissa movement site; Figs 2A and 5A). These sites have been referred to as forelimb sites when forelimb representation size has been analysed. Forelimb movements evoked by threshold current typically consisted of brief twitches of the elbow or shoulder (proximal limb movement), wrist and digit (distal limb movement), or simultaneous twitches of both muscle groups. Forelimbs and hindlimbs were approximately halfway between flexion and extension, and were alternately flexed and extended, particularly at the representational borders.

Histology and lesions reconstruction

At the end of the experimental procedure, the animals were anaesthetized (ketamine, 100 mg/kg) and perfused transcardially. The brains were then removed, postfixed, and transferred to a 30% sucrose solution until they sank. They were then sectioned coronally into 50-μm-thick slices. Sections were stained with thionine and captured using a computer-interfaced light microscopy workstation with a high-resolution digital camera (Fig. 1A). For each section and hemisphere, the total cerebral cortex lesion was obtained using contour tracing software (Adobe System, Mountain View, CA, USA). The lesion extent and placement were reconstructed onto schematic templates of cortical coronal sections. Reconstructions within lesion groups were then overlaid onto one template, and outer boundaries and shared regions of damage were outlined (Fig. 1B).

Map construction and data analysis

Using a dedicated plotting program (written with the Lab View Development System; see Acknowledgements), an on-line grid map was constructed by labeling electrode penetrations according to the distance (in millimeters) from the bregma. At a current intensity of 60 μA or less, threshold values were recorded on a sheet scrolling below the map grid. This procedure breaks down the cortical surface into a square grid where each movement threshold point is the center of a 500-μm-wide square. In each hemisphere, vibrissa and forelimb movements were mapped in order to determine the extent and location of these representations. Map borders were defined as the midpoint between sites with different movement thresholds. If a site eliciting a

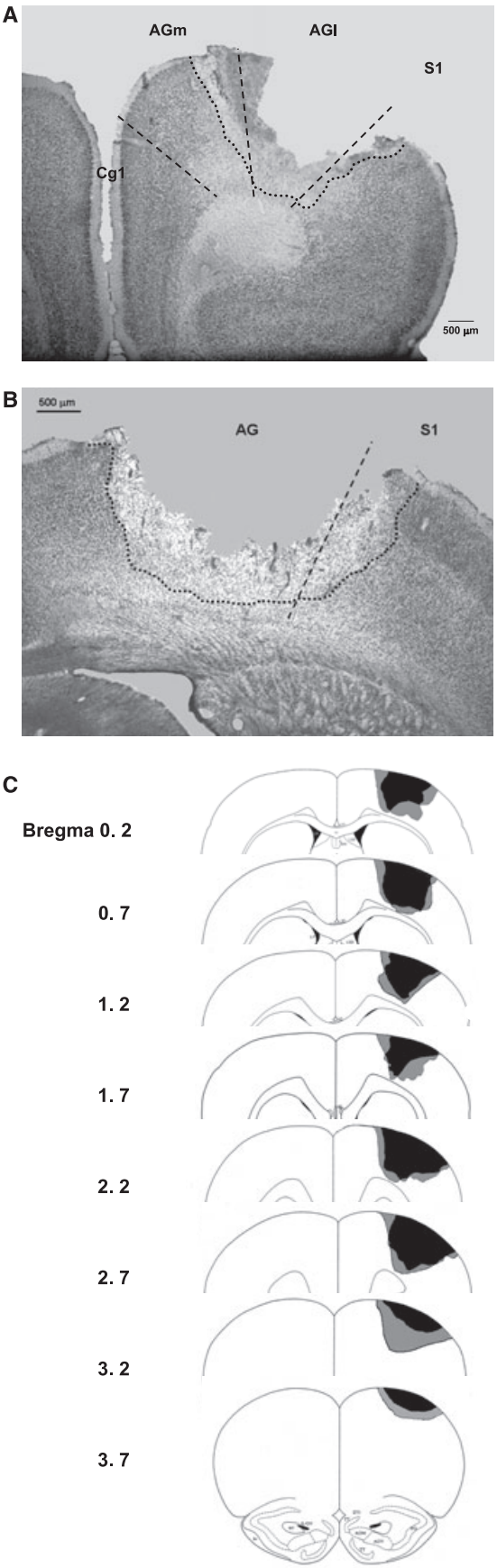

FIG. 1. (A) Representative photomicrographs of typical quinolonic acid-induced lesion of the forelimb motor cortex (FMC) as viewed in Nissl-stained coronal sections. Broken lines define the boundaries of cortical areas according to Brecht *et al*. (2004). (B) Nissl-stained coronal section of caudal part of the quinolinic acid lesion, showing confinement of the lesion to S1. AGl, agranular lateral area; AGm, agranular medial area; CG1, cingulated area 1; S1, primary somatosensory cortex. (C) Reconstructions of the extent and placement of unilateral FMC lesions in the quinolinic acid-induced lesion group of rats with smaller and larger lesions. The regions in light gray indicate the largest extent of all combined lesions, and the areas in black are the regions of damage common to all lesions. Numbers to the left indicate approximate anteroposterior coordinates in millimeters relative to the bregma.

movement was flanked by a site that showed no movement upon stimulation of up to 60 μA, the borderline for the represented movement was set at 250 μm from the movement site. Penetrations not performed in correspondence to large vessels were not taken into account in the calculations. This procedure presents several potential sources of variability that could affect the accuracy of the configuration and size of movement representations. To reduce the effect of experimental sources of variability, similar mapping density was maintained across all animals. The cortex medial to the vibrissa representation was not explored less than 1 mm lateral from the midline. In normal animals, the cortex medial to the vibrissa representation was occupied by a small representation of eye movement (Hall & Lindholm, 1974; Donoghue & Wise, 1982; Guandalini, 1998) and by a thin strip of cortex where ICMS evoked miosis (Gioanni & Lamarche, 1985; Guandalini, 2003). In any case, the eye, pupillar movements and ineffective sites formed the basis for delineating the medial border of the vibrissa representation. The sample of eye and miosis sites in each hemisphere was too small, and these sites have been collectively referred to as 'eye sites'.

In most experimental hemispheres, there is no clear border between rostrally and laterally situated forelimb sites (Fig. 3), so that, in computation of the forelimb sites, no distinction is made between the sites in the rostral and caudal forelimb area.

There is previous evidence that the forelimb representation shares the longest, common border with the vibrissa representation and that the position of the forelimb–vibrissa border can change under a variety of peripheral (Donoghue *et al.*, 1990; Sanes *et al.*, 1990; Franchi, 2000, 2002) and central (Maggiolini *et al.*, 2007) manipulations. In this light, for each group of hemispheres, a quantitative evaluation of the forelimb-vibrissa border configuration was obtained by comparing mediolateral (ML) frequency distributions of sites eliciting vibrissa and forelimb movements from 2 to 3 mm from the midline (see Results). To this end, in each hemisphere, penetrations were divided into 0.5-mm-wide bins into which all sites eliciting movement were grouped, irrespective of their AP coordinates. For each bin – starting 2 mm from the midline and extending 3 mm laterally – the number of vibrissa and forelimb sites were tallied and converted to frequency by expressing data as a percentage of the total number of sites for each movement.

To determine whether any changes in representational movements were related to changes in movement-evoking thresholds, the thresholds for each movement were determined for each group of hemispheres. For each group of hemispheres, a threshold analysis of forelimb movement sites finer than those that emerged within the contralateral M1 was obtained by comparing ML threshold distributions.

Within-group comparisons were determined using the paired *t*-test. Between-group comparisons were determined using one-way ANOVA and the chi-square test. *Post hoc* comparisons of groups were performed when appropriate, using the Scheffé test for contrasts. A probability value of less than 0.05 was considered to be statistically significant. Data are presented as means ± SD.

Results

The mean number of penetrations required to explore the motor region corresponding to the vibrissa and forelimb representations in each hemisphere on this 500-μm sampling grid was 65.9 ± 7. Both hemispheres in each rat were studied, and a threshold-evoked movement map was derived from each hemisphere (Figs 2–4). In presenting the results, we first evaluate interhemispheric variation in the forelimb motor representation using data from the control and sham groups. Next, we present the results testing the effects on the FMC after the inactivation (L-group) and the lesion (Q-group) of the homotopic area in the contralateral hemisphere.

Right vs. left hemisphere in the control and sham groups of animals

In the control hemispheres, the size, shape and location of the forelimb representation conformed to previous descriptions of the rat M1, and included the presence of two distinct forelimb areas (caudal and rostral forelimb area; Fig. 2A) (Donoghue & Wise, 1982; Sievert & Neafsey, 1986). Because, in the experimental animals, the inactivation of forelimb representation includes both caudal and rostral areas, there was no distinction between the sites in the rostral and caudal forelimb areas when forelimb data were analysed. The forelimb motor representation was rostral and slightly medial to the representation of the forelimb in S1. In all presented maps, the most caudolateral forelimb sites overlapped the forelimb representation in S1. The vibrissa representation was situated medially to the forelimb representation at the same AP coordinates. Along the border between the forelimb and vibrissa representations, both movements could occasionally be evoked simultaneously at the current threshold level (dual forelimb–vibrissa movement site; Figs 2A and B, and 5A and B). The hindlimb representation delimited the posterior boundary of the vibrissa and forelimb representations. In the frontal cortex strip situated medially to the vibrissa representation, miosis – or, less commonly, eye movement – was induced under the chosen stimulation conditions (Hall & Lindholm, 1974; Gioanni & Lamarche, 1985; Guandalini, 2003). Ineffective sites formed the basis for delineating the rostral M1 border. Statistical comparison between the right and left hemispheres of the control group of animals showed no significant difference: (i) in the mean size of the forelimb movement representation (Figs 2A, 5A and 6A; right hemisphere, mean number of sites 18.0 ± 1.4, mean size 4.5 ± 0.3 mm^2, range 4.25–5.0 mm^2; left hemisphere, mean number of sites 17.6 ± 3.2, mean size 4.4 ± 0.8 mm^2, range 3.25–5.25.0 mm^2, $P > 0.8$); (ii) in the mean size of the vibrissa movement representation (Fig. 2A and Table 1; right hemisphere, mean number of sites 16.4 ± 0.9; left hemisphere, mean number of sites 16.6 ± 3.2, $P > 0.8$); and (iii) in the percentage of dual movement sites (right hemisphere, mean number of sites 0.6 ± 0.5, mean percentage 1.47 ± 1.3%, range 0–2.7%; left hemisphere, mean number of sites 0.8 ± 0.4, mean percentage 2.1 ± 1.2%, range 0–2.8%, $P > 0.4$). Expressed as a percentage of the total size of the forelimb cortex, the mean percentage of forelimb cortex coding for dual movement did not differ between the right and left hemispheres (right vs. left hemisphere: 3.4% vs. 4.6%, $P > 0.6$). Similarly, no significant differences in evoked movement thresholds were found between the right and left hemispheres in the control group of animals (eye, $P > 0.8$; vibrissa, $P > 0.7$; forelimb, $P > 0.8$; hindlimb, $P > 0.6$). The fact that there were no statistical differences between the right and left hemispheres in the control group of animals ensured that, in the absence of manipulation, sources of variability between the right and left hemispheres were minor and not significant.

Statistical comparison between hemispheres in the control vs. sham groups of animals showed no significant differences: (i) in the mean size of the forelimb and vibrissa movement representations (Fig. 2A vs. Fig. 2B; Fig. 6A; $P > 0.3$); (ii) in the percentage of dual movement sites ($P > 0.9$); and (iii) in evoked movement thresholds (eye, $P > 0.4$; vibrissa, $P > 0.8$; forelimb, $P > 0.7$; hindlimb, $P > 0.5$). The fact that there were no statistical differences between the control and sham groups of animals confirmed that the intracortical injection of saline did not induce changes in the

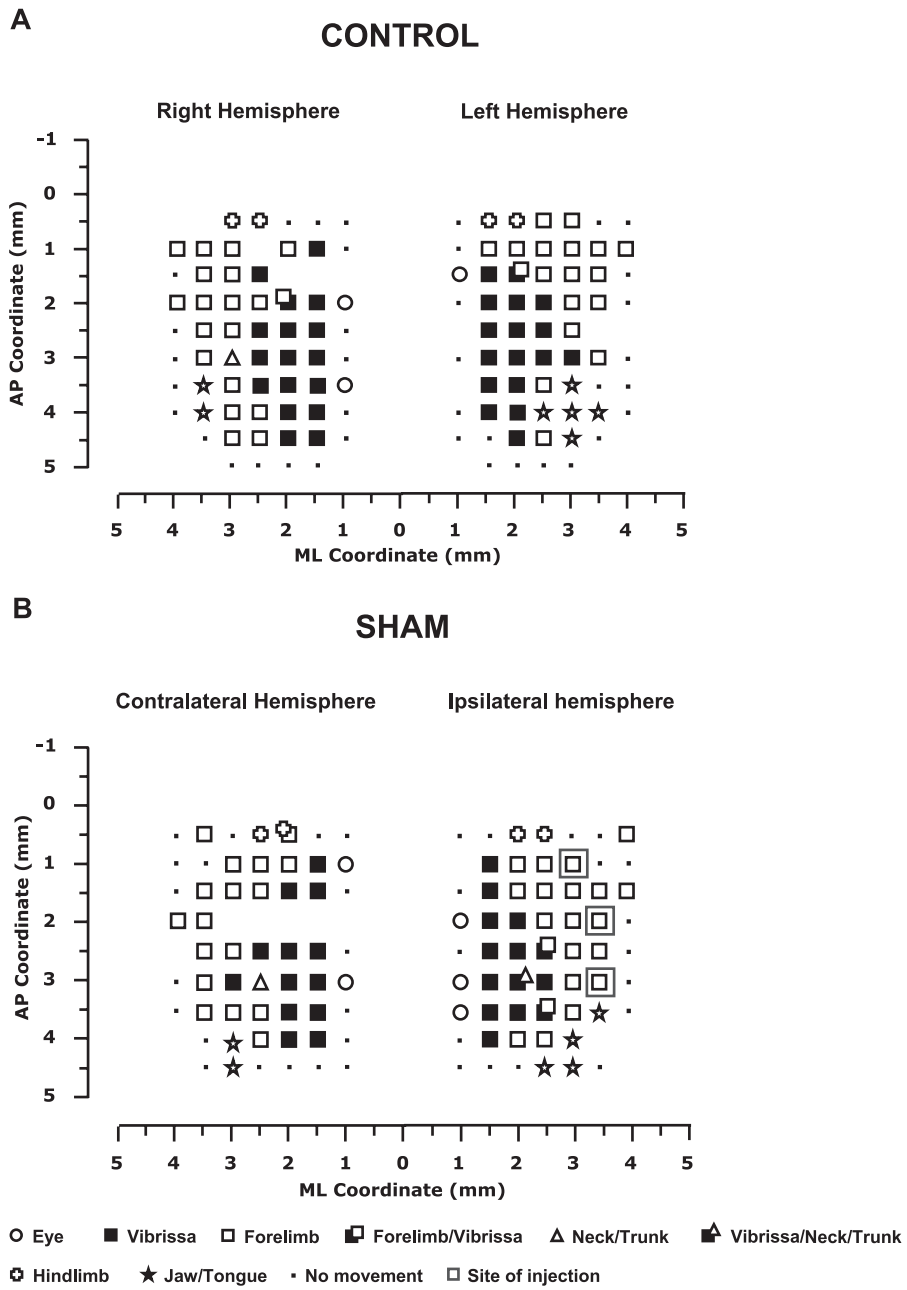

FIG. 2. (A) The top scheme provides an example of representation of the movements evoked at threshold current levels in the right and left hemispheres in the control group of rats. The microelectrode was sequentially introduced to a depth of 1500 μm. Interpenetration distances were 500 μm. In these M1 mapping schemes, frontal poles are at the bottom. In the anteroposterior (AP) coordinate, 0 corresponds to the bregma, and in the mediolateral (ML) coordinate, 0 corresponds to the midline; numbers indicate rostral or caudal distance from the bregma or lateral distance from the midline. Movement evoked at one point is indicated by symbols: double symbol, dual movement at threshold current level; absence of symbol (within or at the border of the maps), penetration not performed due to the presence of a large vessel. (B) The bottom scheme shows a surface view map for the sham group of rats. In the ipsilateral hemisphere, a symbol set in a square frame corresponds to the site of the saline injection. Note that the intracortical injection of saline did not induce changes in the motor representation in either the ipsilateral or contralateral hemisphere.

motor representation in either the ipsilateral or the contralateral hemisphere.

Estimating the area of lidocaine-induced inactivation in the ipsilateral hemisphere

Shortly after topically applying lidocaine into the iFMC, mapping revealed that forelimb movement was evoked in only a few sites (Fig. 3A and B; Fig. 6A; mean number of sites 5.4 ± 4.9; mean size 1.3 ± 0.47 mm^2; range 0.5–2 mm^2; control group vs. L-group ipsilateral hemispheres, $P < 0.0002$), because most of the cortical sites corresponding to the forelimb region were not excitable. Figure 3A and B shows, in the ipsilateral hemispheres, the residual forelimb sites localized at the border between the forelimb and vibrissa representations. The threshold currents required to evoke forelimb movement were greater in these sites than those obtained in controls, although they failed to reach significance (control group vs. L-group

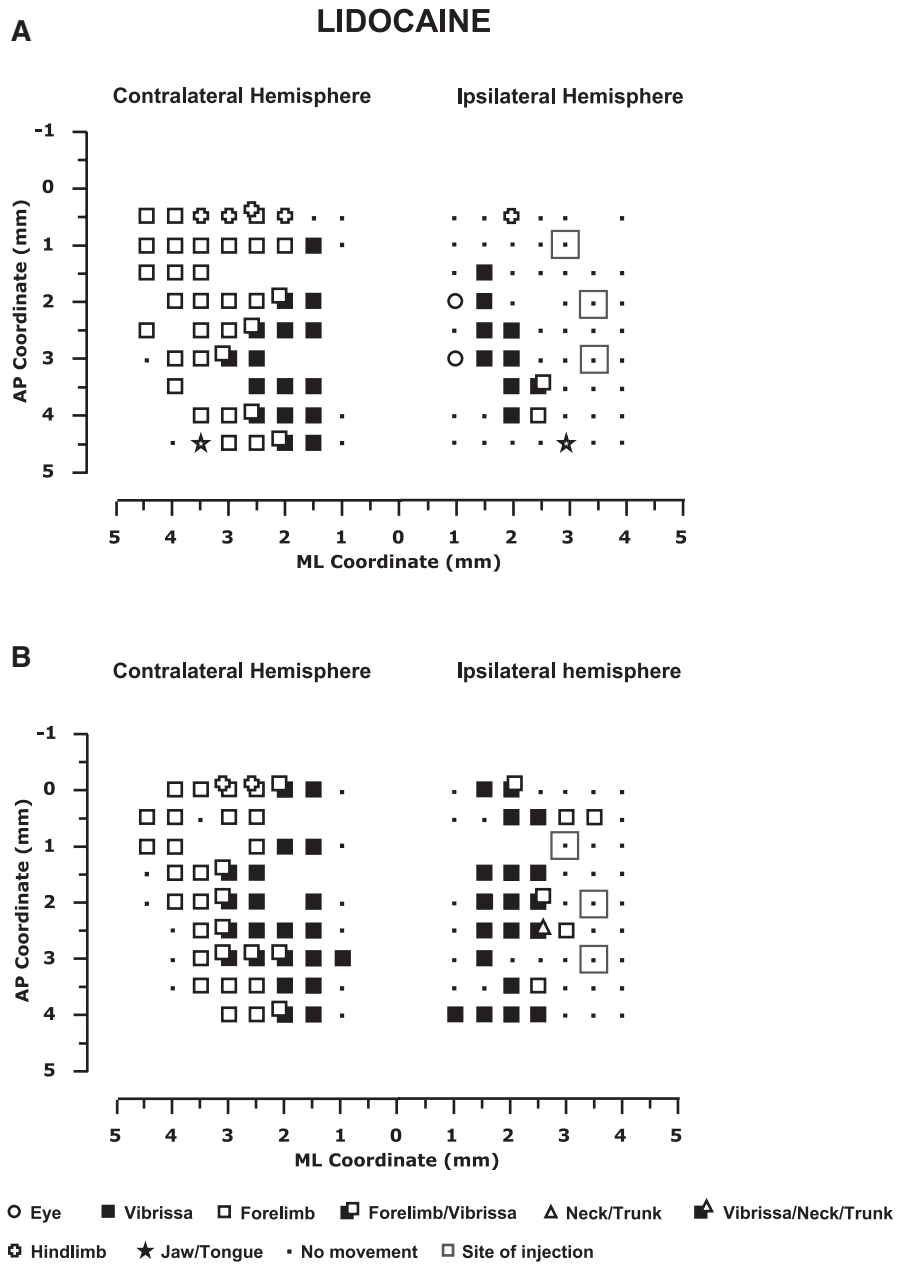

FIG. 3. The top (A) and bottom (B) schemes show two examples of surface view maps in the lidocaine-induced inactivation group of rats. In the ipsilateral hemisphere, symbols set in a square frame correspond to the lidocaine injection sites. Note that, in the ipsilateral hemisphere, the majority of cortical sites corresponding to the forelimb region are not excitable. The contralateral hemisphere shows: (i) enlargement of the forelimb representation; (ii) increase in the number of dual movement sites: sites where the vibrissa and forelimb movements were evoked at threshold current level. AP, anteroposterior; ML, mediolateral.

ipsilateral hemispheres: 20.9 ± 1.2 μA vs. 27.02 ± 7 μA, range 19.4–22.3 vs. 19.3–38.0, $P > 0.08$). Thus, in the ipsilateral hemisphere, the forelimb sites were reduced by 69.1% vs. the controls, and excitability was reduced in five out of seven hemispheres.

Statistical comparison between control group and L-group ipsilateral hemispheres showed that the lidocaine injected within the forelimb representation did not reduce the size (Fig. 3A and B; Table 1; control group vs. L-group ipsilateral hemispheres, $P > 0.7$) and excitability (Table 2; control group vs. L-group ipsilateral hemispheres, $P > 0.05$) of the vibrissa representation. Thus, the ipsilateral hemispheres only showed limited vibrissa site involvement at the border with the FMC (see ipsilateral hemispheres in Fig. 3A and B).

Lidocaine-induced changes in the contralateral hemisphere

The comparison between control group and L-group contralateral hemispheres showed an increase in the size of the forelimb representation in all L-group animals (Fig. 2A vs. Fig. 3A and B; Fig. 6A). The size of the forelimb representation in the L-group was 38.8% higher than those of the control group (L-group contralateral hemispheres, mean size 6.25 ± 0.6 mm^2, range 5.5–7.25 mm^2;

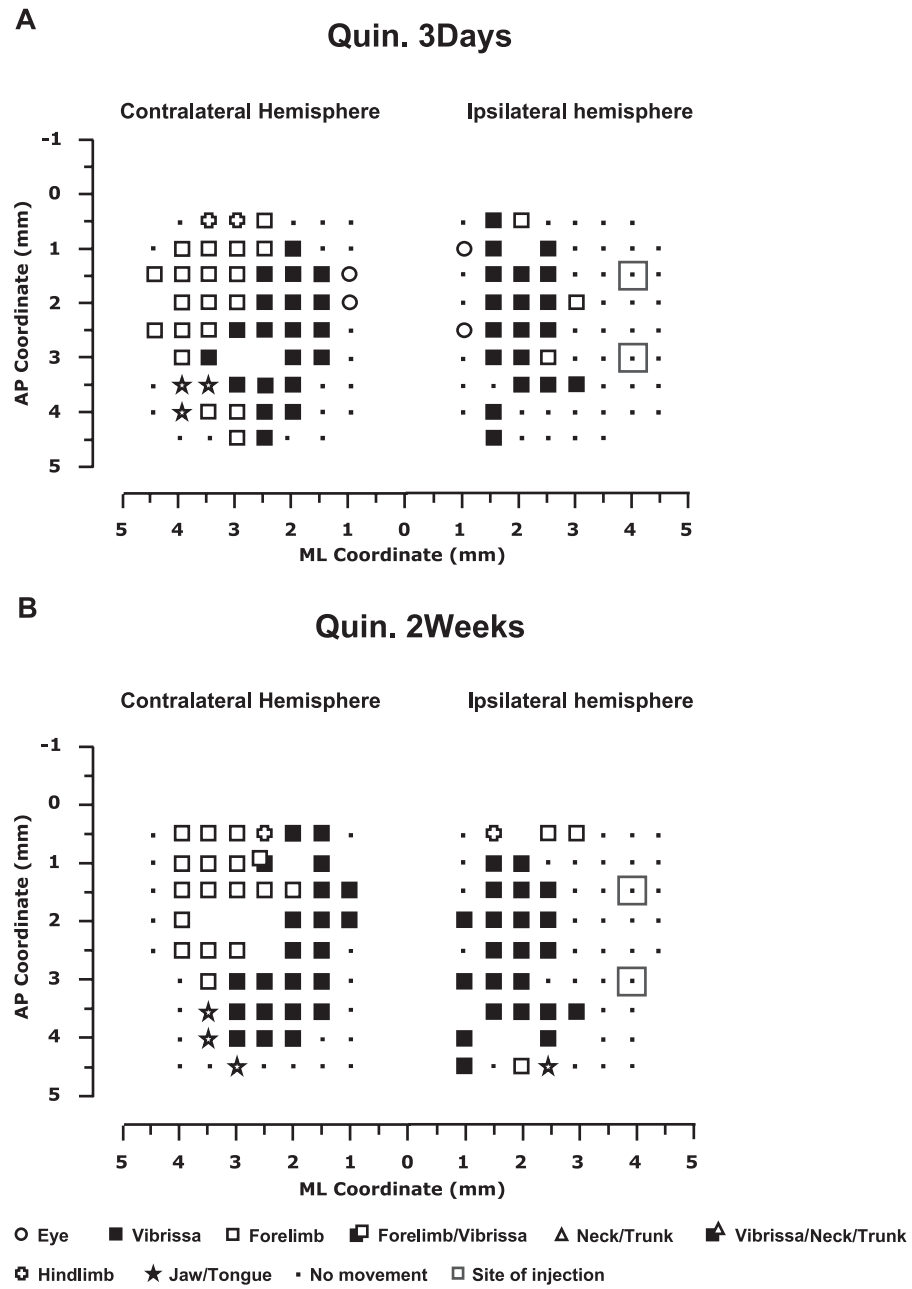

FIG. 4. Examples of bilateral maps from rats 3 days (A) and 2 weeks (B) after quinolinic acid (Quin.) injection. In the ipsilateral hemisphere, the symbol set in a square frame corresponds to the injection site. Note that, in all groups, the ipsilateral hemisphere shows that most of the cortical sites corresponding to the forelimb region are not excitable. The contralateral hemisphere in the 3Ds group and 2Ws group shows a pattern of movement representation similar to that found in the control group. AP, anteroposterior; ML, mediolateral.

control group vs. L-group, $P < 0.0002$). In contrast, the size of the vibrissa representation in the L-group was 15.5% smaller than in the control group (Table 1; control group vs. L-group, $P > 0.1$). Expansion of the forelimb representation was due to increases in the areas of both the distal and proximal forelimb movement representations (Fig. 6B; control group vs. L-group, $P < 0.01$); however, the ratio of the distal forelimb representation to the proximal forelimb representation decreased when L-group contralateral hemispheres were compared to the controls (control group vs. L-group: 4.9 ± 1.6 vs. 3.1 ± 1.3, range 3.2–7.5 vs. 1.4–5.2, $P = 0.07$). Thus, there was an increase in the representation of proximal vs. distal forelimb movement in the L-group, although it failed to reach significance, due to the small sample size and the large variation between L-group contralateral hemispheres. Figure 3A and B shows that the forelimb area expands laterally towards the cortex sites that overlap sites that were not excitable in control maps. The number of cortical sites from which forelimb movement could be elicited at 4 and 4.5 mm from the ML coordinate increased in L-group contralateral hemispheres (mean sites in control group vs. L-group: 2.6 ± 1.4 vs. 5.3 ± 2.7, range 1–4 vs. 2–10, $P = 0.064$). Furthermore, in all L-group contralateral hemispheres, there is strong evidence that the forelimb movement shifted towards medial sites

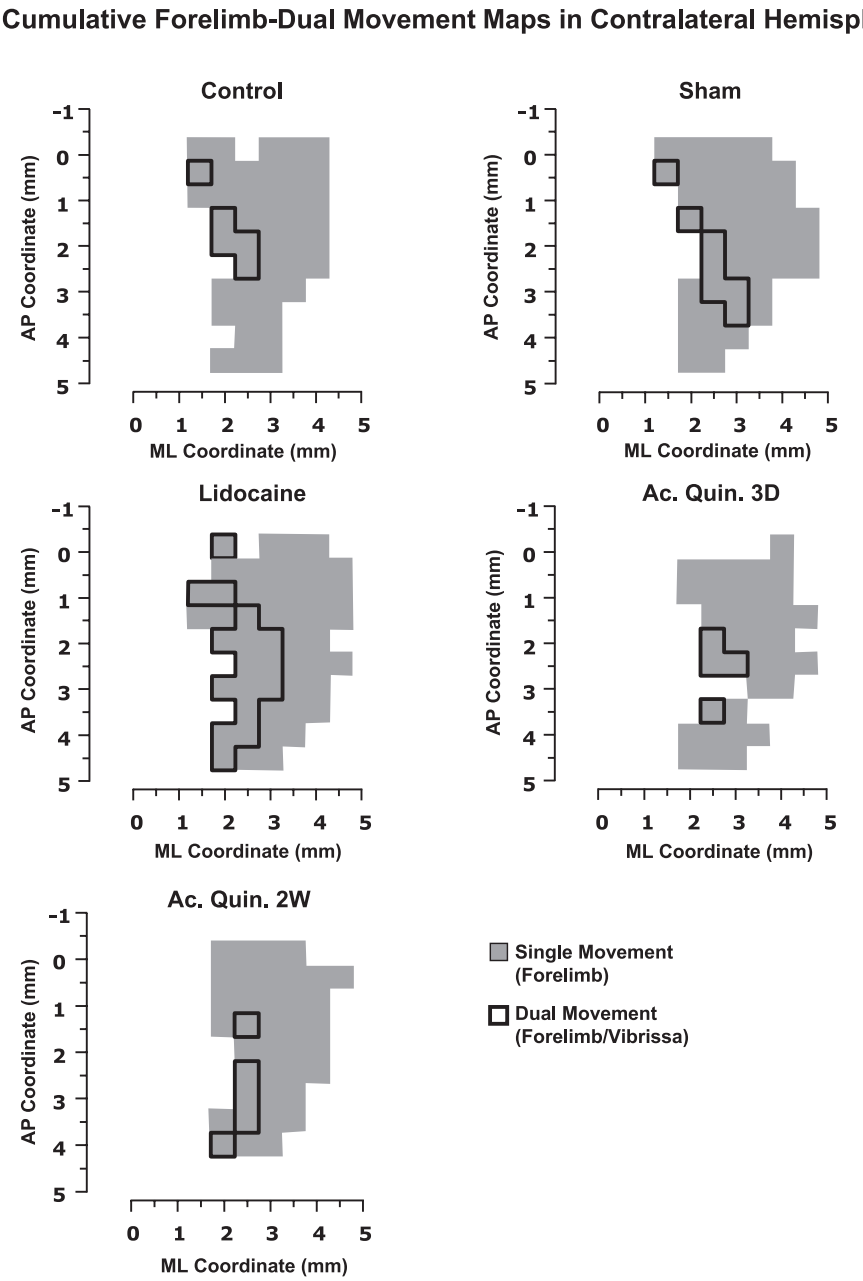

FIG. 5. Overview of the location, size and topographic overlapping of the forelimb (gray area) and dual vibrissa–forelimb movement sites (unbroken line) in control, sham, lidocaine-induced inactivation group (L-group), Q3D group and Q2W group contralateral hemispheres. These are schematic composite maps overlaying the forelimb sites and the dual vibrissa–forelimb sites in all rats in each group. Note that, in the L-group, the dual site composite map is larger than the control group composite map, and it encompasses most of the medial region of the forelimb representation. In contrast, in both the Q3D and Q2W groups, the cumulative map of dual movement sites encompasses cortical territory similar to that in the control and sham groups. Quin., quinolinic acid; AP, anteroposterior; ML, mediolateral.

where vibrissa movement was elicited (Fig. 2A vs. Fig. 3A and B). To quantitatively assess this spatial aspect of L-group maps, and to avoid interindividual biases related to differences in the motor map size and ML position, we expressed forelimb sites as a fraction of the number of movement sites from 2 to 3 mm from the midline in the control group vs. L-group. This cut-off was applied because, from 2 to 3 mm to the midline, the cortex corresponded to the forelimb–vibrissa border in both control group and L-group contralateral hemispheres (Fig. 2A and Fig. 3A and B). After comparison of percentages between the control group and L-group, a significant increase in the percentage of forelimb sites was found in the L-group (control group vs. L-group: 46.85 ± 5.22% vs. 67.01 ± 5.24%, range 42.8–54.5% vs. 58.3–70.5%, $P < 0.0005$). To determine the effect that homotopic cortex inactivation has on dual movement sites, the occurrence of the dual movement site was expressed as a percentage of the total number of movement sites 2–3 mm from the midline. In the L-group contralateral hemispheres, the percentage of dual sites was 22.3 ± 8.1% and was significantly higher than in the control group ($P < 0.0005$). It is of interest to note that this value was similar to the increase in the percentage of forelimb sites from 2 to

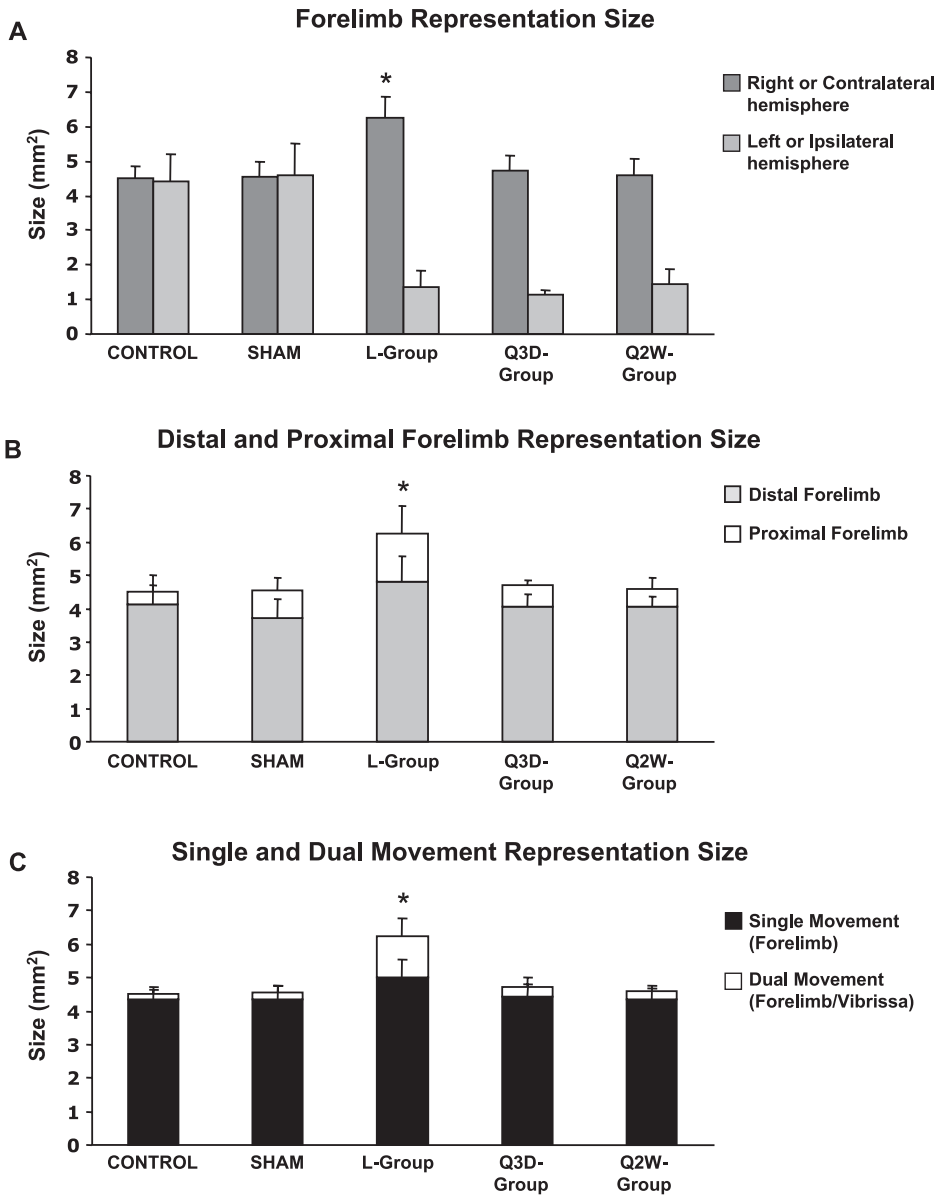

FIG. 6. Across-group comparison of the forelimb size. To compare data between diagrams, all the bars represent mean size values in mm^2 (+SD). (A) In each group, bars show the size of the forelimb representation in the right or contralateral hemispheres and in the left or ipsilateral hemisphere for the control and experimental groups, respectively. Note that, in all experimental groups, the right bar value is far below what it is in the controls ($P < 0.05$, Scheffè test) and there is no difference in this value between experimental groups ($P > 0.05$, ANOVA). In the lidocaine-induced inactivation group (L-group), the value of the left bar was significantly greater than in the control group (*$P < 0.05$, Scheffè test), whereas in the other experimental groups, the left bar value is similar to that found in the controls ($P > 0.05$, Scheffè test). (B) The diagram shows the distal and proximal forelimb movement representation size in the control, sham and experimental groups of rats. The gray bar shows the size of the forelimb representation where distal forelimb movement is evoked at threshold current level (+SD). The open bar shows the size of the forelimb representation where the proximal forelimb movement is evoked at threshold current level (+SD). For each bar, the cumulative value is that of the left bar in diagrams A. Note that, in the L-group, the value of the open bar was significantly greater than in the control group (*$P < 0.05$, Scheffè test). In the other experimental groups, the open bar value is similar to that found in the controls ($P > 0.05$, Scheffè test). (C) The diagram shows the size of the single (black bar) and dual forelimb sites (open bar) in control, sham and experimental groups of rats. For each bar, the cumulative value is that of the left bar in diagrams A. Note that, in the L-group, the value of the open bar was significantly greater than in the control group (*$P < 0.05$, Scheffè test). In the other experimental groups, the open bar value is similar to that found in the controls ($P > 0.05$, Scheffè test).

3 mm from the midline (22.3% vs. 21.7%) and was 66.6% of the forelimb representation size that enlarged in the contralateral L-group hemispheres (Fig. 6C). Thus, we can conclude that forelimb movement expands as dual sites at the border with the vibrissa representation, and that the dual site region occupies a strip of the map along the rostrocaudal border between the forelimb and vibrissa representations (Fig. 5C).

The threshold currents required to evoke forelimb movement in L-group contralateral hemispheres were similar to those in the controls (control group vs. L-group: 21.3 ± 1.9 μA vs. 21.1 ± 1.8 μA, $P > 0.9$). To analyse the spatial aspect of excitability in the enlarged forelimb representation, the current required to evoke forelimb movement was plotted vs. distance to the midline, irrespective of the AP coordinates. In comparing the control group and the L-group,

TABLE 1. Size of vibrissae representation in each hemisphere

Groups	Vibrissae representation (mm^2)	
	Left or ipsilateral hemisphere	Right or contralateral hemisphere
Control	4.1 ± 0.8 (3.00–4.75)	4.1 ± 0.2 (3.75–4.25)
Sham	3.7 ± 1.0 (2.25–4.75)	3.6 ± 0.5 (3.00–4.25)
Lidocaine	3.9 ± 1.1 (2.25–5.25)	3.4 ± 0.9 (2.75–4.25)
Q3D	4.5 ± 0.4 (4.25–5.25)	3.6 ± 0.7 (3.00–4.75)
Q2W	4.4 ± 0.7 (3.75–5.75)	4.0 ± 0.6 (3.25–4.75)

Data are presented as mean ± SD (with range in parentheses). Note that there was no statistical intergroup difference in the vibrissae movement size.

TABLE 2. Threshold currents for vibrissae movement

Groups	Threshold current (μA)	
	Left or ipsilateral hemisphere	Right or contralateral hemisphere
Control	20.9 ± 0.8 (19.6–21.8)	21.4 ± 0.9 (20.0–22.3)
Sham	21.8 ± 1.8 (19.5–23.8)	20.4 ± 0.6 (20.3–28.8)
Lidocaine	24.2 ± 3.3 (20.3–28.8)	19.4 ± 2.8 (15.5–23.0)
Q3D	22.1 ± 2.5 (19.4–23.8)	20.2 ± 1.3 (19.0–24.6)
Q2W	21.6 ± 0.7 (21.0–22.3)	21.0 ± 1.2 (18.3–22.1)

Data are presented as mean ± SD (with range in parentheses). Note that there was no statistical intergroup difference in the vibrissae movement threshold.

this analysis showed that there was no difference in threshold across the ML plane (control group vs. L-group: 3 mm ML coordinate, 18.7 ± 2.6 μA vs. 20.6 ± 4.7 μA; 2.5 mm ML coordinate, 21.08 ± 3.1 μA vs. 17.4 ± 3.1 μA; 2 mm ML coordinate, 15.8 ± 1.4 μA vs. 17.2 ± 5.7 μA, $P > 0.3$). To quantify changes in excitability needed to evoke forelimb movement in dual movement sites, we compared the current needed to evoke suprathreshold forelimb movement in vibrissa sites from 2 to 3 mm from the midline in the control group with the current needed to evoke forelimb movement in dual sites in the L-group. Expressed as a percentage of current required to evoke forelimb movement in those sites where vibrissa movement was evoked at threshold current in the controls, the current for evoking forelimb movement decreased by 47.5% in dual movement sites in the L-group (control group vs. L-group: 26.4 ± 2.4 μA vs. 17.9 ± 6.4 μA, $P > 0.003$).

Estimating the area of quinolinic acid-induced lesion in the ipsilateral hemisphere

Lesions were localized after thionine staining, and photographed to show the relationship between the lesion and the histological borders of the lateral agranular cortex of M1. The histological result from one animal is illustrated in Fig. 1A, and is representative of all the cases studied. Figure 1A and B shows that the borders of the lesions are nearly co-extensive with the lateral agranular cortex where forelimb movements are represented (Brecht *et al.*, 2004). Lesion reconstructions based on thionine staining revealed that all lesions produced damage to the lateral agranular cortex (Fig. 1C). In all Q-group ipsilateral hemispheres, the vast majority of cortical sites lateral to 2.5 mm from the midline were not excitable (Fig. 4). In general, in the Q-group ipsilateral hemispheres, the average number of forelimb sites was reduced by 68.75% as compared to the controls (mean number of sites 5.5 ± 1.5, range 3–8 sites; control group vs. Q-group ipsilateral hemispheres, $P < 0.00001$) and, in these residual sites, excitability was reduced by 19.7% (control group vs. Q-group: $P < 0.004$). Comparison of the control group and Q-group ipsilateral hemispheres showed no statistical difference in the percentage of vibrissa movement sites (mean number of sites in control group vs. Q-group ipsilateral hemispheres 38.5 ± 3.95% vs. 37.0 ± 3.7%, range 33.3–43.2% vs. 30.0–40.4%, $P > 0.5$). Hence the threshold values needed to evoke vibrissa movement were also not significantly different from those for the control group (control group vs. Q-group ipsilateral hemispheres: $P > 0.8$). Thus, the lesion of the FMC does not substantially change the size and excitability of the vibrissa movement representation.

Statistical comparison between ipsilateral hemispheres in the Q-group of animals showed no significant difference in the percentages of vibrissa and forelimb movement sites (vibrissa, $P > 0.4$; forelimb, $P > 0.1$) and in evoked movement thresholds (vibrissa, $P > 0.9$; forelimb, $P > 0.2$; hindlimb, $P > 0.2$). The fact that there were no statistical differences between Q-group ipsilateral hemispheres is evidence that the movement representation in M1 found at 3 days after lesion had not changed by 2 weeks after lesion.

Quinolinic acid-induced changes in the contralateral hemisphere

Three days after lesion of the FMC in the ipsilateral hemisphere, there was no statistical difference in the size and excitability of the cFMC when compared with control values (mean size 4.7 ± 0.5 mm^2, range 4–5.25 mm^2, $P > 0.7$; Figs 4A and 6A; mean excitability 21.7 ± 2.2 μA, range 19.1–23.6 μA, $P > 0.7$). Similarly, there was no difference between the control and Q3D cFMCs in the percentage of dual movement sites and their localization (control group vs. Q3D group: mean number of sites 0.6 ± 0.5 vs. 1.0 ± 1.2, mean percentage 1.47 ± 1.3% vs. 2.4 ± 3.0, range 0–2.7% vs. 0–7.5, $P > 0.7$; Fig. 5A vs. Fig. 5D; Fig. 6C). Thus, we conclude that, under the present experimental conditions, the plastic changes in the cFMC seen after inactivation are evidence of recovery to baseline value at 3 days after lesion.

No comparisons between the Q3D and Q2W groups of animals showed any significant difference in the mean of values and in the range of values: forelimb representation size (Fig. 4A vs. Fig. 4B; Fig. 6A; Q3D group vs. Q2W group, mean size 4.7 ± 0.5 vs. 4.6 ± 0.45 mm^2, range 4–5.25 vs. 4–5, $P > 0.8$), dual movement site percentage (Fig. 6C; Q3D group vs. Q2W group, mean 2.4 ± 3.0% vs. 2.4 ± 0.2%, range 0–2.7% vs. 0–2.6%, $P > 0.7$) and localization (Fig. 5D vs. Fig. 5E), vibrissa representation size (Fig. 4A vs. Fig. 4B; Table 1; Q3D group vs. Q2W group, $P > 0.4$), and evoked movement thresholds [Q3D group vs. Q2W group: vibrissa (Table 2), $P > 0.7$; forelimb, 21.7 ± 2.2 μA vs. 23.1 ± 3.1 μA, $P > 0.2$]. Thus, the normal cFMC output seen at 3 days after the iFMC lesion showed no sign of changes at 2 weeks after iFMC lesion.

Discussion

The aim of the present study was to investigate the contribution of the iFMC to movement representation in the cFMC. The results demonstrate a substantial increase in the contralateral forelimb representation, as assessed by ICMS, after the iFMC had been inactivated. This suggests that the iFMC may play a crucial role in shaping the motor representation, most likely through a trancallosal effect on the cFMC. The present data show that this form of

interhemispheric diaschisis was completely reversed, with recovery of the baseline map, 3 days after the lesion in the iFMC. This restored forelimb map showed no ICMS-induced changes 2 weeks after the iFMC lesion. It is also important to stress that this form of interhemispheric diachisis proved very different in nature from the interhemispheric diachisis after inactivation and lesion in the VMC described in the previous study (Maggiolini *et al.*, 2007).

Interpretation of motor map changes in the cFMC after iFMC inactivation and lesion

For these investigations, cortical inactivation and lesion were produced, respectively, by injecting lidocaine and quinolinic acid. As shown in the previous study (Maggiolini *et al.*, 2007), the advantage of these methods is that they are non-invasive and produce lesions with good reproducibility in terms of size, and a good, sharp boundary between affected motor representations and surrounding motor regions.

In the lidocaine experiments, the level of inactivation was assessed by reviewing injected site responses every 30 min to check for changes in excitability as mapping progressed, and the interpretation of the changes in the contralateral hemisphere is based on the preserved inactivation of the injected sites.

The present study is limited by the fact that experiments with lidocaine were performed without remapping M1 in either hemisphere after lidocaine washout. A map-and-then-remap design would require several hours, and the cortical state could change over such long experimental sections. Nevertheless, the lack of information on recovery after lidocaine washout raises a potential question about the timing of M1 recovery after reversible inactivation of the homologous cortex.

The transcallosal output from the primary motor cortex (M1) has been investigated in humans using transcranial magnetic stimulation (TMS). TMS experiments have demonstrated that transcallosal output inhibits contralateral M1 (Wassermann *et al.*, 1991; Ferbert *et al.*, 1992; Meyer *et al.*, 1995; Gerloff *et al.*, 1998) . TMS was performed by placing a coil tangentially to the scalp at a fixed site over M1 (referred to as a 'motor hot spot') and recording motor-evoked potential and electromyographic activity over arm muscles. The inhibitory effects of transcallosal output were measured either as a period of silence in electromyographic activity or as motor-evoked potential amplitude inhibition by a TMS pulse over M1 of the contralateral hemisphere (Rothwell *et al.*, 1991; Meyer *et al.*, 1995; Boroojerdi *et al.*, 1996).

The present study touches on the issue of short-term vs. long-term effects of contralateral input elimination in the cerebral cortex in an animal model. The standard ICMS was carried out to map movement representations in the rat M1. The inhibitory effects of transcallosal output were measured: (i) as changes in the size and shape of the forelimb representation; (ii) as changes in the border and overlapping between the vibrissa and forelimb representations; and (iii) as changes in the type of movements evoked at both stimulation current threshold and over-threshold levels.

It is important to point out that the area of the cortex defined as the forelimb and vibrissae motor cortex is highly dependent upon the methods used during mapping. In any experiment, the baseline maps reported depend on the technique used (Donoghue & Wise, 1982; Gioanni & Lamarche, 1985; Castro-Alamancos & Borrel, 1995; Kleim *et al.*, 1998; Franchi, 2000; Haiss & Schwarz, 2006; Ramanathan *et al.*, 2006). Moreover, in all ICMS-induced maps, the amount of overlapping between different movements is directly related to the intensity of the stimulus relative to threshold. To avoid biases, in all hemispheres the vibrissae–forelimb overlapping was measured in the threshold current-derived map. In all the present control and sham animals, the topography of movement representations and the amount of vibrissa–forelimb overlapping are consistent with those of previous experiments using similar stimulation parameters (Maggiolini *et al.*, 2007).

The primary finding of the study is that, after inactivation of the iFMC, the cFMC exhibits a substantial increase in the cortex area from which forelimb movement can be elicited at the threshold stimulation current. Then the cFMC undergoes some rapid functional changes due to the inactivation of the iFMC. This functional change facilitates the ability to elicit forelimb movements from cortex sites that would have not previously produced forelimb movements in response to similar stimulation. In all maps, forelimb movement expanded medially within the lateral part of the vibrissa representation, so that all maps showed a larger than normal cortical area where vibrissa and forelimb movements overlapped the same cortical territory.

There is substantial evidence that, via the corpus callosum, each M1 exerts a reciprocal influence on homotopical representations in the opposite hemisphere (Jenny, 1979; Spidalieri & Guandalini, 1983; Gould *et al.*, 1986; Ferbert *et al.*, 1992; Chapman *et al.*, 1998). In the present study, lidocaine inactivation of the iFMC most likely interfered with short-term transcallosal influences between FMCs. If this is the case, changes in the cortical topography could be explained by a loss of interhemispheric inhibitory influence between the FMCs of the two hemispheres. Indeed, by producing iFMC inactivation, we probably impede the transcallosal inhibitory influence that is normally exerted by the iFMC on the opposite hemisphere, leading to a release of the transcallosal inhibition exerted on the cFMC. This interpretation of trancallosal modulation between the bilateral FMCs in rat is in good agreement with the transcallosal modulation between the bilateral hand motor cortices, as investigated by TMS in humans. TMS experiments have shown that transcallosal inhibition between hand motor representations is more prominent than facilitation (Ferbert *et al.*, 1992; Ugawa *et al.*, 1993; Meyer *et al.*, 1995; Hanajima *et al.*, 2001). The interhemispheric inhibitory interactions differ between homologous arm muscle representations in relation to a proximal–distal gradient (Shon *et al.*, 2003) or according to the role that each arm muscle plays in functional movement synergies (Harris-Love *et al.*, 2007).

The equivalent ICMS current required to elicit forelimb movement in the control group and L-group of rats indicates that the suppression of transcallosal inhibition did not alter the basic threshold within the normal forelimb representation but did give rise to a normal-strength functional connection between new forelimb sites and the forelimb motor neuron pool. In some other situations, an alteration in forelimb size can be detected, even when there is no change in motor threshold (Teskey *et al.*, 2002).

The recovery in cFMC size – returning to the size found in the control hemisphere 3 days after iFMC lesion – suggests a rapid adaptive plastic change as a consequence of the rebalancing of excitability that does not depend on the lesion in the contralateral hemisphere. This form of short-lived diaschisis could be explained by a process of rapid recovery of the excitability of inhibitory interneurons so that the cFMC could rapidly be reshaped to the baseline value (Fig. 7). Corticocortical input to the disconnected FMC from SI and SII and thalamocortical activity could both regulate the rate of recovery of inhibitory interneuron excitability.

After a cortical lesion, alterations in dendritic and synaptic morphology (Jones *et al.*, 1996; Jones, 1999) and sprouting of axons (Emerick *et al.*, 2003) could affect the activity (Rema & Ebner, 2003)

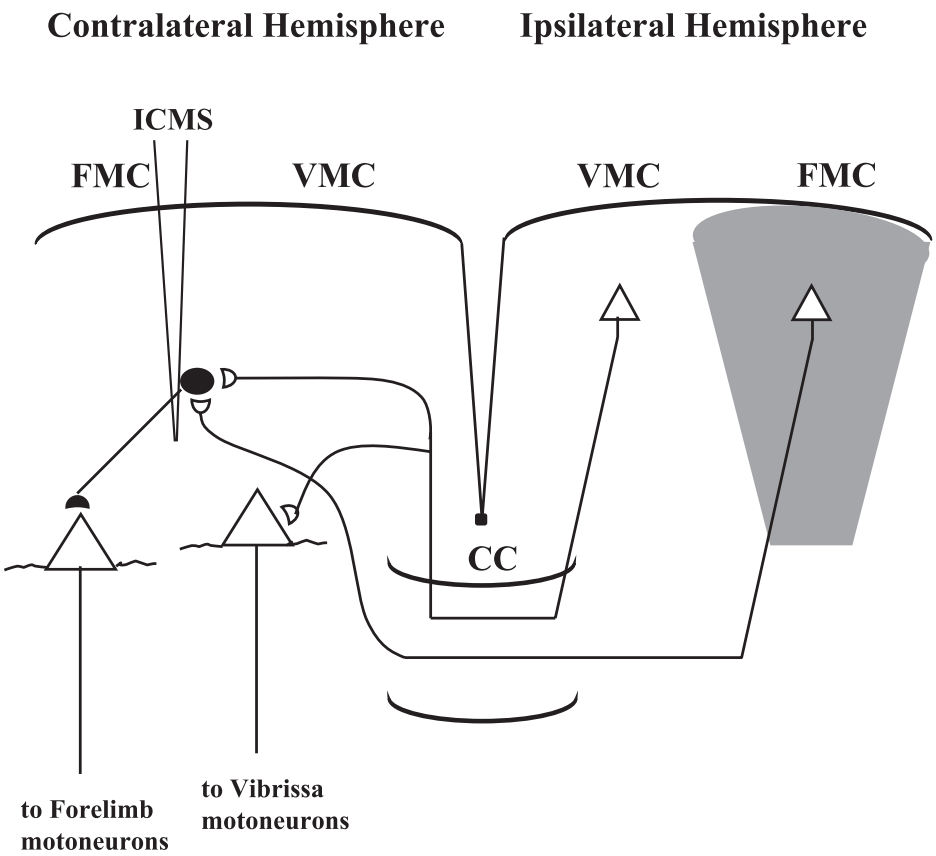

FIG. 7. Proposed circuit model depicting transmission of interhemispheric information of callosal neurons to vibrissa and forelimb neurons at the border between vibrissa and forelimb representations. Axon collaterals provide direct synaptic excitatory connections between callosal afferents and inhibitory interneurons. Inhibitory interneurons at the border of the vibrissa–forelimb representation are well positioned to modulate callosal input onto forelimb motorneurons. Either forelimb motor cortex (FMC) (gray area) inactivation or vibrissa motor cortex (VMC) inactivation causes the forelimb representation to expand within the vibrissa representation, so that it moves in medially. CC, corpus callosum; ICMS, stimulating electrode.

and the ICMS-derived map of the contralateral cortex (Emerick *et al.*, 2003; Maggiolini *et al.*, 2007). All these long-term plastic changes – which could affect the ICMS-derived forelimb map – have proved to be highly dependent on the level of rehabilitative training (Jones & Schallert, 1994; Jones, 1999). Thus, it is not surprising that, in the present experiment, 2 weeks after iFMC lesion, the cFMC proved similar to the controls. However, an alternative possibility is that a subtle, altered excitatory–inhibitory balance in the cFMC might not be sensitive to the ICMS as used in the present experiments.

Comparison between vibrissa–interhemispheric and forelimb–interhemispheric diaschisis

To compare the results from this and previous (Maggiolini *et al.*, 2007) experiments, we can assume that the neurons in the hemisphere opposite the site of inactivation would detect the inactivation as a sudden reduction in activity arising from commissural inputs (Li *et al.*, 2005).

The distinctive feature of the short-term vibrissa–interhemispheric diaschisis was shrinkage in the representation size with reduced excitability of the VMC, whereas the distinctive feature of the forelimb–interhemispheric diaschisis was enlarged representation without any change in baseline excitability. Therefore, we conclude that the VMC and FMC of the two hemispheres continuously interact, respectively, through prominent excitatory and inhibitory influences.

It has proved difficult to explain the observed loss of excitability in the VMC vs. the normal excitability in the FMC after inactivation of the homologous M1 region. The main reason could be that the FMC has fewer homotopical callosal connections than the VMC; moreover, in the FMC, most callosal projections may not be directly linked to corticospinal forelimb motorneurons (Fig. 7). These differences in interhemispheric connectivity could also explain why the recovery of diachisis after FMC lesion was faster than the recovery after VMC lesion.

It should be noted that, in both vibrissa–interhemispheric and forelimb–interhemispheric diaschisis, the forelimb movement expands within the lateral part of the vibrissae representation. Therefore, we propose that the changes in the border between the VMC and FMC, which occur in both forms of diachisis, may be explained by a callosal-driven downregulation in the activity of inhibitory interneurons linked selectively to forelimb motor neurons (Fig. 7).

Interpretation of the motor map changes in relation to movement pattern

ICMS-derived maps of movement representation in M1 are essentially static, and reflect the strength of corticospinal connections within the conditions of the experiment. The present and previous (Maggiolini *et al.*, 2007) studies suggest that the ipsilateral M1 plays a significant role in shaping motor representation in the contralateral M1, allowing changes in the border and overlapping between forelimb and vibrissa

movement representations. Taken together, these data are not consistent with the idea that the vibrissa–forelimb overlapping is simply due to overlapping of the stimuli. The vibrissae–forelimb overlapping appears to be a real feature of rat motor cortex organization after interhemispheric transient disconnection. Amassian *et al.* (1995) suggested that representation overlapping is part of the neural substrate for the motor control of different muscles during natural complex movements. In humans, interhemispheric mechanisms are thought to play a crucial role in motor control by ensuring correct timing of the synergic recruitment of the set of muscles (Devanne *et al.*, 2002, 2006; Holdfer & Miller, 2002). In rats, the final interpretation of the present and previous data could be that the interhemispheric activity between vibrissae and forelimb M1 could promote synergic activity among vibrissa and forelimb muscles or, in contrast, could separate forelimb and vibrissa movement representations into constituent muscles according to different types of movement that reflect animal behavior. Then, the interhemispheric activity could promote differences in the synergic recruitment of vibrissa and forelimb muscles in complex movements such as bringing to the mouth, grooming, or sniffing during explorative behavior. Future studies will be needed to confirm or reject this interpretation of present ICMS-based results.

Acknowledgements

We thank Engineer E. Lodi, Dr V. Muzzioli and S. Zanellati for their technical support. This study was funded by grant from Università degli Studi di Ferrara.

Abbreviations

AP, anteroposterior; cFMC, contralateral forelimb motor cortex; FMC, forelimb motor cortex; ICMS, intracortical microstimulation; iFMC, ipsilateral forelimb motor cortex; ML, mediolateral; TMS, transcranial magnetic stimulation; VMC, vibrissa motor cortex.

References

Amassian, V.E., Cracco, R.Q., Maccabee, P.J., Cracco, J.B. & Henry, K. (1995) Some positive effects of transcranial magnetic stimulation. In Fahn, S., Hallett, M., Luders, H.O. & Marsden, C.D. (Eds), *Advances in Neurology, Negative Motor Phenomena*, **Vol. 67**. Lippincott-Raven, Philadelphia, pp. 79–106.

Biernaskie, J. & Corbett, D. (2001) Enriched rehabilitative training promotes improved forelimb motor function and enhanced dendritic growth after focal ischemic injury. *J. Neurosci.*, **21**, 5272–5280.

Biernaskie, J., Szymanska, A., Windle, V. & Corbett, D. (2005) Bi-hemispheric contribution to functional motor recovery of the affected forelimb following focal ischemic brain injury in rats. *Eur. J. Neurosci.*, **21**, 989–999.

Boroojerdi, B., Diefenbach, K. & Ferbert, A. (1996) Transcallosal inhibition in cortical and subcortical cerebral vascular lesions. *J. Neurol. Sci.*, **144**, 160–170.

Brecht, M., Krauss, A., Muhammad, S., Sinai-Esfahani, L., Bellanca, S. & Margrie, T.W. (2004) Organization of rat vibrissa motor cortex and adjacent areas according to cytoarchitectonics, microstimulation, and intracellular stimulation of identified cells. *J. Comp. Neurol.*, **479**, 360–373.

Brosamle, C. & Schwab, M.E. (1997) Cells of origin, course, and termination patterns of the ventral, uncrossed component of the mature rat corticospinal tract. *J. Comp. Neurol.*, **386**, 293–303.

Castro-Alamancos, M.A. & Borrel, J. (1995) Functional recovery of forelimb response capacity after forelimb primary motor cortex damage in the rat is due to the reorganization of adjacent areas of cortex. *Neuroscience*, **68**, 793–805.

Chapman, C.A., Trepel, C., Ivanco, T.L., Froc, D.J., Wilson, K. & Racine, R.J. (1998) Changes in field potentials and membrane currents in rat sensorimotor cortex following repeated tetanization of the corpus callosum. *Cereb. Cortex*, **8**, 730–742.

Chen, R., Gerloff, C., Hallett, M. & Cohen, L.G. (1997) Involvement of the ipsilateral motor cortex in finger movements of different complexities. *Ann. Neurol.*, **41**, 247–254.

Chen, R., Yung, D. & Li, J.Y. (2003) Organization of ipsilateral excitatory and inhibitory pathways in the human motor cortex. *J. Neurophysiol.*, **89**, 1256–1264.

Cisek, P., Crammond, D.J. & Kalaska, J.F. (2003) Neural activity in primary motor and dorsal premotor cortex in reaching tasks with the contralateral versus ipsilateral arm. *J. Neurophysiol.*, **89**, 922–942.

Davare, M., Duque, J., Vandermeeren, Y., Thonnard, J.L. & Olivier, E. (2007) Role of the ipsilateral primary motor cortex in controlling the timing of hand muscle recruitment. *Cereb. Cortex*, **17**, 353–362.

Devanne, H., Cohen, L.G., Kouchtir-Devanne, N. & Capaday, C. (2002) Integrated motor cortical control of task-related muscles during pointing in humans. *J. Neurophysiol.*, **87**, 3006–3017.

Devanne, H., Cassim, F., Ethier, C., Brizzi, L., Thevenon, A. & Capaday, C. (2006) The comparable size and overlapping nature of upper limb distal and proximal muscle representations in the human motor cortex. *Eur. J. Neurosci.*, **23**, 2467–2476.

Donchin, O., Gribova, A., Steinberg, O., Bergman, H. & Vaadia, E. (1998) Primary motor cortex is involved in bimanual coordination. *Nature*, **395**, 274–278.

Donoghue, J.P. & Wise, S.P. (1982) The motor cortex of the rat: cytoarchitecture and microstimulation mapping. *J. Comp. Neurol.*, **212**, 76–88.

Donoghue, J.P., Suner, S. & Sanes, J.N. (1990) Dynamic organization of primary motor cortex output to target muscles in adult rats. II. Rapid reorganization following motor nerve lesion. *Exp. Brain Res.*, **79**, 492–503.

Emerick, A.J., Neafsey, E.J., Schwab, M.E. & Kartje, G.L. (2003) Functional reorganization of the motor cortex in adult rats after cortical lesion and treatment with monoclonal antibody IN-1. *J. Neurosci.*, **23**, 4826–4830.

Ferbert, A., Priori, A., Rothwell, J.C., Day, B.L., Colebatch, J.G. & Marsden, C.D. (1992) Interhemispheric inhibition of the human motor cortex. *J. Physiol. (Lond.)*, **453**, 525–546.

Franchi, G. (2000) Reorganization of vibrissal motor representation following severing and repair of the facial nerve in adult rats. *Exp. Brain Res.*, **131**, 33–43.

Franchi, G. (2002) Time course of motor cortex reorganization following botulinum toxin injection into the vibrissal pad of the adult rat. *Eur. J. Neurosci.*, **16**, 1333–1348.

Gerloff, C., Cohen, L.G., Floeter, M.K., Chen, R., Corwell, B. & Hallett, M. (1998) Inhibitory influence of the ipsilateral motor cortex on responses to stimulation of the human cortex and pyramidal tract. *J. Physiol. (Lond.)*, **510**, 249–259.

Gioanni, Y. & Lamarche, M. (1985) A reappraisal of rat motor cortex organization by intracortical microstimulation. *Brain Res.*, **344**, 49–61.

Gould, H.J., Cusick, C.G., Pons, T.P. & Kaas, J.H. (1986) The relationship of corpus callosum connections to electrical stimulation maps of motor, supplementary motor, and the frontal eye fields in owl monkeys. *J. Comp. Neurol.*, **247**, 297–325.

Guandalini, P. (1998) The corticocortical projections of the physiologically defined eye field in the rat medial frontal cortex. *Brain Res. Bull.*, **47**, 377–385.

Guandalini, P. (2003) The efferent connections of the pupillary constriction area in the rat medial cortex. *Brain Res.*, **962**, 27–40.

Haiss, F. & Schwarz, C. (2006) Spatial segregation of different modes of movement control in the whisker representation of rat primary motor cortex. *J. Neurosci.*, **25**, 1579–1587.

Hall, D.H. & Lindholm, E. (1974) Organization of motor and somatosensory neocortex in the albino rat. *Brain Res.*, **66**, 23–38.

Hanajima, R., Ugawa, Y., Machii, K., Mochizuki, H., Terao, Y., Enomoto, H., Furubayashi, T., Shiio, Y., Uesugi, H. & Kanazawa, I. (2001) Interhemispheric facilitation of the hand motor area in humans. *J. Physiol.*, **531**, 849–859.

Harris-Love, M., Perez, M.A., Chen, R. & Cohen, L.G. (2007) Interhemispheric inhibition in distal and proximal arm representations in the primary motor cortex. *J. Neurophysiol.*, **97**, 2511–2515.

Hattox, A.M., Priest, C.A. & Keller, A. (2002) Functional circuitry involved in the regulation of whisker movements. *J. Comp. Neurol.*, **442**, 266–276.

Holdfer, R.N. & Miller, L.E. (2002) Primary motor cortical neurons encode functional muscles synergies. *Exp. Brain Res.*, **146**, 233–243.

Jenny, A.B. (1979) Commissural projections of the cortical hand motor area in monkeys. *J. Comp. Neurol.*, **188**, 137–145.

Jones, T.A. (1999) Multiple synapse formation in the motor cortex opposite unilateral sensorimotor cortex lesions in adult rats. *J. Comp. Neurol.*, **414**, 57–66.

Jones, T.A. & Schallert, T. (1992) Overgrowth and pruning of dendrites in adult rats recovering from neocortical damage. *Brain Res.*, **581**, 156–160.
Jones, T.A. & Schallert, T. (1994) Use-dependent growth of pyramidal neurons after neocortical damage. *J. Neurosci.*, **14**, 2140–2252.
Jones, T.A., Kleim, J.A. & Greeniugh, W.T. (1996) Synaptogenesis and dendritic growth in the cortex opposite unilateral sensorimotor cortex damage in adult rats: a quantitative electron microscopic examination. *Brain Res.*, **733**, 142–148.
Kartje-Tillotson, G., Neafsey, E.J. & Castro, A.J. (1985) Electrophysiological analysis of motor cortical plasticity after cortical lesions in newborn rats. *Brain Res.*, **332**, 103–111.
Kartje-Tillotson, G., Neafsey, E.J. & Castro, A.J. (1986) Topography of corticopontine remodelling after cortical lesions in newborn rats. *J. Comp. Neurol.*, **250**, 206–214.
Kleim, J.A., Barbay, S. & Nudo, R.J. (1998) Functional reorganization of the rat motor cortex following motor skill learning. *J. Neurophysiol.*, **80**, 3321–3325.
Li, L., Rema, V. & Ebner, F.F. (2005) Chronic suppression of activity in barrel field cortex downregulates sensory responses in contralateral barrel field cortex. *J. Neurophysiol.*, **94**, 3342–3356.
Maggiolini, E., Veronesi, C. & Franchi, G. (2007) Plastic changes in the vibrissa motor cortex in adult rats after output suppression in the homotopic cortex. *Eur. J. Neurosci.*, **25**, 3678–3690.
Meyer, B.U., Roricht, S., Grafin von Einsiedel, H., Kruggel, F. & Weindl, A. (1995) Inhibitory and excitatory interhemispheric transfers between motor cortical areas in normal humans and patients with abnormalities of the corpus callosum. *Brain*, **118**, 429–440.
Napieralski, J.A., Bultler, A.K. & Chesselet, M.F. (1996) Anatomical and functional evidence for lesion-specific sprouting of corticostriatal input in the adult rat. *J. Comp. Neurol.*, **373**, 484–497.
Papadopoulos, C.M., Tsai, S.Y., Alsbiei, T., O'Brien, T.E., Schwab, M.E. & Kartje, G.L. (2002) Functional recovery and neuroanatomical plasticity following middle cerebral artery occlusion and IN-1 antibody treatment in the adult rat. *Ann. Neurol.*, **51**, 433–441.
Porter, R. & Lemon, R.N. 1993. *Corticospinal Function and Voluntary Movement*. Oxford University Press, New York.
Ramanathan, D., Conner, J.M. & Tuszynski, M.H. (2006) A form of motor cortical plasticity that correlates with recovery of function after brain injury. *Proc. Natl. Acad. Sci. U.S.A.*, **103**, 11370–11375.
Rema, V. & Ebner, F.F. (2003) Lesions of mature barrel field cortex interfere with sensory processing and plasticity in connected areas of the contralateral hemisphere. *J. Neurosci.*, **23**, 11269–11278.
Rothwell, J.C., Colebatch, J., Britton, T.C., Priori, A., Thompson, P.D., Day, B.L. & Marsden, C.D. (1991) Physiological studies in a patient with mirror movements and aganesis of the corpus callosum. *J. Physiol. (Lond.)*, **438**, 34.
Sanes, J.N., Suner, S. & Donoghue, J.P. (1990) Dynamic organization of primary motor cortex output to target muscles in adult rats. I. Long-term pattern of reorganization following motor or mixed peripheral nerve lesion. *Exp. Brain Res.*, **79**, 479–491.
Shon, Y.H., Jung, H.Y., Kaelin-Lang, A. & Hallett, M. (2003) Excitability of the ipsilateral motor cortex during phasic voluntary hand movement. *Exp. Brain Res.*, **148**, 176–185.
Sievert, C.F. & Neafsey, E.J. (1986) A chronic unit study of the sensory properties of neurons in the forelimb areas of rat sensorimotor cortex. *Brain Res.*, **381**, 15–23.
Spidalieri, G. & Guandalini, P. (1983) Motor representation in the rostral portion of the cat corpus callosum as evidenced by microstimulation. *Exp. Brain Res.*, **53**, 59–70.
Steinberg, O., Donchin, O., Gribova, A., Cardosa de Oliveira, S., Bergman, H. & Vaadia, E. (2002) Neuronal populations in primary motor cortex encode bimanual arm movements. *Eur. J. Neurosci.*, **15**, 1371–1380.
Tanji, J., Okano, K. & Sato, K.C. (1988) Neuronal activity in cortical motor areas related to ipsilateral, contralateral, and bilateral digit movements of the monkey. *J. Neurophysiol.*, **60**, 325–343.
Teskey, G.C., Monfils, M.H., VandenBerg, P.M. & Kleim, J.A. (2002) Motor map expansion following repeated cortical and limbic seizures is related to synaptic potentiation. *Cerb. Cortex*, **12**, 98–105.
Ugawa, Y., Hanajima, R. & Kanazawa, I. (1993) Interhemispheric facilitation of the hand area of the human motor cortex. *Neurosci. Lett.*, **160**, 153–155.
Wassermann, E.M., Fuhr, P., Cohen, L.G. & Hallett, M. (1991) Effects of transcranial magnetic stimulation on ipsilateral muscles. *Neurology*, **41**, 1795–1799.
Wassermann, E.M., Pascual-Leone, A. & Hallett, M. (1994) Cortical motor representation of the ipsilateral hand and arm. *Exp. Brain Res.*, **100**, 121–132.
Yarosh, C.A., Hoffman, D.S. & Strick, P.L. (2004) Deficits in movements of the wrist ipsilateral to a stroke in hemiparetic subjects. *J. Neurophysiol.*, **92**, 3276–3285.
Ziemann, U., Ishii, K., Borghesi, A., Yaseen, Z., Battaglia, F., Hallett, M., Cincotta, M. & Wassermann, E.M. (1999) Dissociation of the pathways mediating ipsilateral and contralateral motor-evoked potentials in human hand and arm muscles. *J. Physiol.*, **581**, 895–906.

Neuropsychopharmacology (2009) 34, 341–355

www.neuropsychopharmacology.org

Nociceptin/Orphanin FQ Modulates Motor Behavior and Primary Motor Cortex Output Through Receptors Located in Substantia Nigra Reticulata

Matteo Marti[1,3,5], Riccardo Viaro[1,2,3,5], Remo Guerrini[3,4], Gianfranco Franchi[2,3] and Michele Morari*[,1,3]

[1]Department of Experimental and Clinical Medicine, Section of Pharmacology, University of Ferrara, Ferrara, Italy; [2]Department of Biomedical Sciences and Advanced Therapies, Section of Human Physiology, University of Ferrara, Ferrara, Italy; [3]Center for Neuroscience and Istituto Nazionale di Neuroscienze, University of Ferrara, Ferrara, Italy; [4]Department of Pharmaceutical Sciences and Biotechnology Center; University of Ferrara, Ferrara, Italy

This study was set to investigate whether motor effects of nociceptin/orphanin FQ (N/OFQ) can be related to changes in primary motor cortex output. N/OFQ injected i.c.v. biphasically modulated motor performance, low doses being facilitating and higher ones inhibitory. These effects were counteracted by the N/OFQ receptor antagonist [Nphe[1] Arg[14],Lys[15]]N/OFQ-NH_2 (UFP-101) confirming the specificity of N/OFQ action. However, UFP-101 alone facilitated motor performance, suggesting that endogenous N/OFQ inhibits motor function. N/OFQ and UFP-101 injected into the substantia nigra reticulata but not motor cortex replicated these effects, suggesting motor responses were mediated by subcortical circuits involving the basal ganglia. Intracortical microstimulation technique showed that i.c.v. N/OFQ also biphasically modulated motor cortex excitability and movement representation. Low N/OFQ doses caused a leftward shift of threshold distribution curve in the forelimb area without affecting the number of effective sites. Conversely, high N/OFQ doses increased unresponsive and reduced excitable (movement) sites in vibrissa but not forelimb area. However, increased threshold currents and rightward shift of threshold distribution curve were observed in both areas, suggesting an overall inhibitory effect on cortical motor output. UFP-101 alone evoked effects similar to low N/OFQ doses, suggesting tonic inhibitory control over forelimb movement by endogenous N/OFQ. As shown in behavioral experiments, these effects were replicated by intranigral, but not intracortical, N/OFQ or UFP-101 injections. We conclude that N/OFQ receptors located in the substantia nigra reticulata mediate N/OFQ biphasic control over motor behavior, possibly through changes of primary motor cortex output.
Neuropsychopharmacology (2009) **34,** 341–355; doi:10.1038/npp.2008.56; published online 16 April 2008

Keywords: bar test; drag test; intracortical microstimulation; rotarod test; speed test; UFP-101

INTRODUCTION

Nociceptin/orphanin FQ (N/OFQ) is an endogenous neuropeptide that activates a G-protein-coupled receptor termed NOP. NOP receptors are widely represented in cortical and subcortical motor areas (Darland *et al*, 1998; Neal *et al*, 1999) and are involved in motor control. Both NOP receptor stimulation and blockade affects motor function. In particular, i.c.v. injections of N/OFQ or systemic administration of Ro 64–6198 (a synthetic NOP receptor agonist) facilitated spontaneous locomotion at low doses (Florin *et al*, 1996; Jenck *et al*, 1997; Higgins *et al*, 2001; Kuzmin *et al*, 2004) and inhibited it at higher ones (Reinscheid *et al*, 1995; Devine *et al*, 1996; Rizzi *et al*, 2001; Higgins *et al*, 2001; Kuzmin *et al*, 2004). NOP receptor agonists also inhibited exercise-induced locomotion (as in the rotarod test) although in a monophasic way (Jenck *et al*, 2000; Higgins *et al*, 2001; Marti *et al*, 2004a). In contrast, pharmacological blockade (or genetic deletion) of the NOP receptor did not affect spontaneous locomotion but increased exercise-induced motor activity (Marti *et al*, 2004a). Therefore, it has been proposed that endogenous N/OFQ acts as a physiological constraint of motor function, being its action more relevant under conditions of motor activation rather than at rest (Marti *et al*, 2004a). The neurobiological substrate(s) underlying motor actions of exogenous and endogenous N/OFQ have been investigated. The N/OFQ-induced hypolocomotion has been related to inhibition of mesencephalic mesoaccumbal (Murphy and Maidment, 1999) and/or nigrostriatal (Marti *et al*, 2004a) DA neurons. Consistently, injections of the NOP receptor

*Correspondence: Professor M Morari, Department of Experimental and Clinical Medicine, Section of Pharmacology, University of Ferrara, via Fossato di Mortara 17–19, Ferrara 44100, Italy, Tel: +39 0532 455210, Fax: +39 0532 455205, E-mail: m.morari@unife.it
[5]These authors contributed equally to this work.
Received 15 January 2008; revised 11 March 2008; accepted 12 March 2008

antagonist [Nphe^1 Arg^{14},Lys^{15}]N/OFQ-NH$_2$ (UFP-101) in substantia nigra reticulata (SNr) elevated rotarod performance and striatal DA release (Marti *et al*, 2004a). Evidence that also the hyperlocomotive response induced by i.c.v. N/OFQ is DA-dependent has been presented (Florin *et al*, 1996; Kuzmin *et al*, 2004), although the area involved has not been identified. Endogenous N/OFQ, however, appears to cause motor depressant responses also via non-DAergic mechanisms. Indeed, SNr injections of UFP-101 or systemic administration of 1-[(3R,4R)-1-cyclooctylmethyl-3-hydroxymethyl-4-piperidyl]-3-ethyl-1,3-dihydro-2H benzimidazol-2-one (J-113397) improved motor performance not only in naive but also DA-depleted (6-OHDA hemilesioned) or haloperidol-treated rats (Marti *et al*, 2004b, 2005). In particular, the antiakinetic effect of J-113397 in 6-OHDA hemilesioned rats was associated with reduction of nigrothalamic GABAergic transmission and, possibly, thalamic disinhibition (Marti *et al*, 2007). SNr is the major output nucleus of the basal ganglia. It conveys the motor information generated in the cerebral cortex and processed in the striatum to the thalamus and then back to the motor cortex, forming a functional loop which regulates movement initiation and execution (ie the so-called 'cortico-basal ganglia-thalamo-cortical' loop; Albin *et al*, 1989; Alexander and Crutcher, 1990). On this basis, pharmacological treatments (Marti *et al*, 2004b) or pathological conditions (Marti *et al*, 2005) that alter N/OFQergic transmission in SNr are likely to interfere with the activity of the 'cortico-basal ganglia-thalamo-cortical' loop and, as a consequence, with processing of motor information at the cortical level.

The present study was therefore undertaken to test whether changes in motor behavior produced by activation of central NOP receptors could be associated with changes in motor cortex output. Motor activity has been evaluated in awake rats by means of a battery of behavioral tests involving different motor parameters (ie time to initiate and execute a movement, coordination, and equilibrium). Primary motor cortex (M1) excitability and movement representation (defining motor output) has been investigated in anesthetized rats by intracortical microstimulation (ICMS). This technique allows to excite corticofugal neurons and produce repetitive neuronal discharges, which result in the summation of excitatory synaptic potentials in motoneurons and muscle activity. The role of central NOP receptors in modulation of motor behavior and M1 output has been investigated first by injecting N/OFQ in lateral cerebral ventricle (LCV). UFP-101 has been used to test the specificity of the N/OFQ action and to investigate the influence of endogenous N/OFQ. Finally, the role exerted by NOP receptors located in M1 and SNr has been elucidated by intracortical (layer V) or intranigral injections of N/OFQ and UFP-101.

MATERIALS AND METHODS

Male Sprague–Dawley rats (300–350 g; Stefano Morini, Reggio Emilia, Italy) were kept under regular lighting conditions (12 h light/dark cycle) and given food and water *ad libitum*. The experimental protocols performed in the present study were approved by Ethical Committee of the University of Ferrara and adequate measures were taken to minimize animal pain and discomfort.

Microinjection Technique

A guide cannula (outer diameter 0.55 mm, inner diameter 0.35 mm) was stereotaxically implanted under isoflurane anesthesia (1.4% in air delivered at 1.2 ml/min) 1 mm above the right or left LCV, M1 or SNr, according to the following coordinates from bregma: LCV, AP −0.9, ML ± 1.4, VD −2; M1, AP + 2, ML ± 2, VD −0.5; SNr, AP −5.5, ML ± 2.2, VD −7.3; nose bar positioned at −2.5 (Paxinos and Watson, 1982). The cannula was secured to the skull by acrylic dental cement and metallic screws. A stainless steel obturator (outer diameter 0.30 mm) was left in place inside the guide. After a 7-day recovery period, each rat was opportunely handled and trained before behavioral tests. The day of the experiment, the obturator was removed and saline or pharmacological treatments were injected (volume 0.5 μl) through a stainless-steel injector (outer diameter 0.30 mm; inner diameter 0.15 mm) protruding 1 mm from the cannula tip. At the end of each experiment the placement of the probes was verified by microscopic examination and the rats in which the probes were not correctly positioned were discarded from the study.

Behavioral Studies

Different behavioral tests were used to collect complementary information on different motor parameters in rats.

Bar test. Originally developed to quantify morphine-induced catalepsy (Kuschinsky and Hornykiewicz, 1972), this test measures the ability of the rat to respond to an externally imposed static posture. Also known as the catalepsy test (for a review see Sanberg *et al*, 1988), it can be used to quantify akinesia (ie time to initiate a movement) also under conditions that are not characterized by increased muscle tone (ie rigidity) as in the cataleptic/catatonic state. The rat was placed gently on a table and forepaws were placed alternatively on blocks of increasing heights (3, 6 and 9 cm). The time (in sec) that each paw spent on the block (ie the immobility time) was recorded (cutoff time of 20 s). Akinesia was calculated as total time spent on the different blocks.

Drag test. Modification of the 'wheelbarrow test' (Schallert *et al*, 1979), this test measures the ability of the rat to balance its body posture with forelimbs in response to an externally imposed dynamic stimulus (backward dragging; Marti *et al*, 2005). It gives information regarding the time to initiate and execute (bradykinesia) a movement. The rat was gently handled from the tail leaving the forepaws on the table, and was dragged backwards at a constant speed (about 20 cm/s) for a fixed distance (100 cm). The number of steps made by each paw were recorded. Five to seven determinations were collected for each rat.

Speed test. These tests essentially measure rat speed in an open field. The rat was allowed to habituate in a square arena (150 × 150 cm) for 5 min then elevated 3 cm about the ground (by holding its tail) and finally positioned in the centre of the arena. When the animal touched the floor it started running. Behavior was scored online using the 'correct walking' criteria (see Bouwman *et al*, 2005). Data

acquisition was stopped when the rat changed its acceleration, velocity or direction. Run speed was calculated as distance traveled (cm/s).

Rotarod test. The fixed-speed rotarod test (Rozas *et al*, 1997) measures different motor parameters such as motor coordination, gait ability, balance, muscle tone and motivation to run. It was employed according to a previously described protocol (Marti *et al*, 2004a) which allowed to detect both facilitating and inhibitory drug effects. Briefly, rats were tested in a control session at 4 increasing speeds (30, 35, 40 and 45 r.p.m.; 180 s each), causing a progressive decrement of performance to ~40% of the maximal response (ie the experimental cutoff time). Other two sessions were repeated 10 and 60 min after drug injection, and drug effect expressed as percent of control performance (total time spent on the rod).

Since pharmacological treatment may induce turning in rats, rotational behavior was measured after saline, N/OFQ or UFP-101 treatment. Rats were left to habituate in circular bowls for 20 min before the beginning of the test. Contralateral or ipsilateral turns (ie turns in the same or opposite direction to the injection side) were counted every 5 min, from 15 min before to 90 min after injection.

ICMS

Anesthesia was induced by ketamine hydrochloride (50 mg/kg i.p.) and maintained by supplementary ketamine injections (i.m.) throughout the experiment, such that long-latency, sluggish hindlimb withdrawal was achieved with severe pinching of the hind-foot. The body temperature was maintained at 36–38°C with a heat lamp. The animal was placed in a Kopf stereotaxic apparatus and a large craniotomy was performed over the frontal cortex of one side. The dura remained intact, and was kept moist with a 0.9% saline solution. Drug injections (0.01 or 10 nmol N/OFQ, 10 nmol UFP-101, dissolved in 0.5 μl of saline) were performed in the left or right LCV (AP = −0.8 mm; ML = ± 1.5 mm; VD = −3.5 mm below the pial surface), layer V of central M1 (AP = 2–3 mm and ML = 2.5–3 mm; VD = −1.5 mm) and SNr (AP = −5.5 mm; ML = ± 2.2 mm; VD = −7.6 mm). Drugs were slowly injected and, to prevent the substance from refluxing, the needle was withdrawn from the cortex 120 s later.

In each animal, the movements evoked by ICMS in the frontal agranular cortex were mapped starting 10 min after injection. When drugs were injected in LCV and SNr, the mapping procedure was similar to that described by Donoghue and Wise (1982) and detailed elsewhere (Franchi, 2000a). Briefly, the electrode penetrations were regularly spaced out over a 500 μm grid. Glass-insulated tungsten microelectrodes (0.6–1.2 MΩ impedance at 1 kHz), were used for stimulation. The electrode was lowered perpendicularly to the cortical surface down to layer V of the frontal agranular cortex (−1.5 mm; Franchi, 2000a). Monophasic cathodal pulses (200 μs duration, 30 ms trains at 300 Hz) of a maximum of 60 μA were passed through the electrode with a minimum interval of 2.5 s. Two observers were required for movement detection and threshold determination. Starting with a current of 60 μA, intensity was decreased in 5 μA steps until the movement was no longer evoked; then the intensity was increased to a level at which ~50% of the stimulation elicited movement. This level defined current threshold. If no movements or twitches were evoked with 60 μA, the site was recorded as negative. When a movement was observed in two or more body parts, current thresholds were determined for each component. Body parts activated by ICMS were identified by visual inspection and/or muscle palpation. The terms 'forelimb movement' and 'hindlimb movement' refer collectively to proximal and distal joint movements. When drugs were injected in M1 the procedure was as above, but electrode penetrations were orthogonally spaced out over 200, 400 and 800 μm from injection site. Although the direct current spread is confined to 250 μm from the stimulating electrode, the current can transynaptically activate a wider area of cortex (Jankowska *et al*, 1975). Then, the ICMS applied at different distances to the site of injection ensures a thorough analysis of drug effect. For each set of experiments (injections in LCV, M1, SNr) appropriate controls were run in parallel: five rats were mapped with the cortex untouched (control group) and the other five received a 0.5 μl injection of saline on the correspondent site (sham group).

At the end of the experimental procedures, animals were perfused transcardially with saline and then with 4% paraformaldehyde solution. Brains were removed, post-fixed, sectioned coronally into 50 μm thick slices and then stained with thionine to verify needle and microelectrode positions.

Data Presentation and Statistical Analysis

Motor performance in the bar, drag and speed tests was expressed in absolute values (sec, number of steps, cm/s, respectively) whereas motor performance in the rotarod test as percentage ± SEM of the control session. Statistical analysis was performed by one-way repeated measure (RM) ANOVA followed by contrast analysis to determine group differences. In case a significant time × treatment interaction was found, the sequentially rejective Bonferroni test was used to determine specific differences (ie at the single time-point level) between groups. Drug interaction was studied experimentally according to a 2 × 2 factorial design and data analyzed with conventional two-way ANOVA, factor one being N/OFQ and factor two UFP-101. ICMS data were presented as mean ± SEM. Inter-group comparisons were determined using one-way ANOVA and χ^2 test presented in a two-way contingency table (2 × 2). *P*-values <0.05 were considered to be statistically significant.

Drugs

N/OFQ and UFP-101 were prepared at the University of Ferrara, as previously described (Guerrini *et al*, 2000).

RESULTS

Behavioral Studies

I.c.v. injections of nop receptor ligands. To investigate the role of central NOP receptors in modulation of motor activity, N/OFQ was injected i.c.v. (in LCV). UFP-101 was also administered to test the specificity of N/OFQ action and

to investigate the role of endogenous N/OFQ. Saline injections did not affect motor activity. Indeed, immobility time, number of steps, speed and rotarod performance were similar in saline-injected (0.6 ± 0.2 s, 13.2 ± 0.3, 67.4 ± 2.1 cm/s and 1021 ± 27 s, respectively) and control (0.8 ± 0.3 s, 12.9 ± 0.8, 68.6 ± 6.3 cm/s and 1064 ± 18 s, respectively) rats. As i.c.v. injection of saline, N/OFQ and UFP-101 did not induce forepaw motor asymmetry, results obtained at the contralateral and the ipsilateral forepaw in the bar and drag test were pooled together.

N/OFQ.

(i) *Bar test:* RM ANOVA on the immobility time in the bar test (Figure 1a) showed a significant effect of treatment ($F_{4,28} = 503.91$, $p < 0.0001$) time ($F_{1,4} = 24.85$, $p < 0.0001$) and a significant time × treatment interaction ($F_{4,29} = 11.86$, $p < 0.0001$). *Post hoc* analysis revealed that 0.1 nmol N/OFQ evoked a modest and transient elevation of immobility time (ie caused akinesia) compared to saline while 1 and 10 nmol N/OFQ evoked a more robust and prolonged response, detectable 60 min after injection. No change in immobility time was elicited by 0.01 nmol N/OFQ.

(ii) Drag test: RM ANOVA on the number of steps in the drag test (Figure 1b) showed a significant effect of treatment ($F_{4,28} = 102.07$, $p < 0.0001$), time ($F_{1,4} = 59.13$, $p < 0.0001$) and a significant time × treatment interaction ($F_{4,29} = 23.60$, $p < 0.0001$). *Post hoc* analysis revealed that N/OFQ evoked a biphasic response, namely facilitation at 0.01 nmol and inhibition at higher doses (0.1–10 nmol). Both facilitation and inhibition were detected after 60 min.

(iii) *Speed test:* RM ANOVA on speed values (Figure 1c) showed a significant effect of treatment ($F_{4,28} = 182.51$, $p < 0.0001$), time ($F_{1,4} = 7.15$, $p = 0.012$) and a significant time × treatment interaction ($F_{4,29} = 5.18$, $p = 0.002$). *Post hoc* analysis revealed that, as in the drag test, N/OFQ evoked a biphasic response, improving speed at 0.01 nmol and inhibiting it at higher doses (0.1–10 nmol). Both effects were long-lasting.

(iv) *Rotarod test:* RM ANOVA on rotarod values (Figure 1d) showed a significant effect of treatment ($F_{4,28} = 4980.92$, $p < 0.0001$) but not time ($F_{1,4} = 0.005$, $p = 0.94$) and a non significant time × treatment interaction ($F_{4,29} = 0.61$, $p = 0.66$). *Post hoc* analysis revealed that N/OFQ improved rotarod performance at 0.01 nmol and impaired it at higher doses.

UFP-101.

(i) *Bar test:* RM ANOVA showed a significant effect of treatment ($F_{3,18} = 8.94$, $p = 0.0007$), time ($F_{1,3} = 6.96$, $p = 0.014$) and a non significant time × treatment interaction ($F_{3,24} = 0.94$, $p = 0.43$). UFP-101 caused a reduction of immobility time at 10 nmol (Figure 1e).

(ii) *Drag test*: RM ANOVA showed a significant effect of treatment ($F_{3,18} = 69.29$, $p < 0.0001$) but not time

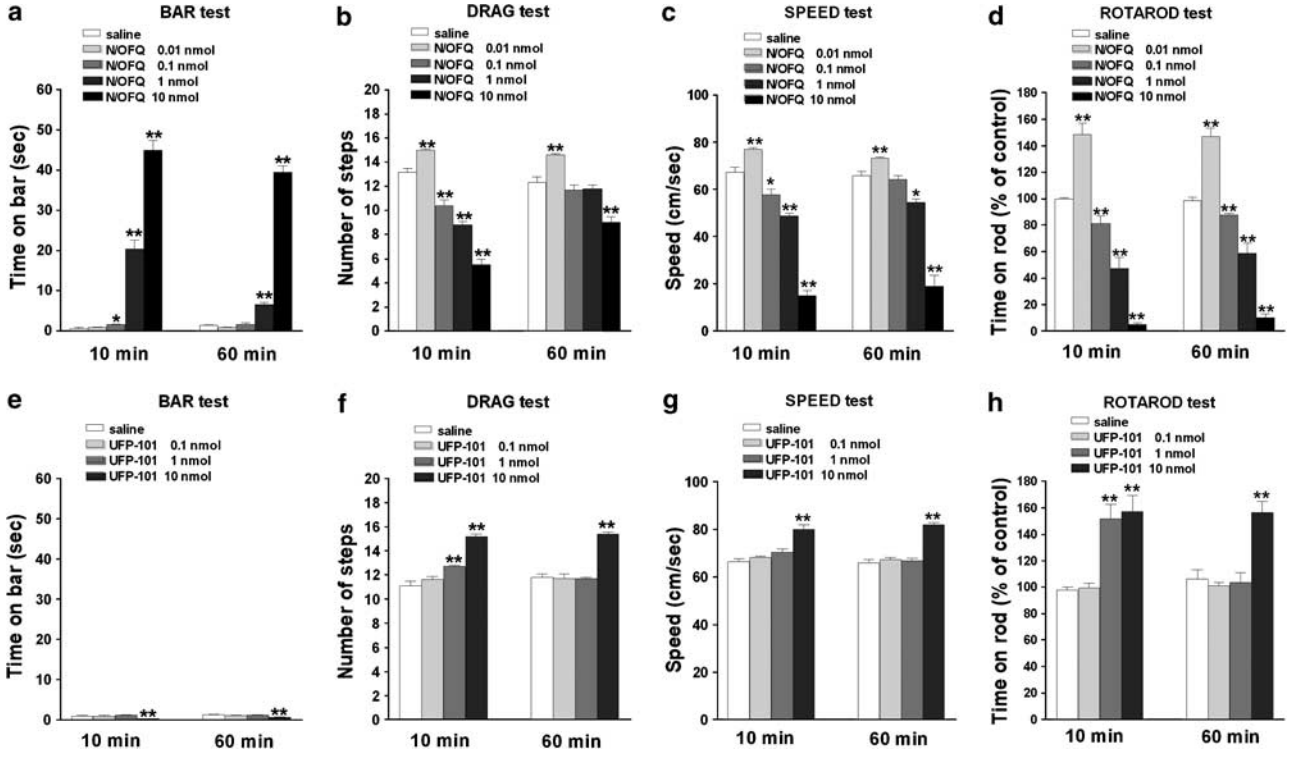

Figure 1 Effect of i.c.v. injection of N/OFQ or UFP-101 on motor activity. N/OFQ (0.01–10 nmol) or UFP-101 (0.1–10 nmol) were injected in the lateral cerebral ventricle and motor activity evaluated in the bar (panels a, e), drag (panels b, f), speed (panels c, g) and rotarod (panels d, h) tests. Each experiment consisted of three different sessions: a control session followed by other two sessions performed 10 and 60 min after saline, N/OFQ or UFP-101 injection (see Materials and Methods). In the bar, drag and speed test data are expressed as absolute values (sec, steps, and cm/s, respectively) whereas in the rotarod test as percentages of motor activity in the control session. Data are means ± SEM of 7–9 determinations per group. $^{*}p < 0.05$ and $^{**}p < 0.01$ significantly different from saline.

($F_{1,3} = 0.01$, $p = 0.93$) and a significant time × treatment interaction ($F_{3,24} = 4.69$, $p = 0.01$). UFP-101 elevated the number of steps at 10 nmol (Figure 1f). The effect of 10 nmol UFP-110 was also detected 60 min after injection.

(iii) *Speed test:* RM ANOVA showed a significant effect of treatment ($F_{3,18} = 81.03$, $p < 0.0001$), but not time ($F_{1,3} = 0.69$, $p = 0.41$) and a non significant time-treatment interaction ($F_{3,24} = 1.63$, $p = 0.20$). UFP-101 induced long-lasting increase in speed at 10 nmol (Figure 1g).

(iv) *Rotarod test:* RM ANOVA showed a significant effect of treatment ($F_{3,18} = 18.70$, $p < 0.0001$), time ($F_{1,3} = 4.80$, $p = 0.022$) and a significant time × treatment interaction ($F_{3,24} = 11.71$, $p < 0.0001$). UFP-101 improved the rotarod performance at 1 and 10 nmol (Figure 1h). The effect of 1 nmol UFP-101 was transient whereas that produced by the higher dose was prolonged.

Co-injection of N/OFQ and UFP-101. To investigate the selectivity of N/OFQ action, co-injections of low and high N/OFQ and UFP-101 doses (1:10 ratio) were performed. We first tested the specificity of 0.01 nmol N/OFQ by challenging it with 0.1 nmol UFP-101 (Figure 2).

RM ANOVA in the drag test (Figure 2a), showed a significant effect of treatment ($F_{3,18} = 57.87$, $p < 0.0001$), but not time ($F_{1,3} = 1.15$, $p = 0.29$) and a non significant time × treatment interaction ($F_{3,24} = 0.04$, $p = 0.98$). N/OFQ elevated the number of steps and UFP-101, ineffective alone, prevented this effect. RM ANOVA on speed values (Figure 2b) revealed a significant effect of treatment ($F_{3,18} = 19.34$, $p < 0.0001$) and time ($F_{1,3} = 6.45$, $p = 0.017$) but not a significant interaction between the two ($F_{3,24} = 1.44$, $p = 0.25$). N/OFQ increased rat speed and UFP-101, ineffective alone, prevented this effect. RM ANOVA on rotarod values (Figure 2c) revealed a significant effect of treatment ($F_{3,18} = 66.09$, $p < 0.0001$), but not time ($F_{1,3} = 0.02$, $p = 0.88$) and a non significant time × treatment interaction ($F_{3,24} = 0.22$, $p = 0.87$). N/OFQ elevated rotarod performance while UFP-101, ineffective alone, prevented N/OFQ action.

We then tested the specificity of high N/OFQ doses by challenging 1 nmol N/OFQ with 10 nmol UFP-101 (Figure 3). RM ANOVA on the bar test (Figure 3a) revealed a significant effect of treatment ($F_{3,18} = 276.13$, $p < 0.0001$), time ($F_{1,3} = 27.19$, $p < 0.0001$) and a significant time × treatment interaction ($F_{3,24} = 34.45$, $p < 0.0001$). N/OFQ elevated immobility time while UFP-101, ineffective alone, prevented this effect. In the drag test (Figure 3b), a significant effect of treatment ($F_{3,18} = 107{,}13$, $p < 0.0001$), time ($F_{1,3} = 12.33$, $p < 0.0017$) and a significant time × treatment interaction ($F_{3,24} = 9.14$, $p = 0.0003$) were found. N/OFQ reduced the number of steps while UFP-101 increased it. The combination of the two was the sum of their effects, that is, no change with respect to saline-treated animals. In the speed test (Figure 3c), a significant effect of treatment ($F_{3,18} = 94.71$, $p < 0.0001$), but not time ($F_{1,3} = 1.47$, $p = 0.23$) and a non significant time × treatment interaction ($F_{3,24} = 1.77$, $p = 0.18$) were observed. N/OFQ reduced, whereas UFP-101 increased speed. Again, combination of the two caused no change in speed when compared to saline-treated animals. Finally, RM ANOVA on the rotarod (Figure 3d) showed a significant effect of treatment ($F_{3,18} = 164.02$, $p < 0.0001$), but not time ($F_{1,3} = 0.14$, $p = 0.70$) and a non significant time × treatment interaction ($F_{3,24} = 0.04$, $p = 0.97$). N/OFQ reduced rotarod performance and UFP-101 improved it. Co-application of N/OFQ and UFP-101 caused a slight increase in performance compared to saline-treated rats.

Turning behavior: LCV injection of N/OFQ or UFP-101 did not induce turning behavior in the range of doses tested.

M1 injections of NOP receptor ligands. To investigate the localization of NOP receptors involved in motor actions elicited by i.c.v. N/OFQ and UFP-101, intracortical injec-

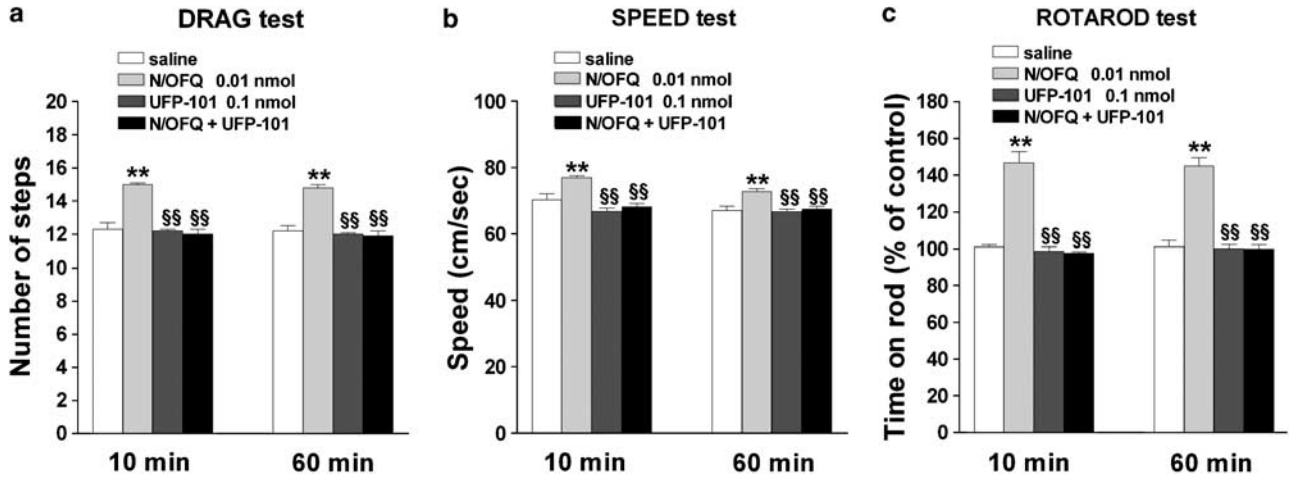

Figure 2 Effect of i.c.v. co-injection of low doses of N/OFQ and UFP-101 on motor activity. N/OFQ (0.01 nmol) and UFP-101 (0.1 nmol) were co-injected in the lateral cerebral ventricle and motor activity evaluated in the drag (panel a), speed (panel b) and rotarod (panel c) test. Each experiment consisted of three different sessions: a control session followed by other two sessions performed 10 and 60 min after saline, N/OFQ or UFP-101 injection (see Materials and Methods). In the drag and speed test data are expressed as absolute values (steps, and cm/s, respectively) whereas in the rotarod test as percentages of motor activity in the control session. Data are means ± SEM of seven determinations per group. $^{**}p < 0.01$ significantly different from saline. $^{\S\S}p < 0.01$ significantly different from N/OFQ.

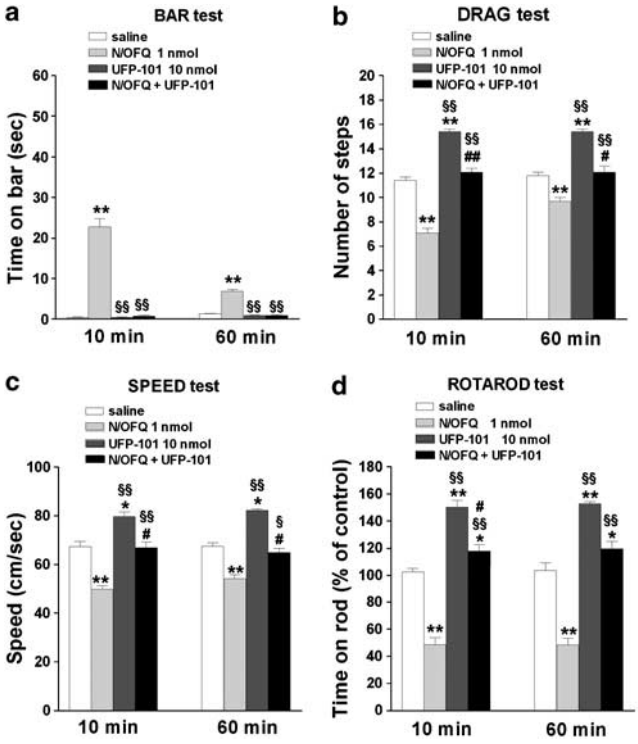

Figure 3 Effect of i.c.v. co-injection of high doses of N/OFQ and UFP-101 on motor activity. N/OFQ (1 nmol) and UFP-101 (10 nmol) were co-injected in the lateral cerebral ventricle and motor activity evaluated in the bar (panel a), drag (panel b), speed (panel c) and rotarod (panel d) test. Each experiment consisted of three different sessions: a control session followed by other two sessions performed 10 and 60 min after saline or UFP-101 injection (see Materials and Methods). In the bar, drag and speed test data are expressed as absolute values (sec, steps, and cm/s, respectively) whereas in the rotarod test as percentages of motor activity in the first session. Data are means ± SEM of seven determinations per group. $^{*}p<0.05$, $^{**}p<0.01$ significantly different from saline. $^{\S}p<0.05$, $^{\S\S}p<0.01$ significantly different from N/OFQ. $^{\#}p<0.05$, $^{\#\#}p<0.01$ significantly different from UFP-101.

tions (layer V of M1) were first made. Saline, N/OFQ (0.01–10 nmol) or UFP-101 (10 nmol) failed to affect rat performance in the bar, drag, speed and rotarod test (Figure S1).

SNr injections of nop receptor ligands. On the basis of our previous finding that NOP receptors located in the SNr modulate rotarod performance in rats (Marti *et al*, 2004a) we investigated whether motor effects induced by i.c.v. N/OFQ and UFP-101 could be reproduced by SNr injections. Since injections were made unilaterally, motor activity was evaluated separately at the ipsilateral and contralateral paw.

N/OFQ.

(i) *Bar test:* Saline did not affect the immobility time at the contralateral (0.9 ± 0.3 s) and ipsilateral (1.0 ± 0.3 s) forepaw compared to control rats (1.1 ± 0.3 s). RM ANOVA on the immobility time at the contralateral paw in the bar test (Figure 4a and b) showed a significant effect of treatment ($F_{4,24} = 80.13$, $p<0.0001$), time ($F_{1,4} = 11.36$, $p = 0.002$) and a significant time × treatment interaction ($F_{4,30} = 3.36$, $p = 0.021$). N/OFQ increased the immobility time dose-dependently and in a prolonged way, being active yet at 0.1 nmol. Qualitatively similar data were obtained at the ipsilateral paw.

(ii) *Drag test:* Saline did not modify the number of steps made by the contralateral (11.9 ± 0.4) and ipsilateral (12.3 ± 0.6) paw compared to control (11.6 ± 0.5) rats. In the drag test (Figure 4c and d), RM ANOVA at the contralateral paw disclosed a significant effect of treatment ($F_{4,24} = 92.03$, $p<0.0001$), time ($F_{1,4} = 11.77$, $p = 0.0017$) and a significant time × treatment interaction ($F_{4,30} = 5.16$, $p = 0.0027$). N/OFQ elevated the number of steps at 0.01 nmol but reduced them in the 0.1–10 nmol range. Conversely, RM ANOVA at the ipsilateral paw showed a significant effect of treatment ($F_{4,24} = 26.35$, $p<0.0001$), but not time ($F_{1,4} = 0.27$, $p = 0.60$) and a non significant time × treatment interaction ($F_{4,30} = 0.48$, $p = 0.88$). N/OFQ dose-dependently reduced the number of steps, the threshold inhibitory dose being 1 nmol.

(iii) *Speed test:* Saline did not affect rat speed (66.7 ± 1.1 and 68.6 ± 6.3 cm/s, respectively, for the saline-treated and control rats). Analysis of speed values (Figure 4e) revealed a significant effect of treatment ($F_{4,24} = 136.15$, $p<0.0001$), time ($F_{1,4} = 6.35$, $p = 0.017$) and a significant time × treatment interaction ($F_{4,30} = 12.37$, $p<0.0001$). N/OFQ biphasically modulated rat speed, low doses (0.01 nmol) being facilitatory and higher ones (0.1–10 nmol) inhibitory.

UFP-101.

(i) *Bar test:* RM ANOVA on the immobility time did not reveal significant effects of UFP-101 at the contralateral and ipsilateral paws (Figure S2).

(ii) *Drag test:* RM ANOVA at the contralateral paw (Figure 4f and g) revealed a significant effect of treatment ($F_{3,18} = 30.22$, $p<0.0001$) but not time ($F_{1,3} = 1.38$, $p = 0.25$) and a non significant time × treatment interaction ($F_{3,24} = 0.66$, $p = 0.58$). UFP-101 (1 and 10 nmol) elevated the number of steps at both 10 and 60 min post injection time. Conversely, RM ANOVA did not reveal any effect of UFP-101 on stepping activity at the ipsilateral paw.

(iii) *Speed test*: RM ANOVA on speed values (Figure 4h) showed a significant effect of treatment ($F_{3,18} = 58.87$, $p<0.0001$), but not time ($F_{1,4} = 0.48$, $p = 0.49$) and a non significant time × treatment interaction ($F_{4,30} = 0.95$, $p = 0.43$). UFP-101 (1 and 10 nmol) consistently elevated speed at 10 and 60 min after injection.

Co-injection of N/OFQ and UFP-101. To investigate the selectivity of N/OFQ action in SNr, co-injections of low and high N/OFQ and UFP-101 doses (1:10 ratio) were performed (Figure 5).

In the drag test (Figure 5a), conventional two-way ANOVA showed a main effect of N/OFQ ($F_{1,24} = 14.72$, $p = 0.0008$), UFP-101 ($F_{1,24} = 22.00$, $p = 0.0001$) and a significant N/OFQ × UFP-101 interaction ($F_{1,24} = 11.63$, $p = 0.0023$). N/OFQ (0.01 nmol) elevated the number of steps and UFP-101 (0.1 nmol), ineffective alone, prevented this increase. Likewise, in the speed test (Figure 5b),

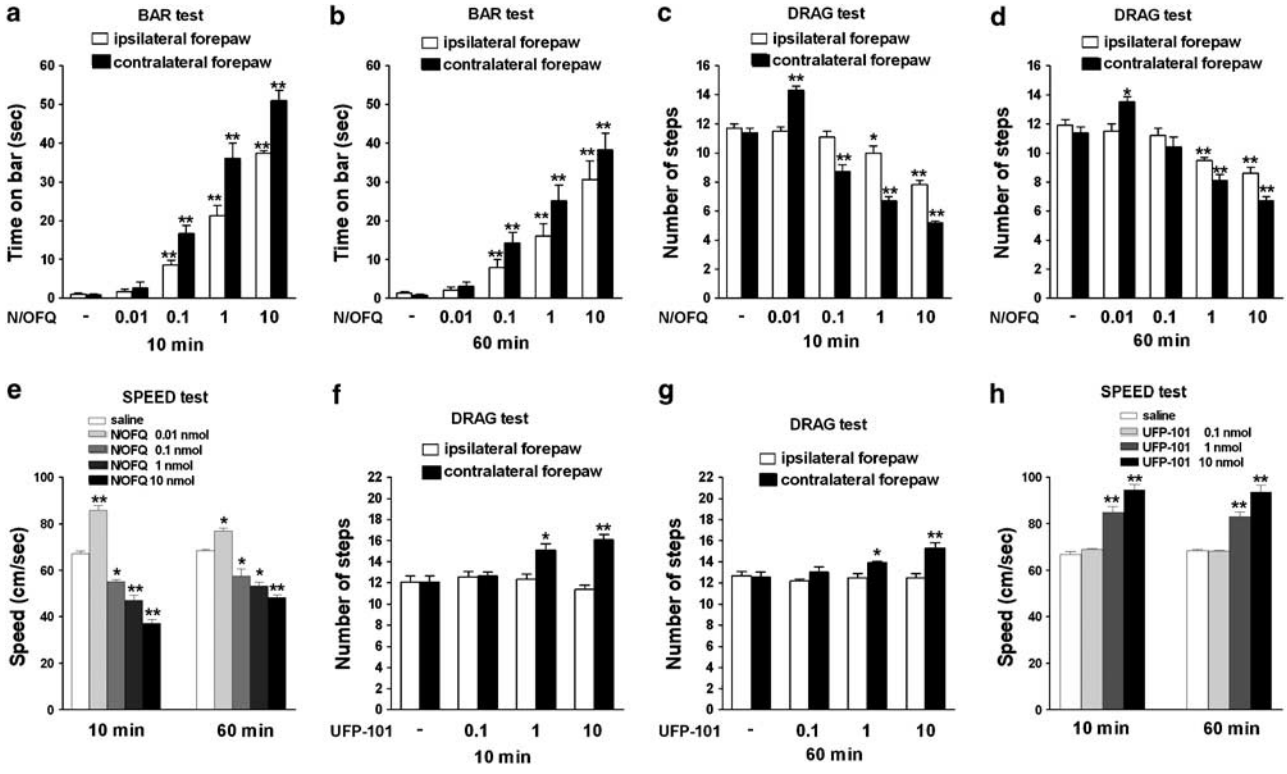

Figure 4 Effect of intranigral injections of N/OFQ or UFP-101 on motor activity. N/OFQ (0.01–10 nmol) or UFP-101 (0.1–10 nmol) were injected in SNr and motor activity evaluated in the bar (panels a–b), drag (panels c–d, f–g) and speed (panels e–h) test. Motor activity in the bar and drag test was evaluated separately at the paws ipsilateral and contralateral to the injection side. Motor activity in the speed test was calculated as distance traveled. Each experiment consisted of three different sessions: a control session followed by other two sessions performed 10 and 60 min after saline, N/OFQ or UFP-101 injection (see Materials and Methods). In the bar, drag and speed test data are expressed as absolute values (sec, steps, and cm/s, respectively) whereas in the rotarod test as percentages of motor activity in the control session. Data are means ± SEM of seven determinations per group. *$p<0.05$ and **$p<0.01$ significantly different from saline.

ANOVA showed a main effect of N/OFQ ($F_{1,24}=32.45$, $p<0.0001$), UFP-101 ($F_{1,24}=21.72$, $p<0.0001$) and a significant N/OFQ × UFP-101 interaction ($F_{1,24}=33.71$, $p<0.0001$). N/OFQ elevated rat speed, and UFP-101, ineffective alone, prevented its effect.

UFP-101 (10 nmol) was also challenged against N/OFQ (1 nmol). In the bar test (Figure 5c), ANOVA showed a main effect of N/OFQ ($F_{1,24}=82.79$, $p<0.0001$), UFP-101 ($F_{1,24}=83.78$, $p<0.0001$) and a significant N/OFQ × UFP-101 interaction ($F_{1,24}=80.45$, $p<0.0001$) at the contralateral paw. N/OFQ increased immobility time and UFP-101, ineffective alone, prevented this effect. Similar results were obtained at the ipsilateral paw. In the drag test (Figure 5d), ANOVA revealed a main effect of N/OFQ ($F_{1,24}=140.84$, $p<0.0001$), UFP-101 ($F_{1,24}=128.00$, $p<0.0001$) and a significant N/OFQ × UFP-101 interaction ($F_{1,24}=11.57$, $p=0.0023$) at the contralateral paw. N/OFQ reduced the number of steps, UFP-101 increased it and the combination of the two did not result in significant changes compared to saline-treated animals. At the ipsilateral paw, a main effect of N/OFQ ($F_{1,24}=7.91$, $p=0.0096$) but not UFP-101 ($F_{1,24}=1.01$, $p=0.32$) and a non significant N/OFQ × UFP-101 interaction ($F_{1,24}=2.59$, $p=0.12$) were found. N/OFQ reduced the number of steps and UFP-101, ineffective alone, prevented this effect. Finally, ANOVA on speed values (Figure 5e) showed a main effect of N/OFQ ($F_{1,24}=22.63$, $p<0.0001$), UFP-101 ($F_{1,24}=68.86$, $p=0.0001$) and a non significant N/OFQ × UFP-101 interaction ($F_{1,24}=4.03$, $p=0.056$). N/OFQ reduced speed, UFP-101 increased it and their combination resulted in a stimulation not different from that evoked by UFP-101 alone.

ICMS

Since NOP receptor stimulation or blockade affected motor activity, the hypothesis was tested that manipulation of central NOP receptors could change output from M1.

I.c.v. injections of NOP receptor ligands. Examination of M1 maps (examples are given in Figure 6) revealed several changes in movement representation in the 10 nmol N/OFQ group (Figure 6e). Contiguous unresponsive sites were consistently observed within M1 after i.c.v. injection of 10 nmol N/OFQ. To quantitatively assess these changes, the percentage of both unresponsive and responsive sites (movement sites in the vibrissa and forelimb areas) was calculated within the total site population (Figure 7a). ANOVA revealed changes in movement representation after injection of NOP receptor ligands ($F_{14,74}=10.45$, $p<0.0001$). N/OFQ 10 nmol doubled the percentage of unresponsive sites. This effect was associated with a significant decrease (~49%) in movement sites in the vibrissa representation and no change in excitable sites in

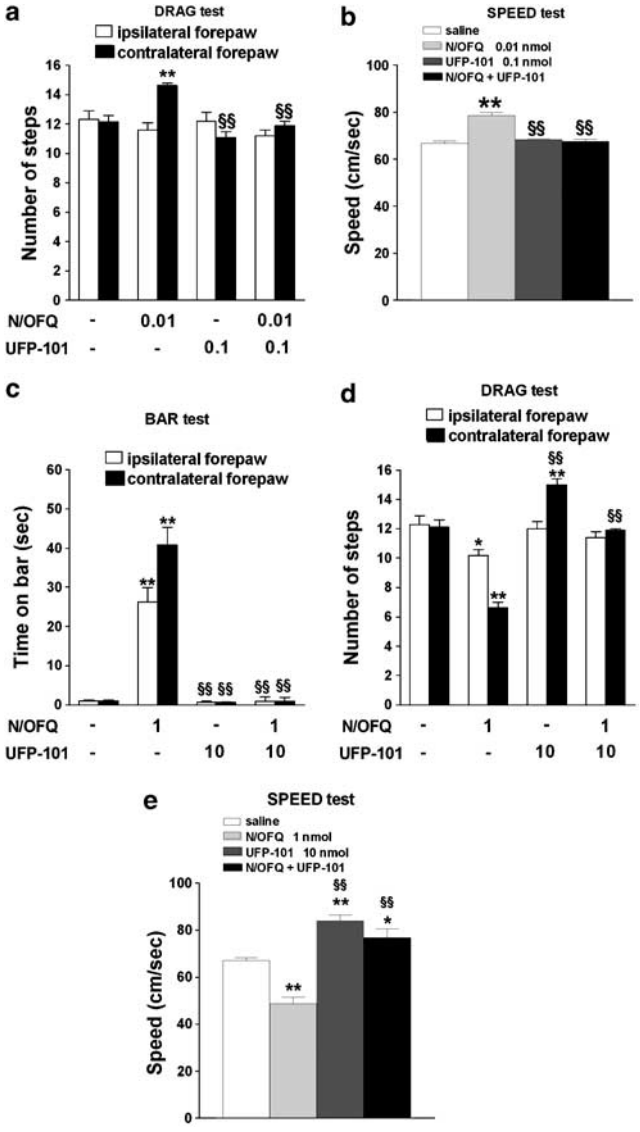

Figure 5 Effect of intranigral co-injection of N/OFQ and UFP-101 on motor activity. N/OFQ and UFP-101 were co-injected at low (0.01 and 0.1 nmol, respectively; panels a–b) and high (1 and 10 nmol, respectively; panels c–e) doses in substantia nigra pars reticulata (SNr) and motor activity evaluated, at 10 min post-injection time, in the drag (panel a, d), speed (panels b, e) and bar (panel c) test. Motor activity in the bar and drag test was evaluated separately at the paws ipsilateral and contralateral to the injection side. Motor activity in the speed test was calculated as distance traveled. In the bar, drag and speed test data are expressed as absolute values (sec, steps, and cm/s, respectively) and are means ± SEM of seven determinations per group. $^{*}p<0.05$, $^{**}p<0.01$ significantly different from saline. $^{\S\S}p<0.01$ significantly different from N/OFQ.

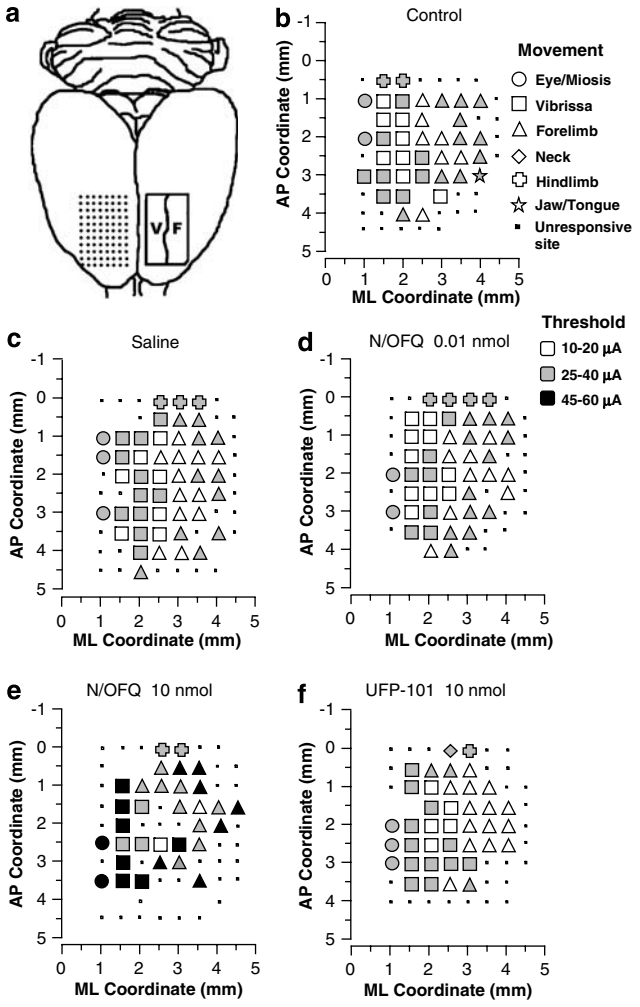

Figure 6 Effect of i.c.v. injection of N/OFQ and UFP-101 on primary motor cortex output. Representative primary motor cortex maps of movements evoked at threshold current levels in the vibrissa and forelimb areas. A schematic of rat brain showing vibrissa and forelimb areas (right) and reporting a coordinate grid (left) is represented (panel a). The maps relative to control rats (panel b) and rats injected with saline (panel c), N/OFQ (0.01 nmol; panel d), N/OFQ (10 nmol; panel e) and UFP-101 (10 nmol; panel f) in the lateral cerebral ventricle are also shown. The microelectrode was sequentially introduced to a depth of 1500 µm. Interpenetration distances were 500 µm. In these mapping schemes, frontal poles are at the bottom. Zero corresponds to bregma; numbers indicate rostral or caudal distance from the bregma or lateral distance from the midline. Movement evoked at one point is indicated by symbols and threshold range by the different grey scale. Absence of symbol (within or at the border of the maps) indicates that penetration was not performed due to presence of a large vessel. In panel e, the presence of dark symbols and unresponsive sites is worth noting.

forelimb representation. ANOVA revealed that NOP receptor ligands significantly affected movement thresholds ($F_{9,49}=31.40$, $p<0.0001$; Figure 7b). N/OFQ (10 nmol) increased threshold currents in both vibrissa and forelimb representations (~55 and ~47%, respectively) whereas both N/OFQ (0.01 nmol) and UFP-101 (10 nmol) reduced them (~17 and ~33%), although only in forelimb representation. The differences in excitability appeared in more detail by looking at the distribution of vibrissa and forelimb movement thresholds. N/OFQ (10 nmol) caused a significant increase in the percentage of those sites where higher currents were necessary to evoke vibrissa (Figure 7c; $\chi^2=59.37$ $p<0.01$) and forelimb (Figure 7d; $\chi^2=40.84$, $p<0.01$) movements (2×2, 35 µA as dividing point). Conversely, N/OFQ (0.01 nmol) and UFP-101 (10 nmol) did not change the distribution of thresholds in the vibrissa but caused a significant leftward shift of the distribution curve in the forelimb representation (N/OFQ 0.01 nmol: $\chi^2=21.26$, $p<0.01$; UFP-101 10 nmol: $\chi^2=41.67$ $p<0.01$, 2×2, 20 µA as a dividing point). In ~40% of sites, currents

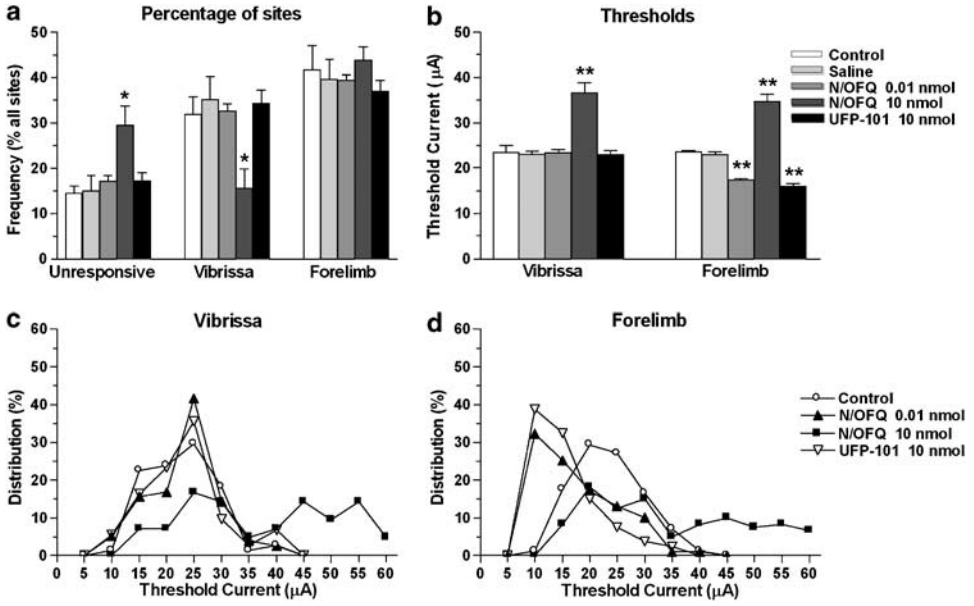

Figure 7 Effect of i.c.v. injection of N/OFQ and UFP-101 on primary motor cortex output. N/OFQ (0.01 and 10 nmol) and UFP-101 (10 nmol) were injected in the lateral cerebral ventricle, and the percentage of unresponsive and excitable sites in the vibrissa and forelimb areas (panel a) or average thresholds currents required to evoke vibrissa and forelimb movements (panel b) were measured. Threshold current distribution is also shown (panels c–d). The percentage of other movement sites (neck, jaw, eye and hindlimb) are not shown because these movements were not extensively explored. Note that N/OFQ (10 nmol) significantly shifted to the right both vibrissa and forelimb threshold distributions whereas N/OFQ (0.01 nmol) and UFP-101 (10 nmol) significantly shifted to the left the forelimb threshold distribution. Data are means ± SEM of five determinations per group. $^{*}p<0.05$, $^{**}p<0.01$ significantly different from control.

lower than 20 μA were usually necessary to evoke forelimb movement.

M1 injections of NOP receptor ligands. To investigate whether NOP receptors located in M1 modulated local excitability, injections of NOP receptor ligands in the layer V of M1 were made (examples are given in Figure 8). ANOVA on threshold currents considered as a whole or at each level away from the injection site (Figure S3) revealed no significant changes in all treated group compared to saline.

SNr injections of NOP receptor ligands. Intranigral injections of NOP receptor ligands were performed to investigate whether NOP receptors located in SNr affected motor excitability. ANOVA on M1 maps derived in SNr (representative examples given in Figure 9) revealed that NOP receptor ligands modulated the numbers of responsive and unresponsive sites ($F_{14,74}=12.09$, $p<0.0001$; Figure 10a). N/OFQ (10 nmol) was ineffective in the vibrissa area but increased (~121%) the number of unresponsive sites and simultaneously reduced (~60%) the number of excitable sites in the forelimb representation. ANOVA also revealed that NOP receptor ligands modulated threshold currents ($F_{9,49}=13.71$, $p<0.0001$; Figure 10b). N/OFQ (10 nmol) enhanced the mean threshold values in the vibrissa (~29%) and forelimb (~58%) areas. Moreover, UFP-101 (10 nmol) reduced (~44%) threshold currents selectively in the forelimb. A slight inhibition (~15%) was also observed with 0.01 nmol N/OFQ in the forelimb area, which however, did not reach the level of significance. Statistical analysis on threshold distribution showed that N/OFQ 10 nmol shifted to the right the distribution in both vibrissa (Figure 10c, $\chi^2=20.99$, $p<0.01$) and forelimb (Figure 10d, $\chi^2=53.27$, $p<0.01$) evoked-movement (2×2, 35 μA as a dividing point). Conversely, N/OFQ (0.01 nmol) and UFP-101 (10 nmol) caused a significant leftward shift in the threshold distribution in forelimb representation (N/OFQ 0.01 nmol $\chi^2=9.89$ $p<0.01$; UFP-101 10 nmol: $\chi^2=62.80$ $p<0.01$, 2×2, 20 μA as a dividing point).

DISCUSSION

Exogenous N/OFQ produced a dose-dependent, biphasic regulation of motor performance in rats. Inhibition was predominant since it was quantitatively larger and detected in a wider dose-range than facilitation. Conversely, UFP-101 monotonically facilitated motor activity suggesting an inhibitory role for endogenous N/OFQ in motor control. NOP receptor ligands produced changes in M1 output, which were consistent with their motor effects. Thus, exogenous N/OFQ biphasically regulated motor cortex excitability, low doses being facilitatory and higher ones inhibitory. Conversely, UFP-101 increased motor cortex excitability (in the forelimb area), suggesting that endogenous N/OFQ tonically inhibits forelimb movement. Both behavioral and electrophysiological effects were evoked by i.c.v. and intranigral, but not intracortical, drug injections, overall suggesting that subcortical NOP receptors regulate motor behavior and motor cortex output via modulation of cortical afferents.

Motor impairment has been consistently reported as one of the main biological effects induced by central NOP

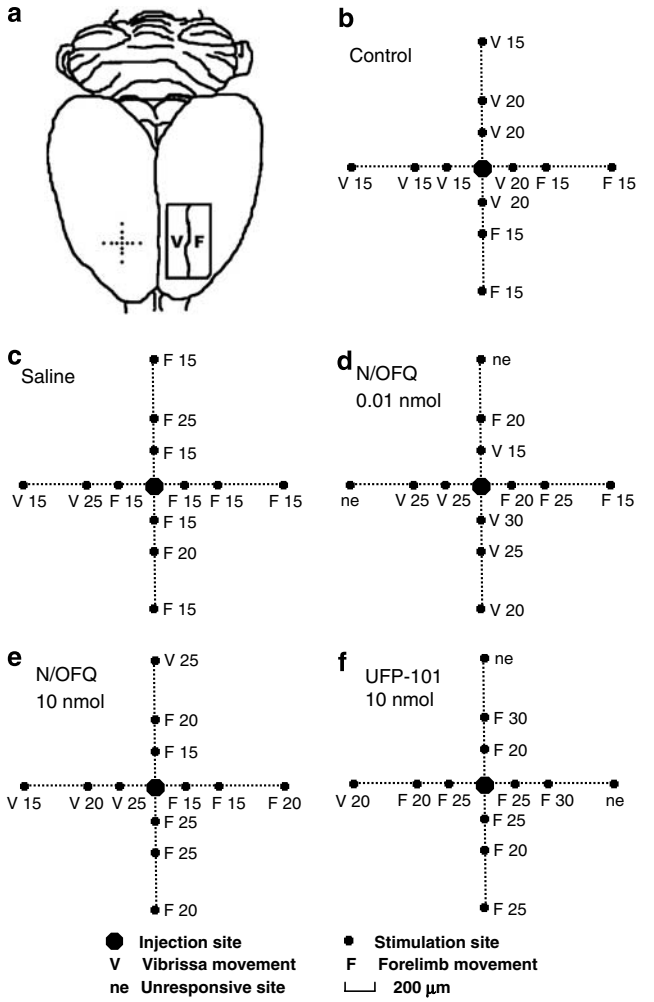

Figure 8 Intracortical injections of N/OFQ and UFP-101. Examples of cross-shaped grids showing injection and stimulation sites in control rats (panel b) or rats injected with saline (panel c), N/OFQ (0.01 and 10 nmol; panels d and e), and UFP-101 (10 nmol; panel f) in primary motor cortex. A schematic of rat brain showing vibrissa and forelimb areas (right) and reporting a coordinate grid (left) is also represented (panel a). For each stimulation site, a letter indicates the type of ICMS-evoked movement and the corresponding number the threshold current (in μA) required to evoke it. Note that threshold values in control and saline groups overlap with those of N/OFQ and UFP-101 groups.

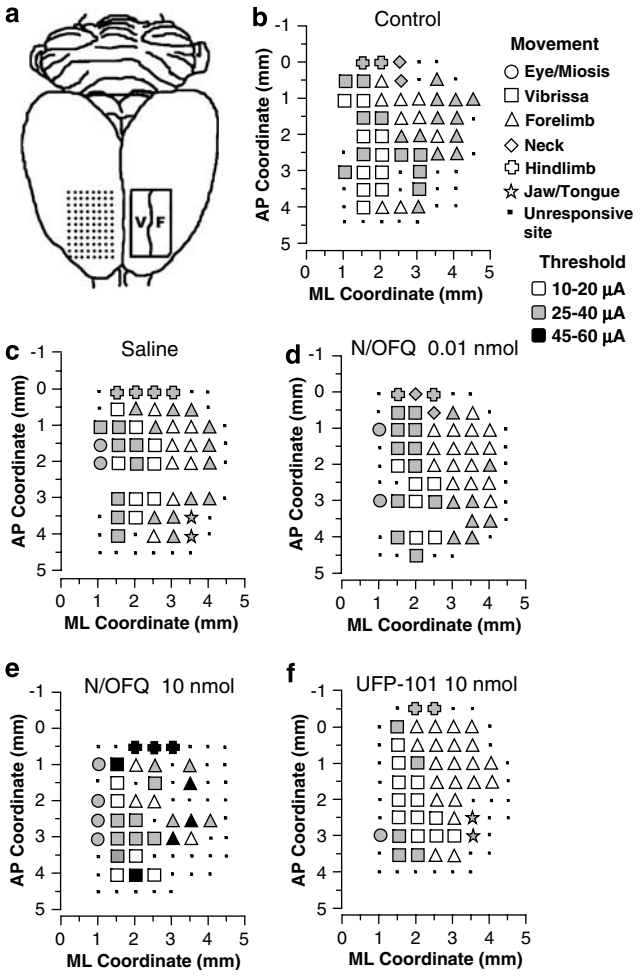

Figure 9 Effect of intranigral injection of N/OFQ and UFP-101 on primary motor cortex output. Representative primary motor cortex maps of movements evoked at threshold current levels in the vibrissa and forelimb areas. A schematic of rat brain showing vibrissa and forelimb areas (right) and reporting a coordinate grid (left) is represented (panel a). The maps relative to control rats (panel b) and rats injected with saline (panel c), N/OFQ (0.01 nmol; panel d), N/OFQ (10 nmol; panel e) and UFP-101 (10 nmol; panel f) in substantia nigra reticulata are also shown. The microelectrode was sequentially introduced to a depth of 1500 μm. Interpenetration distances were 500 μm. In these mapping schemes, frontal poles are at the bottom. Zero corresponds to bregma; numbers indicate rostral or caudal distance from the bregma or lateral distance from the midline. Movement evoked at one point is indicated by symbols and threshold range by the different grey scale. Absence of symbol (within or at the border of the maps) indicates that penetration was not performed due to presence of a large vessel. In panel e, the presence of dark symbols and unresponsive sites is worth noting.

receptor stimulation in rodents. N/OFQ given i.c.v. (Reinscheid *et al*, 1995; Devine *et al*, 1996; Nishi *et al*, 1997; Rizzi *et al*, 2001; Higgins *et al*, 2001; Kuzmin *et al*, 2004) or Ro 64–6198 given systemically (Jenck *et al*, 2000; Higgins *et al*, 2001; Varty *et al*, 2005) depressed both spontaneous and exercise-induced locomotion. Fairly high doses of N/OFQ (1–30 nmol) or Ro 64–6198 (10 mg/Kg) were required to depress motor activity. These doses, although selective for the NOP receptor (Nishi *et al*, 1997; Noda *et al*, 1998; Higgins *et al*, 2001), may induce hypolocomotion and catalepsy by affecting not only motor but also vestibular and cardiovascular functions (Sulaiman *et al*, 1999; Kapusta *et al*, 1999). The battery of complementary behavioral tests used in the present study provides information on the state of activation of the basal ganglia-thalamo-cortical circuit. Indeed, modulation of the time to initiate and to execute a movement, as in the bar and drag test, primarily engage the basal ganglia (Hauber, 1998). Walking activity (as on the rotarod) also engages the dorsolateral striatum, as shown by biochemical (Brown and Sharp, 1995; Holschneider *et al*, 2003) and neurochemical (Bergquist *et al*, 2003; Petzinger *et al*, 2007) evidence. Although the cerebellar-thalamo-cortical circuit is also activated during rotarod performance, its role in motor control predominates (over the basal ganglia-thalamo-cortical circuit) when training period is prolonged to several weeks (Holschneider *et al*, 2007).

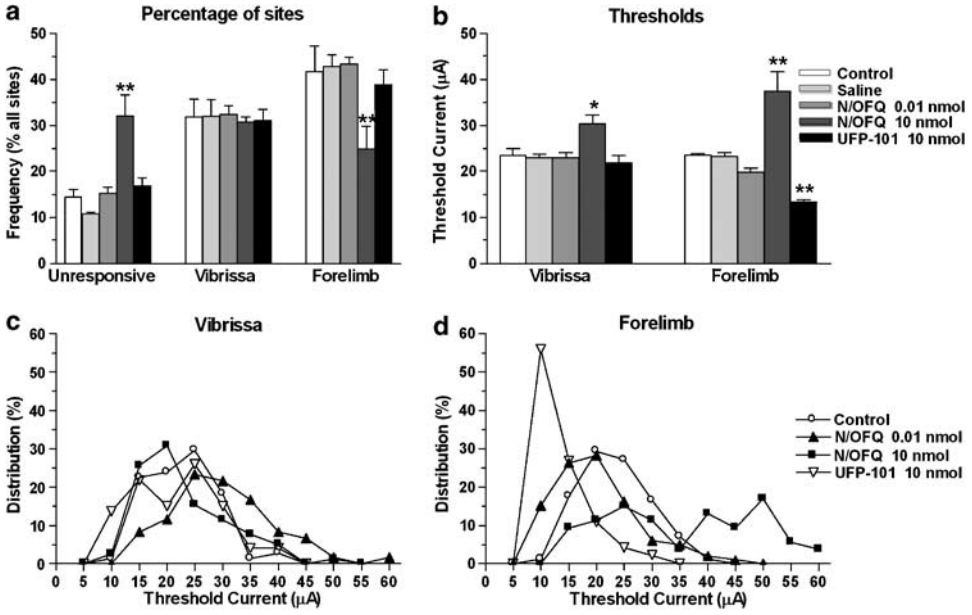

Figure 10 Effect of intranigral injection of N/OFQ and UFP-101 on primary motor cortex output. N/OFQ (0.01 and 10 nmol) and UFP-101 (10 nmol) were injected in substantia nigra reticulata, and the percentage of unresponsive and excitable sites in the vibrissa and forelimb areas (panel a) or the thresholds currents required to evoke vibrissa and forelimb movements (panel b) were measured. Threshold current distribution is also shown (panels c–d). The percentage of other movement sites (neck, jaw, eye and hindlimb) are not shown because these movements were not extensively explored. Note that N/OFQ (10 nmol) significantly shifted to the right both vibrissa and forelimb distributions whereas N/OFQ (0.01 nmol) and UFP-101 (10 nmol) significantly shifted to the left the forelimb distribution. Data are means ± SEM of five determinations per group. $*p < 0.05$, $**p < 0.01$ significantly different from control.

These tests allowed to clearly demonstrate that lower doses of i.c.v. N/OFQ (0.1–1 nmol) inhibited motor behavior by inducing akinesia and bradykinesia, by slowing the time to initiate and to execute a movement. The specificity of these effects is also confirmed by reports that these doses of N/OFQ did not affect other motor parameters such as righting reflex (Devine *et al*, 1996) or muscle strength (Jenck *et al*, 1997) and tone (Devine *et al*, 1996; Marti *et al*, 2004a). Moreover, akinesia and bradykinesia, were replicated by N/OFQ injections in SNr, the motor output of basal ganglia. This confirms and extends our previous studies in naive (Marti *et al*, 2004a) and 6-OHDA hemilesioned (Marti *et al*, 2005) rats, further endorsing the view that nigral NOP receptors are modulators of specific motor patterns.

Inhibition of locomotion was not the only effect induced by central NOP receptor stimulation since very low doses of N/OFQ (0.01 nmol) produced mild but significant facilitation. In previous studies, i.c.v. injection of 0.01–0.5 nmol N/OFQ (Florin *et al*, 1996; Jenck *et al*, 1997; Kuzmin *et al*, 2004; Sakoori and Murphy, 2004) or systemic administration of intermediate doses of Ro 64–6198 (3–6 mg/Kg, Higgins *et al*, 2001) facilitated spontaneous locomotion in rodents. This facilitation was previously related to the well-known anxiolytic effect of NOP receptor agonists (Jenck *et al*, 1997). However, the present study points out that the 0.01 nmol N/OFQ-induced facilitation is a specific motor effect. Indeed, i.c.v. N/OFQ enhanced not only rat speed and rotarod performance but also stepping activity. Moreover, facilitation in the drag and speed test was replicated by stimulation of NOP receptors in the SNr, suggesting activation of motor pathways. To confirm this view, the contralateral limb was selectively affected in the drag test. In fact, we have previously reported that SNr injections of 0.01 nmol N/OFQ did not affect rotarod performance (Marti *et al*, 2004a). The most parsimonious explanation is that the improvements in stepping activity and run speed induced by unilateral SNr N/OFQ injections are too mild to affect exercise-induced locomotion as in the rotarod test.

Despite the fact that exogenous N/OFQ evoked both motor facilitation and inhibition, the latter effect appeared predominant. This is in line with the finding that endogenous N/OFQ physiologically inhibits movement. Indeed, UFP-101, given i.c.v. or injected in SNr, facilitated stepping activity, run speed and rotarod performance (see Marti *et al*, 2004a, for the effect of UFP-101 injections in SNr on rotarod performance). Consistently, deletion of the NOP receptor gene resulted in enhanced rotarod performance (Marti *et al*, 2004a). It is noteworthy that motor activation was induced by doses of UFP-101 (1 nmol i.c.v.) that were found ineffective in modulating spontaneous locomotion (Kuzmin *et al*, 2004; Gavioli *et al*, 2003; Rizzi *et al*, 2007; Sakoori and Murphy, 2008), pain (Calò *et al*, 2002, 2005; Rizzi *et al*, 2006) or depression (Gavioli *et al*, 2003). This finding strengthens the view that exercise-induced movement is the most sensitive biological parameter influenced by endogenous N/OFQ, possibly due to phasic release of N/OFQ under motor activation (Marti *et al*, 2005). This view is not contradicted by the finding that UFP-101 10 nmol improved motor performance also under static conditions (ie reduced the immobility time in the bar test). Indeed, this facilitation was not consistent across groups. This may possibly be due to experimental reasons. Indeed, changes in immobility time below 1 s (which is about the time required to withdraw the paw from the blocks) approach the limits of sensitivity of the method (ie the reaction time of the operator). It is therefore possible that slight changes in

basal activity across different groups of animals may alter the possibility to detect a significant response to UFP-101. Overall, the data obtained with N/OFQ and UFP-101 suggest that exogenous N/OFQ is capable of activating facilitatory and inhibitory motor pathways while endogenous N/OFQ tonically interacts only with the inhibitory ones. Whether these effects are mediated by different receptor subtypes (Marti *et al*, 2003, Kuzmin *et al*, 2004) or receptor located along different and functional opposing pathways remains a matter of conjecture.

Changes in motor behavior observed after stimulation and blockade of NOP receptors in awake rats were in line with changes in motor output observed in anesthetized rats by using ICMS in layer V of M1. Indeed, the efferent neurons located in this area are most intensively involved in movement control (Beloozerova *et al*, 2003). ICMS in layer V elicits movement via direct stimulation of corticofugal and/or intracortical neurons (Jankowska *et al*, 1975), resulting in summation of excitatory synaptic potentials in motoneurons and muscle activity. Thus, movement representation, as assessed by ICMS, is a measure of the output function of the motor cortex. Moreover, it has proven to be highly sensitive to a variety of neural manipulations that influence the balance between excitatory and inhibitory circuits within M1 (Sanes *et al*, 1990; Hess and Donoghue, 1994; Huntley, 1997; Nudo and Milliken, 1996; Franchi, 2000b).

NOP receptors are widely expressed in cortical areas (particularly in layers III–VI; Neal *et al*, 1999), where they can modulate local neurotransmission both at the presynaptic (Sbrenna *et al*, 2000; Marti *et al*, 2003) and postsynaptic (Siniscalchi *et al*, 2002; Bianchi *et al*, 2004) level. However, neither motor output nor behavior was affected by M1 injections of NOP receptor ligands. This indicates that cortical NOP receptors were not involved in local modulation of the normal balance between excitatory and inhibitory circuits or that they did not change the excitability of cortico-fugal neurons belonging to the main subcortical output systems, namely the cortico-spinal, the cortico-pontine, the cortico-striatal and the cortico-thalamic system. Conversely, the fact that SNr injections of N/OFQ and UFP-101 affect motor cortex excitability suggests that the main influence on M1 cortical circuits is due to changes in cortical inputs. M1 receives inputs related to locomotion primarily from the ventrolateral thalamus, and in the absence of this input, the locomotion-related modulation of cortical activity nearly vanishes (Beloozerova and Sirota, 1998). Therefore, a candidate mechanism capable of altering the cortical excitability after injection of NOP receptor ligands might be the modulation of thalamic excitatory input to M1.

Neurobiological Substrates of N/OFQ Actions

Changes in DA transmission may underlie motor effects induced by N/OFQ. Indeed, stimulation of NOP receptors expressed on nigral DA neurons (Norton *et al*, 2002; Maidment *et al*, 2002) hyperpolarized DA cells and reduced their firing activity (Marti *et al*, 2004a). Moreover, motor inhibition induced by intranigral injections of N/OFQ was associated with reduced nigrostriatal DA transmission *in vivo* (Marti *et al*, 2004a). Disruption of motor cortex activity was also associated with motor impairment. M1 receives inputs from basal ganglia circuits that are known to be severely disrupted by striatal DA deficiency (Steiner and Kitai, 2000; Orieux *et al*, 2002; Parr-Brownlie and Hyland, 2005). In haloperidol-treated cats, the activity of the motor thalamus was found to be reduced and the afferent pathways to M1, that influence the segmental apparatus of the spinal cord, inhibited (Voloshin *et al*, 1994). Moreover, haloperidol-induced motor impairment in rats was associated with reduced baseline firing rate, bursting activity and movement-related firing in cortical neurons (Parr-Brownlie and Hyland, 2005). The finding that high N/OFQ doses injected in SNr inhibited motor behavior and cortical motor output, possibly via inhibition of DA transmission, is consistent with an inhibitory effect of N/OFQ on thalamo-cortical transmission. Indeed, reduction of thalamo-cortical inputs leaves the motor cortex functionally deactivated (Wichmann and DeLong, 1993; Obeso *et al*, 2000; Boraud *et al*, 2002; Rolland *et al*, 2007). Evidence that endogenous N/OFQ in SNr also modulates thalamo-cortical projections, although possibly via non-DA mechanisms, has been obtained in the 6-hydroxydopamine hemilesioned rat model of Parkinson's disease. Indeed, NOP receptor antagonists elevated GABA and reduced GLU release in the lesioned SNr, which was associated with reduced nigro-thalamic GABA transmission and attenuation of akinesia at the parkinsonian limb (Marti *et al*, 2007). This finding suggests that endogenous N/OFQ in SNr tonically inhibits thalamic activity. Interestingly, the electrophysiological data indicate that this tonic activity affects forelimb but not vibrissa motor representations. The main reason of this difference may be the nature of vibrissa and forelimb motor systems which involve different cortico-basal ganglia motor circuits (Hoover *et al*, 2003; Miyachi *et al*, 2006).

It proves more difficult to explain the enhanced motor cortex excitability and motor facilitation induced by low N/OFQ doses. Motor facilitation was prevented by D_1 and D_2 receptor antagonists (Florin *et al*, 1996) or catecholamine depletion (Kuzmin *et al*, 2004). It is possible that a low degree of NOP receptor stimulation reduces dendritic DA release in SN. This would remove the inhibitory feedback mediated by somatodendritic D_2 autoreceptors (Cragg and Greenfield, 1997; Bustos *et al*, 2004) and result in a facilitation of rat locomotion (Bergquist *et al*, 2003). Alternatively, as shown for classical opioids (Johnson and North, 1992), low N/OFQ doses may preferentially inhibit GABA interneurons leading to disinhibition of nigral DA neurons (Cobb and Abercrombie, 2002).

Concluding Remarks

A careful analysis of motor behavior using a battery of complementary tests, has demonstrated that exogenous N/OFQ dose-dependently facilitates and inhibits motor behavior while endogenous N/OFQ regulates movement in an inhibitory way. Although we cannot exclude the possibility that other areas also mediate N/OFQ motor effects (eg the VTA and spontaneous locomotion), these data indicate that NOP receptors in SNr mediate specific motor programs such as time to initiate and execute a movement. The present study also demonstrates for the first time that exogenous NOP receptor ligands and endogenous

N/OFQ regulate motor cortex excitability in a way, which is consistent with their motor actions. Although the neurobiological substrates remain to be investigated, the present study suggests that changes in cortical output and behavior are mainly operated by subcortical NOP receptors located in SNr through modulation of the 'cortico-basal ganglia-thalamo-cortical' loop.

DISCLOSURE/CONFLICT OF INTEREST

We declare that this work has been funded by grants from the Italian Ministry of the University (FIRB Internazionalizzazione). We declare that, except for income received from my primary employer, no financial support or compensation has been received from any individual or corporate entity over the past 3 years for research or professional service and there are no personal financial holdings that could be perceived as constituting a potential conflict of interest.

Matteo Marti, Riccardo Viaro, Remo Guerrini, Gianfranco Franchi, Michele Morari are fully paid by the University of Ferrara.

REFERENCES

Albin RA, Young AB, Penney B (1989). The functional anatomy of the basal ganglia disorders. *Trends Neurosci* **12**: 366–375.

Alexander GE, Crutcher MD (1990). Functional architecture of basal ganglia circuits: neural substrates of parallel processing. *Trends Neurosci* **13**: 266–271.

Beloozerova IN, Sirota MG (1998). Cortically controlled gait modifications in the cat. *Ann NY Acad Sci* **860**: 550–554.

Beloozerova IN, Sirota MG, Swadlow HA (2003). Activity of different classes of neurons of the motor cortex during locomotion. *J Neurosci* **23**: 1087–1097.

Bergquist F, Shahabi HN, Nissbrandt H (2003). Somatodendritic dopamine release in rat substantia nigra influences motor performance on the accelerating rod. *Brain Res* **973**: 81–91.

Bianchi C, Marani L, Barbieri M, Marino S, Beani L, Siniscalchi A (2004). Effects of nociceptin/orphanin FQ and endomorphin-1 on glutamate and GABA release, intracellular [Ca2+] and cell excitability in primary cultures of rat cortical neurons. *Neuropharmacology* **47**: 873–883.

Boraud T, Bezard E, Bioulac B, Gross CE (2002). From single extracellular unit recording in experimental and human Parkinsonism to the development of a functional concept of the role played by the basal ganglia in motor control. *Prog Neurobiol* **66**: 265–283.

Bouwman BM, van Lier H, Nitert HE, Drinkenburg WH, Coenen AM, van Rijn CM (2005). The relationship between hippocampal EEG theta activity and locomotor behaviour in freely moving rats: effects of vigabatrin. *Brain Res Bull* **64**: 505–509.

Brown LL, Sharp FR (1995). Metabolic mapping of rat striatum: somatotopic organization of sensorimotor activity. *Brain Res* **686**: 207–222.

Bustos G, Abarca J, Campusano J, Bustos V, Noriega V, Aliaga E (2004). Functional interactions between somatodendritic dopamine release, glutamate receptors and brain-derived neurotrophic factor expression in mesencephalic structures of the brain. *Brain Res Brain Res Rev* **47**: 126–144.

Calò G, Guerrini R, Rizzi A, Salvadori S, Burmeister M, Kapusta DR *et al* (2005). UFP-101, a peptide antagonist selective for the nociceptin/orphanin FQ receptor. *CNS Drug Rev* **11**: 97–112.

Calò G, Rizzi A, Rizzi D, Bigoni R, Guerrini R, Marzola G *et al* (2002). [Nphe^{1},Arg^{14},Lys^{15}]Nociceptin-NH_2, a novel potent and selective antagonist of the nociceptin/orphanin FQ receptor. *Br J Pharmacol* **136**: 303–311.

Cobb WS, Abercrombie ED (2002). Distinct roles for nigral GABA and glutamate receptors in the regulation of dendritic dopamine release under normal conditions and in response to systemic haloperidol. *J Neurosci* **22**: 1407–1413.

Cragg SJ, Greenfield SA (1997). Differential autoreceptor control of somatodendritic and axon terminal dopamine release in substantia nigra, ventral tegmental area, and striatum. *J Neurosci* **17**: 5738–5746.

Darland T, Heinricher MM, Grandy DY (1998). Orphanin FQ/nociceptin: a role in pain and analgesia, but so much more. *Trends Neurosci* **21**: 215–221.

Devine DP, Taylor L, Reinscheid RK, Monsma Jr FJ, Civelli O, Akil H (1996). Rats rapidly develop tolerance to the locomotor-inhibiting effects of the novel neuropeptide orphanin FQ. *Neurochem Res* **21**: 1387–1396.

Donoghue JP, Wise SP (1982). The motor cortex of the rat: cytoarchitecture and microstimulation mapping. *J Comp Neurol* **212**: 76–88.

Florin S, Suaudeau C, Meunier JC, Costentin J (1996). Nociceptin stimulates locomotion and exploratory behaviour in mice. *Eur J Pharmacol* **317**: 9–13.

Franchi G (2000a). Reorganization of vibrissal motor representation following severing and repair of the facial nerve in adult rats. *Exp Brain Res* **131**: 33–43.

Franchi G (2000b). Changes in motor representation related to facial nerve damage and regeneration in adult rats. *Exp Brain Res* **135**: 53–65.

Gavioli EC, Marzola G, Guerrini R, Bertorelli R, Zucchini S, De Lima TC *et al* (2003). Blockade of nociceptin/orphanin FQ-NOP receptor signalling produces antidepressant-like effects: pharmacological and genetic evidences from the mouse forced swimming test. *Eur J Neurosci* **17**: 1987–1990.

Guerrini R, Calò G, Bigoni R, Rizzi A, Varani K, Toth G *et al* (2000). Further studies on nociceptin-related peptides: discovery of a new chemical template with antagonist activity on the nociceptin receptor. *J Med Chem* **43**: 2805–2813.

Hauber W (1998). Involvement of basal ganglia transmitter systems in movement initiation. *Prog Neurobiol* **56**: 507–540.

Hess G, Donoghue JP (1994). Long-term potentiation of horizontal connections provides a mechanism to reorganize cortical motor maps. *J Neurophysiol* **71**: 2543–2547.

Higgins G, Grottick AJ, Ballard TM, Richards JG, Messer J, Takeshima H *et al* (2001). Influence of the selective ORL1 receptor agonist, Ro64–6198, on rodent neurological function. *Neuropharmacology* **41**: 97–107.

Holschneider DP, Maarek JM, Yang J, Harimoto J, Scremin OU (2003). Functional brain mapping in freely moving rats during treadmill walking. *J Cereb Blood Flow Metab* **23**: 925–932.

Holschneider DP, Yang J, Guo Y, Maarek JM (2007). Reorganization of functional brain maps after exercise training: Importance of cerebellar-thalamic-cortical pathway. *Brain Res* **1184**: 96–107.

Hoover JE, Hoffer ZS, Alloway KD (2003). Projections from primary somatosensory cortex to the neostriatum: the role of somatotopic continuity in corticostriatal convergence. *J Neurophysiol* **89**: 1576–1587.

Huntley GW (1997). Correlation between patterns of horizontal connectivity and the extend of short-term representational plasticity in rat motor cortex. *Cereb Cortex* **7**: 143–156.

Jankowska E, Padel Y, Tanaka R (1975). The mode of activation of pyramidal tract cells by intracortical stimuli. *J Physiol* **249**: 617–636.

Jenck F, Moreau J, Martin J, Kilpatrick G, Reinscheid RK, Monsma Jr FJ *et al* (1997). Orphanin FQ acts as an anxiolytic to attenuate behavioural responses to stress. *Proc Natl Acad Sci USA* **94**: 14854–14858.

Jenck F, Wichmann J, Dautzenberg FM, Moreau JL, Ouagazzal AM, Martin JR *et al* (2000). A synthetic agonist at the orphanin FQ/nociceptin receptor ORL1: anxiolytic profile in the rat. *Proc Natl Acad Sci USA* **97**: 4938–4943.

Johnson SW, North RA (1992). Two types of neurone in the rat ventral tegmental area and their synaptic inputs. *J Physiol* **450**: 455–468.

Kapusta DR, Chang JK, Kenigs VA (1999). Central administration of [Phe1psi(CH2-NH)Gly2]nociceptin(1-13)-NH2 and orphanin FQ/nociceptin (OFQ/N) produce similar cardiovascular and renal responses in conscious rats. *J Pharmacol Exp Ther* **289**: 173–180.

Kuschinsky K, Hornykiewicz O (1972). Morphine catalepsy in the rat: relation to striatal dopamine metabolism. *Eur J Pharmacol* **19**: 119–122.

Kuzmin A, Sandin J, Terenius L, Ogren SO (2004). Evidence in locomotion test for the functional heterogeneity of ORL-1 receptors. *Br J Pharmacol* **141**: 132–140.

Maidment NT, Chen Y, Tan AM, Murphy NP, Leslie FM (2002). Rat ventral midbrain dopamine neurons express the orphanin FQ/nociceptin receptor ORL-1. *Neuroreport* **13**: 1137–1140.

Marti M, Mela F, Fantin M, Zucchini S, Brown JM, Witta J *et al* (2005). Blockade of nociceptin/orphanin FQ transmission attenuates symptoms and neurodegeneration associated with Parkinson's disease. *J Neurosci* **95**: 9591–9601.

Marti M, Mela F, Guerrini R, Calò G, Bianchi C, Morari M (2004b). Blockade of nociceptin/orphanin FQ transmission in rat substantia nigra reverses haloperidol-induced akinesia and normalizes nigral glutamate release. *J Neurochem* **91**: 1501–1504.

Marti M, Mela F, Veronesi C, Guerrini R, Salvatori S, Federici M *et al* (2004a). Blockade of nociceptin/orphanin FQ receptor signalling in rat substantia nigra pars reticulata stimulates nigrostriatal dopaminergic transmission and motor behaviour. *J Neurosci* **24**: 6659–6666.

Marti M, Stocchi S, Paganini F, Mela F, De Risi C, Calò G *et al* (2003). Pharmacological profiles of presynaptic nociceptin/orphanin FQ receptors modulatine 5-hydroxytryptamine and noradrenaline release in the rat neocortex. *Br J Pharmacol* **138**: 91–98.

Marti M, Trapella C, Viaro R, Morari M (2007). The nociceptin/orphanin FQ receptor antagonist J-113397 and L-DOPA additively attenuate experimental parkinsonism through overinhibition of the nigrothalamic pathway. *J Neurosci* **27**: 1297–1307.

Miyachi S, Lu X, Imanishi M, Sawada K, Nambu A, Takada M (2006). Somatotopically arranged inputs from putamen and subthalamic nucleus to primary motor cortex. *Neurosci Res* **56**: 300–308.

Murphy NP, Maidment NT (1999). Orphanin FQ/nociceptin modulation of mesolimbic dopamine transmission determined by microdialysis. *J Neurochem* **73**: 179–186.

Neal Jr CR, Mansour A, Reinscheid R, Nothacker HP, Civelli O, Akil H *et al* (1999). Opioid receptor-like (ORL1) receptor distribution in the rat central nervous system: comparison of ORL1 receptor mRNA expression with ^{125}I-[^{14}Tyr]-orphanin FQ binding. *J Comp Neurol* **412**: 563–605.

Nishi M, Houtani T, Noda Y, Mamiya T, Sato K, Doi T *et al* (1997). Unrestrained nociceptive response and dysregulation of hearing ability in mice lacking the nociceptin/orphaninFQ receptor. *EMBO J* **16**: 1858–1864.

Noda Y, Mamiya T, Nabeshima T, Nishi M, Higashioka M, Takeshima H (1998). Loss of antinociception induced by naloxone benzoylhydrazone in nociceptin receptor-knockout mice. *J Biol Chem* **273**: 18047–18051.

Norton CS, Neal CR, Kumar S, Akil H, Watson SJ (2002). Nociceptin/orphanin FQ and opioid receptor-like receptor mRNA expression in dopamine systems. *J Comp Neurol* **444**: 358–368.

Nudo RJ, Milliken GW (1996). Reorganization of movement representations in primary motor cortex following focal ischemic infarcts in adult squirrel monkeys. *J Neurophysiol* **75**: 2144–2149.

Obeso JA, Rodriguez-Oroz MC, Chana P, Lera G, Rodriguez M, Olanow CW (2000). The evolution and origin of motor complications in Parkinson's disease. *Neurology* **5**: S13–S20.

Orieux G, François C, Féger J, Hirsch EC (2002). Consequences of dopaminergic denervation on the metabolic activity of the cortical neurons projecting to the subthalamic nucleus in the rat. *J Neurosci* **22**: 8762–8770.

Parr-Brownlie LC, Hyland BI (2005). Bradykinesia induced by dopamine D2 receptor blockade is associated with reduced motor cortex activity in the rat. *J Neurosci* **25**: 5700–5709.

Paxinos G, Watson C (1982). *The Rat Brain in Stereotaxic Coordinates*. Academic: Sydney.

Petzinger GM, Walsh JP, Akopian G, Hogg E, Abernathy A, Arevalo P *et al* (2007). Effects of treadmill exercise on dopaminergic transmission in the 1-methyl-4-phenyl-1,2,3,6-tetrahydropyridine-lesioned mouse model of basal ganglia injury. *J Neurosci* **27**: 5291–5300.

Reinscheid RK, Nothacker HP, Bourson A, Ardati A, Henningsen RA, Bunzow JR *et al* (1995). Orphanin FQ: a neuropeptide that activates an opioid-like G protein-coupled receptor. *Science* **270**: 792–794.

Rizzi A, Bigoni R, Marzola G, Guerrini R, Salvadori S, Regoli D *et al* (2001). Characterization of the locomotor activity-inhibiting effect of nociceptin/orphanin FQ in mice. *Naunyn Schmiedebergs Arch Pharmacol* **363**: 161–165.

Rizzi A, Nazzaro C, Marzola G, Zucchini S, Trapella C, Guerrini R *et al* (2006). Endogenous nociceptin/orphanin FQ signalling produces opposite spinal antinociceptive and supraspinal pronociceptive effects in the mouse formalin test: pharmacological and genetic evidences. *Pain* **124**: 100–108.

Rizzi A, Spagnolo B, Wainford RD, Fischetti C, Guerrini R, Marzola G *et al* (2007). *In vitro* and *in vivo* studies on UFP-112, a novel potent and long lasting agonist selective for the nociceptin/orphanin FQ receptor. *Peptides* **28**: 1240–1251.

Rolland AS, Herrero MT, Garcia-Martinez V, Ruberg M, Hirsch EC, François C (2007). Metabolic activity of cerebellar and basal ganglia-thalamic neurons is reduced in parkinsonism. *Brain* **130**: 265–275.

Rozas G, Guerra MJ, Labandeira-Garcia JL (1997). An automated rotarod method for quantitative drug-free evaluation of overall motor deficits in rat models of parkinsonism. *Brain Res Brain Res Protoc* **2**: 75–84.

Sakoori K, Murphy NP (2004). Central administration of nociceptin/orphanin FQ blocks the acquisition of conditioned place preference to morphine and cocaine, but not conditioned place aversion to naloxone in mice. *Psychopharmacology* **172**: 129–136.

Sakoori K, Murphy NP (2008). Endogenous Nociceptin (Orphanin FQ) Suppresses Basal Hedonic State and Acute Reward Responses to Methamphetamine and Ethanol, but Facilitates Chronic Responses. *Neuropsychopharmacology* **33**: 877–891.

Sanberg PR, Bunsey MD, Giordano M, Norman AB (1988). The catalepsy test: its ups and downs. *Behav Neurosci* **102**: 748–759.

Sanes JN, Suner S, Donoghue JP (1990). Dynamic organization of primary motor cortex output to target muscles in adult rats. I. Long-term patterns of reorganization following motor or mixed peripheral nerve lesions. *Exp Brain Res* **79**: 479–491.

Sbrenna S, Marti M, Morari M, Calò G, Guerrini R, Beani L *et al* (2000). Modulation of 5-hydroxytryptamine efflux from rat cortical synaptosomes by opioids and nociceptin. *Br J Pharmacol* **130**: 425–433.

Schallert T, De Ryck M, Whishaw IQ, Ramirez VD, Teitelbaum P (1979). Excessive bracing reactions and their control by atropine

and L-DOPA in an animal analog of Parkinsonism. *Exp Neurol* **64**: 33–43.

Siniscalchi A, Rodi D, Morari M, Marti M, Cavallini S, Marino S *et al* (2002). Direct and indirect inhibition by nociceptin/orphanin FQ on noradrenaline release from rodent cerebral cortex *in vitro*. *Br J Pharmacol* **136**: 1178–1184.

Steiner H, Kitai ST (2000). Regulation of rat cortex function by D1 dopamine receptors in the striatum. *J Neurosci* **20**: 5449–5460.

Sulaiman MR, Niklasson M, Tham R, Dutia MB (1999). Modulation of vestibular function by nociceptin/orphanin FQ: an *in vivo* and *in vitro* study. *Brain Res* **828**: 74–82.

Varty GB, Hyde LA, Hodgson RA, Lu SX, McCool MF, Kazdoba TM *et al* (2005). Characterization of the nociceptin receptor (ORL-1) agonist, Ro64-6198, in tests of anxiety across multiple species. *Psychopharmacology (Berl)* **182**: 132–143.

Voloshin MY, Lukhanina EP, Kolomietz BP, Prokopenko VF, Rodionov VA (1994). Electrophysiological investigation of thalamic neuronal mechanisms of motor disorders in parkinsonism: an influence of D2ergic transmission blockade on excitation and inhibition of relay neurons in motor thalamic nuclei of cat. *Neuroscience* **62**: 771–781.

Wichmann T, DeLong MR (1993). Pathophysiology of parkinsonian motor abnormalities. *Adv Neurol* **60**: 53–61.

Supplementary Information accompanies the paper on the Neuropsychopharmacology website (http://www.nature.com/npp)

Experimental Neurology xxx (2010) xxx–xxx

Contents lists available at ScienceDirect

Experimental Neurology

journal homepage: www.elsevier.com/locate/yexnr

Regular Article

Dual motor response to L-dopa and nociceptin/orphanin FQ receptor antagonists in 1-methyl-4-phenyl-1,2,5,6-tetrahydropyridine (MPTP) treated mice: Paradoxical inhibition is relieved by D_2/D_3 receptor blockade

Riccardo Viaro, Matteo Marti, Michele Morari *

Department of Experimental and Clinical Medicine, Section of Pharmacology, University of Ferrara, Ferrara, Italy
Center for Neuroscience and National Institute of Neuroscience, University of Ferrara, Ferrara, Italy

ARTICLE INFO

Article history:
Received 18 November 2009
Revised 19 January 2010
Accepted 23 January 2010
Available online xxxx

Keywords:
Dopamine
MPTP
L-dopa
Pramipexole
Nociceptin/orphanin FQ
Trap-101
J-113397

ABSTRACT

Motor activity of mice acutely treated with the parkinsonian toxin 1-methyl-4-phenyl-1,2,5,6-tetrahydropyridine (MPTP) was monitored for 6 days using behavioral tests which provide complementary information on motor function: the bar, reaction time, drag, stair climbing, grip, rotarod and footprinting tests. These tests consistently disclosed a prolonged motor impairment characterized by akinesia, bradykinesia, speed reduction, loss of coordination and gait patterns. This impairment was associated with ~60% loss of striatal dopamine terminals, as revealed by tyrosine hydroxylase immunohistochemistry, and was attenuated by dopaminergic drugs. Indeed, the dopamine precursor, L-dopa (1–10 mg/kg), and the D_3/D_2 receptor agonist pramipexole (0.0001–0.001 mg/kg) promoted stepping activity in the drag test (a test for akinesia/bradykinesia). The novel nociceptin/orphanin FQ receptor (NOP) antagonist 1-[1-(cyclooctylmethyl)-1,2,3,6-tetrahydro-5-(hydroxymethyl)-4-pyridinyl]-3-ethyl-1,3-dihydro-2*H*-benzimidazol-2-one (Trap-101, 0.001–0.1 mg/kg), an analogue of 1-[(3*R*,4*R*)-1-cyclooctylmethyl-3-hydroxymethyl-4-piperidyl]-3-ethyl-1,3-dihydro-2*H*-benzimidazol-2-one (J-113397), also promoted stepping and synergistically or additively (depending on test) attenuated parkinsonism when combined to dopamine agonists. High doses of L-dopa (100 mg/kg), pramipexole (0.1 mg/kg), Trap-101 and J-113397 (1 mg/kg), however, failed to modulate stepping, worsening immobility time and/or rotarod performance. Low doses of amisulpride (0.1 mg/kg) reversed motor inhibition induced by L-dopa and J-113397, suggesting involvement of D_2/D_3 receptors. This study brings further evidence for a dopamine-dependent motor phenotype in MPTP-treated mice reinforcing the view that this model can be predictive of symptomatic antiparkinsonian activity provided the appropriate test is used. Moreover, it offers mechanistic interpretation to clinical reports of paradoxical worsening of parkinsonism following L-dopa. Finally, it confirms that NOP receptor antagonists may be proven effective in reversing parkinsonism when administered alone or in combination with dopamine agonists.

Introduction

The pathological hallmark of Parkinson's disease (PD) is the death of pigmented dopamine (DA) neurons in substantia nigra compacta (SNc), which triggers a slow onset of motor symptoms such as akinesia/bradykinesia, rigidity, resting tremor and gait/postural abnormalities. Neurodegeneration models have been developed to understand the physiopathological mechanisms underlying PD (Dauer and Przedborski, 2003; Meredith and Kang, 2006). A commonly used neurotoxin is 1-methyl-4-phenyl-1,2,5,6-tetrahydropyridine (MPTP; Langston et al., 1983), which is converted by monoamine oxidase B (MAO-B) to 1-methyl-4-phenylpyridinium ion (MPP^+). This metabolite enters DA cells and inhibits mitochondrial complex I, generating oxidative stress and cell death (Przedborski et al., 2000). Although MPTP-treated nonhuman primates represent the reference PD model, the MPTP-treated mouse is commonly used to investigate the neurotoxicity pathways underlying PD and test the neuroprotective potential of antiparkinsonian drugs. Nonetheless, this model has failed to reproduce the motor impairment seen in PD patients or consistently replicate the phenotype observed in other parkinsonism models. Indeed, mice treated with MPTP can display no change in motor behavior (Miller et al., 1991; Itzhak et al., 1999), transient (Nishi et al., 1991; Sedelis et al., 2000) or sustained (Fredriksson et al., 1994; Haobam et al., 2005) motor impairment, and even hyperlocomotion (Colotla et al., 1990; Chia et al., 1996). Though this variability could be attributed to precise experimental factors (Sedelis et al., 2001;

* Corresponding author. Department of Experimental and Clinical Medicine, Section of Pharmacology, University of Ferrara, via Fossato di Mortara 17-19, 44100 Ferrara, Italy. Fax: +39 0532 455205.
E-mail address: m.morari@unife.it (M. Morari).

0014-4886/$ – see front matter © 2010 Elsevier Inc. All rights reserved.
doi:10.1016/j.expneurol.2010.01.014

Jackson-Lewis and Przedborski, 2007), it has prevented the MPTP model from being used to screen for symptomatic antiparkinsonian drugs, essentially limiting its applications to neurotoxicity studies. We have recently developed a battery of behavioral tests which can be used in a sequence to collect complementary information on motor function: the bar, drag and rotarod tests. These tests allowed us to disclose symptomatic effects of L-dopa in 6-hydroxydopamine (6-OHDA) hemilesioned rats (Marti et al., 2005, 2007) and MPTP-treated mice (Viaro et al., 2008), although in that study only a single dose of L-dopa was investigated. To further validate this approach, a more thorough phenotypic characterization of MPTP-treated mice and evaluation of their motor responses to classical and potential antiparkinsonian drugs was attempted in the present study. Mice were evaluated daily for 6 days after acute MPTP treatment using a broad range of behavioral tests including not only the bar, drag and rotarod but also the reaction time, grip, stair climbing and footprinting tests. Since a parkinsonian-like phenotype emerged from this analysis, we investigated its DA-dependence by measuring striatal tyrosine hydroxylase (TH) density and motor responses to the DA precursor L-dopa and the D_3/D_2 receptor agonist pramipexole. Moreover, we tested the novel nociceptin/orphanin FQ (N/OFQ) receptor (NOP) antagonist 1-(1-Cyclooctyl-methyl-5-hydroxymethyl-1,2,3,6-tetrahydro-pyridin-4-yl)-3-ethyl-1,3-dihydro-benzoimidazol-2-one (Trap-101), a structural analogue of 1-[(3*R*,4*R*)-1-cyclooctylmethyl-3-hydroxymethyl-4-piperidyl]-3-ethyl-1,3-dihydro-2*H*-benzimidazol-2-one (J-113397), administered alone and in combination with DA agonists. These tests revealed dual motor responses, facilitation being observed at low doses and inhibition (or loss of response) at higher ones. Since pramipexole is known to depress motor activity via D_2 (auto)receptors (Mierau and Schingnitz, 1992; Maj et al., 1997; Siuciak and Fujiawara, 2004), we studied whether amisulpride was able to prevent motor inhibition. Indeed, a preferential binding to D_2 autoreceptors was observed at low amisulpride doses (Scatton et al., 1997; Perrault et al., 1997; Schoemaker et al., 1997).

Materials and methods

Animals

Young adult (8 weeks old) male C57BL/6J mice (20–25 g; S.Pietro al Natisone, Harlan, Italy) were used for this study. Animals were housed four for cage, with free access to food and water, and kept under environmentally controlled conditions (12-h light/dark cycle with light on between 07:00 and 19:00). This study was compliant with the European Council Directive of 24 November 1986 (86/609/EEC), and approved by the Ethical Committee of the University of Ferrara and Italian Ministry of Health (license n. 94/2007B). Adequate measures were taken to minimize animal pain as well as the number of animals used.

Experimental design

Prior to pharmacological testing, mice were handled for 1 week by the same operator to reduce stress, and trained daily for an additional week in the behavioral tests until their motor performance became reproducible. The first set of experiments (experiment #1) was aimed at the analysis of behavioral phenotype of MPTP-treated mice. Animals were injected with MPTP (4×20 mg/kg, i.p., 90 min apart) and their motor activity assessed daily for 6 days (beginning 24 h after toxin administration) by a battery of behavioral tests, namely the bar, reaction time, drag, stair climbing, grip, rotarod and footprinting tests. These tests were performed starting at 09.00 in a fixed sequence (as listed). Animals were then sacrificed, their brain removed and processed for TH immunohistochemistry to quantify the degree of striatal denervation.

The second set of experiments (experiment #2) was aimed at studying the DA-dependence of motor deficit, and mice responsiveness to classical and potential antiparkinsonian compounds. Three tests only were used for these experiments: the bar, drag and rotarod tests. Mice were treated with MPTP as above and drug testing was performed 7 days later. DA agonists (L-dopa and pramipexole) and Trap-101 were administered systemically (i.p.) over a wide dose range. L-Dopa was associated with benserazide (4:1 ratio). After dose–response curves were obtained, low doses (subthreshold or threshold depending on test) of Trap-101, L-dopa and pramipexole were also tested in combination. Appropriate controls (saline, benserazide 25 mg/kg) were run in parallel. These experiments revealed that high doses of DA agonists and Trap-101 were either ineffective or caused mild inhibition. The same phenomenon was previously reported for J-113397 (Viaro et al., 2008). Therefore, the D_2/D_3 antagonist amisulpride was tested alone or in combination with L-dopa, pramipexole and J-113397 (20 min pre-treatment), to investigate whether D_2/D_3 receptors were involved. The three tests were performed in a sequence (bar, drag and rotarod) before (control session) and after (10 and 60 min) drug injections.

Behavioral motor studies

Bar test

This test, also known as the catalepsy test (Sanberg et al., 1988), measures the ability of the animal to respond to an externally imposed static posture. Each mouse was placed gently on a table and the right and left forepaws were placed alternatively on blocks of increasing heights (1.5, 3 and 6 cm). The immobility time (in seconds) of each forepaw on the block was recorded (cut-off time 20 s/step, 60 s maximum). Akinesia was calculated as total time spent on the blocks (mean between the two forepaws).

Reaction time test

This test measures motor reactivity of the animal in an open field. Mice were allowed to habituate to the center of a square arena (150×150 cm) for 5 min, then elevated 3 cm above the surface (lifting from the tail), and finally left to fall. When the animal touched the floor, the latency time for the first forelimb movement was recorded.

Drag test

This test (modification of the "wheelbarrow" test; Schallert et al., 1979), measures the ability of the animal to balance its body posture using forelimbs in response to an externally imposed dynamic stimulus (backward dragging; Marti et al., 2005). Each mouse was gently lifted from the tail (allowing the forepaws on the table) and dragged backwards at a constant speed (about 20 cm/s) for a fixed distance (100 cm). The number of touches made by each forepaw was counted by two separate observers (mean between the two forepaws).

Stair climbing test

This test (modification of the SCA test; Kumar and Sehgal, 2007) analyzed the motivation and the motor skill during a climb-walk. Each mouse was positioned on the first step (2 cm height, 2 cm long, 5 cm wide) of a 45°-sloping staircase. At the top of the staircase a food pellet was lodged in a small dark goal box. The time needed for climbing 20 consecutive steps (50 cm) was recorded and the average speed calculated (cm/s). Steps made at the beginning and the end of the climb were excluded because of velocity changes or obvious acceleration/deceleration.

Grip test

This test was used to evaluate the skeletal muscle strength in mice (Meyer et al., 1979). The grip-strength apparatus (ZP-50N, IMADA, Japan) is comprised of a wire grid (5×5 cm) connected to an

Please cite this article as: Viaro, R., et al., Dual motor response to L-dopa and nociceptin/orphanin FQ receptor antagonists in 1-methyl-4-phenyl-1,2,5,6-tetrahydropyridine (MPTP) traeted mice: Paradoxical..., Exp. Neurol. (2010), doi:10.1016/j.expneurol.2010.01.014

isometric force transducer (dynamometer). In the grip-strength test mice were held by their tails and allowed to grasp the grid with their forepaws. The mice were then gently pulled backward by the tail until the grid was released. The average force exerted by the mouse before losing grip was recorded. The mean of 10 measurements for each animal was calculated and the mean average force was determined. The skeletal muscle strength in mice was expressed in grams force (gf) and was recorded and processed by IMADA ZP-Recorder software.

Rotarod test

This test analyzes the ability of the mouse to run on a rotating cylinder (diameter 8 cm) and provides information on different motor parameters such as coordination, gait, balance, muscle tone and motivation to run (Rozas et al., 1997). The fixed-speed rotarod test was employed according to a previously described protocol (Marti et al., 2004; Viaro et al., 2008). Briefly, mice were tested at stepwise increasing speeds (usually from 5 to 45 rpm for naïve and from 5 to 35 rpm for MPTP-treated mice; 180 s each step) and time spent on the rod calculated (in seconds). In experiment #2, a shorter protocol was used to allow measurement of drug effect at two different time-points. This protocol was specifically developed to measure both facilitatory and inhibitory drug effects on rotarod performance (Marti et al., 2004). After obtaining reproducible motor performance during training, mice were tested over a narrower speed window (usually from 20 to 35 rpm, stepwise, 180 s each step) which was found to cause a progressive decrement of performance to ~40% of the maximal response (i.e. the experimental cut-off time). Drug effect was then calculated by comparing the performances (time on rod) over these narrow speed windows, before and after drug treatment.

Footprinting test

This test provides information on gait patterns (Klapdor et al., 1997). Mice paws were marked with ink and gait patterns (stride length and width, foot angle, overlap, speed) analyzed after walking over a sheet of paper (Fig. 1F). The apparatus was composed of a white runway (5 cm wide, 70 cm long, with borders of 10 cm height) arranged to lead out into a dark goal box (20×20×30 cm). The parameters were measured by wetting forepaws and hindpaws with commercially available pencil nontoxic ink (the paws were painted with different colored inks) and allowing the mice to trot on a strip of paper (5 cm wide, 70 cm long) onto the runway. Pawprints made at the beginning and the end of the run were excluded because of velocity changes or obvious acceleration/deceleration. Stride length is the average distance (in millimeters) of forward movement between each forepaw and hindpaw footprint. Stride width is the average lateral distance (in millimeters) between opposite left and right forepaw and opposite left and right hindpaw. This was determined by measuring the perpendicular distance of a given step to a line connecting its opposite preceding and succeeding steps. Foot angle is the angle of hindpaw (in degrees) with respect to main direction. This was determined by measuring the amplitude of angle between the direction of run and each direction of the hindpaw (line starting at center of paw to the third finger). Placement of paws is the footprint overlap (in millimeters) and is calculated by measuring the distance between the center of the forepaw footprint and the ipsilateral hindpaw footprint, taken from successive steps. Speed of run (in centimeters/second), was calculated by the ratio between the length of runway and time spent along the runway. After the run, animals were placed in a cage filled with 0.5 cm warm water for 1 min in order to wash off the dye.

Histological evaluation

Mice were deeply anesthetized (ketamine 85 mg/kg, xylazine 15 mg/kg, i.p.), transcardially perfused with phosphate-buffered saline (PBS; 20 mM, pH 7.4, at room temperature) and fixed with cold 4% paraformaldheyde in PBS. Brains were removed, post-fixed in the fixative overnight and transferred to 20% sucrose solution in PBS for cryoprotection. Serial coronal sections of 30 μm thickness were made using a freezing microtome. Every second section in the striatum was

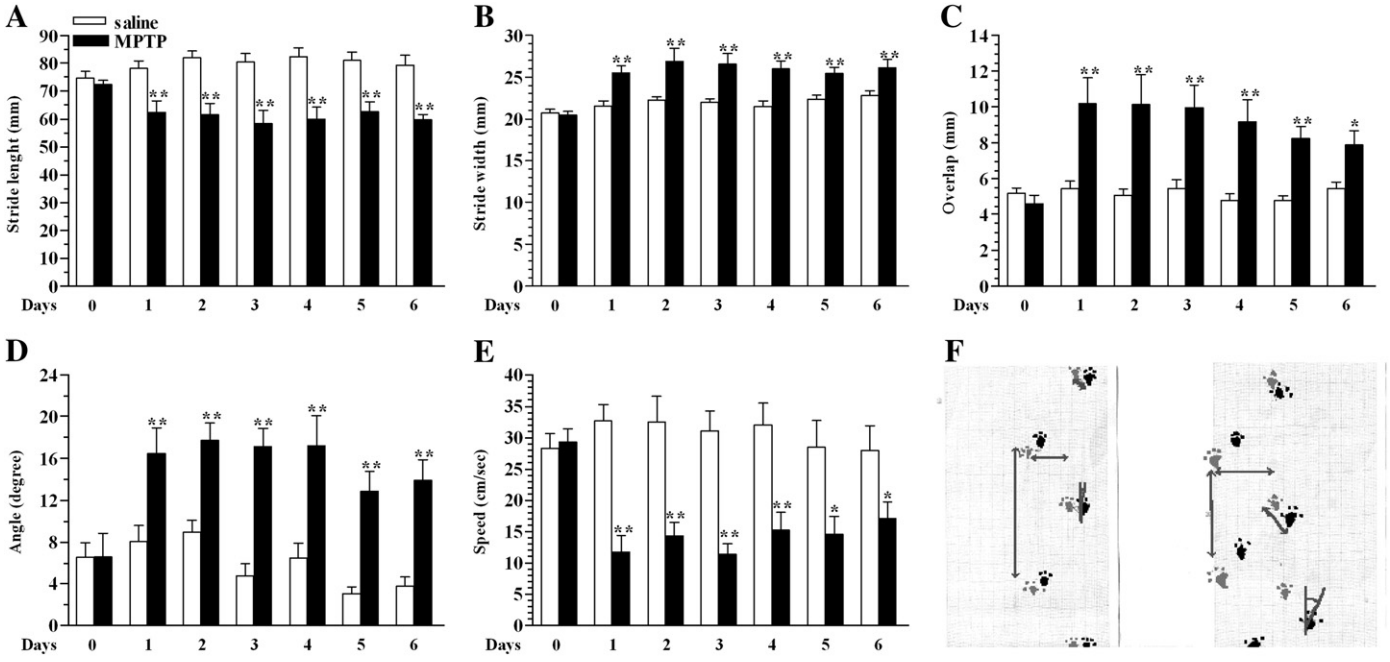

Fig. 1. MPTP-treatment induced abnormalities of gait and posture in mice. (A–E) Systemic administration of MPTP reduced the stride length of hindlimbs (in millimeters; A), increased the stride width of hindlimbs (in millimeters; B), the distance of matching (in millimeters; C) and the angle of hindpaws (in degrees; D) and reduced the speed of run (in centimeters per second; E). (F) Complete set of parameters in the footprints of a saline (left) and MPTP-treated mouse (right). All tests were performed before and after (daily for 6 days) MPTP-treatment. Data are means ± SEM of 10 determinations per group. *$p<0.05$, **$p<0.01$ different from saline (RM ANOVA followed by contrast analysis and the sequentially rejective Bonferroni's test for multiple comparisons).

Please cite this article as: Viaro, R., et al., Dual motor response to L-dopa and nociceptin/orphanin FQ receptor antagonists in 1-methyl-4-phenyl-1,2,5,6-tetrahydropyridine (MPTP) traeted mice: Paradoxical..., Exp. Neurol. (2010), doi:10.1016/j.expneurol.2010.01.014

selected from the region spanning from bregma −0.8 to +1.3, and processed for TH immunohistochemistry. Sections were rinsed three times in PBS and incubated for 15 min in 3% H_2O_2 and 10% methanol in PBS to block the endogenous peroxidase activity. After washing in PBS, the sections were preincubated in blocking serum (5% normal horse serum and 0.3% Triton X 100 in PBS) for 60 min, followed by incubation in anti-TH mouse monoclonal antibody solution (1:2000, Chemicon, Temecula, CA) for 16 h at room temperature. The sections were then rinsed in PBS and incubated for 1 h in biotinylated horse anti-mouse IgG secondary antibody (1:200; Vector Laboratories, Burlingame, CA). After rinsing, sections were incubated with avidin–biotin–peroxidase complex (Vector Laboratories) for 30 min at room temperature. After rinsing with PBS, immunoreactivity was visualized by incubating the sections in a solution containing 0.05% 3,3-diaminobenzidine (DAB) in 0.013% H_2O_2 in PBS for about 1 min. The sections were rinsed in PBS, mounted on gelatine-coated slides, dried with ethanol and xylene, and coverslipped with mounting medium. The sections were viewed with a Zeiss Axioskop (Carl Zeiss, Germany). Sections were acquired (AxioCam ICc3, Carl Zeiss) at five antero-posterior (AP) levels (−0.10, +0.20, +0.50, +0.80, +1.10 mm) and TH-immunoreactive fiber density analyzed using ImageJ software (Wayne Rasband; NIH, USA). For each animal, optical density was calculated as the mean of the five striatal levels and corrected for non-specific background, measured in the corpus callosum.

Drugs

Benserazide, L-dopa and MPTP were purchased from Sigma Chemical Company (St. Louis, MO, USA). Amisulpride and domperidone were purchased from Tocris Bioscience (Bristol, UK). Pramipexole was purchased from McTony Bio and Chem (Vancouver, Canada). J-113397 and Trap-101 were synthesized in the laboratories of the Department of Pharmaceutical Chemistry at the University of Ferrara. All drugs were freshly dissolved in saline just prior to use and the volume injected was 10 μl/g body weight.

Data presentation and statistical analysis

Data are expressed as means ± SEM of 10 (experiment #1) or 6–8 (experiment #2) determinations per group. Motor performance in the behavioral tests has been indicated in absolute values (experiment #1) or as percentage of the control session (i.e. the session performed before treatment, which represents the internal control for each mouse; experiments #2). Statistical analysis was performed by two-way repeated measure (RM) ANOVA, implemented on a spreadsheet. In the case these tests yielded a significant F score, post-hoc analysis was performed by contrast analysis to determine group differences and the sequentially rejective Bonferroni test was used to determine specific differences (i.e. at the single time-point level) between groups. To compare TH density the Student's t-test was performed. P values <0.05 were considered to be statistically significant.

Results

MPTP induced long-lasting motor deficits (experiment #1)

MPTP administration induced a variety of acute behavioral changes observed unsystematically, such as muscular hypotonia, piloerection, elevated bowed stiff tail (i.e. Straub tail), increased respiration (i.e. hyperpnea). These phenomena appeared immediately after the first injection and vanished within 16 h. About 30% of MPTP-treated mice died within 24 h after toxin administration. Body weight of surviving MPTP-treated mice did not change with respect to vehicle-injected mice over time (data not shown).

MPTP treatment caused akinesia and bradykinesia

Acute MPTP treatment increased the immobility and reaction times, and decreased the number of steps, the climbing speed, the pulling force and the time spent on the rod. Motor impairment was usually maximal at D1 after MPTP and, despite a tendency to subside over time, it was still evident after 6 days.

Bar test

RM ANOVA on bar test values (Fig. 2A) showed a significant effect of treatment ($F_{1,9}=43.92$, $p<0.0001$), but not time ($F_{6,6}=1.00$, $p=0.50$) and a significant time × treatment interaction ($F_{6,108}=12.30$, $p=0.0038$). Post hoc analysis revealed that MPTP increased the immobility time, which was maximal at D1 after MPTP and subsided from D4 onward. At 6 days after MPTP, mice were still akinetic.

Reaction time test

RM ANOVA on reaction time test values (Fig. 2B) showed a significant effect of treatment ($F_{1,9}=33.02$, $p<0.0001$), but not time ($F_{6,6}=1.10$, $p=0.46$) and a nonsignificant time × treatment interaction ($F_{6,108}=3.38$, $p=0.08$). Post hoc analysis revealed that MPTP caused a marked loss of reactivity that was substantially unchanged from D1 through D6.

Drag test

RM ANOVA on stepping values (Fig. 2C) showed a significant effect of treatment ($F_{1,9}=95.48$, $p<0.001$), but not time ($F_{6,6}=1.01$, $p=0.50$), and a significant time × treatment interaction ($F_{6,108}=10.99$, $p<0.001$). Post hoc analysis revealed that MPTP caused a decrease in stepping activity. The effect was maximal at D1 and D2 (~60%) and still detectable, albeit attenuated (~15%), at D6.

Stair climbing test

RM ANOVA on climbing test values (Fig. 2D) showed a significant effect of treatment ($F_{1,9}=69.83$, $p<0.001$), but not time ($F_{6,6}=0.93$, $p=0.53$), and a significant time × treatment interaction ($F_{6,108}=5.22$, $p=0.032$). Post hoc analysis revealed that MPTP caused a marked impairment of climbing speed at D1 (~70%) which tended to revert back over time (~40% at D6).

Grip test

RM ANOVA on force values (Fig. 2E) showed a significant effect of treatment ($F_{1,9}=18.41$, $p=0.002$), but not time ($F_{6,6}=2.02$, $p=0.21$), and a nonsignificant time × treatment interaction ($F_{6,108}=2.59$, $p=0.14$). Post hoc analysis revealed that MPTP caused a maximal reduction of pulling force in the D1–D4 range. After 6 days, however, the pulling force was normalized.

Rotarod test

RM ANOVA on time-on-rod values (Fig. 2F) showed a significant effect of treatment ($F_{1,9}=13.57$, $p=0.005$), but not time ($F_{6,6}=0.97$, $p=0.52$), and a significant time × treatment interaction ($F_{6,108}=10.48$, $p=0.0058$). Post hoc analysis revealed that MPTP caused a maximal ~65% impairment of the rotarod performance at D1. In the following days, attenuation of motor impairment settled to ~30%.

MPTP treatment caused abnormalities in gait and posture

In addition to akinesia and bradykinesia, MPTP caused long lasting loss of gait ability and correct posture, as shown by reductions in stride length and speed, increases in stride width and angle of paw, and mismatch of paw placement.

Stride length

RM ANOVA on stride length values (Fig. 1A) showed a significant effect of treatment ($F_{1,9}=14.18$, $p=0.0045$), but not time

Please cite this article as: Viaro, R., et al., Dual motor response to L-dopa and nociceptin/orphanin FQ receptor antagonists in 1-methyl-4-phenyl-1,2,5,6-tetrahydropyridine (MPTP) traeted mice: Paradoxical..., Exp. Neurol. (2010), doi:10.1016/j.expneurol.2010.01.014

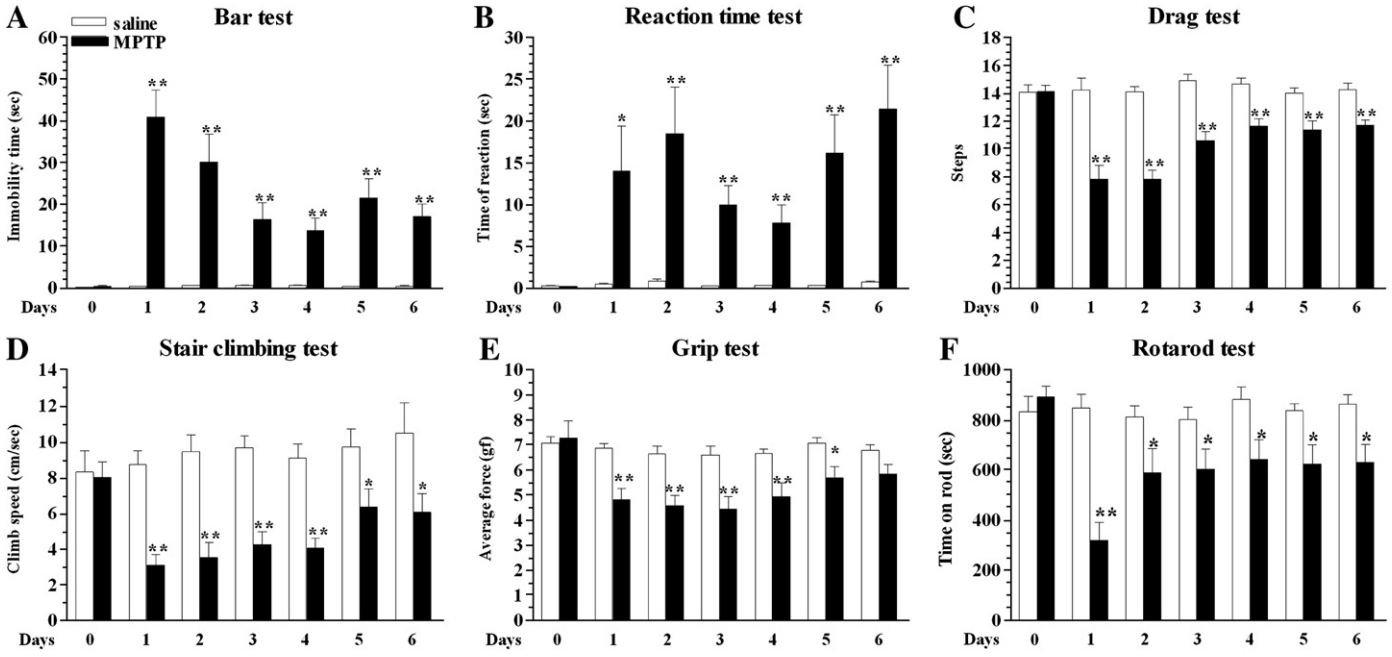

Fig. 2. MPTP-treatment induced akinesia and bradykinesia in mice. (A–F) Systemic administration of MPTP increased the immobility and reaction time (in seconds; bar and reaction time tests; A, B) and decreased the number of steps (drag test; C), the climbing speed (stair climbing test; cm/s; D), the pulling force (grip test; gram force; E) and the time spent on the rod (in seconds, rotarod test; F). All tests were performed before and after (daily for 6 days) MPTP-treatment. Data are means ± SEM of 10 determinations per group. $*p<0.05$, $**p<0.01$ different from saline (RM ANOVA followed by contrast analysis and the sequentially rejective Bonferroni's test for multiple comparisons).

($F_{6,6}=1.74$, $p=0.26$), and a significant time × treatment interaction ($F_{6,108}=7.97$, $p=0.012$). Post hoc analysis revealed that MPTP caused a slight reduction (~16%) of hindpaw stride length. A parallel impairment was detectable by measuring forepaw stride length (data not shown).

Stride width

RM ANOVA on stride width values (Fig. 1B) showed a significant effect of treatment ($F_{1,9}=60.38$, $p<0.001$), but not time ($F_{6,6}=2.46$, $p=0.14$), and a nonsignificant time × treatment interaction ($F_{6,108}=2.57$, $p=0.14$). Post hoc analysis revealed that MPTP caused a long lasting increase (~20%) of hindpaw stride width.

Overlap

RM ANOVA on overlap values (Fig.1C) showed a significant effect of treatment ($F_{1,9}=19.79$, $p=0.002$), but not time ($F_{6,6}=0.94$, $p=0.54$) and a nonsignificant time × treatment interaction ($F_{6,108}=3.81$, $p=0.064$). Post hoc analysis revealed that MPTP caused a mismatch in the overlap of the ipsilateral paw that showed a tendency to recover over time.

Angle

RM ANOVA on placement angle values (Fig. 1D) showed a significant effect of treatment ($F_{1,9}=36.06$, $p<0.001$), but not time ($F_{6,6}=1.56$, $p=0.30$), and a nonsignificant time × treatment interaction ($F_{6,108}=3.04$, $p=0.10$). Post hoc analysis revealed that MPTP caused a stable increase in the angle amplitude between hindpaws and the main direction.

Speed

RM ANOVA on speed values (Fig. 1E) showed a significant effect of treatment ($F_{1,9}=29.09$, $p<0.001$), but not time ($F_{6,6}=0.47$, $p=0.81$), and a significant time × treatment interaction ($F_{6,108}=4.83$, $p=0.039$). Post hoc analysis revealed that MPTP caused a marked decrease of running speed, which was almost halved with respect to saline-treated animals.

MPTP induced loss of TH staining in the striatum

Seven days after treatment, MPTP-treated mice displayed partial (~60%) bilateral loss of TH-positive DA terminals compared to vehicle-injected mice (Figs. 3A–C).

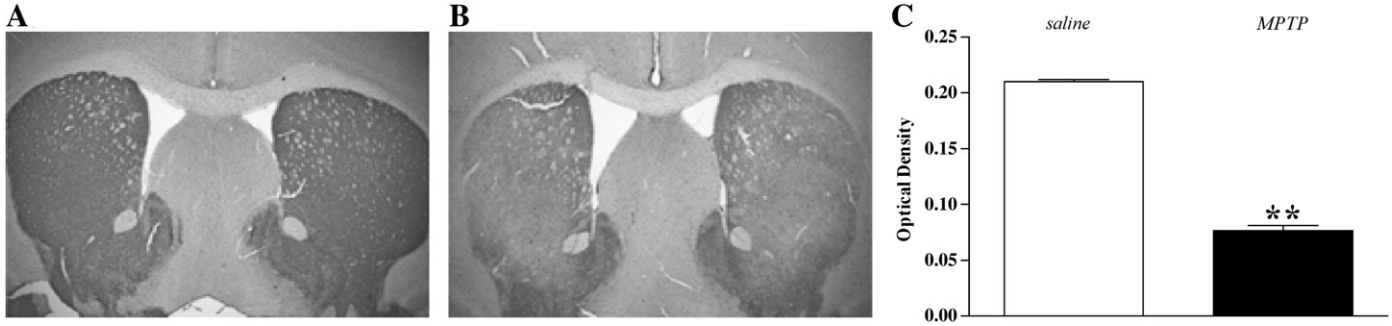

Fig. 3. MPTP-treatment reduced the tyrosine hydroxylase (TH)-positive (TH^+) fiber density in the mouse striatum. (A–B) Photomicrographs of TH^+ fibers in the striatum of a saline (A) and MPTP-treated (B) mouse. (C) Optical density of TH^+ fibers in the striatum. Data are means ± SEM of 10 determinations per group. $**p<0.01$ different from saline (Student's *t*-test).

Pharmacological treatments in MPTP-treated mice (experiment #2)

To investigate whether the MPTP-induced phenotype was generated by DA deficiency, the ability of DA agonists (i.e. L-dopa and pramipexole) to attenuate motor deficit was investigated. The novel NOP receptor antagonist Trap-101 was also tested since this compound was found effective in promoting movement in 6-OHDA hemilesioned rats (Marti et al., 2008). Animals were challenged in the bar, drag and rotarod test only.

L-Dopa

L-Dopa dually modulated motor performance, causing motor facilitation at low doses (1–10 mg/kg) and inhibition (or no effect) at higher ones (100 mg/kg).

Bar test

RM ANOVA on bar test values (Fig. 4A) showed a significant effect of treatment ($F_{4,28}=25.27$, $p<0.001$) but not time ($F_{1,4}=0.03$, $p=0.86$) and a nonsignificant time × treatment interaction ($F_{4,29}=0.40$, $p=0.80$). Post hoc analysis revealed that L-dopa caused dual and prolonged changes of immobility time, namely a reduction at 10 mg/kg and an increase at 100 mg/kg.

Drag test

RM ANOVA on drag test values (Fig. 4B) showed a significant effect of treatment ($F_{4,28}=12.45$, $p<0.001$), but not time ($F_{1,4}=0.02$, $p=0.87$) and a nonsignificant time × treatment interaction ($F_{4,29}=1.16$, $p=0.34$). Post hoc analysis revealed that L-dopa elevated the number of steps at 1 and 10 mg/kg, being ineffective at higher doses. The effect of 1 mg/kg was transient whereas that produced by 10 mg/kg was detected also 60 min after injection.

Rotarod test

RM ANOVA on rotarod test values (Fig. 4C) showed a significant effect of treatment ($F_{4,28}=133.25$, $p<0.0001$) but not time ($F_{1,4}=0.14$, $p=0.71$) and a nonsignificant time × treatment interaction ($F_{4,29}=0.19$, $p=0.94$). Post hoc analysis revealed that L-dopa increased motor performance at 10 mg/kg and reduced it at 100 mg/kg. These effects were long lasting.

Since L-dopa was administered in combination with benserazide (ratio 4:1), benserazide alone was tested at the highest does (25 mg/kg). Benserazide did not affect motor performance with respect to saline (data not shown).

Pramipexole

Different from L-dopa, pramipexole effects were strictly dependent on dose and test used. Low doses (0.0001–0.001 mg/kg) promoted performance in the drag test but did not affect that in the bar and rotarod test. Conversely, higher doses (0.01–0.1 mg/kg) caused inhibition in the bar and rotarod test being mildly effective or ineffective in the drag test.

Bar test

RM ANOVA on bar test values (Fig. 4D) showed a significant effect of treatment ($F_{4,24}=5.18$, $p=0.003$) and time ($F_{1,4}=6.05$, $p=0.019$) but not a significant time × treatment interaction ($F_{4,32}=1.32$, $p=0.28$). Post hoc analysis revealed that pramipexole 0.01 and 0.1 mg/kg increased the immobility time, although the effect of the lower dose appeared only 60 min after injection. Lower pramipexole doses were ineffective.

Drag test

RM ANOVA on drag test values (Fig. 4E) showed a significant effect of treatment ($F_{4,24}=10.25$, $p=0.0001$), but not time ($F_{1,4}=0.22$,

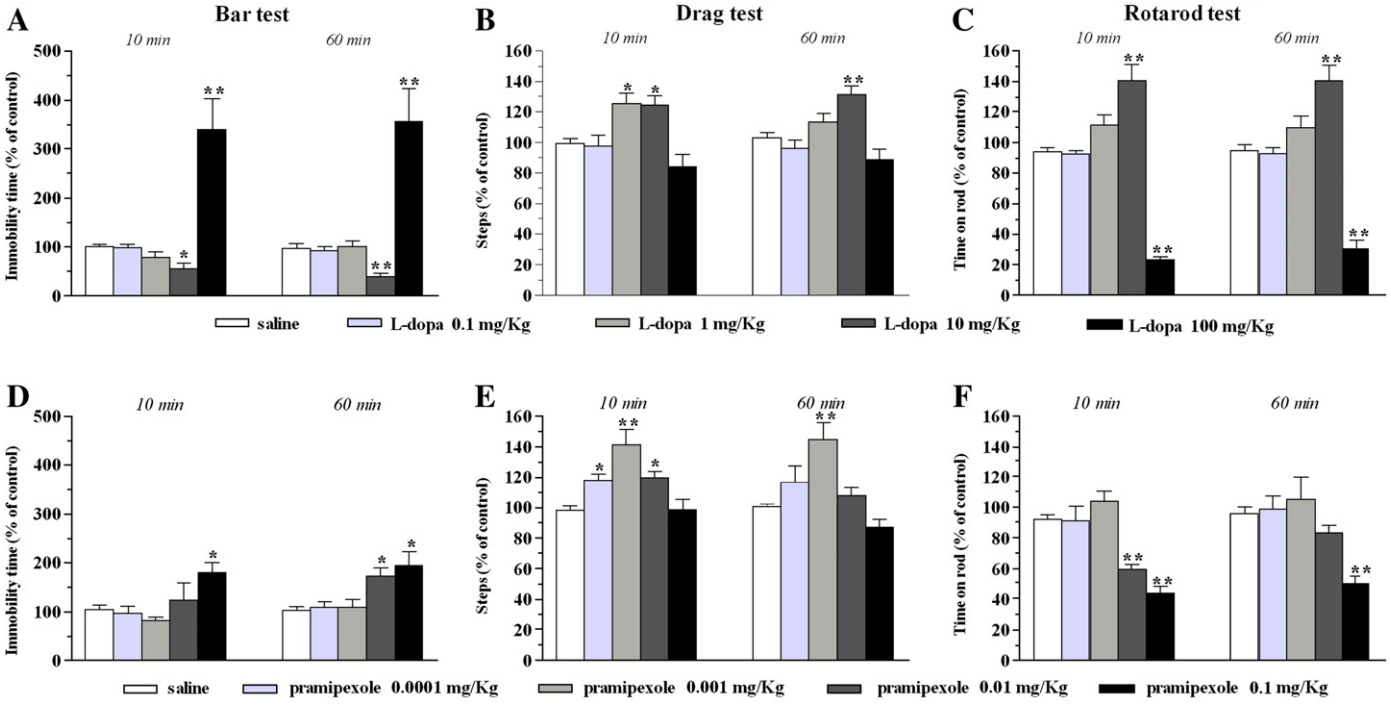

Fig. 4. Dopamine agonists attenuated parkinsonian symptoms in MPTP-treated mice. (A–F) Systemic administration of L-dopa (0.1–100 mg/kg, i.p.) or pramipexole (0.0001–0.1 mg/kg, i.p.) affected the immobility time in the bar test (A, D), the number of steps in the drag test (B, E) and the time spent on the rod in the rotarod test (C, F). All tests were performed at 7 days after MPTP administration, before (control session) and after (10 and 60 min) drug injection. Data are means ± SEM of 7–8 determinations per group and were calculated as percentage of the control session. *$p<0.05$, **$p<0.01$ different from saline (RM ANOVA followed by contrast analysis and the sequentially rejective Bonferroni's test for multiple comparisons).

Please cite this article as: Viaro, R., et al., Dual motor response to L-dopa and nociceptin/orphanin FQ receptor antagonists in 1-methyl-4-phenyl-1,2,5,6-tetrahydropyridine (MPTP) traeted mice: Paradoxical..., Exp. Neurol. (2010), doi:10.1016/j.expneurol.2010.01.014

$p=0.63$) and a nonsignificant time×treatment interaction ($F_{4,32}=1.39$, $p=0.25$). Post hoc analysis revealed that pramipexole elevated the number of steps in the 0.0001–0.01 mg/kg dose range but was ineffective at higher doses (0.1 mg/kg). Only the facilitation induced by 0.001 mg/kg was long lasting.

Rotarod test

RM ANOVA on rotarod test values (Fig. 4F) showed a significant effect of treatment ($F_{4,24}=13.04$, $p<0.001$) and time ($F_{1,4}=6.76$, $p=0.014$) but not a significant time×treatment interaction ($F_{4,32}=1.47$, $p=0.23$). Post hoc analysis revealed that pramipexole was ineffective up to 0.001 mg/kg while it impaired motor performance at 0.01 and 0.1 mg/kg.

Trap-101

Similar to pramipexole, Trap-101 caused motor changes that were dependent on dose and test used. Low doses (0.001–0.1 mg/kg) facilitated motor activity in the bar and drag test being ineffective in the rotarod test. Higher doses caused (mild) inhibition of rotarod performance being otherwise ineffective.

Bar test

RM ANOVA on bar test values (Fig. 5A) showed a significant effect of treatment ($F_{4,24}=7.96$, $p=0.0003$), time ($F_{1,4}=15.18$, $p=0.0005$) and a nonsignificant time×treatment interaction ($F_{4,32}=1.26$, $p=0.31$). Post hoc analysis revealed that Trap-101 caused a transient reduction of immobility time at 0.01 and 0.1 mg/kg but was ineffective at 1 mg/kg.

Drag test

RM ANOVA on drag test values (Fig. 5B) showed a significant effect of treatment ($F_{4,24}=10.44$, $p<0.0001$), but not time ($F_{1,4}=0.92$, $p=0.34$) and a nonsignificant time×treatment interaction ($F_{4,32}=2.06$, $p=0.11$). Post hoc analysis revealed that Trap-101 elevated the number of steps in the 0.001–0.1 mg/kg dose range, being ineffective at 1 mg/kg. Only the facilitation induced by Trap-101 0.1 mg/kg was detected at 60 min after injection.

Rotarod test

RM ANOVA on rotarod test values (Fig. 5C) showed a significant effect of treatment ($F_{4,24}=3.47$, $p=0.022$) but not time ($F_{1,4}=1.87$, $p=0.18$) and a nonsignificant time×treatment interaction ($F_{4,32}=0.86$, $p=0.49$). Post hoc analysis revealed that Trap-101 was ineffective up to 0.1 mg/kg and transiently reduced rotarod performance at 1 mg/kg.

Interaction between DA agonists and Trap-101

We previously demonstrated (Marti et al., 2007, 2008) that co-administration of L-dopa and J-113397 or Trap-101 produced additive attenuation of parkinsonism in 6-OHDA hemilesioned rats. Therefore, we first tested whether low doses of L-dopa (1 mg/kg) and Trap-101 (0.001 mg/kg) could synergistically or additively attenuate parkinsonism in MPTP-treated mice. Indeed, synergistic interaction was observed in the bar test (where both compounds were ineffective alone) whereas additive interaction were observed in the drag test (where both compounds were effective alone). No interaction was observed in the rotarod test.

Bar test

RM ANOVA on bar test values (Fig. 6A) showed a significant effect of treatment ($F_{3,18}=3.27$, $p=0.045$), time ($F_{1,3}=8.52$, $p=0.007$) and a nonsignificant time×treatment interaction ($F_{3,26}=0.78$, $p=0.51$). Post hoc analysis revealed that L-dopa and Trap-101 alone were ineffective whereas their combination reduced the immobility time. This effect was observed only at 10 min after injection.

Drag test

RM ANOVA on drag test values (Fig. 6B) showed a significant effect of treatment ($F_{3,18}=12.24$, $p<0.001$), but not time ($F_{1,3}=3.23$, $p=0.083$) and a nonsignificant time×treatment interaction ($F_{3,26}=1.73$, $p=0.18$). Post hoc analysis at 10 min after injection revealed that L-dopa and Trap-101 slightly increased the number of steps, their combination producing an additive effect. The combination effect was even more evident at 60 min, since both compounds were ineffective alone.

Rotarod test

No change in rotarod performance was observed after administration of low doses of L-dopa and Trap-101, either alone or in combination (Fig. 6C).

We then co-administered low doses of pramipexole (0.0001 mg/kg) and Trap-101 (0.001 mg/kg). Additive interaction was observed in the drag test, the combination being otherwise ineffective.

Bar test

No change in immobility time was observed after administration of pramipexole and Trap-101, alone or in combination (Fig. 6D).

Drag test

RM ANOVA on drag test values (Fig. 6E) showed a significant effect of treatment ($F_{3,18}=7.69$, $p=0.002$), but not time ($F_{1,3}=0.88$,

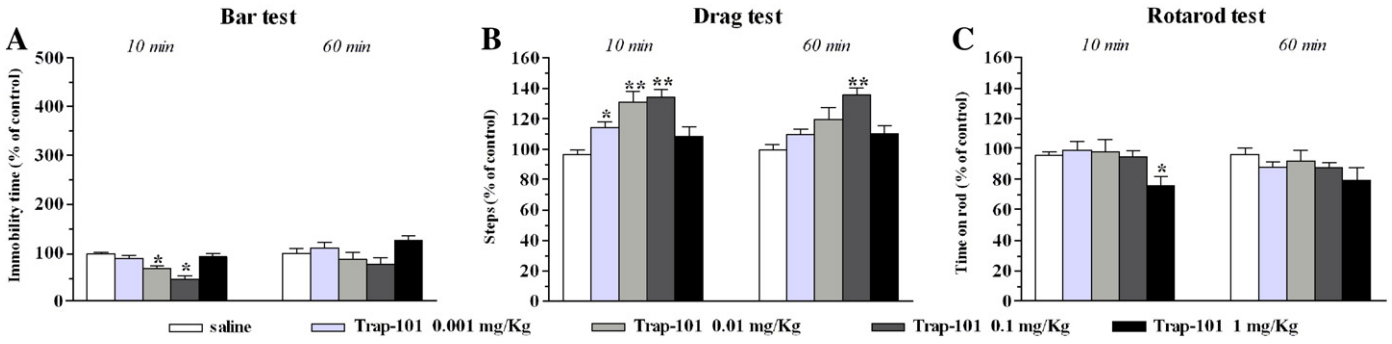

Fig. 5. Trap-101 attenuated parkinsonian symptoms in MPTP-treated mice. (A–C) Systemic administration of Trap-101 (0.001–1 mg/kg, i.p.) affected the immobility time in the bar test (A), the number of steps in the drag test (B) and the time spent on the rod in the rotarod test (C). All tests were performed at 7 days after MPTP administration, before (control session) and after (10 and 60 min) drug injection. Data are means ± SEM of 7–8 determinations per group and were calculated as percentage of the control session. *$p<0.05$, **$p<0.01$ different from saline (RM ANOVA followed by contrast analysis and the sequentially rejective Bonferroni's test for multiple comparisons).

Please cite this article as: Viaro, R., et al., Dual motor response to L-dopa and nociceptin/orphanin FQ receptor antagonists in 1-methyl-4-phenyl-1,2,5,6-tetrahydropyridine (MPTP) traeted mice: Paradoxical..., Exp. Neurol. (2010), doi:10.1016/j.expneurol.2010.01.014

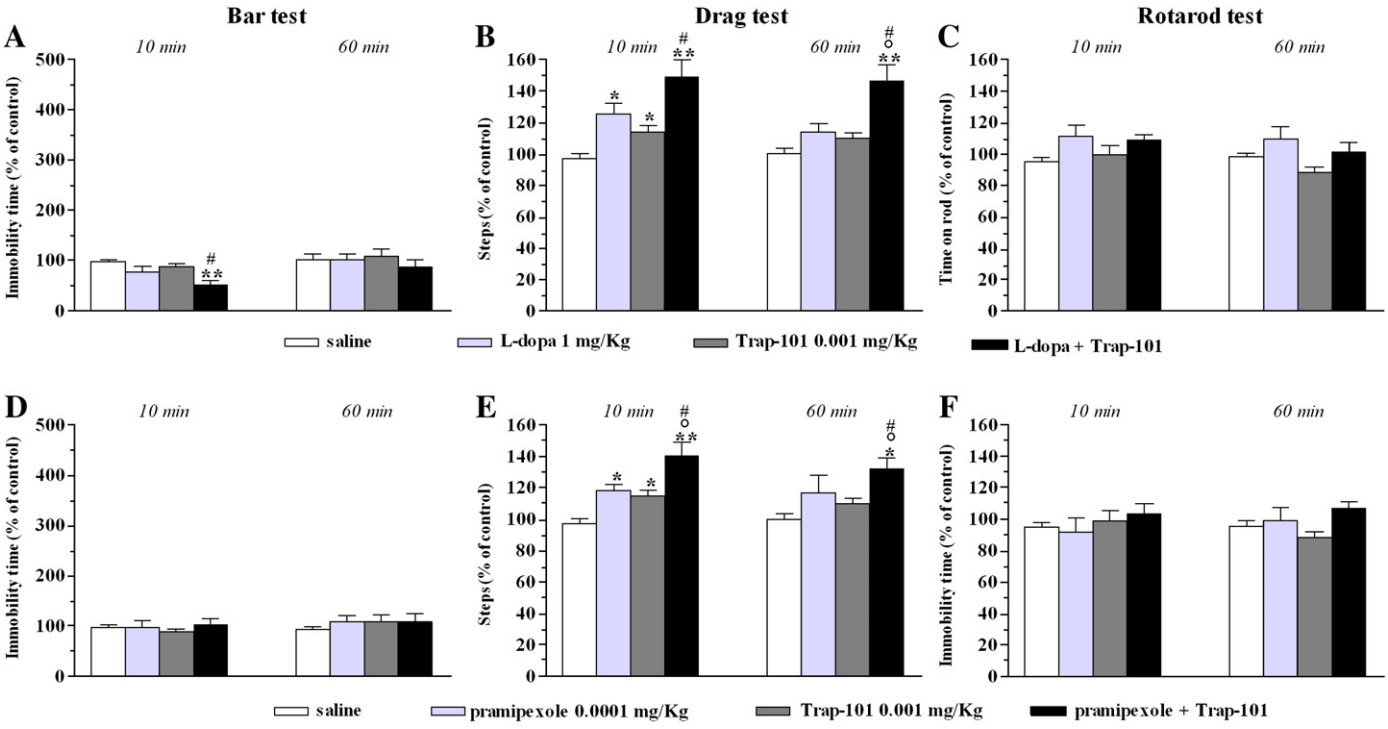

Fig. 6. Combination of L-dopa and pramipexole with Trap-101 synergistically or additively attenuated parkinsonian symptoms in MPTP-treated mice. (A–C) Combined administration of L-dopa (1 mg/kg, i.p.) and Trap-101 (0.001 mg/kg, i.p.) affected the immobility time in the bar test (A) and the number of steps in the drag test (B) but not the time spent on the rod in the rotarod test (C). (D–F) Combined administration of pramipexole (0.0001 mg/kg, i.p.) and Trap-101 (0.001 mg/kg, i.p.) affected only the number of steps in the drag test (E) but not the immobility time in the bar test (D) and the time spent on the rod in the rotarod test (F). All tests were performed at 7 days after MPTP administration, before (control session) and after (10 and 60 min) drug injection. Data are means ± SEM of 7–8 determinations per group and were calculated as percentage of the control session. $^{*}p<0.05$, $^{**}p<0.01$ different from saline; $^{\circ}p<0.05$ different from L-dopa; $^{\#}p<0.05$ different from Trap-101 (RM ANOVA followed by contrast analysis and the sequentially rejective Bonferroni's test for multiple comparisons).

$p = 0.35$) and a nonsignificant time × treatment interaction ($F_{3,26} = 0.53$, $p = 0.66$). Post hoc analysis at 10 min revealed that pramipexole and Trap-101 transiently elevated the number of steps, while their combination produced a greater (additive) and sustained improvement.

Rotarod test

No change in rotarod performance was observed after administration of subthreshold doses of pramipexole and Trap-101, either alone or in combination (Fig. 6F).

Amisulpride prevented hypomotility induced by L-dopa and NOP receptor antagonist

Pramipexole is known to depress motor activity (Mierau and Schingnitz, 1992; Maj et al., 1997; Siuciak and Fujiawara, 2004), likely via stimulation of presynaptic D_{2S} (short isoform) autoreceptors (Usiello et al., 2000; Vallone et al., 2000). We therefore tested the hypothesis that motor inhibition induced by L-dopa and pramipexole could be reversed by the D_2/D_3 receptor antagonist amisulpride. Indeed, this antagonist preferentially binds to D_2 autoreceptors at low doses (Scatton et al., 1997; Perrault et al., 1997; Schoemaker et al., 1997). To investigate the DA-dependence of the motor inhibition produced by NOP receptor blockade, we used J-113397 instead of Trap-101 since, differently from Trap-101, J-113397 caused marked motor inhibition also in the bar test (Viaro et al., 2008). The effect of amisulpride alone was first assessed in a dose-finding study. Amisulpride caused consistent motor inhibition in the three tests at 0.5 and 5 mg/kg.

Bar test

RM ANOVA on bar test values (Fig. 7A) showed a significant effect of treatment ($F_{3,15} = 31.30$, $p<0.001$) but not time ($F_{1,3} = 0.01$, $p = 0.97$), and a nonsignificant time × treatment interaction ($F_{3,20} = 0.37$, $p = 0.77$). Post hoc analysis revealed that amisulpride caused a prolonged increase of immobility time at the highest dose tested (5 mg/kg).

Drag test

RM ANOVA on drag test values (Fig. 7B) showed a significant effect of treatment ($F_{3,15} = 13.24$, $p<0.001$), but not time ($F_{1,3} = 3.55$, $p = 0.07$) and a nonsignificant time × treatment interaction ($F_{3,20} = 0.42$, $p = 0.74$). Post hoc analysis revealed that amisulpride caused a prolonged reduction in stepping activity at 5 mg/kg.

Rotarod test

RM ANOVA on rotarod test values (Fig. 7C) showed a significant effect of treatment ($F_{3,15} = 19.03$, $p<0.001$) but not time ($F_{1,3} = 1.17$, $p = 0.29$) and a nonsignificant time × treatment interaction ($F_{3,20} = 0.62$, $p = 0.62$). Post hoc analysis revealed that amisulpride caused sustained motor impairment at 0.5 and 5 mg/kg, which could be detected also at 60 min after injection.

Based on these preliminary findings we selected an ineffective dose of amisulpride (0.1 mg/kg) and challenged it with motor inhibiting doses of L-dopa (100 mg/kg), pramipexole (0.1 mg/kg) or J-113397 (1 mg/kg). The outcome of the interaction was dependent on compound and test used. Essentially, amisulpride prevented (or reversed into facilitation) motor inhibition induced by L-dopa and J-113397 in the bar and rotarod test, being ineffective against pramipexole. Moreover, in the presence of amisulpride, high (ineffective) doses of J-113397 were able to increase stepping activity in the drag test.

Bar test

RM ANOVA on bar test values (Fig. 7D) showed a significant effect of treatment ($F_{7,35} = 24.13$, $p<0.001$), but not time ($F_{1,7} = 1.10$, $p = 0.29$) and a nonsignificant time × treatment interaction ($F_{7,40} = 1.03$,

Please cite this article as: Viaro, R., et al., Dual motor response to L-dopa and nociceptin/orphanin FQ receptor antagonists in 1-methyl-4-phenyl-1,2,5,6-tetrahydropyridine (MPTP) traeted mice: Paradoxical..., Exp. Neurol. (2010), doi:10.1016/j.expneurol.2010.01.014

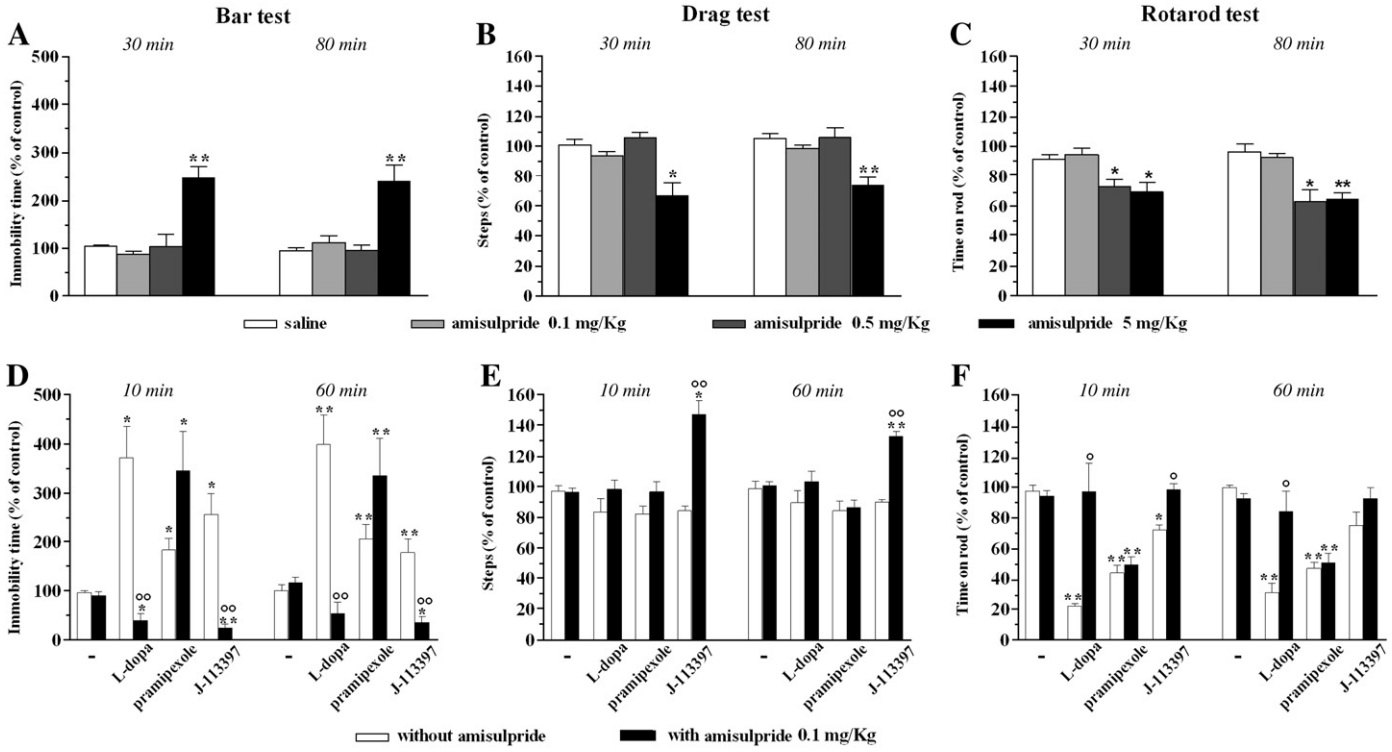

Fig. 7. Amisulpride prevented motor inhibition induced by high doses of L-dopa and J-113397 but not pramipexole in MPTP-treated mice. (A–C) Systemic administration of amisulpride (0.1–5 mg/kg, i.p.) increased the immobility time in the bar test (A), reduced the number of steps in the drag test (B) and the time spent on the rod in the rotarod test (C). (D–F) Twenty minute pretreatment with amisulpride (0.1 mg/kg, i.p.) differentially affected motor inhibition induced by L-dopa (100 mg/kg, i.p.) and J-113397 (1 mg/kg, i.p.) in the bar (D), drag (E) and rotarod (F) test but was ineffective against hypomotility induced by pramipexole (0.1 mg/kg; i.p.). (A–F) All tests were performed at 7 days after MPTP administration, before (control session) and after (10 and 60 min) L-dopa, pramipexole and J-113397 administration. When amisulpride were tested alone, behavioral testing was performed 30 and 80 min after administration. Data are means ± SEM of six determinations per group and were calculated as percentage of the control session. *$p<0.05$, **$p<0.01$ different from saline; °$p<0.05$, °°$p<0.01$ different from amisulpride alone (RM ANOVA followed by contrast analysis and the sequentially rejective Bonferroni's test for multiple comparisons).

$p = 0.43$). Post hoc analysis revealed that motor inhibition caused by L-dopa (100 mg/kg) and J-113397 (1 mg/kg) was reversed into facilitation in the presence of amisulpride. Conversely, amisulpride did not prevent the effect of pramipexole.

Drag test

RM ANOVA on drag test values (Fig. 7E) showed a significant effect of treatment ($F_{7,35} = 11.25$, $p<0.001$), but not time ($F_{1,7} = 0.02$, $p = 0.89$) and a nonsignificant time × treatment interaction ($F_{7,40} = 0.15$, $p = 0.99$). Post hoc analysis revealed that L-dopa and pramipexole were ineffective either alone or in combination with amisulpride. Conversely, J-113397, ineffective alone, caused a prolonged increase in stepping activity in the presence of amisulpride.

Rotarod test

RM ANOVA on rotarod test values (Fig. 7F) showed a significant effect of treatment ($F_{7,35} = 15.64$, $p<0.001$) but not time ($F_{1,7} = 0.01$, $p = 0.99$) and a nonsignificant time × treatment interaction ($F_{7,40} = 1.14$, $p = 0.36$). Post hoc analysis revealed that motor impairment caused by L-dopa (100 mg/kg) and J-113397 (1 mg/kg) was prevented by amisulpride. However, amisulpride failed to attenuate the impairment in rotarod performance induced by pramipexole.

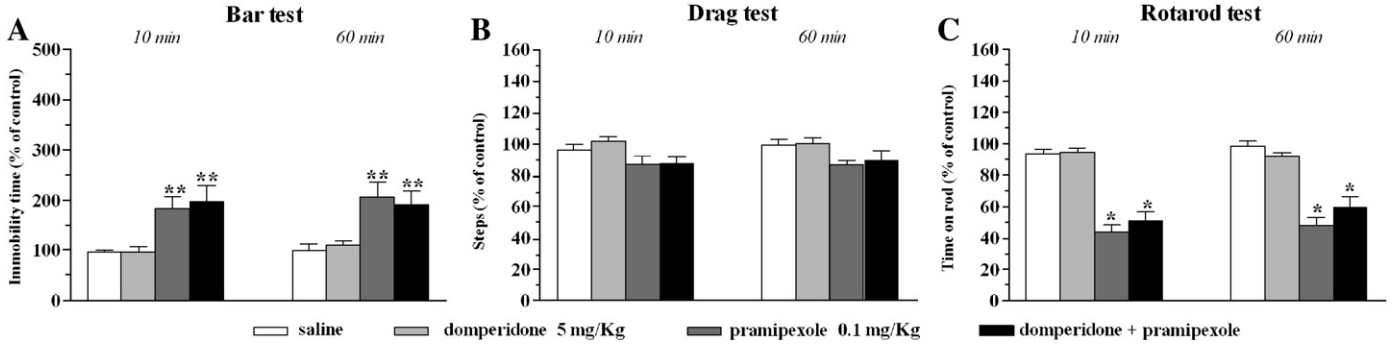

Fig. 8. Motor inhibition induced by pramipexole was insensitive to domperidone in MPTP-treated mice. (A–C) Twenty minute pretreatment with domperidone (5 mg/kg, i.p.) did not attenuate motor inhibition caused by pramipexole (0.1 mg/kg, i.p.) in the bar (A), drag (B) and rotarod (C) test. All tests were performed at 7 days after MPTP administration, before (control session) and after (10 and 60 min) pramipexole administration. When domperidone was tested alone, behavioral testing was performed 30 and 80 min after administration. Data are means ± SEM of six determinations per group and were calculated as percentage of the control session. *$p<0.05$, **$p<0.01$ different from saline (RM ANOVA followed by contrast analysis and the sequentially rejective Bonferroni's test for multiple comparisons).

Please cite this article as: Viaro, R., et al., Dual motor response to L-dopa and nociceptin/orphanin FQ receptor antagonists in 1-methyl-4-phenyl-1,2,5,6-tetrahydropyridine (MPTP) traeted mice: Paradoxical..., Exp. Neurol. (2010), doi:10.1016/j.expneurol.2010.01.014

We finally tested whether the pramipexole-induced hypolocomotion had a peripheral origin. The peripheral DA receptor antagonist domperidone (5 mg/kg) alone failed to affect the immobility time (Fig. 8A), number of steps (Fig. 8B) or rotarod performance (Fig. 8C) and was not able to counteract the inhibitory effect of pramipexole.

Discussion

Motor phenotype in MPTP-treated mice

The use of a broad range of motor tasks allowed for the collection of information on different motor parameters in MPTP-treated mice such as the time required to initiate (akinesia) and execute (bradykinesia) a movement, muscle strength, gait patterns and coordinated motor performance in freely moving or exercise-driven conditions. These tests showed that the MPTP-induced bilateral partial (~60%) lesions of striatal DA terminals was associated with an increase of immobility and reaction time, a reduction of stepping activity, climbing speed, time on rod and muscle strength, as well as gait abnormalities such as reduced stride length and increased stride width. Consistent with the evidence that loss of nigral DA cells and striatal DA terminal is maximal at 2 and 7 days after MPTP, respectively (Sundström et al., 1988), motor deficits were maximal the day following MPTP administration and subsided 3–4 days afterward, being still detectable a week later. These observations are in line with studies reporting reduced performance in the bar (Kato et al., 2004; Watanabe et al., 2008) and treadmill (Petzinger et al., 2007) tests as well as gait abnormalities in the footprinting test (Tillerson et al., 2002) at 7 days after MPTP intoxication. The evidence of a parkinsonian-like phenotype at 7 days after intoxication was further confirmed by positive response to DA agonists.

Response to DA agonists

L-Dopa (1–10 mg/kg) attenuated MPTP-induced motor impairment in the bar, drag and rotarod tests. Consistently, L-dopa (15–20 mg/kg) attenuated hypoactivity (Fredriksson et al., 1990; Sundström et al., 1990) and gait abnormalities (Tillerson et al., 2002) in mice at 7 days after MPTP administration. These data also confirm previous findings in 6-OHDA hemilesioned rats (Marti et al., 2005, 2007) though L-dopa was overall more potent (effective yet at 0.1 mg/kg) possibly due to greater striatal denervation in this model (~95%). Motor testing however disclosed paradoxical effects of L-dopa, high doses causing exacerbation of parkinsonism. This is the first evidence for a dual motor response to L-dopa in a model of parkinsonism. Nonetheless, opposite dose-dependent effects of L-dopa on sleep have been detected in MPTP-treated mice (Laloux et al., 2008), and a biphasic effect on pain (hyperalgesia followed by antinociception) was described in naïve rats at high L-dopa doses (Paalzow, 1992). Interestingly, antinociception was reversed by the D_2 receptor antagonist sulpiride and the catecholamine depletor alpha-methyl-*p*-tyrosine, suggesting its dependence on presynaptic mechanisms.

Extending previous findings in 6-OHDA hemilesioned or reserpinized rats, reserpinized mice and MPTP-treated non human primates (Mierau and Schingnitz, 1992; Maj et al., 1997), pramipexole exerted symptomatic antiparkinsonian effects in MPTP-treated mice by promoting stepping in the drag test. This effect was observed at very low doses (0.0001–0.001 mg/kg) but vanished at higher ones (0.1 mg/kg). In fact, overt motor inhibition in the bar and rotarod tests emerged at this dose. As for L-dopa, this dual response has not been previously reported for pramipexole. Nonetheless, a dual effect of DA receptor agonists cabergoline and bromocriptine on spontaneous locomotion in mice made hypoactive with MPTP has been described, low doses being facilitatory and higher ones inhibitory (Archer et al., 2003).

A possible explanation of the dual motor responses of pramipexole (and L-dopa) calls for a different contribution of D_2 pre- and postsynaptic receptors. Indeed, pramipexole (0.001–1 mg/kg) causes hypolocomotion in naïve mice via stimulation of D_2 autoreceptors (Mierau and Schingnitz, 1992; Maj et al., 1997, Siuciak and Fujiawara, 2004) of the D_{2S} isoform (Usiello et al., 2000; Vallone et al., 2000). However, under parkinsonian conditions, DA deafferentation causes compensatory supersensitvity in striatal postsynaptic D_2 receptors, which allows DA agonists to promote movement (Seeman, 2007) outweighing the negative contribution of D_2 autoreceptors. Since compensatory increase in striatal D_2 receptor binding has been detected at 7 days after MPTP (Smith et al., 1997), it may be speculated that the increased stepping activity observed with low doses of pramipexole and L-dopa is mediated by stimulation of striatal postsynaptic D_2 receptors while the hypokinesia induced by higher doses reflects progressive recruitment of D_2 autoreceptors, leading to reduction in DA release. This possibility may be further underpinned by experiments with amisulpride. Amisulpride is an atypical neuroleptic reported to inhibit D_2 autoreceptors at low doses and block postsynaptic D_2 receptors at higher ones (Scatton et al., 1997; Perrault et al., 1997; Schoemaker et al., 1997). Indeed, amisulpride caused overt motor impairment in MPTP-treated mice, an effect reported for other D_2 receptor antagonists in this model (Weihmuller et al., 1990), and related to the blockade of D_{2L} (long isoform) postsynaptic striatal receptors (Wang et al., 2000). However, at lower doses, per se ineffective on motor activity, amisulpride prevented the motor inhibition induced by L-dopa. This may suggest that high L-dopa doses not only activate D_2 postsynaptic receptors but also D_2 autoreceptors, leading to a reduction of neurosecretion and firing activity at DA pathways. Consistent with this view, low doses of L-dopa elevated striatal DA levels in reserpinized rats while higher ones (100 mg/kg) were ineffective (Fisher et al., 2000). In this context, reversal of L-dopa motor inhibition into facilitation (bar test) by amisulpride may be explained on the basis of a removal of D_2 autoreceptor inhibition leading to disclosure of a D_2 postsynaptic facilitation. The possibility that high L-dopa doses cause hypolocomotion by recruiting populations of amisulpride-sensitive postsynaptic receptors should also be considered. Amisulpride is a D_2/D_3 receptor selective antagonist with high affinity at 5-HT_{2B} and 5-HT_{7A} receptors (Schoemaker et al., 1997; Abbas et al., 2009). The involvement of 5-HT receptors in L-dopa hypolocomotion appears remote in view of the fact that 5-HT_2 receptors stimulate locomotion whereas 5-HT_7 receptors do not influence it (Millan et al., 2003; Clemett et al., 1998). However, D_3 receptors have been shown to inhibit locomotion (Sautel et al., 1995; Pritchard et al., 2007; Mela et al., 2010). It should also be considered that amisulpride displays some limbic selectivity (Schoemaker et al., 1997), suggesting that L-dopa hypolocomotion may be due to impact on subpopulations of "normosensitive" D_2 receptors located in (extrastriatal) areas in which DA transmission has been less impacted by MPTP.

The failure of amisulpride in preventing pramipexole-induced hypolocomotion remains puzzling. One possible reason could be a suboptimal antagonist/agonist dose ratio, in view of the poor brain penetrability of amisulpride (Assié et al., 2006) and the different mechanisms of action of L-dopa and pramipexole. L-Dopa replenishes DA stores, favoring synaptic DA release via activity-dependent mechanisms and activation of a full set of DA receptors (D_1–D_5) while pramipexole is a D_3/D_2 selective agonist with preferential action on extrasynaptic (Pickel et al., 2002) D_2 autoreceptors (Mierau and Schingnitz, 1992). Moreover, differently from pramipexole, L-dopa may also operate those populations of D_2 receptors whose activity is enabled by D_1 receptor coupling (Clark and White, 1987).

Response to NOP receptor antagonists

The novel NOP receptor antagonist Trap-101 is a J-113397 derivative with 3-fold lower selectivity and potency at recombinant NOP receptors but comparable activity at native NOP receptors, and

Please cite this article as: Viaro, R., et al., Dual motor response to L-dopa and nociceptin/orphanin FQ receptor antagonists in 1-methyl-4-phenyl-1,2,5,6-tetrahydropyridine (MPTP) traeted mice: Paradoxical..., Exp. Neurol. (2010), doi:10.1016/j.expneurol.2010.01.014

similar selectivity for NOP over classical opioid receptors (Trapella et al., 2006). Consistently, Trap-101 and J-113397 attenuated parkinsonism and enhanced the antiparkinsonian action of L-dopa in 6-OHDA hemilesioned rats through blockade of NOP receptors located in SNr and overinhibition of nigro-thalamic transmission (Marti et al., 2007, 2008). The present study demonstrates that Trap-101 also shares with J-113397 (Viaro et al., 2008) the ability to improve parkinsonism in MPTP-treated mice. In addition, Trap-101 synergistically or additively (depending on test) attenuated MPTP-induced akinesia/bradykinesia when combined with L-dopa and pramipexole. The antiparkinsonian action of Trap-101 appeared at much lower doses (0.001–0.1 mg/kg) than those effective in promoting movement naïve mice (1–10 mg/kg; Marti et al., 2008), suggesting that MPTP caused a leftward shift of the Trap-101 dose–response curve. Increased sensitivity to J-113397 was previously observed in both 6-OHDA hemilesioned rats (Marti et al., 2005, 2008) and MPTP mice and nonhuman primates (Viaro et al., 2008) and may be related to up-regulation of N/OFQ transmission following DA depletion (Marti et al., 2005; Di Benedetto et al., 2009).

A major concern regarding possible clinical use of NOP receptor antagonists was that high doses of J-113397 caused motor inhibition in MPTP-treated mice and nonhuman primates (Viaro et al., 2008). The present study sheds some light on this phenomenon. Indeed, as for L-dopa, amisulpride reversed the pro-akinetic effect of J-113397 and prevented its inhibition of rotarod performance. In addition, it disclosed a J-113397-mediated facilitation in the drag test. This suggests that motor inhibition induced by NOP receptor antagonists is mediated by endogenous DA. Consistently, NOP receptor antagonists were capable of increasing striatal DA release in naïve rats, revealing a tonic inhibitory influence of endogenous N/OFQ over nigro-striatal DA transmission (Marti et al., 2004). In mice, however, there is no firm evidence that NOP receptor blockade elevates striatal DA release. Indeed, UFP-101 (a peptide NOP receptor antagonist) elevated accumbal DA levels but via NOP-independent mechanisms (Koizumi et al., 2004). Nonetheless, the possibility that NOP receptor blockade elevates DA levels in other motor areas cannot be ruled out.

Concluding remarks

Motor phenotype of mice acutely treated with MPTP was monitored daily using a broad range of behavioral tests. Specifically, the drag test (a test for akinesia/bradykinesia) revealed that MPTP-induced motor deficit was attenuated by classical antiparkinsonian drugs such as L-dopa and pramipexole. This test appeared most predictive of antiparkinsonian activity and suitable to screen for novel antiparkinsonian drugs (also) in the MPTP model. Possibly relevant from a clinical perspective, the present study provides evidence that L-dopa can cause paradoxical worsening of motor performances at high doses. Responsiveness to L-dopa and DA agonists is a diagnostic criterion for idiopathic PD. However, reports that L-dopa can exacerbate symptoms, especially in those patients suffering from parkinsonism, have been published (Wiener et al., 1978; Jenkins and Pearce, 1992; Merello and Lees, 1992; Cicarelli et al., 2002). This phenomenon may be clinically underestimated and contribute to motor fluctuations (Nutt et al., 1988). Although various mechanism(s) have been put forward, the present study suggests that low doses of a D_2/D_3 receptor antagonist, possibly acting on D_2 (auto)receptors, can reverse it.

Finally, NOP receptor antagonists were confirmed in their ability to attenuate MPTP-induced parkinsonism, also providing additive/synergistic symptomatic benefit when given in combination with DA agonists. The strong analogies between motor responses to NOP receptor antagonists in 6-OHDA lesioned rats (Marti et al., 2005, 2007, 2008) and MPTP-treated mice (Viaro et al., 2008, present data) strengthen the pathogenic contribution of N/OFQ across species and experimental models of parkinsonism, endorsing the view that NOP receptor antagonists may represent a promising therapeutic approach to PD.

Acknowledgments

This work has been supported by grants from the Michael J. Fox Foundation for Parkinson's Research and from the Italian Ministry of the University (FIRB Internazionalizzazione n. RBIN047W33) to M. Morari. We thank Prof S Salvadori for generous gift of J-113397 and Trap-101.

References

Abbas, A.I., Hedlund, P.B., Huang, X.P., Tran, T.B., Meltzer, H.Y., Roth, B.L., 2009. Amisulpride is a potent 5-HT7 antagonist: relevance for antidepressant actions in vivo. Psychopharmacology (Berl.) 205, 119–128.

Archer, T., Palomo, T., McArthur, R., Fredriksson, A., 2003. Effects of acute administration of DA agonists on locomotor activity: MPTP versus neonatal intracerebroventricular 6-OHDA treatment. Neurotox. Res. 5, 95–110.

Assié, M.B., Dominguez, H., Consul-Denjean, N., Newman-Tancredi, A., 2006. In vivo occupancy of dopamine D2 receptors by antipsychotic drugs and novel compounds in the mouse striatum and olfactory tubercles. Naunyn Schmiedebergs Arch. Pharmacol. 373, 441–450.

Chia, L.G., Ni, D.R., Cheng, L.J., Kuo, J.S., Cheng, F.C., Dryhurst, G., 1996. Effects of 1-methyl-4-phenyl-1,2,3,6-tetrahydropyridine and 5,7 dihydroxytryptamine on the locomotor activity and striatal amines in C57BL/6 mice. Neurosci. Lett. 218, 67–71.

Cicarelli, G., Pellecchia, M.T., De Michele, G., Pizzolato, G., Barone, P., 2002. Paradoxical response to apomorphine in a case of atypical parkinsonism. Mov. Disord. 17, 604–606.

Clark, D., White, F.J., 1987. D1 dopamine receptor—the search for a function: a critical evaluation of the D1/D2 dopamine receptor classification and its functional implications. Synapse 1, 347–388.

Clemett, D.A., Cockett, M.I., Marsden, C.A., Fone, K.C., 1998. Antisense oligonucleotide-induced reduction in 5-hydroxytryptamine7 receptors in the rat hypothalamus without alteration in exploratory behaviour or neuroendocrine function. J. Neurochem. 71, 1271–1279.

Colotla, V.A., Flores, E., Oscos, A., Meneses, A., Tapia, R., 1990. Effects of MPTP on locomotor activity in mice. Neurotoxicol. Teratol. 4, 405–407.

Dauer, W., Przedborski, S., 2003. Parkinson's disease: mechanisms and models. Neuron 39, 889–909.

Di Benedetto, M., Cavina, C., D'Addario, C., Leoni, G., Candeletti, S., Cox, B.M., Romualdi, P., 2009. Alterations of N/OFQ and NOP receptor gene expression in the substantia nigra and caudate putamen of MPP+ and 6-OHDA lesioned rats. Neuropharmacology 56, 761–767.

Fisher, A., Biggs, C.S., Eradiri, O., Starr, M.S., 2000. Dual effects of L-3,4-dihydroxyphenylalanine on aromatic L-amino acid decarboxylase, dopamine release and motor stimulation in the reserpine-treated rat: evidence that behaviour is dopamine independent. Neuroscience 95, 97–111.

Fredriksson, A., Plaznik, A., Sundström, E., Jonsson, G., Archer, T., 1990. MPTP-induced hypoactivity in mice: reversal by L-dopa. Pharmacol. Toxicol. 67, 295–301.

Fredriksson, A., Plaznik, A., Sundström, E., Archer, T., 1994. Effects of D1 and D2 agonists on spontaneous motor activity in MPTP treated mice. Pharmacol. Toxicol. 75, 36–41.

Haobam, R., Sindhu, K.M., Chandra, G., Mohanakumar, K.P., 2005. Swim-test as a function of motor impairment in MPTP model of Parkinson's disease: a comparative study in two mouse strains. Behav. Brain Res. 163, 159–167.

Itzhak, Y., Martin, J.L., Black, M.D., Ali, S.F., 1999. Effect of the dopaminergic neurotoxin MPTP on cocaine-induced locomotor sensitization. Pharmacol. Biochem. Behav. 63, 101–107.

Jackson-Lewis, V., Przedborski, S., 2007. Protocol for the MPTP mouse model of Parkinson's disease. Nat. Protoc. 1, 141–151.

Jenkins, J.R., Pearce, J.M., 1992. Paradoxical akinetic response to apomorphine in parkinsonism. J. Neurol. Neurosurg. Psychiatry 55, 414–415.

Kato, H., Kurosaki, R., Oki, C., Araki, T., 2004. Arundic acid, an astrocyte-modulating agent, protects dopaminergic neurons against MPTP neurotoxicity in mice. Brain Res. 1030, 66–73.

Klapdor, K., Dulfer, B.G., Hamman, A., Van der Staay, F.J., 1997. A low-cost method to analyse footprints patterns. J. Neurosci. Methods 75, 49–54.

Koizumi, M., Sakoori, K., Midorikawa, N., Murphy, N.P., 2004. The NOP (ORL1) receptor antagonist Compound B stimulates mesolimbic dopamine release and is rewarding in mice by a non-NOP-receptor-mediated mechanism. Br. J. Pharmacol. 143, 53–62.

Kumar, V.L., Sehgal, R., 2007. Calotropis procera latex-induced inflammatory hyperalgesia—effect of bradyzide and morphine. Auton. Autacoid Pharmacol. 27, 143–149.

Laloux, C., Derambure, P., Houdayer, E., Jacquesson, J.M., Bordet, R., Destée, A., Monaca, C., 2008. Effect of dopaminergic substances on sleep/wakefulness in saline- and MPTP-treated mice. J. Sleep Res. 17, 101–110.

Langston, J.W., Ballard, P., Tetrud, J.W., Irwin, I., 1983. Chronic Parkinsonism in humans due to a product of meperidine-analog synthesis. Science 219, 979–980.

Maj, J., Rogóz, Z., Skuza, G., Kołodziejczyk, K., 1997. The behavioural effects of pramipexole, a novel dopamine receptor agonist. Eur. J. Pharmacol. 324, 31–37.

Marti, M., Mela, F., Veronesi, C., Mela, F., Veronesi, C., Guerrini, R., Salvadori, S., Federici, M., Mercuri, N.B., Rizzi, A., Franchi, G., Beani, L., Bianchi, C., Morari, M., 2004. Blockade of nociceptin/orphanin FQ receptor signalling in rat substantia nigra pars reticulata stimulates nigrostriatal dopaminergic transmission and motor behaviour. J. Neurosci. 24, 6659–6666.

Please cite this article as: Viaro, R., et al., Dual motor response to L-dopa and nociceptin/orphanin FQ receptor antagonists in 1-methyl-4-phenyl-1,2,5,6-tetrahydropyridine (MPTP) traeted mice: Paradoxical..., Exp. Neurol. (2010), doi:10.1016/j.expneurol.2010.01.014

Marti, M., Mela, F., Fantin, M., Zucchini, S., Brown, J.M., Witta, J., Di Benedetto, M., Buzas, B., Reinscheid, R.K., Salvadori, S., Guerrini, R., Romualdi, P., Candeletti, S., Simonato, M., Cox, B.M., Morari, M., 2005. Blockade of nociceptin/orphanin FQ transmission attenuates symptoms and neurodegeneration associated with Parkinson's disease. J. Neurosci. 95, 9591–9601.

Marti, M., Trapella, C., Viaro, R., Morari, M., 2007. The nociceptin/orphanin FQ receptor antagonist J-113397 and L-dopa additively attenuate experimental parkinsonism through overinhibition of the nigrothalamic pathway. J. Neurosci. 27, 1297–1307.

Marti, M., Trapella, C., Morari, M., 2008. The novel nociceptin/orphanin FQ receptor antagonist Trap-101 alleviates experimental parkinsonism through overinhibition of the nigro-thalamic pathway: positive interaction with L-DOPA. J. Neurochem. 107, 1683–1696.

Mela, F., Millan, M.J., Brocco, M., Morari, M., 2010. The selective D(3) receptor antagonist, S33084, improves parkinsonian-like motor dysfunction but does not affect L-dopa-induced dyskinesia in 6-hydroxydopamine hemi-lesioned rats. Neuropharmacology 58, 528–536.

Meredith, G.E., Kang, U.J., 2006. Behavioral models of Parkinson's disease in rodents: a new look at an old problem. Mov. Disord. 21, 1595–1606.

Merello, M., Lees, A.J., 1992. Beginning-of-dose motor deterioration following the acute administration of levodopa and apomorphine in Parkinson's disease. J. Neurol. Neurosurg. Psychiatry 55, 1024–1026.

Meyer, O.A., Tilson, H.A., Byrd, W.C., Riley, M.T., 1979. A method for the routine assessment of fore- and hindlimb grip strength of rats and mice. Neurobehav. Toxicol. 1, 233–236.

Mierau, J., Schingnitz, G., 1992. Biochemical and pharmacological studies on Pramipexole, a potent and selective dopamine D_2 receptor agonist. Eur. J. Pharmacol. 215, 161–170.

Millan, M.J., Veiga, S., Girardon, S., Brocco, M., 2003. Blockade of serotonin 5-HT1B and 5-HT2A receptors suppresses the induction of locomotor activity by 5-HT reuptake inhibitors, citalopram and fluvoxamine, in NMRI mice exposed to a novel environment: a comparison to other 5-HT receptor subtypes. Psychopharmacology (Berl.) 168, 397–409.

Miller, D.B., Reinhard Jr, J.F., Daniels, A.J., O'Callaghan, J.P., 1991. Diethyldithiocarbamate potentiates the nuerotoxicity of in vivo 1-methyl-4-phenyl-1,2,3,6-tetrahydropyridine and of in vitro 1-methyl-4-phenylpyridinium. J. Neurochem. 57, 541–549.

Nishi, K., Kondo, T., Narabayashi, H., 1991. Destruction of norephinephrine terminals in 1-methyl-4-phenyl-1,2,3,6-tetrahydropyridine (MPTP)-treated mice reduces locomotor activity induced by L-dopa. Neurosci. Lett. 123, 244–247.

Nutt, J.G., Gancher, S.T., Woodward, W.R., 1988. Does an inhibitory action of levodopa contribute to motor fluctuations? Neurology 38, 1553–1557.

Paalzow, G.H., 1992. L-dopa induces opposing effects on pain in intact rats: (−)-sulpiride, SCH 23390 or alpha-methyl-DL-p-tyrosine methylester hydrochloride reveals profound hyperalgesia in large antinociceptive doses. J. Pharmacol. Exp. Ther. 263, 470–479.

Perrault, G.H., Scatton, B., Sanger, D.J., Morel, E., Depoortere, R., 1997. Psychopharmacological profile of amisulpride: an antipsychotic drug with presynaptic D_2/D_3 dopamine receptor antagonist activity and limbic selectivity. J. Pharmacol. Exp. Ther. 280, 73–82.

Petzinger, G.M., Walsh, J.P., Akopian, G., Hogg, E., Abernathy, A., Arevalo, P., Turnquist, P., Vucković, M., Fisher, B.E., Togasaki, D.M., Jakowec, M.W., 2007. Effects of treadmill exercise on dopaminergic transmission in the 1-methyl-4-phenyl-1,2,3,6-tetrahydropyridine-lesioned mouse model of basal ganglia injury. J. Neurosci. 27, 5291–5300.

Pickel, V.M., Chan, J., Nirenberg, M.J., 2002. Region-specific targeting of dopamine D2-receptors and somatodendritic vesicular monoamine transporter 2 (VMAT2) within ventral tegmental area subdivisions. Synapse 45, 113–124.

Pritchard, L.M., Newman, A.H., McNamara, R.K., Logue, A.D., Taylor, B., Welge, J.A., Xu, M., Zhang, J., Richtand, N.M., 2007. The dopamine D3 receptor antagonist NGB 2904 increases spontaneous and amphetamine-stimulated locomotion. Pharmacol. Biochem. Behav. 86, 718–726.

Przedborski, S., Jackson-Lewis, V., Djaldetti, R., Liberatore, G., Vila, M., Vukosavic, S., Almer, G., 2000. The parkinsonian toxin MPTP: action and mechanism. Restor. Neurol. Neurosci. 16, 135–142.

Rozas, G., Guerra, M.J., Labandeira-Garcia, J.L., 1997. An automated rotarod method for quantitative drug-free evaluation of overall motor deficits in rat models of parkinsonism. Brain Res. Brain Res Protoc. 2, 75–84.

Sanberg, P.R., Bunsey, M.D., Giordano, M., Norman, A.B., 1988. The catalepsy test: its ups and downs. Behav. Neurosci. 102, 748–759.

Sautel, F., Griffon, N., Sokoloff, P., Schwartz, J.C., Launay, C., Simon, P., Costentin, J., Schoenfelder, A., Garrido, F., Mann, A., Wermuth, C.G., 1995. Nafadotride, a potent preferential dopamine D3 receptor antagonist, activates locomotion in rodents. J. Pharmacol. Exp. Ther. 275, 1239–1246.

Scatton, B., Claustre, Y., Cudennec, A., Oblin, A., Perrault, G., Sanger, D.J., Schoemaker, H., 1997. Amisulpride: from animal pharmacology to therapeutic action. Int. Clin. Psychopharmacol 12, S29–S36.

Schallert, T., De Ryck, M., Whishaw, I.Q., Ramirez, V.D., Teitelbaum, P., 1979. Excessive bracing reactions and their control by atropine and L-DOPA in an animal analog of Parkinsonism. Exp. Neurol. 64, 33–43.

Schoemaker, H., Claustre, Y., Fage, D., Rouquier, L., Chergui, K., Curet, O., Oblin, A., Gonon, F., Carter, C., Benavides, J., Scatton, B., 1997. Neurochemical characteristics of amisulpride, an atypical dopamine D2/D3 receptor antagonist with both presynaptic and limbic selectivity. J. Pharmacol. Exp. Ther. 280, 83–97.

Sedelis, M., Hofele, K., Auburger, G.W., Morgan, S., Huston, J.P., Schwarting, R.K.W., 2000. Evidence for resistance to MPTP in C57BL/6×BALB/c F1 hybrids as compared with their progenitor strains. NeuroReport 11, 1093–1096.

Sedelis, M., Schwarting, R.K.W., Huston, J.P., 2001. Behavioral phenotyping of the MPTP mouse model of Parkinson's disease. Behav. Brain Res. 125, 109–125.

Seeman, P., 2007. Antiparkinson therapeutic potencies correlate with their affinities at dopamine D2(High) receptors. Synapse 61, 1013–1018.

Siuciak, J.A., Fujiwara, R.A., 2004. The activity of pramipexole in the mouse forced swim test is mediated by D_2 rather than D_3 receptors. Psychopharmacology 175, 163–169.

Smith, T.S., Trimmer, P.A., Khan, S.M., Tinklepaugh, D.L., Bennett Jr, J.P., 1997. Mitochondrial toxins in models of neurodegenerative diseases: II. Elevated zif268 transcription and independent temporal regulation of striatal D1 and D2 receptor mRNAs and D1 and D2 receptor-binding sites in C57BL/6 mice during MPTP treatment. Brain Res. 765, 189–197.

Sundström, E., Luthman, J., Goldstein, M., Jonsson, G., 1988. Time course of MPTP-induced degeneration of the nigrostriatal dopamine system in C57 BL/6 mice. Brain Res. Bull. 21, 257–263.

Sundström, E., Fredriksson, A., Archer, T., 1990. Chronic neurochemical and behavioral changes in MPTP-lesioned C57BL/6 mice: a model for Parkinson's disease. Brain Res. 528, 181–188.

Tillerson, J.L., Caudle, W.M., Reveron, M.E., Miller, G.W., 2002. Detection of behavioral impairments correlated to neurochemical deficits in mice treated with moderate doses of 1-methyl-4-phenyl-1,2,3,6-tetrahydropyridine. Exp. Neurol. 178, 80–90.

Trapella, C., Guerrini, R., Piccagli, L., Calò, G., Carrà, G., Spagnolo, B., Rubini, S., Fanton, G., Hebbes, C., McDonald, J., Lambert, D.G., Regoli, D., Salvadori, S., 2006. Identification of an achiral analogue of J-113397 as potent nociceptin/orphanin FQ receptor antagonist. Bioorg. Med. Chem. 14, 692–704.

Usiello, A., Baik, J.H., Rougé-Pont, F., Picetti, R., Dierich, A., LeMeur, M., Piazza, P.V., Borrelli, E., 2000. Distinct functions of the two isoforms of dopamine D2 receptors. Nature 408, 199–203.

Vallone, D., Picetti, R., Borrelli, E., 2000. Structure and function of dopamine receptors. Neurosci. Biobehav. Rev. 24, 125–132.

Viaro, R., Sanchez-Pernaute, R., Marti, M., Trapella, C., Isacson, O., Morari, M., 2008. Nociceptin/orphanin FQ receptor blockade attenuates MPTP-induced parkinsonism. Neurobiol. Dis. 30, 430–438.

Wang, Y., Xu, R., Sasaoka, T., Tonegawa, S., Kung, M.P., Sankoorikal, E.B., 2000. Dopamine D2 long receptor-deficient mice display alterations in striatum-dependent functions. J. Neurosci. 20, 8305–8314.

Watanabe, Y., Kato, H., Araki, T., 2008. Protective action of neuronal nitric oxide synthase inhibitor in the MPTP mouse model of Parkinson's disease. Metab. Brain Dis. 23, 51–69.

Weihmuller, F.B., Hadjiconstantinou, M., Bruno, J.P., 1990. Dopamine receptors and sensorimotor behavior in MPTP-treated mice. Behav. Brain Res. 38, 263–273.

Wiener, W.J., Kramer, J., Nausieda, P.A., Klawans, H.L., 1978. Paradoxial response to dopaminergic agents in parkinsonism. Arch. Neurol. 35, 453–455.

Please cite this article as: Viaro, R., et al., Dual motor response to L-dopa and nociceptin/orphanin FQ receptor antagonists in 1-methyl-4-phenyl-1,2,5,6-tetrahydropyridine (MPTP) traeted mice: Paradoxical..., Exp. Neurol. (2010), doi:10.1016/j.expneurol.2010.01.014

Different subpopulations of D2 receptors mediate dual motor responses of nociceptin/orphanin FQ receptor antagonists in mice

R Viaro[1,2], M Marti[1,2] and M Morari[1,2]

[1]*Department of Experimental and Clinical Medicine, Section of Pharmacology,* [2]*Neuroscience Center and National Institute of Neuroscience, University of Ferrara, Ferrara (Italy).*

Running title: NOP ligands and D2 receptors

Correspondence:

Michele Morari
Department of Experimental and Clinical Medicine, Section of Pharmacology
University of Ferrara, via Fossato di Mortara 17-19,
44100 Ferrara (Italy)
Phone: +39-0532-455210
Fax: +39-0532-455205
E-mail: m.morari@unife.it

Abbreviations:

5-HT, 5-hydroxytryptamine (serotonin); DA, dopamine; ED50, median effective dose; GBR12783, (1-[2-(diphenylmethoxy)ethyl]4-(3-phenyl-2-(propenyl)-piperazine); N/OFQ, nociceptin/orphanin FQ; NOP, nociceptin opioid receptor; NOP-/-, nociceptin opioid receptor knockout; NOP+/+ nociceptin opioid receptor wild-type; J-113397, 1-[(3R,4R)-1-cyclooctylmethyl-3-hydroxymethyl-4-piperidyl]-3-ethyl-1,3-dihydro-2H-benzimidazol-2-one; PPX, pramipexole; S33084, (3aR, 9bS)-N-[4-(8-cyano-1,3a,4,9b-tetrahydro-3H-benzopyrano[3,4-c]pyrrole-2-yl)-butyl]-(4-phenyl) benzamide; SB-277011-A, (trans-N-[4-[2-(6-cyano-1,2,3, 4-tetrahydroisoquinolin-2-yl)ethyl]cyclohexyl]-4-quinolininecarboxamide); SCH23390, 7-chloro-8-hydroxy-1-phenyl-2,3,4,5-tetrahydro-1H-3-benzazepine; SNr, substantia nigra reticulata; Trap-101, 1-[1-(cyclooctylmethyl)-1,2,3,6-tetrahydro-5-(hydroxymethyl)-4-pyridinyl]-3-ethyl-1,3-dihydro-2H-benzimidazol-2-one; UFP-101, [Nphe^{1},Arg^{14},Lys^{15}]N/OFQ-NH_2.

Summary

Background and purpose: Nociceptin/orphanin FQ (N/OFQ) reduces dopamine release in rat mesencephalic areas while antagonists at the N/OFQ receptor (NOP) elevate it. We therefore investigated the contribution of endogenous dopamine in motor actions of NOP receptor ligands in naïve mice.

Experimental approach: The motor profiles of N/OFQ and NOP receptor antagonists [Nphe^{1},Arg^{14},Lys^{15}]N/OFQ-NH_2 (UFP-101), 1-[(3R,4R)-1-cyclooctylmethyl-3-hydroxymethyl-4-piperidyl]-3-ethyl-1,3-dihydro-2H-benzimidazol-2-one (J-113397) and 1-[1-(cyclooctylmethyl)-1,2,3,6-tetrahydro-5-(hydroxymethyl)-4-pyridinyl]-3-ethyl-1,3-dihydro-2H-benzimidazol-2-one (Trap-101) were characterized using behavioral tests providing complementary information on motor function. NOP receptor knockout mice were used to confirm the specificity of motor responses. D1/D5 (SCH23390), D2/D3 (raclopride, amisulpride) and D3 (S33084) dopamine receptor antagonists, the dopamine precursor L-dopa and the D3/D2 receptor agonist pramipexole were used to unravel the specific contribution of dopamine receptor subtypes. A preparation of striatal synaptosomes preloaded with [^{3}H]-dopamine was employed to study presynaptic effects of L-dopa and pramipexole.

Key results: Both NOP receptor antagonists and N/OFQ facilitated motor activity at low doses and inhibited it at higher ones, being ineffective in NOP receptor knockout mice. Motor facilitation was selectively prevented by raclopride while motor inhibition (induced by NOP receptor antagonists) by amisulpride. Amisulpride also prevented hypolocomotion induced by L-dopa and pramipexole. Pramipexole and L-dopa caused inhibition and facilitation of K^{+}-evoked synaptosomal [^{3}H]-dopamine release, which were reversed by amisulpride and SCH23390, respectively.

Conclusions and implications: Motor responses to NOP receptor antagonists in naïve mice are dopamine-dependent and mediated by D2 postsynaptic (facilitation) and D2 presynaptic

autoreceptors (inhibition). L-dopa can stimulate D1/D5 dopamine receptors in vitro prior to dopamine conversion.

Key words: dopamine receptors, J-113397, L-dopa, motor activity, nociceptin/orphanin FQ, pramipexole, synaptosomes, Trap-101, UFP-101.

Introduction

Nociceptin/orphanin FQ (N/OFQ; Meunier *et al.,* 1995; Reinscheid *et al.,* 1995) is a neuropeptide belonging to the opioid family, and the endogenous ligand of the N/OFQ peptide (NOP) receptor. The N/OFQ-NOP receptor system shares with classical opioid systems the ability to modulate a number of central functions such as pain, reward, mood, and locomotion (Mogil and Pasternak, 2001) and the NOP receptor is an emerging target with broad therapeutic potential (Lambert, 2008), including movement disorders (Marti *et al.,* 2005). Endogenous N/OFQ exerts a physiologically inhibitory control over motor function (Marti *et al.,* 2004; 2008). Indeed, NOP receptor selective antagonists such as [Nphe^{1},Arg^{14},Lys^{15}]N/OFQ-NH_2 (UFP-101; Calò *et al.,* 2002), 1-[(3R,4R)-1-cyclooctylmethyl-3-hydroxymethyl-4-piperidyl]-3-ethyl-1,3-dihydro-2H benzimidazol-2-one (J-113397 or Compound B; Kawamoto *et al.,* 1999) and its achiral analogue 1-[1-(cyclooctylmethyl)-1,2,3,6-tetrahydro-5-(hydroxymethyl)-4-pyridinyl]-3-ethyl-1,3-dihydro-2H-benzimidazol-2-one (Trap-101; Trapella *et al.,* 2006) increased stepping activity, run speed and rotarod performance in naïve rats (Marti *et al.,* 2004; 2008, 2009). J-113397 and Trap-101 also elevated motor performance in naïve mice (Viaro *et al.,* 2008; Marti *et al.,* 2008), while J-113397 increased arm movement speed in nonhuman primates (Viaro *et al.,* 2008). The view of N/OFQ as a physiological constraint over motor activity was also corroborated by the finding that NOP receptor knockout (NOP$^{-/-}$) mice had greater stepping activity and rotarod performance than wild-type mice (Marti *et al.,* 2004, 2005; Viaro *et al.,* 2008). Recent data, however, suggested that endogenous N/OFQ may play a more complex role in motor control. Indeed, J-113397 and Trap-101 facilitated motor activity at low doses and impaired it at higher ones through NOP receptor blockade in naïve rodents (Viaro *et al.,* 2008; Marti *et al.,* 2008). A similar dual response was also reported after i.c.v. administration of N/OFQ, low doses facilitating (Florin *et al.,* 1996; Jenck *et al.,* 1997; Higgins *et al.,* 2001; Kuzmin *et al.,* 2004, Marti *et al.,* 2009) and higher ones inhibiting (Reinscheid *et al.,* 1995; Devine *et al.,* 1996; Rizzi *et al.,* 2001; Higgins *et al.,* 2001; Kuzmin *et al.,* 2004; Marti *et al.,* 2009) spontaneous locomotion. Importantly, we found that N/OFQ-induced motor facilitation was a true motor

response (Marti *et al.,* 2009) and not a result of an anxiolytic effect of N/OFQ as previously thought (Florin *et al.,* 1996; Jenck *et al.,* 1997). In fact, motor improvement induced by low N/OFQ doses given i.c.v. or injected into substantia nigra reticulata (SNr) was associated with enhanced motor cortex excitability and motor output, while motor impairment induced by higher N/OFQ doses was accompanied by opposite electrophysiological changes (Marti *et al.,* 2009). Interestingly, NOP receptor antagonists replicated the electrophysiological and behavioral changes induced by low N/OFQ doses, overall suggesting that i) dual motor responses to NOP receptor ligands are mediated by NOP receptors in SNr and ii) NOP receptor antagonists and N/OFQ (at low doses) activate common pathways.

Evidence that mesencephalic dopamine (DA) neurons transduce motor actions of NOP receptor ligands has been presented. Indeed, N/OFQ and NOP receptor antagonists, given systemically or into SNr, inhibited and facilitated DA release in dorsal striatum, respectively (Marti *et al.,* 2004). Moreover, N/OFQ inhibited DA release in limbic striatum (Murphy *et al.,* 1999; Narayanan *et al.,* 2004) while J-113397 elevated it, although via NOP-unrelated mechanisms (Koizumi *et al.,* 2004). Finally, even the hyperlocomotive response to N/OFQ was reported to be DA-dependent (Florin *et al.,* 1996; Kuzmin *et al.,* 2004).

In the present study, we investigated the role of endogenous DA in motor actions of NOP receptor ligands in mice. The motor profile of chemically unrelated NOP receptor antagonists, namely UFP-101 (peptide), J-113397 and Trap-101 (nonpeptides), was evaluated by using a battery of previously validated behavioral tests (the bar, drag and rotarod tests; Marti *et al.,* 2004, 2005, 2008, 2009; Viaro *et al.,* 2008) providing complementary information on akinesia, bradykinesia and gait ability. The effect of i.c.v. administration of N/OFQ was also investigated. $NOP^{-/-}$ mice were used to confirm the specificity of the motor responses of NOP receptor ligands. To unravel the specific contribution of DA receptor subtypes, D1/D5 (SCH23390), D2/D3 (raclopride, amisulpride) and D3 selective (S33084) receptor antagonists were tested alone and in combination with NOP receptor ligands. Since a specific role for D2 receptors emerged from these experiments, the motor responses

to the DA precursor, L-dopa, and the DA agonist pramipexole (PPX) were also analyzed. Finally, the presynaptic effects of PPX and L-dopa were more specifically investigated in a preparation of striatal synaptosomes preloaded with [^{3}H]-DA.

Methods

Animals

Young adult (8 weeks old) male C57BL/6J mice (20-25 g; Harlan, Italy, S.Pietro al Natisone) and CD1/C57BL6J/129 NOP$^{+/+}$ and NOP$^{-/-}$ mice (20-25 g; Ferrara vivarium; Nishi *et al.,* 1997) were housed with free access to food and water and kept under environmentally controlled conditions (12-h light/dark cycle with light on between 07:00 and 19:00). The experimental protocols were approved by the Italian Ministry of Health (license n. 94/2007B) and Ethical Committee of the University of Ferrara. Adequate measures were taken to minimize animal pain and discomfort.

Experimental design

Prior to pharmacological testing, mice were handled for 1 week by the same operator to reduce stress, and trained daily for an additional week on the behavioral tests until their motor performance became reproducible. Motor activity was assessed by a battery of previously validated behavioral tests specific for different motor abilities: the bar, drag and rotarod test (Marti *et al.,* 2004, 2005, 2008, 2009; Viaro *et al.,* 2008). On the day of experiment, drugs were administered systemically (i.p.). N/OFQ and UFP-101 were injected in the lateral cerebral ventricle (i.c.v.). L-dopa was administered in combination with benserazide (4:1 ratio). The three tests were repeated in a fixed sequence (bar, drag and rotarod) before (control session) and after (10 and 60 min) drug injection. When DA receptor antagonists were used, motor analysis was performed 30 and 80 min after injection to match time of administration in the interaction studies (i.e. 20 min before NOP receptor antagonists or DA receptor agonists).

Since in most cases we did not observe differences in motor responses between the first (10 or 30 min) and the second time point (60 or 80 min) evaluated after drug administration, for the sake of

clarity, drug effects as 10 or 30 min were presented in figures 1 through 10 while effects at 60 or 80 min as supplementary material (Fig S1).

Microinjection technique

The injections in the lateral cerebral ventricle were given according to the procedure described by Laursen and Belknap (1986). Briefly, the syringe was held at an approximate 45° angle to the skull. Bregma was found by lightly rubbing the point of the needle over the skull until the suture was felt. Once found, care was taken to maintain the approximate 45° angle and the needle was inserted about 2 mm lateral to the midline. The skull is relatively thin at this point, so only mild pressure was required to insert and remove the needle. Drugs were slowly injected (0.5 µl in about 5 sec) and to prevent the substance from refluxing, the needle was withdrawn from the skull 5 sec later.

Behavioral studies

Bar test. Originally developed to quantify morphine-induced catalepsy (Kuschinsky and Hornykiewicz, 1972), this test measures the ability of the mouse to respond to an externally imposed static posture. Also known as the catalepsy test (for a review see Sanberg *et al.,* 1988), it can be used to quantify akinesia (i.e. time to initiate a movement) also under conditions that are not characterized by increased muscle tone (i.e rigidity) as in the cataleptic/catatonic state. The mouse was placed gently on a table and forepaws were placed alternatively on blocks of increasing heights (1.5, 3 and 6 cm). The time (in sec) that each paw spent on the block (i.e. the immobility time) was recorded (cut-off time of 20 sec). Akinesia was calculated as total time spent on the different blocks.

Drag test. Modification of the "wheelbarrow test" (Schallert *et al.,* 1979), this test measures the ability of the animal to balance its body posture with forelimbs in response to an externally imposed dynamic stimulus (backward dragging; Marti *et al.,* 2005). It gives information regarding the time to initiate and execute (bradykinesia) a movement. The animal was gently lifted from the tail leaving the forepaws on the table, and was dragged backwards at a constant speed (about 20

cm/sec) for a fixed distance (100 cm). The number of steps made by each paw were recorded by two separate observers. Five to seven determinations were collected for each animal.

Rotarod test. The fixed-speed rotarod test (Rozas *et al.,* 1997) measures different motor parameters such as motor coordination, gait ability, balance, muscle tone and motivation to run. It was employed according to a previously described protocol (Marti *et al.,* 2004), in which mice were tested at stepwise increasing speeds (from 5 to 50 rpm; 180 sec each).

Synaptosome preparation and [^{3}H]-DA analysis

To minimize pain and discomfort, mice were decapitated under light ether anesthesia and the striatum was quickly excised to prepare synaptosomes, as previously described (Morari *et al.,* 1998). Briefly, striata were homogenized in ice-cold 0.32 M sucrose buffer at pH 7.4 then centrifuged for 10 min at 2,500 g_{max} (4°C). The supernatant was then centrifuged for 20 min at 9,500 g_{max} (4°C) with the synaptosomal pellet being resuspended in oxygenated (95% O_2, 5% CO_2) Krebs solution (mM: NaCl 118.5, KCl 4.7, $CaCl_2$ 1.2, $MgSO_4$ 1.2, KH_2PO_4 1.2, $NaHCO_3$ 25, glucose 10) containing ascorbic acid (0.05 mM) and disodium EDTA (0.03 mM). Synaptosomes were pre-loaded with [^{3}H]-DA by incubation in medium containing 50 nM [^{3}H]-DA (specific activity 27.8 Ci/mmol, NEN DuPont, Boston, MA, USA.) for 25 min.

One milliliter aliquots of the suspension (~0.35 mg protein) were slowly injected into nylon syringe filters (outer diameter 13 mm, 0.45 µM pore size, internal volume of about 100 µl; MSI, Westporo, MA, USA) which were then connected to a peristaltic pump. Filters were maintained at 36.5 °C in a thermostatic bath and superfused at a flow rate of 0.4 ml/min with a pre-oxygenated Krebs solution. Under these experimental conditions, spontaneous [^{3}H]-DA efflux was essentially unaffected by reuptake. Sample collection (every 3 min) was initiated after a 20 min period of filter washout. The effect of drugs was evaluated on both spontaneous and K^+-stimulated neurotransmitter outflow. In this case, drugs were added to the perfusion medium 6 (agonist) or 9 (antagonist) min before a 10 mM KCl pulse (120 sec) and maintained until the end of the experiment. [^{3}H]-DA levels in the samples were measured by liquid scintillation spectrophotometry. Sample superfusate (1.2

ml/sample) and filter retained (dissolved with 1 ml of 1 M NaOH followed by 1 M HCl) were opportunely mixed with Ultima Gold XR scintillation fluid (Packard Instruments B.V., Groningen, The Netherlands) and radioactivity was determined by a Beckman LS 1800 β-spectrophotometer.

Data presentation and statistical analysis

Data are expressed as means ± SEM of 6-8 determinations per group. Motor performance in the behavioral tests has been expressed as percentage of the control session (i.e. the session performed before treatment, which represents the internal control for each mouse). Statistical analysis was routinely (Fig 1-11) performed (CoStat 6.3, CoHort Software, Monterey, CA, USA) by two-way repeated measure ANOVA on percent values. In the case these tests yielded a significant F score, post-hoc analysis was performed by contrast analysis to determine group differences followed by the sequentially rejective Bonferroni test to determine specific differences (i.e. at the single time-point level) between groups. Data obtained in synaptosomes were treated by one-way ANOVA on percent (Fig. 11A-B) or area-under-the curve (AUC; Fig. 12A-C) values followed by the Newman-Keuls test. ANOVA values have been presented as supplemental material (Fig. S2). P values <0.05 were considered to be statistically significant.

Materials

Benserazide, L-dopa methyl ester and L-dopa free-base were purchased from Sigma (St. Louis, MO, USA). Amisulpride, domperidone, GBR12783, raclopride and SCH23390 were purchased from Tocris (Bristol, UK). PPX was purchased from McTony Bio&Chem (Vancouver, Canada). S33084 was provided by Institut de Recherches Servier (Croissy-sur-Seine, France). J-113397, N/OFQ, Trap-101 and UFP-101 were synthesized in the laboratories of Department of Pharmaceutical Chemistry at the University of Ferrara. All drugs were freshly dissolved in the vehicle just prior to use. For in vivo experiments, the volume injected was 10 µl/g body weight (systemic administration) or 0.5 µl (i.c.v. administration).

Results

NOP receptor antagonists dually modulated motor activity

The motor profiles of three NOP receptor antagonists were investigated in C57BL/6J mice by using static and dynamic tests providing complementary information on motor parameters: the bar, drag and rotarod tests. The non peptide antagonist J-113397 and its achiral analogue Trap-101 were administered systemically while the peptide antagonist UFP-101 was given i.c.v. Basal activity in absolute values was 0.8 ± 0.1 sec (immobility time in the bar test), 16.5 ± 0.9 steps (drag test) and 937.9 ± 62.1 sec (time on rod). Motor activity was not different at the right and left paw so data were pooled together.

J-113397 did not affect the immobility time in the bar test up to 1 mg/Kg and increased it at 10 mg/Kg (Fig. 1A). J-113397 caused a biphasic regulation of stepping activity in the drag test (Fig. 1B) and overall gait ability in the rotarod test (Fig. 1C). In both tests, facilitation was observed at 0.3 and 1 mg/Kg and reduction at 10 mg/Kg. Trap-101 did not affect the immobility time at any of the doses tested (Fig. 1D). However, Trap-101 biphasically modulated motor activity in the drag and rotarod test, increasing the number of steps (Fig. 1E) and time on rod (Fig. 1F) at 10 mg/Kg and reducing them at 30 mg/Kg. UFP-101 increased the immobility time at 30 nmol (Fig. 1G) and caused dual responses in the drag (Fig. 1H) and rotarod test (Fig. 1I), namely facilitation at 1 and 3 nmol and marked inhibition at 30 nmol. Differently from non peptide antagonists, the effects of UFP-101 were detected also at 60 min after injection (Fig. S1.1).

Dopamine receptor antagonists differentially modulate motor actions of NOP receptor antagonists

We previously reported that NOP receptor antagonists elevate striatal DA release in rats, suggesting that endogenous N/OFQ tonically inhibits nigro-striatal DA transmission (Marti *et al.,* 2004). We therefore employed selective DA receptor antagonists to unravel the contribution of endogenous DA to motor actions of NOP receptor antagonists. The D1/D5 receptor antagonist SCH23390, the D2/D3 receptor antagonists raclopride and amisulpride, and the D3 selective receptor antagonist

S33084 were tested alone and in combination with motor facilitating or inhibiting doses of NOP receptor antagonists.

Raclopride dose-dependently inhibited motor performance, as shown by an increase in immobility time (Fig. 2A) and reduction in both the number of steps (Fig. 2B) and time on rod (Fig. 2C). These effects were evoked at 0.1 and 0.3 mg/Kg and observed both 30 and 80 min (Fig. S1.2) after administration. Amisulpride partially replicated motor inhibiting action of raclopride, causing a prolonged increase in immobility time (Fig. 2D) and inhibition of rotarod performance (Fig. 2F) at the highest dose tested (15 mg/Kg). Delayed impairment of rotarod performance was observed also at 5 mg/Kg (Fig. S1.2). Different from raclopride, amisulpiride did not affect stepping activity in the drag test (Fig. 2E). SCH23390 produced consistent motor inhibition in the three tests (Fig. 3). Increased immobility time (Fig. 3A), reduced stepping activity (Fig. 3B) and rotarod performance (Fig. 3C) were observed at 0.01 and 0.03 mg/Kg. The effects in the bar and drag tests were prolonged (Fig. S1.3), while those in the rotarod were detected only 30 min after injection. S33084 did not produce marked changes in motor activity (Fig. 3D-F), the only effect observed being mild inhibition of stepping at 0.64 mg/Kg (Fig. 3E).

To disclose the role of endogenous DA, we challenged NOP receptor antagonists with doses of DA receptor antagonists per se ineffective on motor activity. The effect of DA receptor antagonists on motor facilitation was first investigated. Raclopride (0.03 mg/Kg) prevented the increase in stepping activity (Fig. 4B) and rotarod performance (Fig. 4C) induced by J-113397 (0.3 mg/Kg), Trap-101 (0.3 mg/Kg) and UFP-101 (3 nmol, see also Fig. S1.4). Conversely, amisulpride (0.5 mg/Kg), SCH23390 (0.003 mg/Kg) and S33084 (0.16 mg/Kg) were ineffective (Fig. 4E-F).

Differently from facilitation, motor inhibition caused by J-113397 (10 mg/Kg), Trap-101 (30 mg/Kg) and UFP-101 (30 nmol) in the bar (Fig. 5A), drag (Fig. 5B) and rotarod test (Fig. 5C) was prevented by amisulpride while raclopride was ineffective (Fig. 5D-F). It is noteworthy that individual doses of J-113397 and Trap-101 which caused inhibition of stepping activity in the drag

test induced significant stimulation in the presence of amisulpride (Figs. 5B and S1.5). A similar reversal of action was observed for J-113397 on rotarod performance (Fig. 5C).

Raclopride prevented motor facilitation induced by N/OFQ

The data collected thus far indicate that the dual action profile of NOP antagonists is mediated by endogenous DA acting on populations of D2 receptors differently sensitive to amisulpride and raclopride. Previous studies in mice have reported that N/OFQ given i.c.v. stimulates spontaneous locomotion through DA-dependent mechanisms (Florin *et al.,* 1996; Kuzmin *et al.,* 2004). We therefore investigated the role of D2 receptors in motor facilitation induced by N/OFQ in the bar, drag and rotarod tests.

N/OFQ produced different effects on motor activity depending on the dose and motor task used. In particular, N/OFQ monotonically increased immobility time (Fig. 6A) and dually regulated both stepping activity (Fig. 6B) and rotarod performance (Fig. 6C). The effects were also detected after 60 min from administration (Fig. S1.6). Motor facilitation in the drag and rotarod tests was observed at 0.01 nmol while motor inhibition predominated at higher doses (0.1-10 nmol) in all tests. Increases in stepping activity and rotarod performance induced by 0.01 nmol N/OFQ were prevented by raclopride (Fig. 6E-F and S1.6).

UFP-101 and N/OFQ modulated motor activity in $NOP^{+/+}$ mice being ineffective in $NOP^{-/-}$ mice

To test the specificity of NOP receptor ligands, motor facilitating and inhibitory doses of UFP-101 and N/OFQ were challenged in $NOP^{+/+}$ and $NOP^{-/-}$ mice. Low doses of UFP-101 (3 nmol) and N/OFQ (0.01 nmol) did not affect immobility time (Fig 7A) but facilitated stepping activity (Fig. 7B) and rotarod performance (Fig. 7C) in $NOP^{+/+}$ mice. Higher doses of UFP-101 (30 nmol) and N/OFQ (10 nmol) elevated immobility time and inhibited stepping and rotarod performance (Fig. 7A-C). These effects were detectable also at 60 min after treatment (Fig. S1.7). No major difference was observed between C57BL/6J and $NOP^{+/+}$ mice in terms of sensitivity to N/OFQ or duration of the response. Conversely, UFP-101 and N/OFQ were not effective in $NOP^{-/-}$ mice at any of the

doses tested, suggesting that the dual responses they evoked in $NOP^{+/+}$ mice relied on the interaction (blockade and stimulation, respectively) with NOP receptors.

Dopamine receptor antagonists prevented motor inhibition induced by L-dopa and PPX

To strengthen the role of D2 receptors in motor control, we first analyzed motor responses to the DA precursor, L-dopa (in combination with benserazide), and the D3/D2 agonist PPX.

L-dopa inhibited motor activity at the highest dose tested (100 mg/Kg), elevating immobility time (Fig. 8A) and reducing both stepping activity (Fig. 8B) and rotarod performance (Fig. 8C). Impaired rotarod performance was also detected at the lower 10 mg/Kg dose. Similar to L-dopa, PPX evoked a marked increase in immobility time (Fig. 8D) and rotarod performance (Fig. 8F) at 0.1 and 1 mg/Kg. Stepping activity, however, was minimally and transiently reduced only at the highest PPX dose tested (1 mg/Kg; Fig. 8E). These effects were also observed at 60 min post-injections time (Fig. S1.8).

Since motor inhibition was the only effect detected following DA agonists, amisulpride and raclopride were used to demonstrate the involvement of D2/D3 receptors. Amisulpride consistently prevented motor inhibition induced by high doses of L-dopa (100 mg/Kg) in the bar, drag and rotarod tests (Figs. 9A-C and S1.9). Conversely, it modulated the effects of PPX depending on the test and agonist dose used. Thus, amisulpride prevented the increase in immobility time induced by 0.1 mg/Kg PPX (Fig. 9A) but failed to attenuate the impairment in rotarod performance induced by the same dose (Fig. 9C). Amisulpride also did not affect motor inhibition induced by the higher PPX dose (1 mg/Kg) in the bar and drag tests (Fig. 9A-B) but slightly attenuated impairment in rotarod performance (Fig. 9C). On the other hand, raclopride did not prevent motor inhibition induced by PPX on the rotarod (Fig. 9F) and even worsened the inhibition of immobility time (Fig. 9D) and stepping activity (Figs. 9E and S1.9) induced by PPX in the bar and drag tests, respectively. Since PPX is a potent D3 receptor agonist, we investigated whether motor inhibition could be mediated by D3 receptors (Figs. 10 and S1.10). Not only did S33084 not prevent motor inhibition induced by both doses of PPX in the three tests (Fig. 10A-C) but it even worsened

impairment of stepping activity induced by the PPX 1 mg/Kg in the drag test (Fig. 10B). Likewise, S33084 enhanced inhibition of stepping activity induced by 100 mg/Kg L-dopa (Figs. 10B and S1.10) leaving unaffected its motor responses in the bar (Fig. 10A) and rotarod (Fig. 10C) tests. A combination of S33084, amisulpride and raclopride failed to attenuate PPX-induced inhibition (data not shown). We finally investigated whether peripheral D2-like receptors could contribute to motor inhibition induced by PPX, e.g. by inducing hypotension. The peripheral non selective D2 receptor antagonist domperidone (5 mg/Kg; Figs. 10D-F and S1.10) did not affect motor activity alone and also failed to prevent the effect of 0.1 mg/Kg PPX.

L-dopa and PPX oppositely modulated [^{3}H]-DA release in striatal synaptosomes

Previous in vivo data suggest that motor inhibitory actions of L-dopa and PPX rely on an interaction with presynaptic D2 autoreceptors. We therefore analyzed the effects of L-dopa (free-base) and PPX in a preparation of striatal synaptosomes preloaded with [^{3}H]-DA (Fig 11-12). This would also demonstrate whether L-dopa might have biological activity per se or if its effects are due to its conversion to DA. Basal synaptosomal [^{3}H]-DA efflux was 0.021 ± 0.001 pmol mg prot^{-1} min^{-1} (n=68) and corresponded to a fractional release of 6.79 ± 0.15 %. A 2 minute pulse of KCl 10 mM evoked a tritium overflow of 0.006 ± 0.001 pmol mg prot^{-1} min^{-1} (n=24) which was attenuated by ~70 % in the absence of Ca^{++} (Fig. 11A). PPX (100 nM) decreases [^{3}H]-DA overflow (~51 %) and this effects was prevented by pre-treatment with amisulpride (100 nM), ineffective per se (Fig. 11A). Conversely, L-dopa (1 µM) doubled [^{3}H]-DA overflow (Fig. 11B). This effect was prevented by SCH23390 (100 nM) but not by the DA transporter blocker GBR12783 (300 nM; Fig 11B). Neither compound affected the K^+-evoked tritium overflow. L-dopa (1-100 µM) also increased in a dose-dependent manner tritium efflux (Fig. 12A). GBR12783 (300 nM) prevented the response to 10 µM L-dopa (Fig. 12B) and attenuated that of 100 µM L-dopa (Fig. 12C), while SCH23390 (1 µM) was ineffective. GBR12783 and SCH23390 did not affect spontaneous tritium efflux at the doses tested.

Discussion

DA receptor ligands and motor activity

The role of endogenous DA in the modulation of motor activity has been largely investigated using DA selective antagonists, DA lesioning techniques and DA receptor knockout mice (Clark and White, 1997; Millan *et al.,* 2004; Scatton *et al.,* 1997; Vallone *et al.,* 2000). In keeping with these studies, raclopride and amisulpride dose-dependently increased akinesia (bar test) and bradykinesia (drag test), and impaired overall gait abilities (rotarod test), likely through the blockade of striatal D2L (long isoform) postsynaptic receptors (Wang *et al.,* 2000). D3 receptors appear to be minimally involved in tonic regulation of motor activity in naïve animals since S33084 alone did not produce marked changes in motor performance. Consistently, S33084 (Millan *et al.,* 2000, 2004) or another D3 receptor selective antagonist (SB-277011-A; Reavill *et al.,* 2000) failed to alter spontaneous locomotion. Mimicking D2/D3 receptor antagonists, SCH23390 induced dose-dependent motor impairment (Clark and White, 1997). Disruption of cooperative D1-D2 receptor interaction at the postsynaptic level (Clark and White, 1997) or blockade of D2-independent D1 receptor pathways (Usiello *et al.,* 2000) may underlie this effect. The major role played by D2 receptors in movement control was further confirmed with DA receptor agonists. In fact, PPX caused monotonic motor inhibition in the 0.01-1 mg/Kg dose-range, as previously reported (Mierau and Schingnitz, 1992; Siuciak and Fujiawara, 2004). It has been proposed (Usiello et al., 2000; Vallone et al., 2000) that such hypomotility is mediated by central (domperidone-insensitive) DA receptors, possibly presynaptic D2S (short isoform) receptors, via reduced striatal DA release (Carter and Müller, 1991). L-dopa replicated the PPX-induced hypomotility, suggesting that not only in DA-depleted but also in naïve animals endogenous DA newly formed from L-dopa decarboxylation can be incorporated in releasable vesicular pools and exert receptor-mediated central biological effects. The finding that L-dopa and PPX-induced motor inhibition was counteracted by amisulpride further strengthened the role of D2 autoreceptors, although PPX effects (particularly on rotarod performance) appeared poorly sensitive to amisulpride. This may be due to

the different levels of DA receptor occupancy required to induce the biological response and/or to the different spectrum of DA receptors activated by the two agonists. Additional mechanisms not involving classical D2 receptors may also be recruited by PPX to inhibit rotarod performance. As a possibility, we could speculate involvement of pharmacologically distinct receptor entities such D2/D3 heterodimers (Maggio *et al.,* 2003). Interestingly, although D3 receptors appear not to be tonically activated, they markedly contributed to motor responses to PPX and L-dopa. Indeed, S33084 worsened inhibition of stepping activity induced by both agonists in the drag test, suggesting that D3 receptors play a specific role in facilitation of movement initiation and execution. The worsening of PPX-induced motor inhibition observed in the presence of raclopride may also rely on the high affinity of this compound for the D3 receptor. Alternatively, the opposite modulation of the PPX response exerted by raclopride (enhancement) and amisulpride (attenuation) may be due to blockade of different D2 receptor subpopulations, namely post- and presynaptic. In fact, amisulpride given systemically was reported to inhibit D2 autoreceptors at low doses (ED_{50} 3.7 mg/Kg) and block postsynaptic D2 receptors, thereby causing akinesia and catalepsy, at higher ones (ED_{50} ~60 mg/Kg; Scatton *et al.,* 1997). Nonetheless, different from raclopride (Roth et al., 1994), amisulpride also blocks 5-HT_{2B} and 5-HT_{7A} receptors with high affinity (Schoemaker *et al.,* 1997; Abbas et al., 2009). However, the involvement of 5-HT receptors in PPX and L-Dopa hypolocomotion action appears remote in view of the fact that 5-HT_2 receptors stimulate locomotion whereas 5-HT_7 receptors do not influence it (Millan et al., 2003; Clemett et al., 1998). The possibility that high doses of L-dopa activate D2 autoreceptors may be further corroborated by the bell-shaped profile of L-dopa on striatal DA release in reserpinized rats, low doses being stimulatory and higher ones (100 mg/Kg) ineffective (Fisher *et al.,* 2000).

An important finding of the present study is that L-dopa modulated [^{3}H]-DA release from a preparation of nerve terminals (synaptosomes). Expectedly, the synaptosomal K^+-evoked tritium overflow was largely Ca^{++}-dependent, thus exocitotic in nature (Marti *et al.*, 2003), and was inhibited by PPX via activation of amisulpride-sensitive D2 receptors. Indeed, striatal D2 receptors

mainly serve as autoreceptors (Stamford *et al.,* 1991; Kennedy *et al.,* 1992). Unexpectedly however, L-dopa elevated tritium overflow via SCH23390-sensitve D1/D5 receptors. D1 receptors are indeed expressed by striatal nerve terminals (Hersch *et al.,* 1995) and their activation leads to a SCH23390-sensitive rise in synaptosomal Ca^{++} levels (Wu *et al.,* 2006). Although D1 presynaptic receptors are mainly heteroreceptors and expressed by cholinergic and GABAergic terminals, D1 receptors also co-localize with tyrosine hydroxylase, suggesting a role as autoreceptors (Wu *et al.,* 2006). In addition to vesicular [^{3}H]-DA release, L-dopa also increased spontaneous tritium efflux at higher concentrations, through different mechanisms. Indeed, spontaneous [^{3}H]-DA efflux is Ca^{++}-insensitive (Marti *et al.,* 2003) mainly reflecting non vesicular release. The finding that GBR12783 prevented L-dopa action, suggests that L-dopa is uptaken by the DA transporter, causing reversal of its action and promoting tritium efflux. The ineffectiveness of GBR12783 alone relies on superfusion conditions, since continuous removal of the neurotransmitter from the perfusion medium minimizes the role of uptake. Despite the evidence that L-dopa can have biological activity and stimulate presynaptic D1/D5 receptors in vitro, motor inhibition induced by high doses was mediated by D2/D3 receptors, suggesting that in vivo, its actions are mediated by endogenous DA. Although not operative in naïve mice however, this facilitatory control may become important in Parkinson's disease, where storage capability of DA nerve terminals is compromised and D1 receptor transmission up-regulated. Under these conditions, direct stimulation of D1/D5 presynaptic (even postsynaptic) receptors may contribute to L-dopa sensitization and development of dyskinesia (Bezard et al., 2001).

NOP receptor ligands and motor activity

We previously reported that UFP-101 microinjections in rat SNr (Marti *et al.,* 2004) or systemic administrations of J-113397 (Viaro *et al.,* 2008) and Trap-101 (Marti *et al.,* 2008) in naïve rodents facilitated motor activity at low doses and inhibited it at higher ones. The present study confirms that dual motor response is indeed a consequence of progressive central NOP receptor blockade, further demonstrating the involvement of endogenous DA. Motor facilitation induced by NOP

receptor antagonists was raclopride-sensitive but amisulpride-insensitive, suggesting that NOP receptor blockade can ultimately lead to postsynaptic D2L receptor activation. Indeed, J-113397 elevated striatal DA release via blockade of an inhibitory N/OFQ tone on nigral DA neurons (Marti *et al.,* 2004), although in rats this effect was observed at higher doses (3 mg/Kg) than those facilitating motor activity in mice. J-113397 (10 mg/Kg) also elevated DA release in the mouse nucleus accumbens although in a NOP-independent manner (Koizumi *et al.,* 2004). Motor facilitation induced by low N/OFQ doses was also raclopride-sensitive. This extends previous findings that N/OFQ-induced facilitation was prevented by haloperidol (Florin *et al.,* 1996) or by lesioning the DA system (Kuzmin *et al.,* 2004), further suggesting that low doses of N/OFQ and NOP antagonists activate common pathways. To support this view, both 0.01 nmol N/OFQ or 0.1 nmol UFP 101 injected into SNr evoked motor activation associated with increases in excitability and output from motor cortex (Marti *et al.,* 2009), likely via inhibition of nigro-thalamic output neurons and thalamic disinhibition (Deniau and Chevalier, 1985). At present, however, evidence that N/OFQ stimulates nigral efferent DA pathways is still lacking. Rather, exogenous N/OFQ inhibits the activity of nigro-striatal (Marti *et al.,* 2004) and meso-accumbal (Murphy and Maidment, 1999) DA neurons, an effect related to N/OFQ induced hypolocomotion (Marti *et al.,* 2004; Murphy and Maidment, 1999; Narayanan *et al.,* 2004). Contrary to facilitation, motor inhibition induced by NOP antagonists was amisulpride-sensitive and raclopride-insensitive, suggesting that high doses of NOP receptor antagonists cause excessive DA release leading to stimulation of negative feedback mechanisms via D2 autoreceptors. Indeed, motor inhibition was reversed into facilitation in the presence of amisulpride. Consistently, motor impairment induced by high Trap-101 doses in naïve rats was turned into motor facilitation after striatal DA depletion (Marti *et al.,* 2008).

Conclusions

NOP receptor antagonists evoked dual motor responses in mice. Motor facilitation was raclopride-sensitive and amisulpride-insensitive while the opposite was true for motor inhibition. Raclopride

also blocked motor facilitation induced by N/OFQ whereas amisulpride attenuated motor impairment induced by PPX and L-dopa, suggesting that facilitation and inhibition are mediated by different populations of D2 receptors, likely postsynaptic and presynaptic (autoreceptors), respectively. D1/5 and D3 receptors do not contribute to motor responses to NOP receptor ligands. However, D3 receptors shape motor responses to both PPX and L-Dopa, opposing their D2 autoreceptor-mediated inhibitory actions in a test specific for movement initiation and execution. Moreover, D1/D5 receptors mediate presynaptic facilitatory actions of L-dopa on DA release occurring prior to its conversion to DA. This finding may be clinically relevant as D1/D5 receptor stimulation underlie L-dopa-induced dyskinesia during Parkinson's disease therapy (Obeso et al., 2000). In conclusion, the present study demonstrates the involvement of endogenous DA in motor action of NOP receptor antagonists in naïve mice, suggesting that the dual motor response can be shaped by pharmacological manipulations of D2 pre- or postsynaptic receptors, or be influenced by physio-pathological changes of their expression. Further studies are warranted to investigate the dopaminergic component of the dual motor response to NOP receptor antagonists in DA-depleted rodents (Viaro et al., 2008), in view of the proposed clinical application as antiparkinsonian agents (Marti et al., 2005, 2007).

Acknowledgments

This work has been funded by grants from the Italian Ministry of the University (FIRB Internazionalizzazione n RBIN047W33 to M Morari). We gratefully thank Prof S Salvadori for the generous gift of J-113397, N/OFQ, Trap-101 and UFP-101, and Dr MJ Millan for providing S33084.

References

Abbas AI, Hedlund PB, Huang XP, Tran TB, Meltzer HY, Roth BL (2009). Amisulpride is a potent 5-HT7 antagonist: relevance for antidepressant actions in vivo. *Psychopharmacology (Berl)* **205:** 119-128.

Bezard E, Brotchie JM, Gross CE (2001). Pathophysiology of levodopa-induced dyskinesia: potential for new therapies. *Nat Rev Neurosci* **2:** 577-588.

Calò G, Rizzi A, Rizzi D, Bigoni R, Gerrini R, Marzola G, *et al.* (2002). [Nphe1, Arg14, Lys^{15}]Nociceptin-NH_2, a novel potent and selective antagonist of the nociceptin/orphanin FQ receptor. *Br J Pharmacol* **136:** 303-311.

Carter AJ, Müller RE (1991). Pramipexole, a dopamine D2 autoreceptor agonist, decreases the extracellular concentration of dopamine in vivo. *Eur J Pharmacol* **200:** 65-72.

Clark D, White FJ (1997). D1 dopamine receptor--the search for a function: a critical evaluation of the D1/D2 dopamine receptor classification and its functional implications. *Synapse* **1:** 347-388.

Clemett DA, Cockett MI, Marsden CA, Fone KC (1998). Antisense oligonucleotide-induced reduction in 5-hydroxytryptamine7 receptors in the rat hypothalamus without alteration in exploratory behaviour or neuroendocrine function. *J Neurochem* **71:** 1271-1279.

Deniau JM, Chevalier G (1985). Disinhibition as a basic process in the expression of striatal functions. II. The striato-nigral influence on thalamocortical cells of the ventromedial thalamic nucleus. *Brain Res* **334:** 227-233.

Devine DP, Taylor L, Reinscheid RK, Monsma FJ Jr, Civelli O, Akil H (1996). Rats rapidly develop tollerance to the locomotor-inhibiting effects of the novel neuropeptide orphanin FQ. *Neurochem Res* **21:** 1387-1396.

Fisher A, Biggs CS, Eradiri O, Starr MS (2000). Dual effects of L-3,4-dihydroxyphenylalanine on aromatic L-amino acid decarboxylase, dopamine release and motor stimulation in the reserpine-treated rat: evidence that behaviour is dopamine independent. *Neuroscience* **95:** 97-111.

Florin S, Suaudeau C, Meunier JC, Costentin J (1996). Nociceptin stimulates locomotion and exploratory behaviour in mice. *Eur J Pharmacol* **317:** 9-13.

Hersch SM, Ciliax BJ, Gutekunst CA, Rees HD, Heilman CJ, Yung KK, *et al.* (1995). Electron microscopic analysis of D1 and D2 dopamine receptor proteins in the dorsal striatum and their synaptic relationships with motor corticostriatal afferents. *J Neurosci* **15:** 5222-5237.

Higgins GA, Grottick AJ, Ballard TM, Richards JG, Messer J, Takeshima H, *et al.* (2001). Influence of the selective ORL1 receptor agonist, Ro64-6198, on rodent neurological function. *Neuropharmacology* **41:** 97-107.

Jenck F, Moreau J, Martin J, Kilpatrick G, Reinschied RK, Monsma FJ Jr, *et al.* (1997). Orphanin FQ acts as an anxiolitic to attenuate behavioural responses to stress. *Proc Natl Acad Sci* **94:** 14854-14858.

Kawamoto H, Ozaki S, Itoh Y, Miyaji M, Arai S, Nakashima H, *et al.* (1999). Discovery of the fist potent and selective small molecule opioid receptor-like (ORL-1) antagonist: 1-[(3R,4R)-1-cyclooctymethyl-3-hydroxymethyl-4-piperidyl]-3-ethyl-1,3-diydro-2H-benzimidazol-2-one (J-113397). *J Med Chem* **42:** 5061-5063.

Kennedy RT, Jones SR, Wightman RM (1992). Dynamic observation of dopamine autoreceptor effects in rat striatal slices. *J Neurochem* **59:** 449-455.

Koizumi M, Sakoori K, Midorikawa N, Murphy NP (2004). The NOP (ORL1) receptor antagonist Compound B stimulates mesolimbic dopamine release and is rewarding in mice by a non-NOP-receptor-mediated mechanism. *Br J Pharmacol* **143:** 53-62.

Kuschinsky K, Hornykiewicz O (1972). Morphine catalepsy in the rat: relation to striatal dopamine metabolism. *Eur J Pharmacol* **19:** 119-122.

Kuzmin A, Sandin J, Terenius L, Ogren SO (2004). Evidence in locomotion test for the functional heterogeneity of ORL-1 receptors. *Br J Pharmacol* **141:** 132-140.

Lambert DG (2008). The nociceptin/orphanin FQ receptor: a target with broad therapeutic potential. *Nat Rev Drug Discov* **7:** 694-710.

Laursen SE, Belknap JK (1986). Intracerebroventricular injections in mice. Some methodological refinements. *J Pharmacol Methods* **16:** 355-357.

Maggio R, Scarselli M, Novi F, Millan MJ, Corsini GU (2003). Potent activation of dopamine D3/D2 heterodimers by the antiparkinsonian agents, S32504, pramipexole and ropinirole. *J Neurochem* **87:** 631-641.

Marti M, Mela F, Ulazzi L, Hanau S, Stocchi S, Paganini F, *et al.* (2003). Differential responsiveness of rat striatal nerve endings to the mitochondrial toxin 3-nitropropionic acid: implications for Huntington's disease. *Eur J Neurosci* **18:** 759-767.

Marti M, Mela F, Veronesi C, Marti M, Mela F, Veronesi C, *et al.* (2004). Blockade of nociceptin/orphanin FQ receptor signalling in rat substantia nigra pars reticulata stimulates nigrostriatal dopaminergic transmission and motor behaviour. *J Neurosci* **24:** 6659-6666.

Marti M, Mela F, Fantin M, Zucchini S, Brown JM, Witta J, *et al.* (2005). Blockade of nociceptin/orphanin FQ transmission Attenuates Symptoms and Neurodegeneration Associated with Parkinson's Disease. *J Neurosci* **25:** 9591-9601.

Marti M, Trapella C, Viaro R, Morari M (2007). The Nociceptin/Orphanin FQ Receptor antagonist J-113397 and L-Dopa additively attenuate experimental parkinsonism through overinhibition of the nigrothalamic pathway. *J Neurosci* **27:** 1297-1307.

Marti M, Trapella C, Morari M (2008). The novel nociceptin/orphanin FQ receptor antagonist Trap-101 alleviates experimental parkinsonism through inhibition of the nigro-thalamic pathway: positive interaction with L-DOPA. *J Neurochem* **107:** 1683-1696.

Marti M, Viaro R, Guerrini R, Franchi G, Morari M (2009). Nociceptin/orphanin FQ modulates motor behavior and primary motor cortex output through receptors located in substantia nigra reticulata. *Neuropsychopharmacology* **34:** 341-355.

Meunier JC, Mollerau C, Toll L, Saudeau C, Moisand C, Alvinerie P, *et al.* (1995). Isolation and structure of the endogenus agonist of opioid receptor-like ORL1 receptor. *Nature* **377:** 532-535.

Mierau J, Schingnitz G (1992). Biochemical and pharmacological studies on Pramipexole, a potent and selective dopamine D_2 receptor agonist. *Eur J of Pharmacology* **215:** 161-170.

Millan MJ, Dekeyne A, Rivet JM, Dubuffet T, Lavielle G, Brocco M (2000). S33084, a novel, potent, selective, and competitive antagonist at dopamine D(3)-receptors: II. Functional and behavioral profile compared with GR218,231 and L741,626. *J Pharmacol Exp Ther* **293:** 1063-1073.

Millan MJ, Veiga S, Girardon S, Brocco M (2003). Blockade of serotonin 5-HT1B and 5-HT2A receptors suppresses the induction of locomotor activity by 5-HT reuptake inhibitors, citalopram and fluvoxamine, in NMRI mice exposed to a novel environment: a comparison to other 5-HT receptor subtypes. *Psychopharmacology (Berl)* **168:** 397-409.

Millan MJ, Seguin L, Gobert A, Cussac D, Brocco M (2004). The role of dopamine D3 compared with D2 receptors in the control of locomotor activity: a combined behavioural and neurochemical analysis with novel, selective antagonists in rats. *Psychopharmacology (Berl)* **174:** 341-357.

Mogil JS, Pasternak GW (2001). The molecular and behavioral pharmacology of the orphanin FQ/nociceptin peptide and receptor family. *Pharmacological Reviews* **53:** 381-415.

Morari M, Sbrenna S, Marti M, Caliari C, Bianchi C, Beani L (1998). NMDA and non-NMDA ionotropic glutamate receptors modulate striatal acetylcholine release via pre-and postsynaptic mechanisms. *J Neurochem* **71:** 2006-2017.

Murphy NP, Maidment NT (1999). Orphanin FQ/nociceptin modulation of mesolimbic dopamine transmission determined by microdialisis. *J Neurochem* **73:** 179-186.

Narayanan S, Lam H, Carroll FI, Lutfy K (2004). Orphanin FQ/nociceptin suppresses motor activity through an action along the mesoaccumbens axis in rats. *J Psychiatry Neurosci* **29:** 116-123.

Nishi M, Houtani T, Noda Y, Mamiya T, Sato K, Doi T, *et al.* (1997). Unrestrained nociceptive response and disregulation of hearing ability in mice lacking the nociceptin/orphaninFQ receptor. *EMBO J* **16:** 1858-1864.

Reavill C, Taylor SG, Wood MD, Ashmeade T, Austin NE, Avenell KY, *et al.* (2000). Pharmacological actions of a novel, high-affinity, and selective human dopamine D(3) receptor antagonist, SB-277011-A. *J Pharmacol Exp Ther* **294:** 1154-1165.

Reischeid RK, Nothacker HP, Burson A, Adati A, Henningens RA, Bunzow JR, *et al.* (1995). Orphanin FQ: a neuropeptide that activates an opioid-like G protein-coupled receptor. *Science* **270:** 792-794.

Rizzi A, Marzola G, Bigoni R, Guerrini R, Salvadori S, Mogil JS, *et al.* (2001). Endogenous nociceptin signaling and stress-induced analgesia. *Neuroreport* **12:** 3009-3013.

Roth BL, Craigo SC, Choudhary MS, Uluer A, Monsma FJ Jr, Shen Y, *et al.* (1994). Binding of typical and atypical antipsychotic agents to 5-hydroxytryptamine-6 and 5-hydroxytryptamine-7 receptors. *J Pharmacol Exp Ther* **268:** 1403-1410.

Rozas G, Guerra MJ, Labandeira-Garcia JL (1997). An automated rotarod method for quantitative drug-free evaluation of overall motor deficits in rat models of parkinsonism. Brain Res Brain *Res Protoc* **2:** 75-84.

Sanberg PR, Bunsey MD, Giordano M, Norman AB (1988). The catalepsy test: its ups and downs. *Behav Neurosci* **102:** 748-759.

Scatton B, Claustre Y, Cudennec A, Oblin A, Perrault G, Sanger DJ, *et al.* (1997). Amisulpride: From Animal Pharmacology To Therapeutic Action. *International Clinical Psychopharmacology* **12:** S29-S36.

Schallert T, De Ryck M, Whishaw IQ, Ramirez VD, Teitelbaum P (1979). Excessive bracing reactions and their control by atropine and L-DOPA in an animal analog of Parkinsonism. *Exp Neurol* **64:** 33-43.

Schoemaker H, Claustre Y, Fage D, Rouquier L, Chergui K, Curet O, *et al.* (1997). Neurochemical characteristics of amisulpride, an atypical dopamine D2/D3 receptor antagonist with both presynaptic and limbic selectivity. *J Pharmacol Exp Ther* **280**: 83-97.

Siuciak JA, Fujiawara RA (2004). The activity of pramipexole in the mouse forced swim test is mediated by D_2 rather than D_3 receptors. *Psychopharmacology* **175:** 163-169.

Stamford JA, Kruk ZL, Millar J (1991). Differential effects of dopamine agonists upon stimulated limbic and striatal dopamine release: in vivo voltammetric data. Br J Pharmacol 102: 45-50.

Trapella C, Guerrini R, Piccagli L, Calò G, Carra' G, Spagnolo B, *et al.* (2006). Identification of an achiral analogue of J-113397 as potent nociceptin/orphanin FQ receptor antagonist. *Bioorg Med Chem* **14:** 692-704.

Usiello A, Baik JH, Rougé-Pont F, Picetti R, Dierich A, LeMeur M, *et al.* (2000). Distinct functions of the two isoforms of dopamine D2 receptors. *Nature* **408:** 199-203.

Vallone D, Picetti R, Borrelli E (2000). Structure and function of dopamine receptors. Neurosci Biobehav Rev 24: 125-132.

Viaro R, Sanchez-Pernaute R, Marti M, Trapella C, Isacson O, Morari M (2008). Nociceptin/orphanin FQ receptor blockade attenuates MPTP-induced parkinsonism. Neurobiol Dis 30: 430-438.

Wang Y, Xu R, Sasaoka T, Tonegawa S, Kung MP, Sankoorikal EB (2000). Dopamine D2 long receptor-deficient mice display alterations in striatum-dependent functions. J Neurosci 20: 305-314.

Wu J, Dougherty JJ, Nichols RA (2006). Dopamine receptor regulation of Ca2+ levels in individual isolated nerve terminals from rat striatum: comparison of presynaptic D1-like and D2-like receptors. J Neurochem 98: 481-494.

Figures and Legends

Figure 1. NOP receptor antagonists dually modulated motor activity in mice. Systemic (i.p.) administration of J-113397 (0.1-10 mg/Kg) and Trap-101 (0.1-30 mg/Kg), or i.c.v. injection of UFP-101 (0.1-30 nmol) produced motor facilitation or inhibition depending on dose. Motor activity has been evaluated as immobility time in the bar test (**A, D, G**), number of steps in the drag test (**B, E, H**) and time spent on the rod in the rotarod test (**C, F, I**). All tests were performed before (control session) and after (10 and 60 min) drug administration. Data (collected 10 min after treatment) are means ± SEM of 6 determinations per group and were expressed as percentage of the control session. Data collected 60 min after treatment have been presented as supplementary material (Fig. S1.1). *p<0.05, **p<0.01 different from saline (RM ANOVA followed by contrast analysis and the sequentially rejective Bonferrroni's test for multiple comparisons).

Figure 2. D2/D3 receptor antagonists decreased motor activity in mice. Systemic (i.p.) administration of raclopride (0.03-0.3 mg/Kg) and amisulpride (0.5-15 mg/Kg) increased immobility time in the bar test (**A, D**) and reduced time spent on the rod in the rotarod test (**C, F**). Raclopride also reduced the number of steps in the drag test (**B**), amisulpride being ineffective (**E**). All tests were performed before (control session) and after (30 and 80 min) drug administration. Data (collected 30 min after treatment) are means ± SEM of 6 determinations per group and were calculated as percentage of the control session. Data collected 80 min after treatment have been presented as supplementary material (Fig. S1.2). *p<0.05, **p<0.01 different from saline (RM ANOVA followed by contrast analysis and the sequentially rejective Bonferrroni's test for multiple comparisons).

Figure 3. D1/D5 and D3 receptor selective antagonists differentially affected motor activity in mice. Systemic (i.p.) administration of the D1/D5 selective antagonist SCH23390 (0.003-0.03

mg/Kg) increased immobility time in the bar test (**A**), reducing both the number of steps in the drag test (**B**) and time spent on the rod in the rotarod test (**C**). Systemic (i.p.) administration of the D3 receptor selective antagonist S33084 (0.04-0.64 mg/Kg) did not affect immobility time (**D**) and time spent on the rod (**F**), slightly reducing the number of steps (**E**). All tests were performed before (control session) and after (30 and 80 min) drug administration. Data (collected 30 min after treatment) are means ± SEM of 6 determinations per group and were calculated as percentage of the control session. Data collected 80 min after treatment have been presented as supplementary material (Fig. S1.3). *p<0.05, **p<0.01 different from saline (RM ANOVA followed by contrast analysis and the sequentially rejective Bonferrroni's test for multiple comparisons).

Figure 4. Facilitation of motor activity induced by NOP receptor antagonists was selectively prevented by raclopride. Pretreatment (20 min in advance) with raclopride (0.03 mg/Kg, i.p.) prevented motor facilitation induced by low doses of J-113397 (0.3 mg/Kg, i.p.), Trap-101 (10 mg/Kg, i.p.) and UFP-101 (3 nmol, i.c.v.) in the drag (**B**) and rotarod (**C**) tests. Raclopride and NOP receptor antagonists did not affect immobility time in the bar test (**A**). Pretreatment with amisulpride (0.5 mg/Kg, i.p.), S33084 (0.16 mg/Kg, i.p.) and SCH23390 (0.003 mg/Kg, i.p.) did not affect motor facilitation induced by J-113397 (0.3 mg/Kg, i.p.) in the drag (**E)** and rotarod (**F**) tests. Amisulpride, S33084, SCH23390 and J-113397 (alone or in combination) did not affect immobility time in the bar test (**D**). All tests were performed before (control session) and after (10 and 60 min) NOP receptor antagonist administration. When DA receptor antagonists were tested alone, behavioral testing was performed 30 and 80 min after drug administration. Data (collected 10 min after treatment) are means ± SEM of 6 determinations per group and were calculated as percentage of the control session. Data collected 60 min after treatment have been presented as supplementary material (Fig. S1.4). *p<0.05, **p<0.01 different from saline; °p<0.05, °°p<0.01 different from the same group in the absence of raclopride or J-113397 (RM ANOVA followed by contrast analysis and the sequentially rejective Bonferrroni's test for multiple comparisons).

Figure 5. Inhibition of motor activity induced by NOP receptor antagonists was selectively prevented by amisulpride. Pretreatment (20 min in advance) with amisulpride (0.5 mg/Kg) reduced motor inhibition caused by high doses of J-113397 (10 mg/Kg, i.p.), Trap-101 (30 mg/Kg, i.p.) and UFP-101 (30 nmol, i.c.v) in the bar (**A**), drag (**B**) and rotarod (**C**) tests. Conversely, pretreatment with raclopride (0.03 mg/Kg, i.p.) was ineffective (**D-F**). All tests were performed before (control session) and after (10 and 60 min) NOP receptor antagonist administration. When DA receptor antagonists were tested alone, behavioral testing was performed 30 and 80 min after drug administration. Data (collected 10 min after treatment) are means ± SEM of 6 determinations per group and were expressed as percentage of the control session. Data collected 60 min after treatment have been presented as supplementary material (Fig. S1.5). *p<0.05, **p<0.01 different from saline; °p<0.05, °°p<0.01 different from the same group in the absence of amisulpride (RM ANOVA followed by contrast analysis and the sequentially rejective Bonferrroni's test for multiple comparisons).

Figure 6. Nociceptin/orphanin FQ (N/OFQ) dually modulated motor activity in mice. I.c.v. injections of N/OFQ (0.01-10 nmol) produced motor facilitation or inhibition in the drag (**B**) and rotarod (**C**) tests depending on dose. Only motor inhibition was observed in the bar test (**A**). Pretreatment (20 min in advance) with raclopride (0.03 mg/Kg, i.p.) prevented increases in the number of steps (**E**) and time on rod (**F**) induced by low doses of N/OFQ (0.01 nmol, i.c.v.). Low doses of N/OFQ, alone or in combination with raclopride, did not affect immobility time in the bar test (**D**). All tests were performed before (control session) and after (10 and 60 min) N/OFQ injection. When raclopride was tested alone, behavior was assessed 30 and 80 min after drug administration. Data (collected 10 min after treatment) are means ± SEM of 6 determinations per group and were calculated as percentage of the control session. Data collected 60 min after treatment have been presented as supplementary material (Fig. S1.6). *p<0.05, **p<0.01 different

from saline (RM ANOVA followed by contrast analysis and the sequentially rejective Bonferrroni's test for multiple comparisons).

Figure 7. Specificity of action of UFP-101 and nociceptin/orphanin FQ (N/OFQ). I.c.v. injections of UFP-101 (3 and 30 nmol, respectively) and N/OFQ (0.01 and 10 nmol, respectively) differentially affected immobility time in the bar test (**A**), number of steps in the drag test (**B**) and time spent on the rod in the rotarod test (**C**) in $NOP^{+/+}$ mice, being ineffective in $NOP^{-/-}$ mice. All tests were performed before (control session) and 10 min and 60 min after N/OFQ and UFP-101 injection. Data (collected 10 min after treatment) are means ± SEM of 6 determinations per group and were calculated as percentage of the control session. Data collected 60 min after treatment have been presented as supplementary material (Fig. S1.7). **p<0.01 different from saline (RM ANOVA followed by contrast analysis and the sequentially rejective Bonferrroni's test for multiple comparisons).

Figure 8. DA receptor agonists decreased motor activity in mice. Systemic administration of L-dopa (1-100 mg/Kg combined with benserazide 4:1 ratio, i.p.) and pramipexole (PPX; 0.0001-1 mg/Kg, i.p.) increased immobility time in the bar test (**A, D**), and reduced both the number of steps in the drag test (**B, E**) and time spent on the rod in the rotarod test (**C, F**). All tests were performed before (control session) and after (10 and 60 min) drug administration. Data (collected 10 min after treatment) are means ± SEM of 6 determinations per group and were calculated as percentage of the control session. Data collected 60 min after treatment have been presented as supplementary material (Fig. S1.8). *p<0.05, **p<0.01 different from saline (RM ANOVA followed by contrast analysis and the sequentially rejective Bonferrroni's test for multiple comparisons).

Figure 9. Amisulpride differentially affected motor inhibition induced by L-dopa and pramipexole (PPX). Pretreatment (20 min in advance) with amisulpride (0.5 mg/Kg) differentially affected motor

inhibition induced by L-dopa (100 mg/Kg plus benserazide 25 mg/Kg) and PPX (0.1 and 1 mg/Kg, i.p.) in the bar (**A**), drag (**B**) and rotarod (**C**) tests. Amisulpiride consistently counteracted the effect of L-dopa in the three test but was partially effective against PPX, only prevented the increase in immobility time induced by PPX 0.1 mg/Kg in the bar test (**A**) and attenuated impairment in rotarod performance induced by PPX 1 mg/Kg (**C**). Pretreatment with raclopride (0.03 mg/Kg, i.p.) did not attenuate motor inhibition induced by L-dopa and PPX and even worsened it (**D-F**). All tests were performed before (control session) and after (10 and 60 min) L-dopa and PPX administration. When DA receptor antagonists were tested alone, behavioral testing was performed 30 and 80 min after drug administration. Data (collected 10 min after treatment) are means ± SEM of 6 determinations per group and were calculated as percentage of the control session. Data collected 60 min after treatment have been presented as supplementary material (Fig. S1.9). *p<0.05, **p<0.01 different from saline; °p<0.05, °°p<0.01 different from the same group in the absence of amisulpride or raclopride (RM ANOVA followed by contrast analysis and the sequentially rejective Bonferrroni's test for multiple comparisons).

Figure 10. Motor inhibition induced by L-dopa or pramipexole (PPX) was insensitive to the D3 selective receptor antagonist S33084 or the peripheral non selective DA receptor antagonist domperidone. Pretreatment (20 min in advance) with S33084 (0.16 mg/Kg, i.p.; **A-C**) or domperidone (5 mg/Kg, i.p.; **D-F**) did not attenuate motor inhibition caused by L-dopa (100 mg/Kg plus benserazide 25 mg/Kg; i.p.) and PPX (0.1 and 1 mg/Kg) in the bar (**A, D**), drag (**B, E**) and rotarod (**C, F**) test. S33084 alone even increased the inhibition of stepping activity induced by both DA receptor agonists in the drag test (**B**). All tests were performed before (control session) and after (10 and 60 min) DA receptor agonist administration. When DA receptor antagonists were tested alone, behavioral testing was performed 30 and 80 min after drug administration. Data (collected 10 min after treatment) are means ± SEM of 6 determinations per group and were calculated as percentage of the control session. Data collected 60 min after treatment have been presented as

supplementary material (Fig. S1.10). *p<0.05, **p<0.01 different from saline; °p<0.05, °°p<0.01 different from the same group in the absence of S33084; #p<0.05 different from PPX 1 mg/Kg (RM ANOVA followed by contrast analysis and the sequentially rejective Bonferrroni's test for multiple comparisons).

Figure 11. Pramipexole (PPX) and L-dopa oppositely modulated K^+-evoked DA release from synaptosomes. PPX (100 nM) inhibited (**A**) while L-dopa (1 µM) elevated (**B**) the [^{3}H]-DA overflow evoked by a 2 min pulse of 10 mM KCl from a preparation of striatal synaptosomes in superfusion. The inhibition induced by PPX was prevented by the D2-like receptor antagonist amisulpride (**A**) while the stimulation induced by L-dopa was prevented by the D1-like receptor antagonist SCH23390 (**B**). PPX and L-dopa were administered 6 min prior to KCl whereas antagonists 3 min before agonists. Data are means ± SEM of 8 determinations per group and were expressed as percentage of control (i.e. the K^+-evoked tritium overflow). *p<0.05, **p<0.01 different from control (ANOVA followed by the Newman-Keuls test).

Figure 12. L-dopa increased spontaneous tritium efflux from synaptosomes. L-dopa (1-100 µM) elevated spontaneous tritium efflux from a preparation of striatal synaptosomes in superfusion pre-loaded with [^{3}H]-DA (**A**). The dopamine transporter blocker GBR12783 but not the D1-like selective antagonist SCH23390 prevented the elevation of tritium efflux induced by the lower L-dopa concentration (10 µM; **B**) and attenuated that induced by the higher L-dopa concentration (100 µM; **C**). GBR12783 and SCH23390 were given 3 min prior to L-dopa and maintained until the end of experiments. Data are means ± SEM of 6 determinations per group and were expressed as percentage of basal tritium efflux (calculated as the mean between the two samples before L-dopa). *p<0.05, **p<0.01 different from washout; °°p<0.01 different from L-dopa alone (ANOVA followed by the Newman-Keuls test performed on AUC values).

Statement of conflicts of interest

None

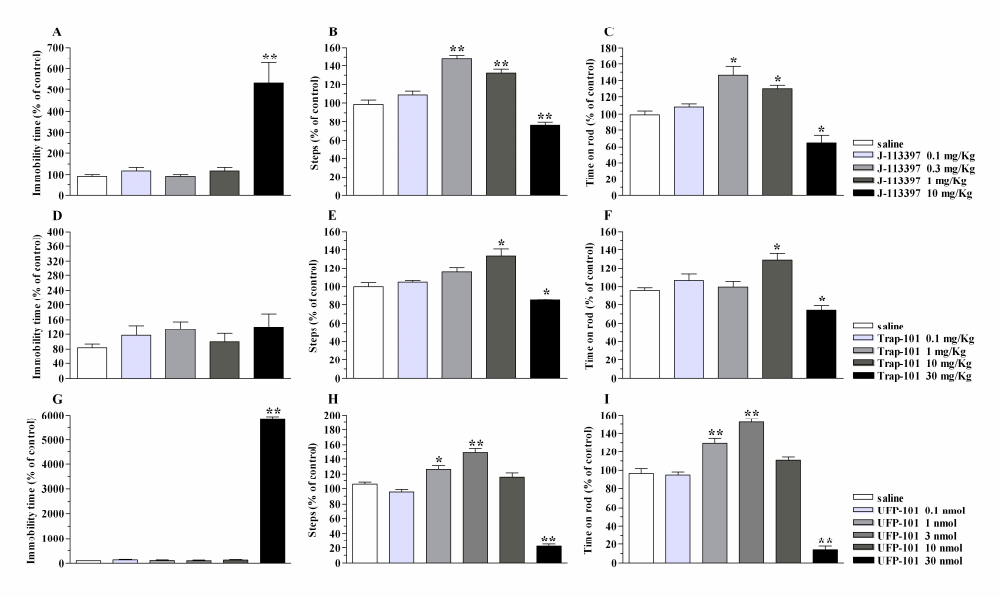

Fig. 1
246x147mm (600 x 600 DPI)

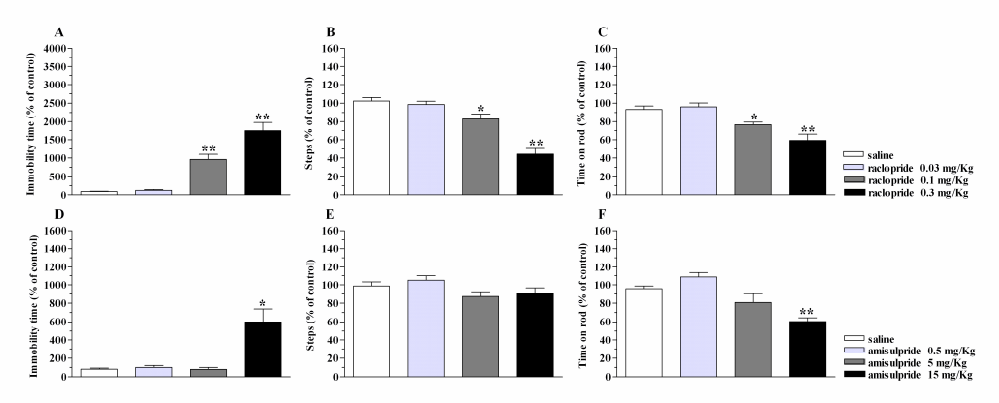

Fig. 2
246x100mm (600 x 600 DPI)

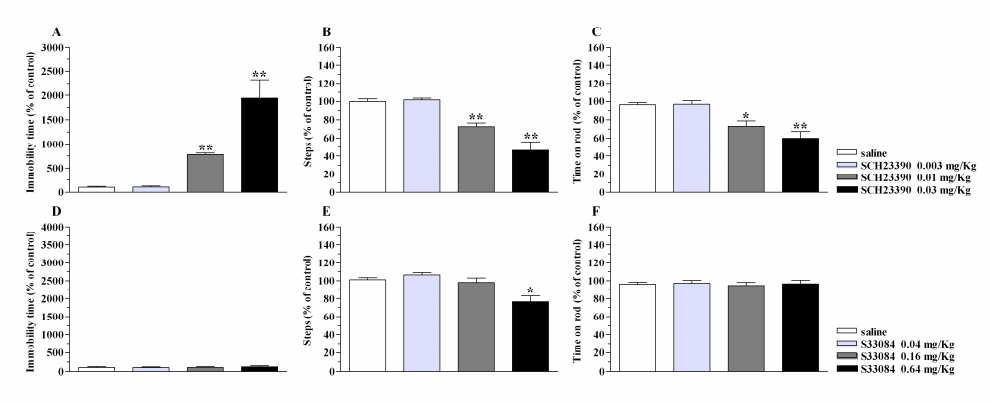

Fig. 3
246x100mm (600 x 600 DPI)

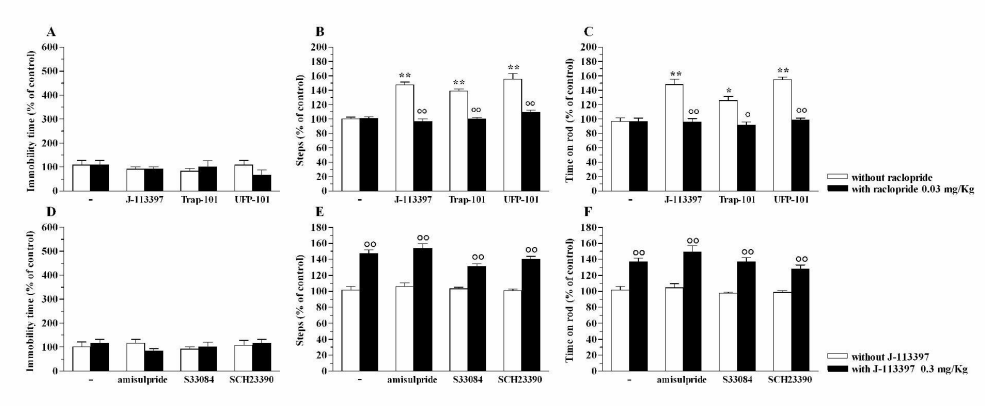

Fig. 4
246x101mm (600 x 600 DPI)

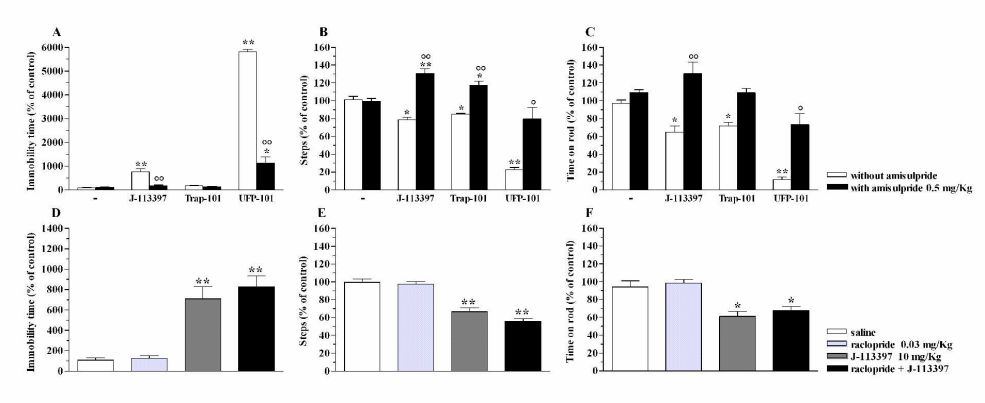

Fig. 5
246x100mm (600 x 600 DPI)

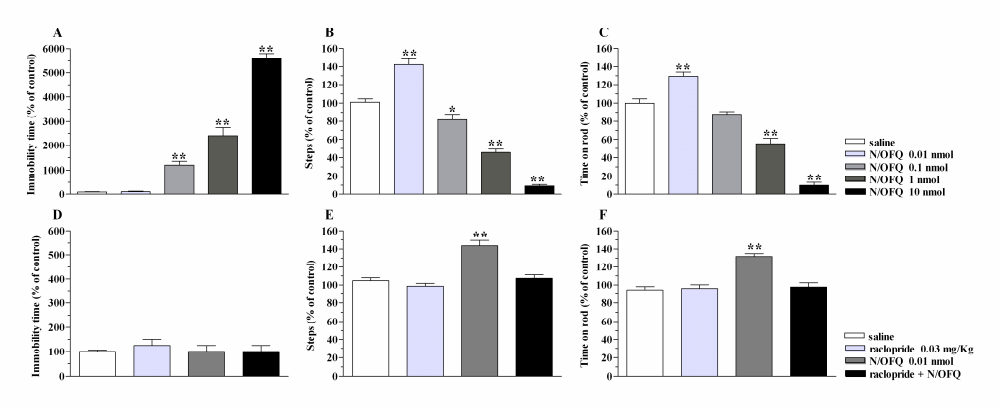

Fig. 6
246x101mm (600 x 600 DPI)

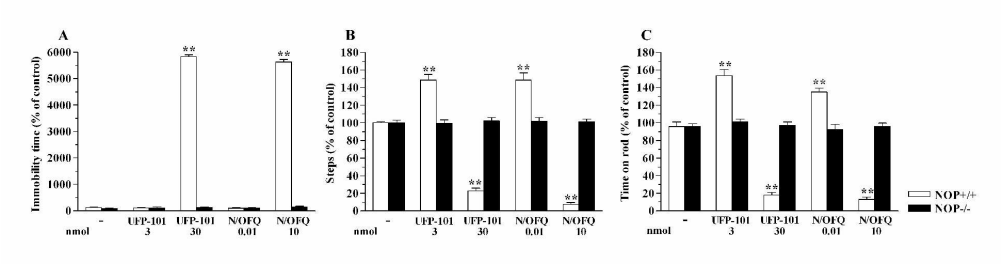

Fig. 7
246x65mm (600 x 600 DPI)

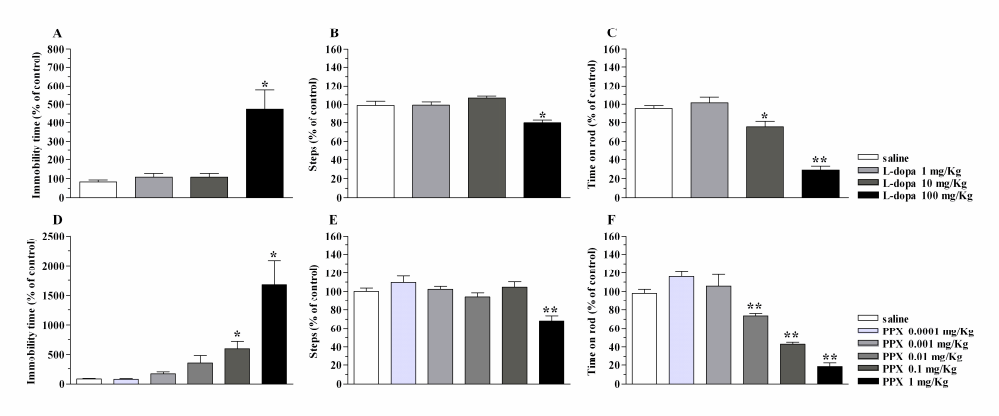

Fig. 8
246x103mm (600 x 600 DPI)

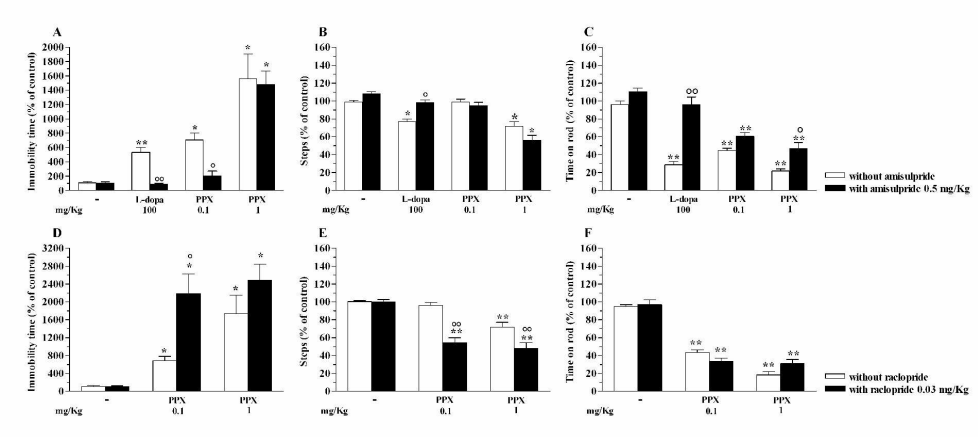

Fig. 9
246x108mm (600 x 600 DPI)

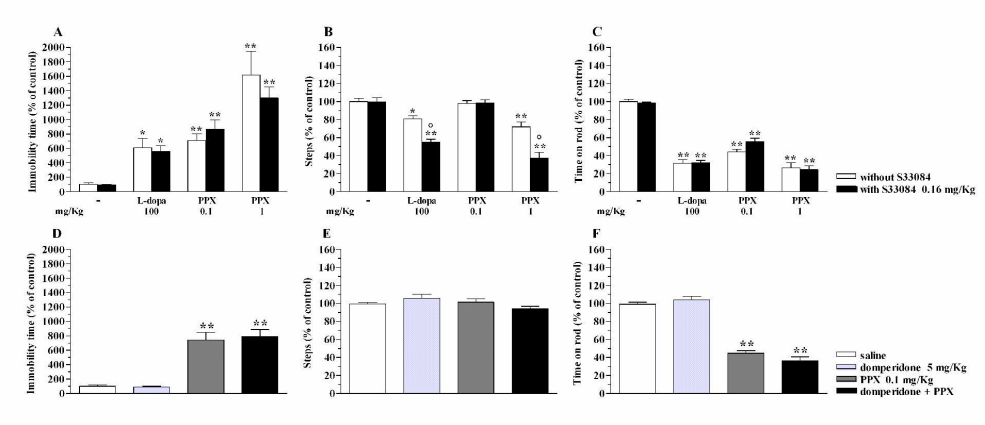

Fig. 10
246x105mm (600 x 600 DPI)

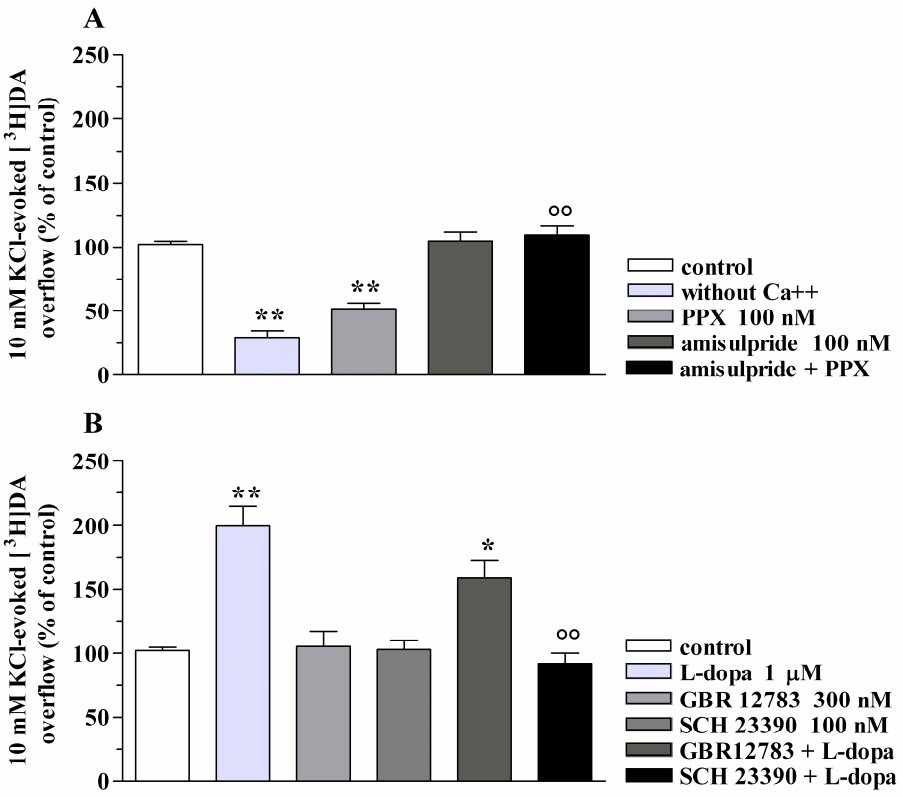

Fig. 11
246x222mm (600 x 600 DPI)

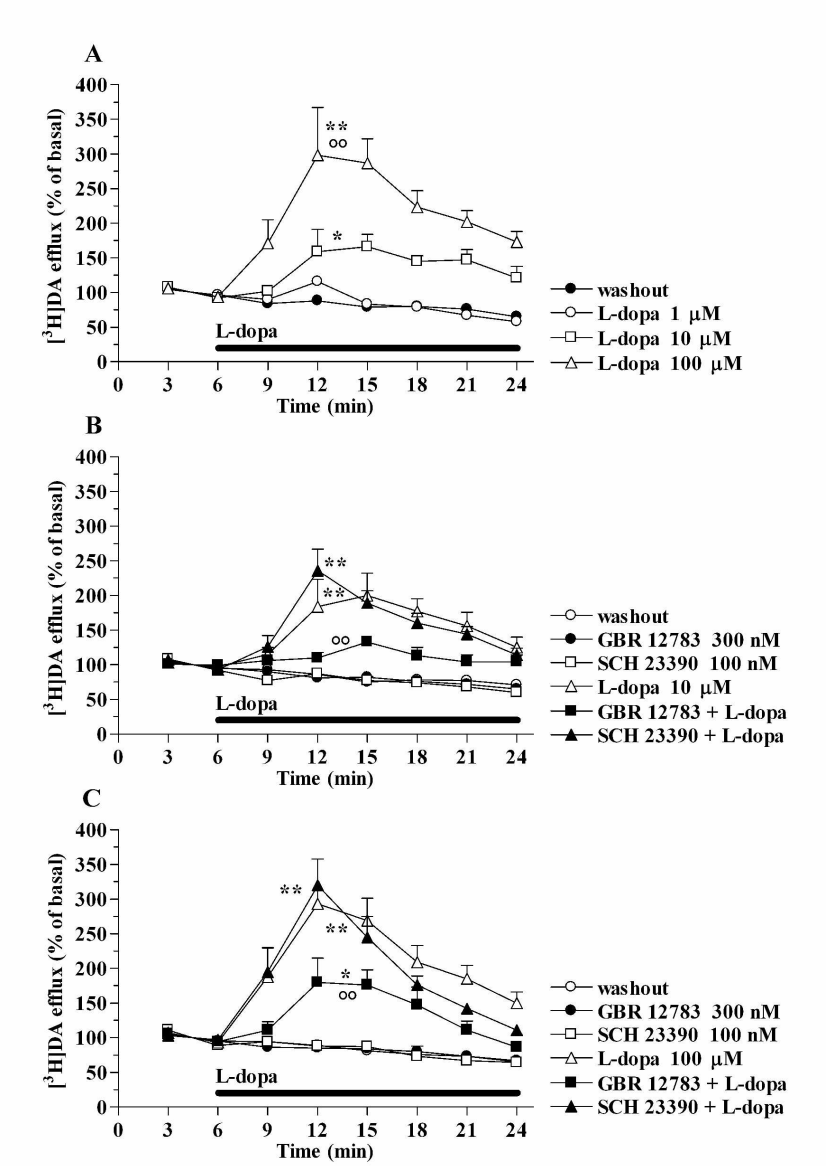

Fig. 12
147x214mm (600 x 600 DPI)